STUDIES ON THE DEACTIVATION AND REACTIVATION OF SPENT HYDROPROCESSING CATALYST

By

MEENA ABDUL-NABI MARAFI

Doctor of Philosphy

The University of Aston in Birmingham

October, 1996

The University of Aston in Birmingham

Studies on the Deactivation and Reactivation of Spent Hydroprocessing Catalyst

Doctor of Philosphy Meena Abdul-Nabi Marafi 1996

SUMMARY

A study is reported on the deactivation of hydroprocessing catalysts and their reactivation by the removal of coke and metal foulants. The literature on hydrotreating catalyst deactivation by coke and metals deposition, the environmental problems associated with spent catalyst disposal, and its reactivation /rejuvenation process was reviewed.

Experimental studies on catalyst deactivation involved problem analysis in industrial hydroprocessing operations, through characterization of the spent catalyst, and laboratory coking studies. A comparison was made between the characteristics of spent catalysts from fixed bed and ebullating bed residue hydroprocessing reactor units and the catalyst deactivation pattern in both types of reactor systems was examined. In the laboratory the nature of initial coke deposited on the catalyst surface and its role on catalyst deactivation were studied. The influence of initial coke on catalyst surface area and porosity was significant. Both catalyst acidity and feedstock quality had a remarkable influence on the amount and the nature of the initial coke. The hydrodenitrogenation function (HDN) of the catalyst was found to be deactivated more rapidly by the initial coke than the hydrodesulphurization function (HDS).

In decoking experiments, special attention was paid to the initial conditions of coke combustion, since the early stages of contact between the coke on the spent catalyst surface and the oxygen are crucial in the decoking process. An increase in initial combustion temperature above 440°C and the oxygen content of the regeneration gas above 5% vanadium led to considerable sintering of the catalyst. At temperatures above 700°C there was a substantial loss of molybdenum from the catalyst, and phase transformations in the alumina support.

The preferred leaching route (coked vs decoked form of spent catalyst) and a comparison of different reagents (i.e., oxalic acid and tartaric acid) and promoters (i.e., Hydrogen Peroxide and Ferric Nitrate) for better selectivity in removing the major foulant (vanadium), characterization and performance evaluation of the treated catalysts and modelling of the leaching process were addressed in spent catalyst rejuvenation studies. The surface area and pore volume increased substantially with increasing vanadium extraction from the spent catalyst; the HDS activity showed a parallel increase. The selectivity for leaching of vanadium deposits was better, and activity recovery was higher, for catalyst rejuvenated by metal leaching prior to decoking.

A model for foulant metals leaching from spent catalyst was developed based upon kinetic and mass transfer aspects. Good agreement was obtained between experimental and simulated results based on the model.

Key Words: Catalyst, Deactivation, Hydroprocessing, Coke Removal, Metal Removal, Rejuvenation.

DEDICATED TO

MY LIBERATED COUNTRY, KUWAIT

MY FAMILY

AND

THE DEPARTED SOUL OF MY MOTHER

AND

MY LOVING CHILDREN

TAREK AND MONA

ACKNOWLEDGEMENTS

I wish to express my deepest gratitude and thanks to Dr. A. Stanislaus and Dr. C. J. Mumford for their help and supervision throughout this study. I also wish to express my appreciation and thanks to the Catalyst Characterization Group for carrying out the analysis of the catalyst samples and TPO testing at Kuwait Institute for Scientific Research.

My thanks also to the Central Analytical Laboratories at K.I.S.R for their cooperation and assistance in conducting NMR, TGA and DTA tests.

Special thanks to Ms. Grace Pereira for her help in typing the thesis.

CONTENTS

LIST OF TABLES

LIST OF FIGURES

1.0. INTRODUCTION

Catalytic hydroprocessing is used extensively to upgrade petroleum heavy oils and residues to more valuable, cleaner transportation fuels in the presence of hydrogen and a catalyst under high temperature and pressure. The catalysts promotes the removal of undesirable impurities such as sulfur, nitrogen, oxygen and metals present in the residual oil by hydrodesulphurization (HDS), hydrodenitrogenation (HDN), hydrodeoxygenation (HDO) and hydrodemetallation (HDM) reactions, and fragmentation of the high-molecular-weight components of the heavy oils to lighter products by hydrocracking.

However, these catalysts lose activity with time due to, e.g. fouling resulting from the formation of carbonaceous deposits on the active sites of the catalyst surface and deposition of heavy metals (such as nickel and vanadium) from the feedstock.

Poisoning and sintering are other causes of catalyst deactivation. Poisoning is caused by strong chemisorption of reactants, products or impurities on the active catalytic sites. Sintering results from decreasing catalyst surface area and porosity, usually associated with high temperature. High temperature may also lead to phase transformation of catalytic components and the support. The deactivated catalysts constitute hazardous wastes since they contain toxic compounds that may be leached by water if disposed of without proper treatment. Disposal of spent catalyst in an environmentally-acceptable way poses a major problem.

Attention therefore has been focused worldwide on developing different methods of handling spent catalysts. A comprehensive review of the literature on the subject revealed that the following options are available to resolve the problem.

One.Treatment of catalyst to allow safe disposal.

Two.Recovery of metals/metal salts from catalysts, coupled with safe disposal.

Three.Recovery of metal/metal salts, coupled with regeneration.

Four.Treatment of catalyst to produce useful material from which deleterious chemical could not be leached during normal use.

Five.Utilization of spent catalyst in catalyst preparation.

Selection of any one option depends upon its technical and economic feasibility. Metal recovery is technically viable, but fluctuation in prices for the recovered materials sometimes renders the process uneconomical. Moreover, the current technologies available for this option are themselves a potential source of chemical pollution arising from the chemicals used to leach the metals; hence the application of this option is limited. Regeneration by the conventional procedure using a nitrogen/air mixture does not result in complete reactivation of the catalyst. Although coke is removed completely, metallic impurities, such as vanadium and nickel, remain on the catalyst pores and act as a diffusion barrier to the reactants. The regeneration/rejuvenation option is considered to be the most attractive approach and has potential advantages from both the economic and environmental points of view. In this process, both foulants (coke and metal deposits) are removed from the spent catalyst and it can be reused. However, the technology is not well-developed although worldwide R&D effort is being directed at it.

Environmental problems associated with the disposal of spent catalysts have greatly affected Kuwait. The country has a huge capacity for petroleum refining. Current production of refined petroleum products at Kuwait's three refineries is nearly 700,000 barrels per day. It is planned to increase the refining capacity to 900,000 barrels per day based on international market requirements until the year 2000 and beyond. These refining operations generate large quantities of spent catalysts that contain toxic chemicals. Disposal of these catalyst wastes in an environmentally-safe way poses a serious problem.

A major portion (about 6000 t/y) of the waste catalysts generated in Kuwait is generated from the residual oil hydroprocessing units. The capacity to process and upgrade residual oils was increased several-fold during 1983/1988. Several units were introduced at KNPC's Mina Abdulla and Mina Al-Ahmadi refineries as part of refinery modernization and upgrading projects to hydrotreat atmospheric residue to low sulfur fuel oils and to produce feedstocks with low contaminant levels for further processing in catalytic cracking and coking units.

Currently, about 250,000 barrels of atmospheric and vacuum residues are hydroprocessed daily in Kuwait refineries bringing substantial economic returns to the country. However, the catalysts used in these processes deactivate rapidly. The deactivated catalysts are not regenerated and reused, but are discarded as solid wastes at a rate of 6000 t/y. Development of a cost-effective method to utilize or dispose of, these

spent catalysts safely would substantially reduce the environmental impact associated with disposal.

In recognition of the potential problems associated with spent catalyst disposal in Kuwait, in the present study attention was focused on understanding the mechanisms of catalyst deactivation caused by metal and coke deposition and on the development of a process to rejuvenate spent hydroprocessing catalysts. A few processes for removal of metal and coke deposits have been reported in the patent literature but information on selective removal of the foulant metal, is relatively scarce in the open literature. Furthermore, no detailed studies have been reported on the development of technically-acceptable processes for spent catalyst rejuvenation. The scope for R&D in areas of residue hydroprocessing and particularly in the reactivation and utilization of spent catalysts, is considerable.

A part of the present work, namely, metals leaching from spent residue hydroprocessing catalysts for rejuvenation is a continuation of the research conducted by the author for the M.Phil degree (102). The effectiveness of different organic acids for selective leaching of the metal foulants from the spent catalyst was compared (123). The kinetics and mechanism of leaching metal sulfides from spent catalyst were also investigated (119). However, several important questions such as the role of oxidizing agents on the leaching efficiency of acids, the preferred leaching route for selective leaching of the deposited metal foulants, the effect of leaching treatment on the concentration and distribution of catalytically-active metals (Co and Mo) orginally present in the catalyst and on the morphology of alumina support, were not addressed in that earlier study.

In the present work, new results are presented on metal leaching from spent catalyst. A model for simulating the metal leaching process has also been developed as part of the study. In addition, factors influencing hydroprocessing catalyst deactivation by coke and its removal by combustion are studied in detail. However to provide a background and to identify specific areas for further research on the subject, the literature on catalyst deactivation problems in residue hydroprocessing and the methods of reactivation and utilization of spent catalysts, will first be reviewed.

2.0. LITERATURE REVIEW

Background

The Role of Catalysts in Petroleum Refining

Catalysts are used extensively in the refining of petroleum crude oils. Figure. 2.1 shows the various catalytic units in a modern refinery. Crude oils are complex mixtures, mostly of hydrocarbons which range from associated gases up to non-distillable residue. The first refinery operation is distillation which is carried out to separate the crude oil into different boiling range fractions typically shown in Table 2.1.

Table 2.1. Boiling Ranges of Typical Crude Oil Fractions

Fraction	ASTM Boiling Range (°C)
Butanes and lighter	
Light straight-run gasoline (LSR)	32.2 - 104.4
Naphtha (heavy straight-run gasoline)	82.0 - 204
Kerosene	176.6 - 282
Light gas oil (LGO)	215.5 - 338
Heavy gas oil	288.0 - 443
Vacuum gas oil (VGO)	398.8 - 565.5
Vacuum reduced crude	538 and above

Heavy oils and residues represent the fraction of the crude oil remaining after atmospheric distillation at 350°C (1). These oils are high in viscosity and molecular weight, and low in volatility and hydrogen-to-carbon ratio, and include high concentrations of inorganic atoms such as sulphur, nitrogen, vanadium and nickel (1, 2) which are associated with large organic molecules. The distillation products are further refined to yield the desired products by catalytic processes such as hydrotreating, isomerization, reforming, catalytic cracking, hydrocracking, etc Figure.2.1

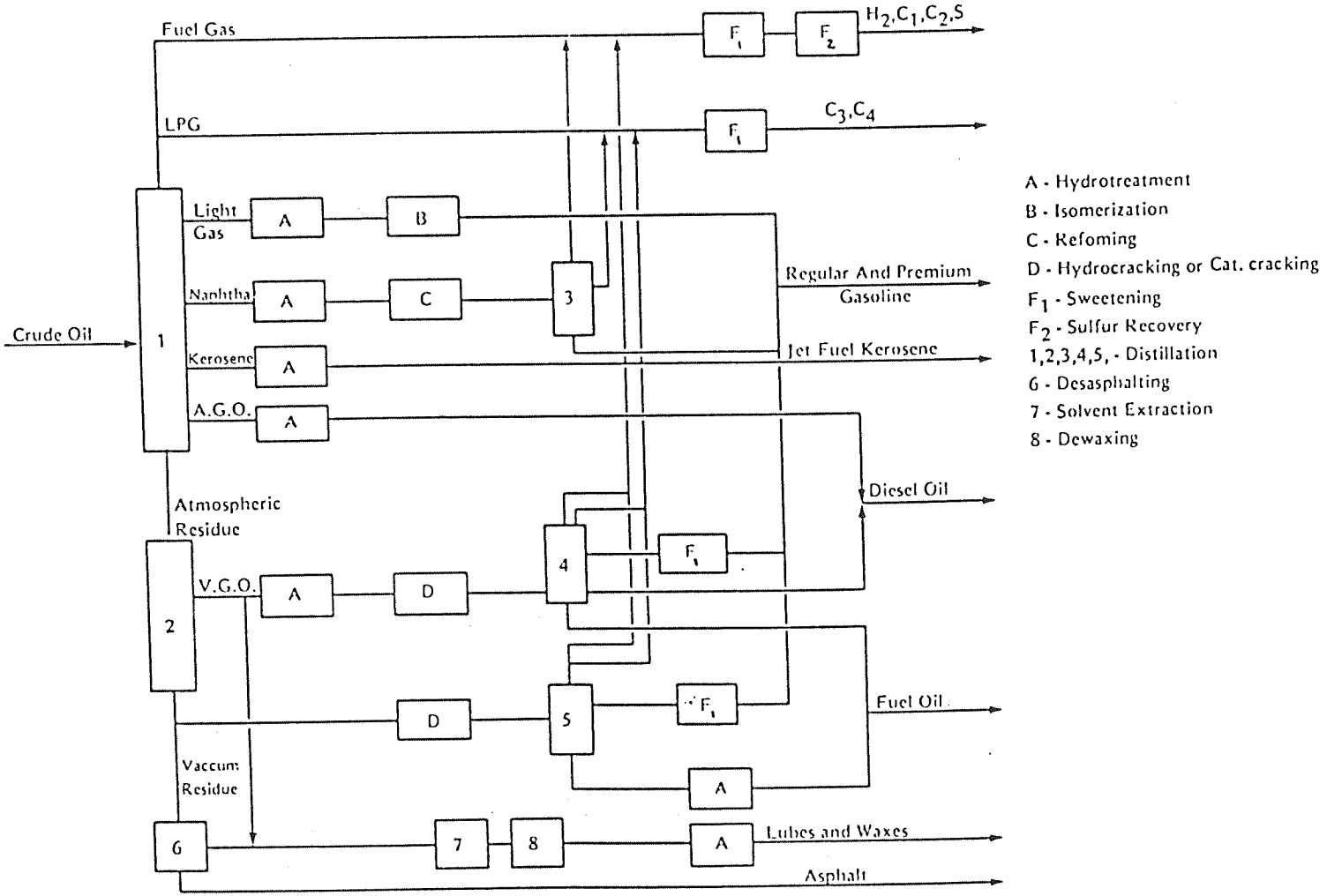

Figure 2.1. Catalytic Units in a Refinery Scheme

Heavy oils and residues which have low economic values are upgraded by conversion into lighter products such as transportation fuels (gasoline, kerosene, diesel, etc.) and petrochemical feedstocks. Catalytic processes such as hydrotreating, hydrocracking, catalytic cracking, etc. have been widely-used to remove undesirable elements such as S, N and metals (Ni and V) from the residues and to convert them into valuable lighter products. The catalysts used in various refinery processes are listed in Table 2.2.

Table 2.2. Catalysts Used in Various Refinery Processes

Process	Reason for Operation	Catalyst
Cat-reforming	To increase octane in gasoline	Pt on Al_2O_3 Pt-Re on Al_2O_3
Cat-cracking	To convert large petroleum molecules into smaller hydrocarbon mainly for high octane gasoline.	Silica alumina Zeolite
Hydrotreating	To remove S, N and metals and to produce valuable lighter products.	Co-Mo-Al_2O_3 Ni-Mo-Al_2O_3
Isomerization	To improve the quality and the quantity of gasoline	Friedel Craft $AlCl_3$, HCl Pt on alumina Silica or zeolite
Hydrocracking (hydroconversion)	To convert heavy oils and residues to transportation fuels.	Ni-Mo-Al_2O_3 Ni-W-Al_2O_3,SiO_2-Al_20_3 or Zeolite.

Catalyst Deactivation

Hydroprocessing of heavy residues to produce lighter, more valuable, products such as transportation fuels and petrochemical feedstocks, has achieved considerable importance in recent years (3,4,5). Hydroprocessing is a generic term which covers a variety of catalytic processes by which oil fractions are treated with hydrogen (2, 6). The most important processes are hydrodesulphurization (HDS), hydrodemetallation (HDM), hydrogenation (HG), hydrodenitrogenation (HDN) and hydrocracking (HC). The catalysts most commonly used in hydrotreating are derived from alumina-supported sulphides of cobalt-molybdenum or nickel-molybdenum. However these catalysts lose catalytic activity after a time as a result of several processes such as fouling from the deposition of

carbonaceous materials (coke) on the active sites of catalyst surfaces and deposits of heavy toxic metals from feedstock such as nickel (Ni) and vanadium (V) on the catalyst pellet (7). Sintering, phase transformation and poisoning are other causes of catalyst deactivation (8). The causes of deactivation obviously differ with duty, type and service conditions. The causes and basic mechanisms of various modes of catalyst deactivation are briefly reviewed in this section.

Fouling

Fouling involves physical deposition of species from the fluid or gas phase onto the catalyst surface resulting in blockage of reaction sites or pores. Deposition of coke or carbon on porous catalysts is considered as fouling. The coke covers the active surface, hinders the contact between the reactants and the catalytic sites and reduces the reaction rate.

Coke is a general term which describes carbonaceous deposits on catalysts. These can include high molecular weight polycyclic aromatics and carbons, which may be formed in the gas phase or on a surface. Coke deposition on catalysts is a complex process affected by several factors. The net accumulation of coke is usually a balance between coke formation, which occurs as a result of adsorption, dehydrogenation and polymerization of carbonaceous residues, and coke removal which occurs via gasification. The balance depends upon the operating conditions and the nature of the catalyst. Possible routes of carbon formation are shown in Figure 2.2. Coke accumulation can be minimized by adjusting reaction conditions, or mass and heat transfer effects and controlling the catalyst chemistry.

Deposition of metal sulphides on the catalyst pores during hydroprocessing of heavy residues is also an example of fouling. The heavy residues contain high concentrations of large-sized (M.Wt. 20,000 g/mole), organometallic compounds of (e.g., vanadium or nickel) present predominantly in the asphaltenes, which decompose by hydrodemetallation (HDM) reactions during hydroprocessing to give metal sulphides and hydrocarbons. Due to diffusion limitations, the metal sulphides tend to concentrate on the outer edges of the catalyst pellets and particularly in the pore mouths of the catalyst. Deposition of metal sulphides in large amounts at the pore mouth plugs the pores and physically restricts

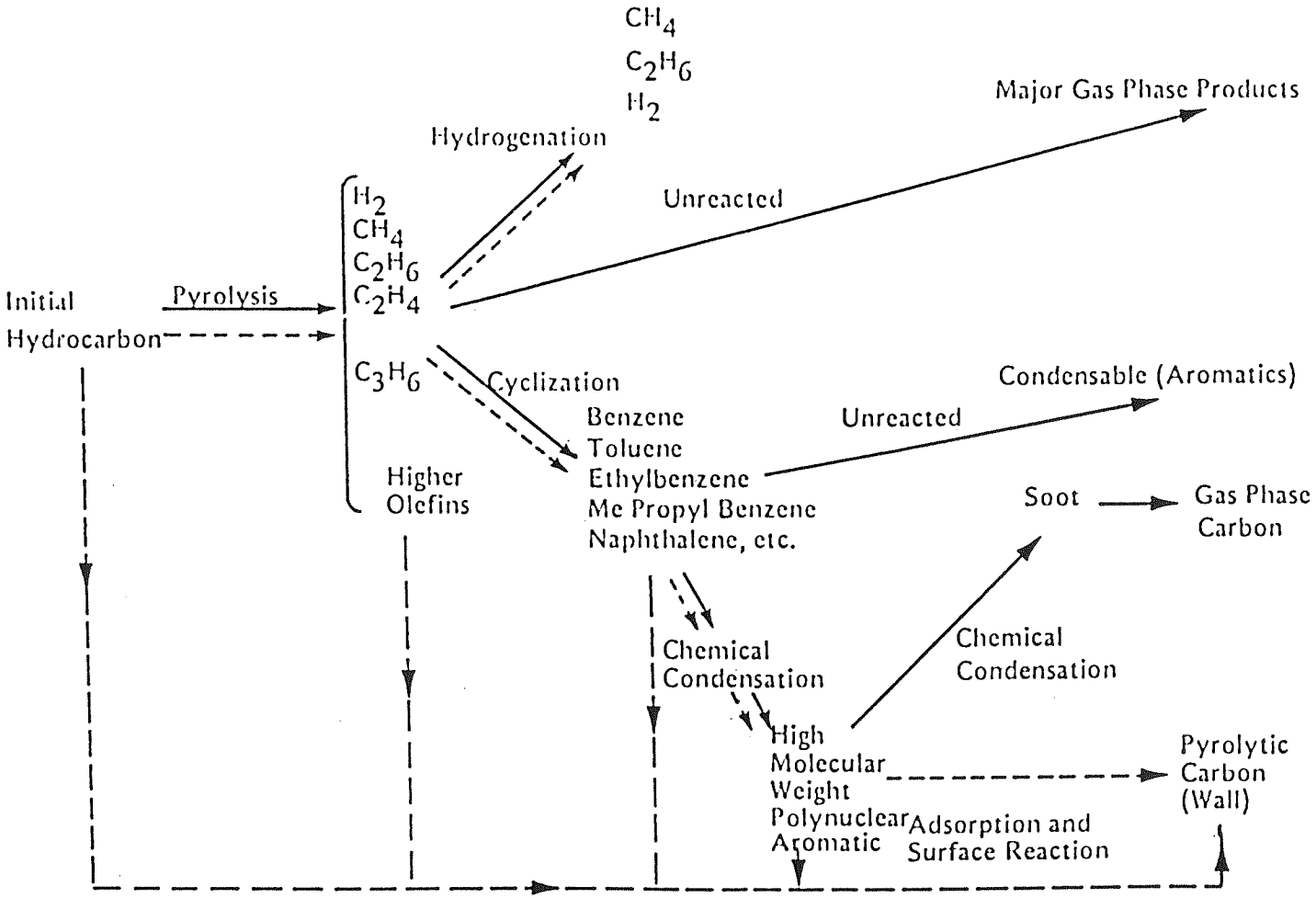

Figure 2.2. Possible Routes of Carbon Formation. ____ Gas Phase Reactions

------- Catalytic Reactions on the Wall _ _ _ _ _ Wall Reactions

access of the reactant molecules to the active sites on the catalyst surface within the pores. This leads to catalyst deactivation (9, 10). Extensive fouling by coke and metal deposition may also plug the reactor void space and result in a high pressure drop across the catalyst bed.

Poisoning

Catalyst poisoning is one of the most severe problems associated with their commercial application. It involves the strong chemisorption of reactants, products or impurities onto the active catalytic sites. A poison blocks the active sites as a result of very strong adsorption (9, 11). Catalyst poisons tend to be selective, i.e., a certain species may be a poison in some reactions but not in others, depending on its adsorption strength relative to that of other species which compete for catalytic sites. Some of the most severe poisoning encountered in catalytic systems is that induced by sulphur, nitrogen or metals on metal catalysts. Sulphur apparently bonds so strongly to metal surfaces that the presence of only ppm quantities of sulphur compounds in the feed is significant (12). Because of the essentially irreversible adsorption of sulphur compounds onto metal, regeneration is usually impossible. Sulphur compounds include H_2S, CS_2, MeSH, EtSH, Me_2S, Et_2S, thiophene, CoS, SO_2 and SO_3.

In general, catalyst poisons can be classified according to chemical species, the types of reaction poisoned, and the selectivity for active catalyst sites. For example, organic bases and ammonia are poisons for acidic oxides catalysts used in cracking and hydrocracking; sulphur and arsenic compounds are poisons for metals (e.g., Pt, Ni) in hydrogenation, dehydrogenation and steam reforming reactions (13a, 13b). A selective poisoning process is one that initially poisons the most active sites.

Sintering

Sintering is a major factor determining catalyst life, since it involves loss of surface area and porosity that can only be reversed with considerable difficulty, if at all. It arises because, in order to obtain maximum gas - solid contact, catalysts are usually prepared with high surface areas. Thus, there is always a thermodynamic driving force to minimize surface free energy, a force resisted only by an activation barrier. As the temperature increases this barrier is overcome and the catalyst sinters.

The mechanism of sintering can differ widely. As the temperature of the solid increases, atoms on the surface first become mobile (surface diffusion). This leads to the smoothing of very unstable surfaces and to the development of faceted or spherical particles, a process which may be enhanced by the gases present. Huttig (14) proposed that in theory surface diffusion - related sintering should become important at about one-third of the melting point of the solid, a prediction which has been borne out by some experimental measurements. However the influence of gases, or of trace impurities in the surface, can have a major effect on the temperature at which sintering starts (15, 16, 17).

At higher temperatures, i.e. > 600°C, volume diffusion of material starts to become important, and gross changes in the structure of the solid can occur. Eventually, and usually at very high temperatures, i.e. > 800°C, evaporation-condensation processes can also lead to gross sintering or to loss of solid.

Some success has been achieved in stabilizing materials against sintering by the addition of small amounts of a second component. For example in the case of alumina sintering can be enhanced, or inhibited, by the addition of small (< 3 wt%) amounts of appropriate additives (18). The addition of metal, necessarily present as the catalyst, retards sintering slightly in small amounts and enhances sintering in higher amounts. The addition of very small amounts (ca 0.1 wt %) of rare earth oxides (either Ce, Nd, Sm, Eu, Dy, Er, Y or Yb) was found to affect the temperature at which sintering occurred without deleterious effects on the catalytic activity. The mode of these stabilizing oxides, or of the metals, is often open to considerable question.

The sintering of metals on a support is a process of particular industrial importance, and considerable attention has been devoted to establishing empirical relationships and models which describe the process (19, 20). Two mechanisms have been advanced for metal sintering in supported metal catalysts.

- Crystallite migration: entire metal crystallites move over the support surface, collide and coalesce.
- Atomic migration: metal atoms detach from the crystallites, migrate over the surface and are captured by larger crystallites.

Crystallite migration is important in the early stages of sintering, when crystallites are small. Atomic migration becomes important and influences sintering at higher temperatures (i.e. > 800°C) in the later stages when the crystallites are larger.

Sintering of catalysts and supports is clearly very undesirable, since it is usually very difficult or impossible to reverse. As a result, there is considerable interest in the prevention of sintering. An obvious way to achieve this is to keep the temperature low, (less than 500°C) and particular care should be taken if the catalyst is to be regenerated by burning-off coke deposits.

Phase Transformations and Solid State Reactions

Migration of atoms in a crystal lattice can also result in changes of phase. Thus, in the case of alumina it is well-known that various crystal forms can exist, even though the alpha phase is thermodynamically most stable. As a result, as temperature is increased, phase changes occur, and Gitzern (18) has produced a very useful guide to the temperature stability of the various phases. That these phase changes result in a loss of surface area and porosity is evident from the dimensions of the unit cells of the crystal forms, (Table 2.3).

High temperatures can also cause interaction between the catalyst components and the support leading to the transformation of the active catalytic phase to non-catalytic ones (21). For example, in alumina-based steam reforming catalysts, reaction between nickel oxide and the alumina support can occur under reforming conditions resulting in the formation of nickel aluminate spinel (22).

$$NiO + Al_2O_3 \rightarrow Ni\,Al_2O_4$$

Table 2.3. Unit Cell Dimensions of Alumina Phases

Alumina Phase	Crystallinity	a(Å)	b(Å)	c(Å)
η	Cubic	7.90		
θ	Monoclinic	5.62	2.86	11.74
γ	Cubic	7.90		
δ	Tetragonal	7.96	7.96	11.74
α	Rhombohedral-hexagonal	5.13		

Nickel bound in nickel aluminate spinel does not contribute to catalyst activity; consequently, the activity of the catalyst declines. In alumina based cobalt-molybdenum or nickel-molybdenum hydrotreating catalysts the reaction between MoO_3 and Al_2O_3 can occur, resulting in the formation of a catalytically inactive aluminium molybdate phase.

Another thermal effect is the volatilization of the catalytic materials. In hydrotreating catalysts, loss of active molybdena phase has been observed on heating at temperatures above 700°C (23). Loss of catalytic metals is also possible through formation of compounds such as carbonyls, sulphides, halides, etc. in environments containing CO, H_2S, HCl or halogens.

The deactivation of catalysts used in the hydroprocessing of heavy residues due to fouling is reviewed in the following section.

2.1. Hydrotreating Catalyst Deactivation by Coke Deposition.

Catalysts used in the hydrotreating of petroleum distillates and residues can be deactivated by several mechanisms, namely, deposition of carbonaceous residues, accumulation of poisonous compounds and fouling by the deposition of metals such as vanadium, nickel and iron from the oil. In commercial operation, it is a common practice to increase the temperature gradually with time on-stream to compensate for loss of catalytic activity and to maintain a constant level of activity, e.g., HDS conversion. A typical temperature profile for catalytic hydroprocessing of residual oils is shown in Figure 2.3. which indicates three different stages of deactivation (7, 24, 25).

Although the extent of the three zones may differ widely depending on the process conditions, feedstock characteristics and catalyst properties, it is generally accepted that the deactivation is caused by coke and metal deposits. Coke is believed to be primarily responsible for the rapid deactivation of the catalyst during the early period of the process run which may extend for (11-12) months. As early as 1963, Beuther and Schmid (26) observed that half of the total carbon deposited on the residue hydrotreating catalyst in 16 days of operation, was deposited in the first 12 hours. This has been confirmed by several later studies (27,28,29). It is now widely accepted that coke lay-down on residue hydrotreating catalysts is most extensive during the very early stages of the operation (30).

This coking is accompanied by a large loss of surface area and fairly rapid deactivation. After this initial period, coking slows down to a nearly stable value and the

catalyst exhibits a pseudo-steady state level of activity for several months in spite of the relatively large amount of coke deposited during the early stages of the operation. The nearly stable value for coke on the catalyst is explained by a dynamic equilibrium between the hydrocracking (HC) rate and the hydrogenation (HG) rate on the catalyst surface. Metals (V and Ni) gradually accumulate on the catalyst throughout the run. Activity slowly decreases; the loss of activity during the operation may be offset by increase of temperature. Increased temperature can, however, lead to the deposition of more coke and metals. Catalyst deactivation occurs through diffusional resistance of reacting molecules in the heavy oils. Both coke deposition and metals accumulation contribute to diffusional resistance by blocking catalyst pores (7,31,32,33).

2.1.1. Nature of Coke.

The coke deposits which form on a catalyst surface during hydroprocessing of petroleum residues are complex mixtures of compounds containing carbon, hydrogen, nitrogen, sulphur and oxygen. (30,33,34). Available evidence indicates that the initial deposits consist of asphaltenes adsorbed on the most acidic sites of the catalyst. Studies of the adsorption of Boscan residues on Mo/Al_2O_3 and $Co\text{-}Mo/Al_2O_3$ catalysts at room temperature have shown preferential adsorption of asphaltenes (30). Similar results have also been observed for Kuwaiti and Safania asphaltenes (35). The nitrogen atoms buried deep in the asphaltene molecules are believed to be primarily responsible for the preferential adsorption of asphaltenes on hydrotreating catalysts. A significant increase in the nitrogen:carbon ratio in coke compared with that in the hydroprocessing feed has been reported by several researchers (30,34,36,37). Interaction between basic nitrogen-containing groups in the asphaltene molecule and the acidic sites on the catalyst during the early stages of hydroprocessing would certainly lead to preferential adsorption.

Recent studies have shown that asphaltene are not the only source of coke, and that not all the coke in the asphaltene rich feedstocks originates from the asphaltenes. Polynuclear aromatics, or even structures which are precursors to the formation of polynuclear aromatics, are potential sources for coke formation (29, 30). Wivel et al., (29) compared mono-di-, tri- and polynuclear aromatic fractions as coke precursors and noticed that the polynuclear aromatics contributed significantly to initial coke formation. This fraction also contained the most nitrogen.

The presence of two types of coke, one inactive and the other active, on heavy oil hydrotreating catalysts has been observed by some researchers (38,39). The inactive form of coke is the main contributor to catalyst deactivation. Two types of coke were also identified in the hydroprocessing of Venezuelan crude (39). One type contained predominantly asphaltenic material and a higher hydrogen:carbon ratio (1.0 to1.3) than the other (0.4 to 0.6). TPO studies of spent hydroprocessing catalysts have shown two peaks for SO_2 formation, one at about 250°C and the other between 400 and 450°C, (34,37,44).

The SO_2 formation profiles indicated the presence of two types of sulfur species in the spent catalyst. There is general agreement that the low temperature peak at about 250°C originates from the oxidation of metal sulfides (e.g. CoS and MoS_2).

The high temperature peak at around 450°C, has been attributed to the oxidation of organic sulfur in coke. This has been confirmed by thermal gravimetric analysis (TGA) and differential thermal analysis (DTA) techniques as well as by isothermal decoking studies at various temperatures between 100 and 600°C (45).

The chemical nature of the coke usually changes with time on-stream. It has been well established that the hydrogen:carbon ratio in the coke changes with increases in processing time (30,40,41), and solubility of the deposit decreases. The aromaticity of the coke deposits increases and the reactivity decreases with increased time on-stream. It has been suggested that the initial deposits dehydrogenate and polymerize (30,42,43), resulting in changes in the nature of the coke during the lifetime of the catalyst on-stream.

2.1.2. Mechanisms of Coke Formation.

The mechanisms of coke formation on catalysts during the hydroprocessing of heavy oils is not clearly understood. Several researchers have attempted to elucidate the coking mechanism through the characterization of coke on the used catalyst by means of nuclear magnetic resonance (NMR), x-ray photoelectron spectroscopy (XPS), Temperature Programme Oxidation (TPO), electron microscopy and other techniques. Use of various techniques has provided valuable information on the aromaticity, structure and reactivity of the coke.

Sanders et al., (46) isolated the carbonaceous deposits from spent HDS catalysts by acid treatment. Examination of the isolate by high resolution electron microscopy (HREM) revealed curved and buckled structures with occasional concentric circles. The morphology

of the carbonaceous material was comparable to heat-treated carbon although somewhat less well-developed. Recently, HREM analysis of coked iron sulfide catalysts used for hydroliquefaction of coal has shown the presence of two type of carbon deposits (47). A range of deposits from randomly-oriented coke structures to highly-ordered graphite layers has been reported in the HREM examination of coked catalysts (44).

The hydrogen:carbon ratio in coke is usually low, varying between 0.3 and 1.0. The bonding in coke is reported to be similar to that in aromatic compounds.

Coke formation may involve several different reaction pathways and several different chemicals. The process is obviously very complicated and studies of the system are rendered difficult by the fact that the end product may be essentially the same even when produced via different routes, (Figure 2.4). Beuther et al., (48)
classified coke deposits occuring on the sulfide catalyst during the HDS of petroleum residue into three groups.

- Aromatics that adsorb reversibly on surface sites at low temperatures; once adsorbed, these may polymerize;
- Asphaltenes that adsorb reversibly on surface sites;
- Aromatic concentrates that condense into clusters and then crystallize. This crystalline mesophase is formed after a long time at high temperatures (at about 400°C). This coke causes severe deactivation of catalysts.

Several reviews have highlighted the complex structure of the three main types of carbon deposits: polymeric, filamentous and graphitic (24,49,50). Different mechanisms have been proposed to explain the formation of these various types (49, 30). Absi-Halabi et al., (30) suggested that the mechanism of coke formation during the hydroprocessing of heavy oils may involve the reaction pathways shown in schemes 1, 2 and 3 (Fig. 2.5).

Absi-Halabi et al., (30) used examples from recent studies to suggest that asphaltenes were the major source of coke in residual oil hydroprocessing. In a study by Cotte and Calderon (51) using TGA and mass spectroscopy (MS) on Boscan asphaltenes, three stages of pyrolysis were identified. In the first, at temperatures up to 300°C, no chemical change was observed. The second stage, at temperatures between 300 and 425°C, was characterized by partial depolymerisation of asphaltenes, cracking, deoxygenation and

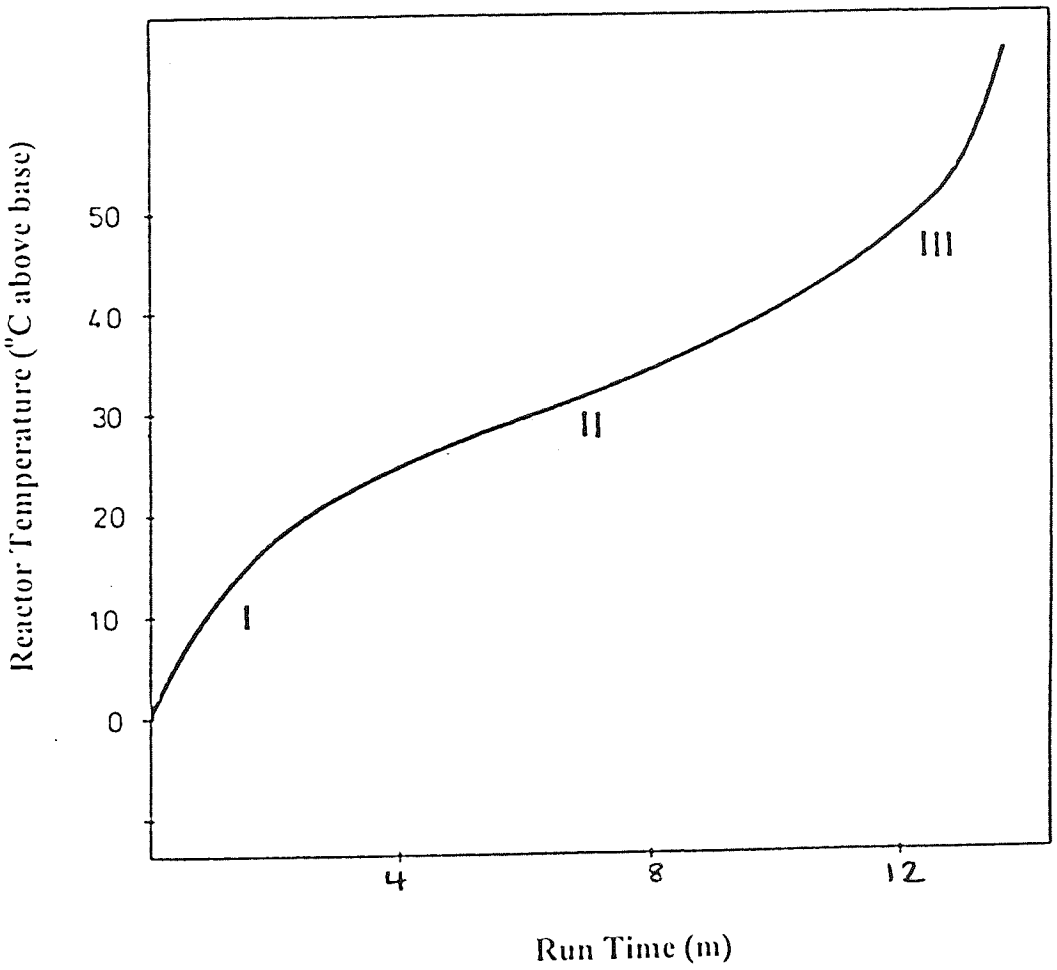

i. An initial period with a very rapid rate of deactivation.

ii. An intermediate period with a slower, almost constant deactivation rate

iii. A final period with a rapidly increasing deactivation rate

Fig. 2.3. Catalyst Deactivation Behaviour in Residual Oil Hydrotreating.

desulphurisation. The products included hydrogen sulphide, carbon monoxide, light hydrocarbons and resins. The authors attributed their observations mainly to depolymerisation into resins, while the slate of products indicates that cracking of side chains is one dominant reaction at this stage. In the third stage, at temperatures between 425 and 550°C, cracking appears to be dominant in the formation of coke and light products.

Speight (42) investigated the thermal pyrolysis of asphaltenes as part of a study of the initial reactions in the coking of residua. Thermal decomposition increased markedly in the temperature range from 350 to 400°C, as evidenced by a significant increase in benzene-insoluble products and in gas production. This finding is in agreement with the suggestion that the molecules dealkylate and form an aromatic, condensed coke. Significant decreases in the nitrogen:carbon ratio in the benzene-insoluble product were observed and these were suggested to have arisen from the incorporation of some low-nitrogen species into the coke rather than from nitrogen elimination. This suggestion was particularly relevant to coking in that Speight suggested, in agreement with earlier findings by Fitzer et al (52), that the presence of nitrogen accelerated coke formation.

Similar effects have been reported for the catalytic hydroprocessing of heavy residue (53). Asphaltene conversion increased significantly at temperatures above 430°C; the toluene-insoluble materials also started to become significant at that temperature. The sulphur:carbon and the vanadium:carbon ratios decreased steadily as the temperature increased (Figure 2.6), but no such trends were noted for nickel or nitrogen in the asphaltene. Sulphur and vanadium appear to be distributed through out asphaltene molecules, and thus, are removed as the severity of hydroprocessing increases. Conversely nickel and nitrogen, appear to be concentrated in the asphaltenes fractions that are more resistant to attack; hence, removal is more effective at temperatures greater than 430°C.

The average molecular weight of the asphaltenes was found to decrease steadily with time over the whole temperature range (Figure 2.7). (53). However, the hydrogen:carbon ratio first increased and then decreased with temperature. The separation of some individual groups coupled to HG seems to occur in the temperature range 380°C to 410°C. Above 410°C, scission of side chains from the asphaltenes becomes important leaving large aromatic structures which are deposited as toluene-insoluble materials. The hydrogen:carbon ratio drops and the molecular weight loss reflects depolymerisation with more loss of side chains and the deposition of (unmeasured) coke. These highly aromatic, more refractory, nitrogen-rich species may be the coke precursors.

These studies clearly demonstrate that asphaltenic oils have a higher propensity to form coke at high processing temperatures. However, asphaltenes are not the only source of coke. The overall mechanism is probably complex. Coke may form when the reaction intermediates, such as unstable radicals produced by thermal cracking, are reconstituted into large polymers. Various types of microscopically observable coke are often accompanied by the appearance of anisotropic mesophase spheres that grow through coalescence and ultimately form coke. The nucleation of mesophase spheres has been attributed to the condensation and polymerization of medium-sized molecules in the isotropic phase as well as to selective transfer of such molecules to mesophase. Condensed-ring polyaromatic hydrocarbons were identified as nucleation agents (54). Beuther et al., (48) used hot-stage microscopy to observe the formation of coke during the hydroprocessing of residual oil over Co Mo/Al_2 O_3 catalyst. The actual coking process was found to be preceded by an ordering and stacking of aromatic molecules (48).

2.2. Hydrotreating Catalyst Deactivation by Metal Deposition

Unlike coke deposition, the rate of metals deposition is nearly constant with time. Oxenreiter et al. (55) reported the amount of deposited vanadium to be as high as 56% and nickel to be up to 17% wt. Several investigators (55-58) studied metal deposition on the catalyst with a scanning electron X-ray microprobe analyzer. All found that vanadium deposits in the thin outer shell of the catalyst, whereas nickel tends to be more uniformly distributed across the diameter of the catalyst. From a study applying microprobe analysis in combination with pore diffusion theory, Takayama et al. (58) concluded that the effective diffusivity for vanadium is less than 10% of that for nickel. However, Todo et al. (59) reported that the maximum deposition of both vanadium and nickel occurred near the outer edge and the concentration profiles were U-shaped for both metals.

These findings suggest that hydro-demetallation (HDM) reactions are diffusion-controlled and are themselves active sites for the HDM reaction. High metal concentration at the edge of the catalyst pellet slowly blocks the pores and renders the interior of the catalyst inaccessible to the reactants. It has been proposed that pore mouth plugging is the major cause in limiting the total catalyst life in residue hydroprocessing (28, 60,61).

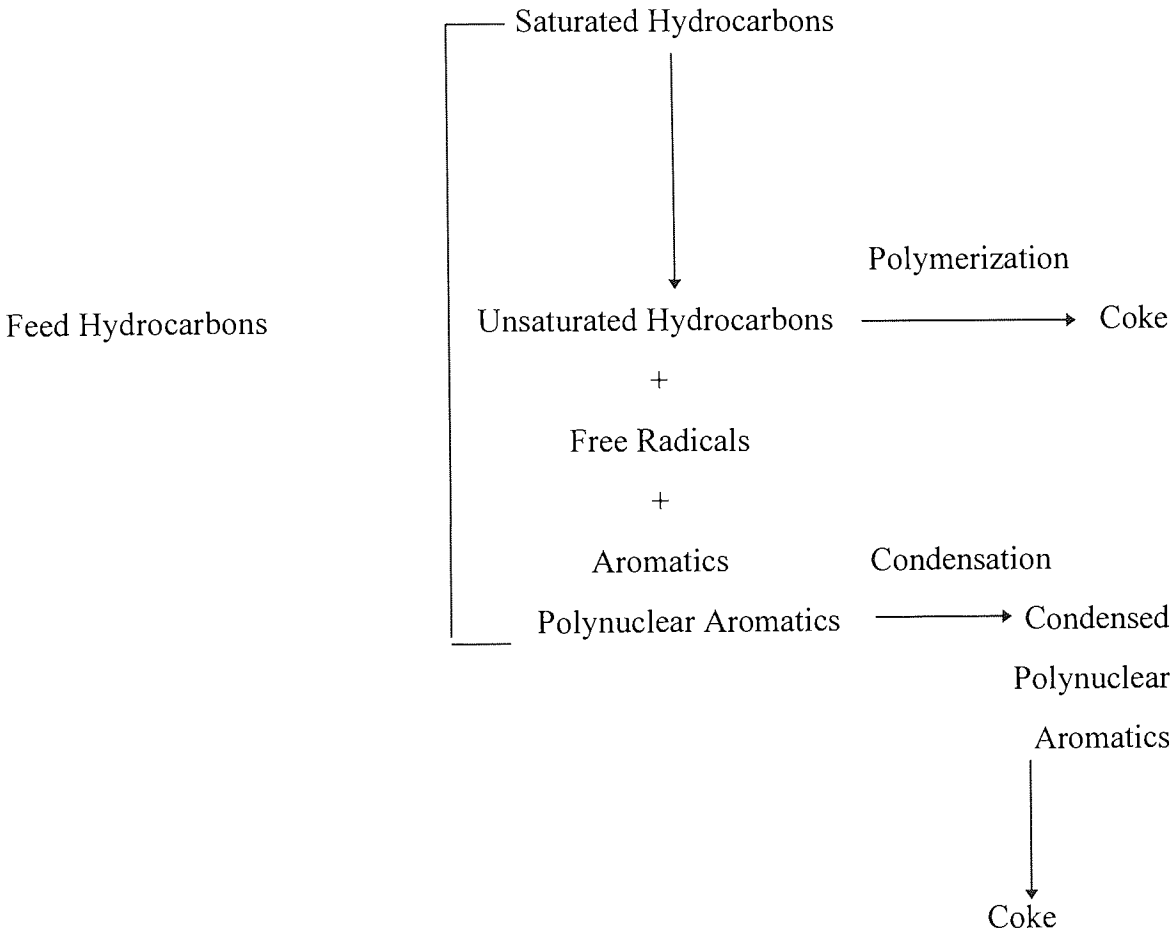

Figure 2.4. General Routes for Coke Formation

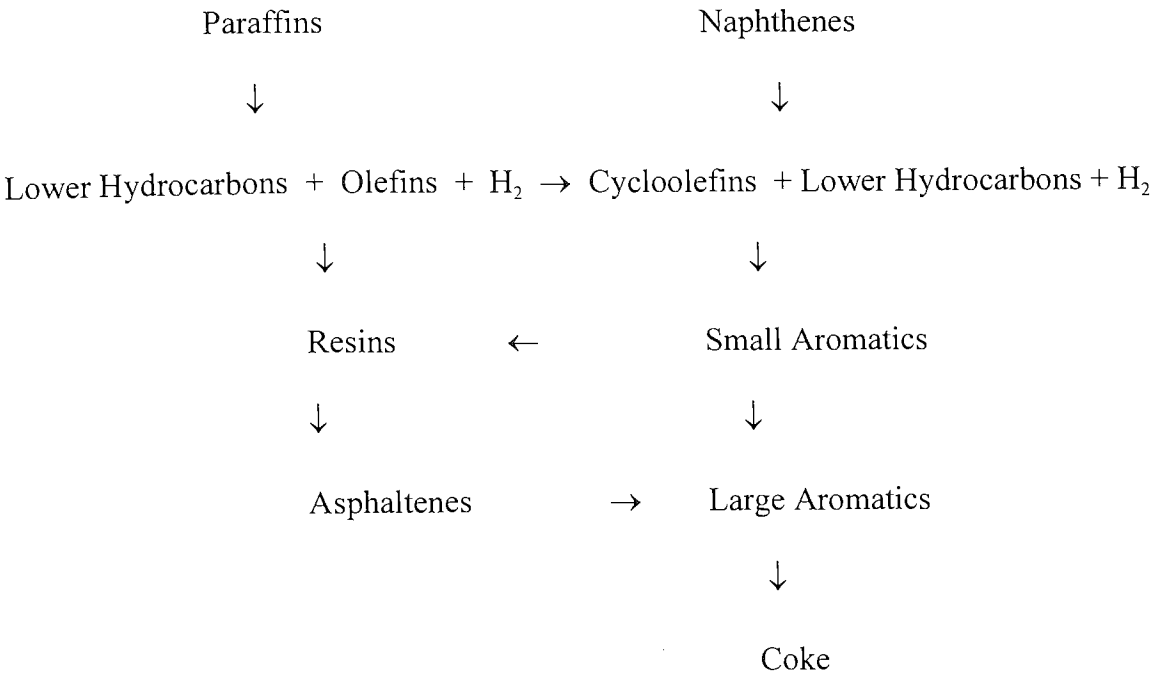

Scheme 1

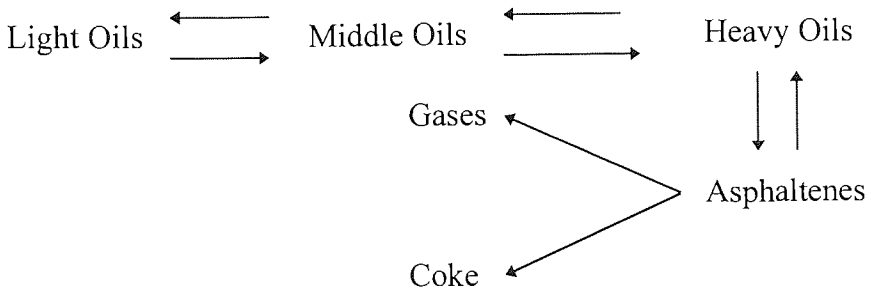

Scheme 2

Figure 2.5. Reaction Pathways for Coke Formation.

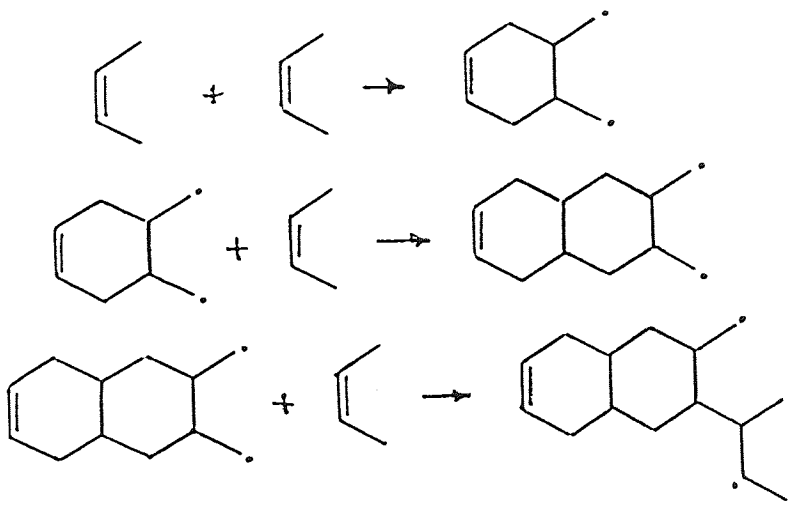

Scheme 3

Figure 2.5. Reaction Pathways for Coke Formation.

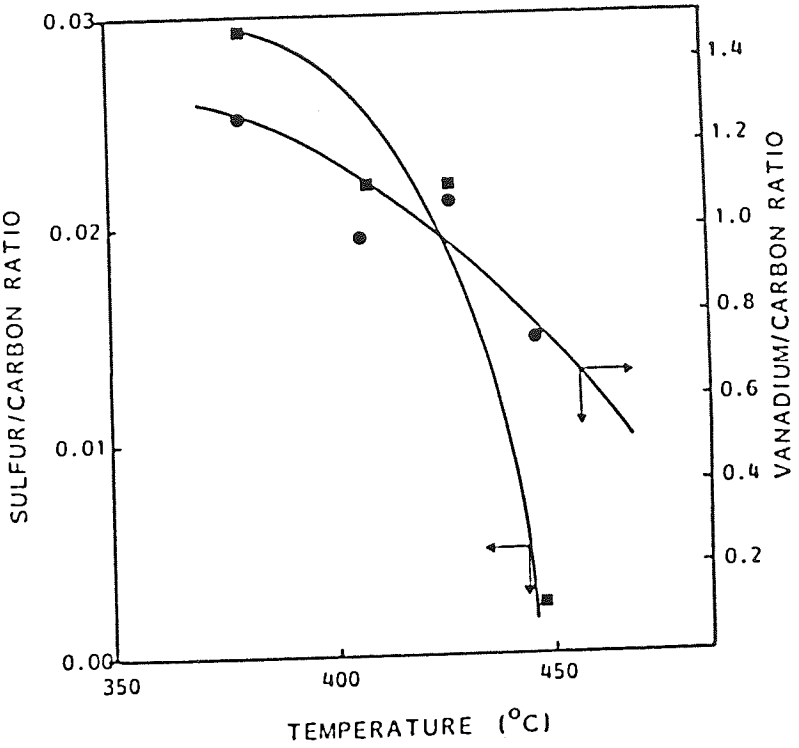

Figure 2.6. Sulphur/Carbon and Vanadium/Carbon Ratios of Asphaltenes from Products at Different Temperature.

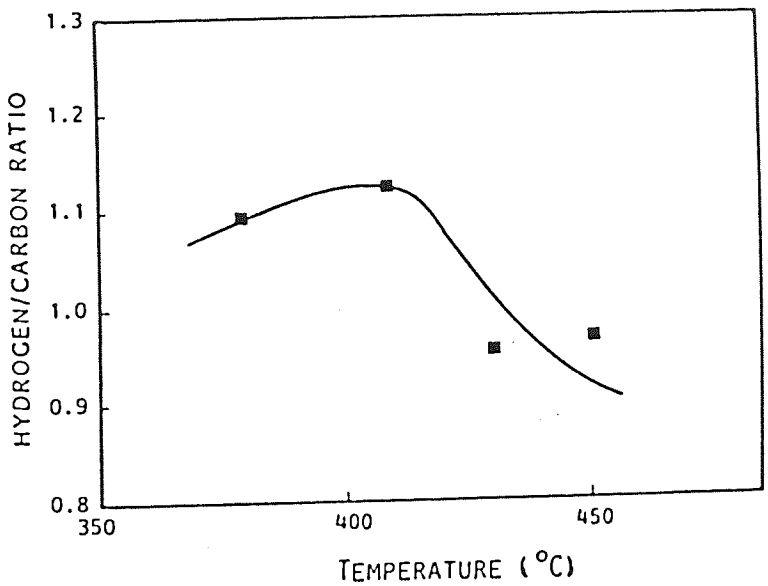

Figure 2.7. Hydrogen/Carbon (H/C) Ratio of Asphaltenes from Product at Different Temperatures.

Although pore blockage by metal deposits is a major reason for discarding used residue hydrotreating catalysts, Bogdanor and Rase (62) demonstrated that decline in activity can result from molybdenum and nickel migration and an apparent molybdenum agglomeration that occurs under operating and regeneration conditions. The rate and extent of deposition of coke and metals on the hydroprocessing catalyst are governed to a large extent by various parameters such as feedstock characteristics, catalyst characteristics and operating conditions. It is therefore important to understand the relation between these parameters and catalyst deactivation by fouling. Catalyst fouling by metal deposition has been studied extensively and the subject has been reviewed by Quan et al (33). Factors influencing catalyst deactivation by fouling are discussed in detail in the following section with particular reference to coke formation.

2.3. Factors that Influence Catalyst Deactivation by Fouling in Residue Hydrotreating

The rate of deactivation of a residue hydrotreating catalyst is influenced by a number of factors which include:

* Feed properties
* Catalyst properties
* Operating conditions
* Reactor or process technology

Feedstock Effects

Feedstock quality has a significant impact on the rate of catalyst deactivation in residue hydroprocessing (24,25,27). It is widely accepted that the presence of high concentrations of asphaltenes, carbon residues and metals in the heavy residues cause serious catalyst deactivation problems (30,49). The amounts of carbon residues, asphaltenes, organometallic impurities and other contaminants (e.g., S and N) can vary widely depending on the source of the residual oil feed as shown in Table 2.4. (24,63,66).

Residues with the lowest metal content, asphaltene content and the Conradson carbon residue usually give the longest cycle length or catalyst life (64,65), because the

rates of both coke and metals deposition on the catalyst are relatively lower with such feedstocks. Feed pretreatment by deasphalting and demetallization has been found to improve catalyst life substantially (65, 66).

Beuther and Schmid (26) showed that coke formation can be alleviated to some extent by deasphalting the residues. Other investigators have reported remarkable improvements in catalyst life by feed pretreatment (65,66). Silbernagel and Riley (67) performed deactivation tests on three feeds: a high metal content Venezuelan whole crude, its deasphalted oil and the hydrogen fluoride treated, demetallized version of the same crude. The HDS activity was higher for deasphalted oil (DAO) than for the other two feeds, while the deactivation rate was slower for the demetallized HF-treated feed. Recently, Wivel and co-workers (29) studied coke formation on hydrotreating catalysts using various feeds with different distributions of aromatic fractions and found that only the amount of polynuclear aromatic hydrocarbons (PNA) fraction in the feed correlated well with the coke formation (Figure 2.8). Nitrogen-containing compounds also strongly adsorbed onto the surface of the catalyst and contributed to coke formation.

Studies (68) on the comparison of hydrotreating catalysts deactivated by coke deposition with different feeds such as VGO and anthracene revealed that the coke in the VGO-coked catalysts resulted in lower pore volumes and appreciable pore plugging than the anthracene coked catalyst (Figure 2.9).

In another study, Furimsky et al. (71) used three different feedstocks with widely varying properties to examine the effect of feedstock on coke formation during catalytic hydroprocessing. The results are shown in Table 2.5.

The larger amount of coke after hydroprocessing of the naphtha compared with that for heavy gas oil, in spite of the markedly lower average molecular weight, may be attributed to the higher aromaticity of the former. The contribution of N-containing species to coke formation is evident from the significantly increased N/C ratio in the coke compared with that in these two feeds. It appears that for bitumen, most of the coke originated from a physical interaction of large asphaltene molecules with the catalyst surface. Thus, the increase in the N/C ratio from feed to coke was much less pronounced. The difference in N/C and S/C ratios as between feeds and benzene extracts may indicate a relative contribution of N- and S-containing species to coke formation. It is evident, that for heavy gas oil and bitumen, S-containing compounds make a significant contribution to coke formation.

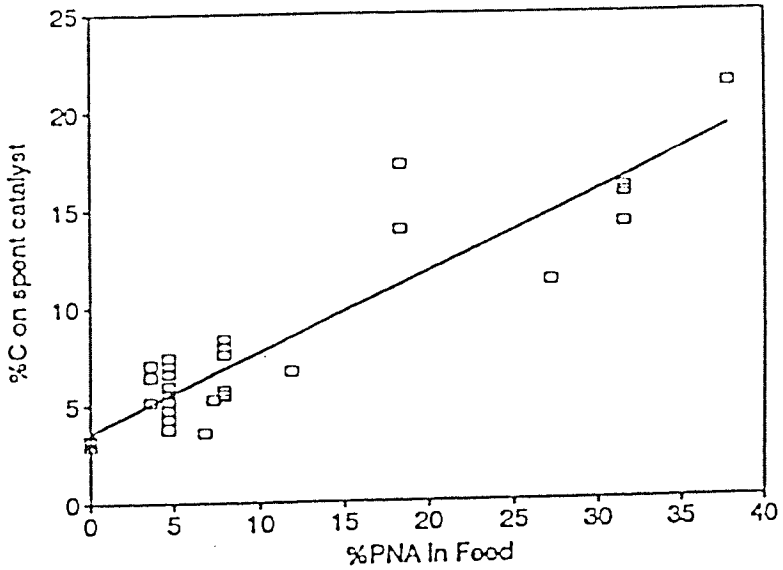

Figure 2.8. Amount of coke vs. % PNA in feed (Different conditions and feeds).

Table. 2.4. Typical Properties of Petroleum Resids

	Arabian Gulf Crudes			North Sea Brent	W-Africa Nigeria	Venezuala Lago-medio	China Taching	USA West Taxas	Russia Export	Mexican Maya
	Kuwait	Arab. Berry	Eocene							
Crude API	31	38	18.6	38	37	31.5	21	39	32.5	22
Atm. Resid (Vol %)	45	39	65	39	27	49	76	35	54	56
API°	16.5	21	10	22	22	18.1	18	22	17	7.7
S (%)	3.8	2.1	4.9	0.8	0.4	2.0	0.2	0.6	2.6	5.0
V/Ni ppm	60/20	3/2	80/40	6/2	2/10	180/60	1/16	10/6	75/25	500/90
Conradson Carbon (%)	12	4.2	14.8	4	2.5	9	8	4.7	8	18
Pour Pt (°F)	70	70	60	100	--	--	86	83	--	115

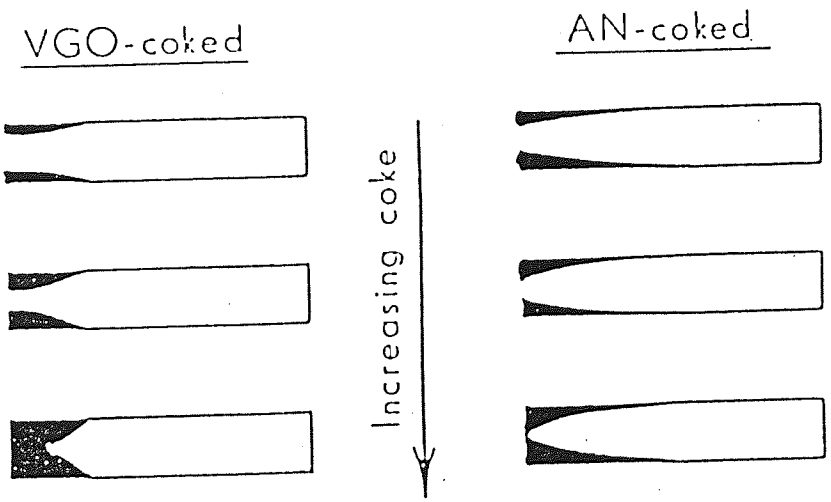

Figure 2.9. Idealized Model of Coked Pores with VGO and Anthracene.

Effect of Operating Conditions

Temperature. Increase in temperature usually leads to an increase in coke formation and metal deposition rates and thus to an increase in the deactivation rate. During hydroprocessing of residual oils a large amount (17 wt%) of carbon deposition occurred even at low temperatures e.g., 380°C. The amount of coke on catalyst increased to 22% when the reactor temperature increased above 430°C (Figure 2.10). In industrial hydrotreating operations the reactor temperature is gradually increased with time on stream, from 370°C to 410°C, to compensate for loss of catalyst activity. Bartholdy and Cooper (31) observed that more coke builds up and deactivation by coke occurs each time the operating temperature is increased to compensate for loss of activity during the process. In high severity residue hydroprocessing operations, deactivation due to coke build-up is more severe. Pazoz et al., (72) and Tamm et al. (7), found higher metal build-up near the catalyst edge with increasing temperature.

As mentioned earlier, the metal build-up at the catalyst edge or external surface is detrimental to catalyst life as it will progressively block the diffusion of the reactant molecules into the interior of the catalyst. Metal-controlled deactivation occurs at low severity operation.

Hydrogen Pressure. An increase in hydrogen pressure within the range 5-12 x $10^6 N/m^2$ has been found to decrease the coke content of the catalyst but to increase metal deposition at the exterior surface of the catalyst pellet (7,25,31,72) as shown in (Figure 2.11). Thus, an increase in hydrogen partial pressure has a favourable effect if the catalyst deactivation is caused by coke formation demonstrated by Kriz et al., (73, 74), but results in shorter catalyst life if metal deposition is the primary cause of catalyst ageing (24,33). The beneficial effect of hydrogen pressure on reducing coke deposition has been attributed to an increase in hydrogenation activity that is kinetically favoured at higher pressure. This enhanced activity reduces the coke formation on the catalyst by removal of olefinic coke precursors by hydrogenation.

Space Velocity (LHSV)

The liquid hourly space velocity (LHSV) has been found to have a significant effect on catalyst deactivation by the deposition of coke and metals. In residual oil hydroprocessing an increase in the LHSV (>1 h^{-1}) decreases coke deposition, but increases metals

Table 2.5. Chemical Composition of Feedstocks, Benzene Extract and Coke from Hydroprocessing of three Different Feedstocks.

	Coal Derived Naphtha	Heavy Gas Oil	Bitumen
Feedstocks			
Av. mol. weight	140.0	350.0	800.0
Carbon total (wt%)	85.3	84.5	83.0
^{13}C NMR (wt%) arom. + olef.	52.7	27.4	30.6
H/C	1.35	1.47	1.52
N/C	0.005	0.004	0.004
S/C	--	0.016	0.021
Benzene Extract			
H/C	1.06	1.09	1.09
N/C	0.023	0.017	0.008
S/C	--	0.019	0.022
Coke			
Carbon (wt%)	7.0	4.6	13.9
Nitrogen (wt%)	0.40	0.48	0.29
N/C	0.050	0.091	0.018

deposition (Figure. 2.12.). Thus whilst the rate of coke-controlled deactivation is low at higher space velocities, the metal-controlled deactivation is high (75a&75b). A decrease in LHSV usually increases catalyst efficiency and life in residual hydrotreating processes.

Impact of ReactorType on Catalyst Fouling

Fixed bed and ebullating bed reactor technologies are commonly employed for hydroprocessing heavy residues.

Figures 2.13. and Figure 2.14. show schematic diagrams of fixed bed and ebullating bed reactors, respectively. In the fixed bed process, preheated feed and hydrogen pass first over a guard bed and then over a series of reactors packed with catalysts (76). In the ebullating bed process (6), preheated feed and hydrogen enter the bottom of the reactor. The catalyst bed is maintained in an ebullated (expanded) state by an upward flow of feed and the internal liquid recycle. In order to maintain a steady state activity, provision is

made for periodic catalyst addition and withdrawal. The deactivation behaviour of catalysts in both types of units is discussed below based on the information obtained from the analysis of spent catalysts.

Rapid coke build-up was observed during the initial period of operation (7,27,77) in both types of reactors.

Carbon content of the catalyst in fixed bed reactors was found to increase from the entrance (Guard Reactor) to the exit (last reactor) (Figure 2.15). These indicated that in fixed bed units, the coke content of a catalyst pellet depends upon its location; deposition of both vanadium and nickel occured near the inlet of the reactor and decreased towards the reactor outlet. Analysis of carbon content in spent catalyst (78) from a 4-reactor fixed bed Atmospheric Residue Hydrodesulphurization (ARDS) showed the lowest amount of carbon deposits in the first and the highest contents in the last reactor. In the ebullating bed reactor, since the catalyst particles are in continuous motion, the coke content of the catalyst does not depend upon its location (27). The coke content of a catalyst pellet was found to increase very slightly with increasing catalyst residence time in the reactor (77). In the ebullated bed reactor metal deposits on the catalysts were also independent of its location. Several workers (7,79,81) observed that at the entrance of the bed, the maximum metal deposition occurs inside the catalyst so that the metal deposition profiles resemble an M-shape. Tamm et al. (7) and Jacobson et al. attributed this to the diffusion controlled reaction of metal species with hydrogen sulphide inside the catalyst extrudate. At the exit section of the bed, the maximum moved to the external surface and the metal deposition profiles were U-shaped.

Effect of Catalyst Properties

Pore Size Effect

Catalyst deactivation in residue hydroprocessing is believed to be caused primarily by pore blocking which decreases diffusional accessibility (7,27,68 and 81). Several researchers have studied the effect of catalyst pore blockage on catalyst deactivation and suggested that the deactivation rate would be slower, and the life of the catalyst longer, if the proportion of large pores in the catalyst is increased. Macroporous catalyst can accommodate more coke and metals prior to total pore blockage (9,32,33).

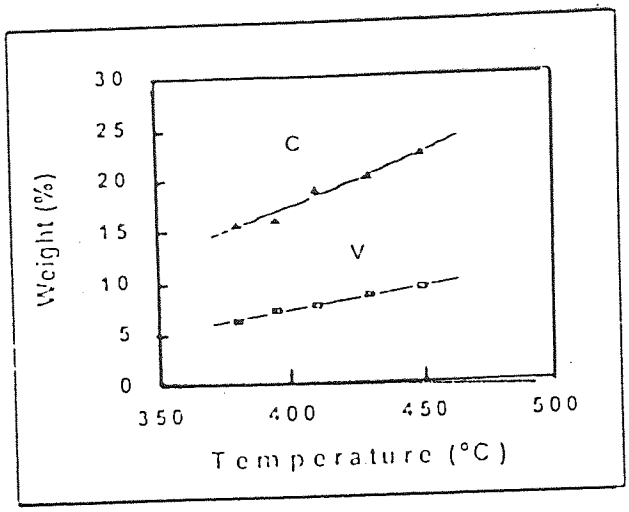

Figure 2.10. Effect of Operating Temperature on Coke and Metal Deposition.

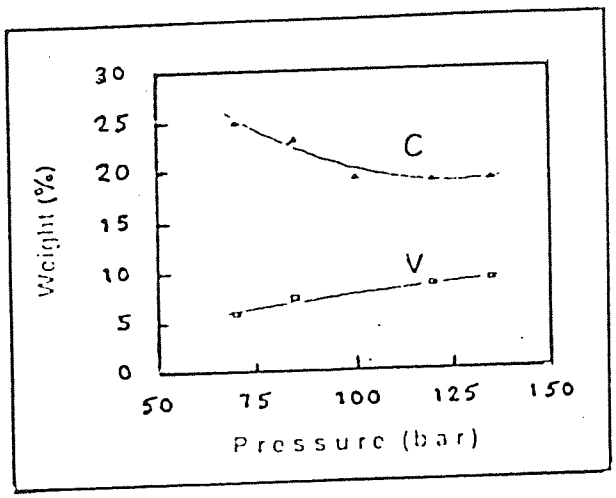

Figure 2.11. Effect of Hydrogen Pressure on Coke and Metal Deposition.
C= Carbon, V = Vanadium

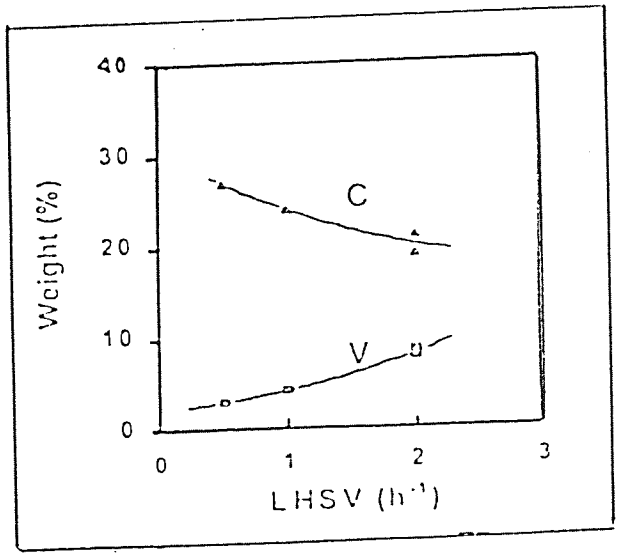

Figure 2.12. Effect of LHSV on Coke and Metal Deposition.

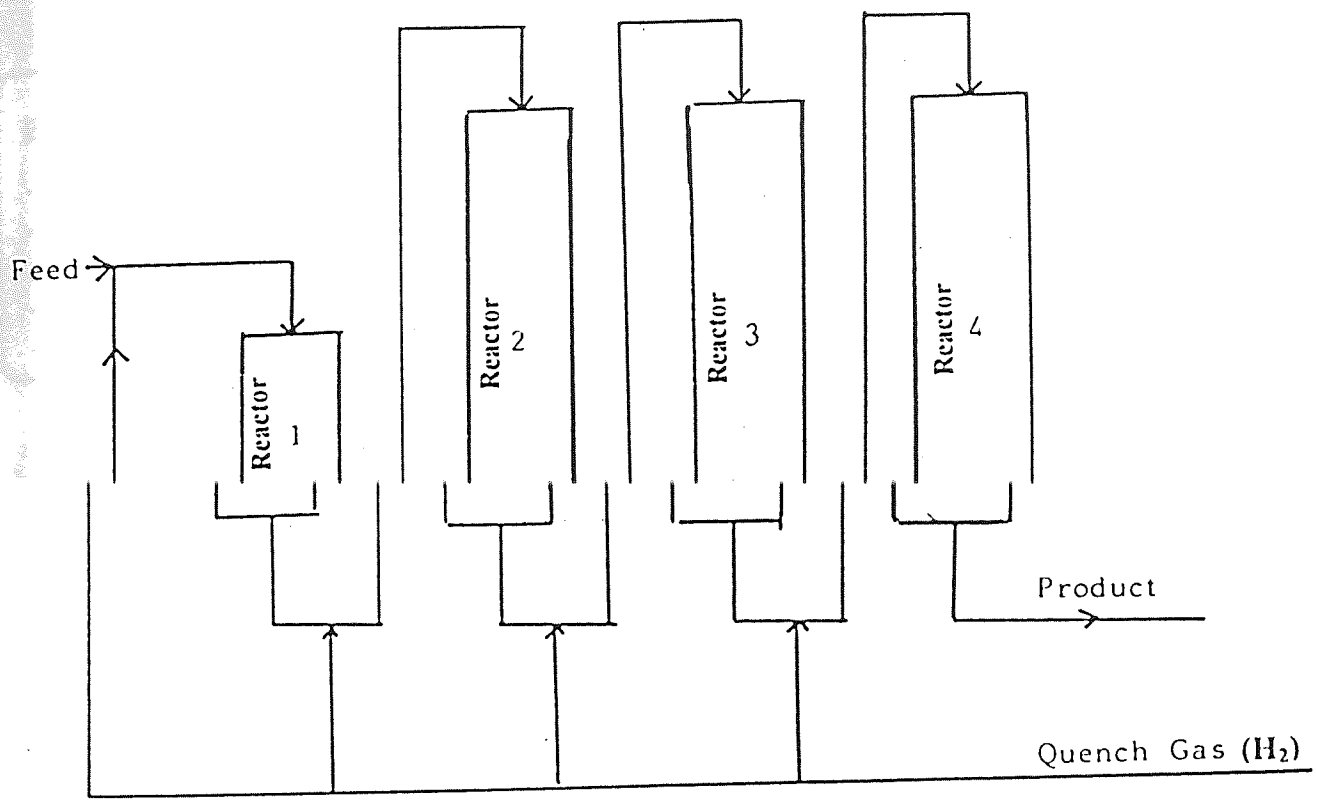

Figure. 2.13. Multiple Reactor Fixed Bed Hydrotreating Reactor.

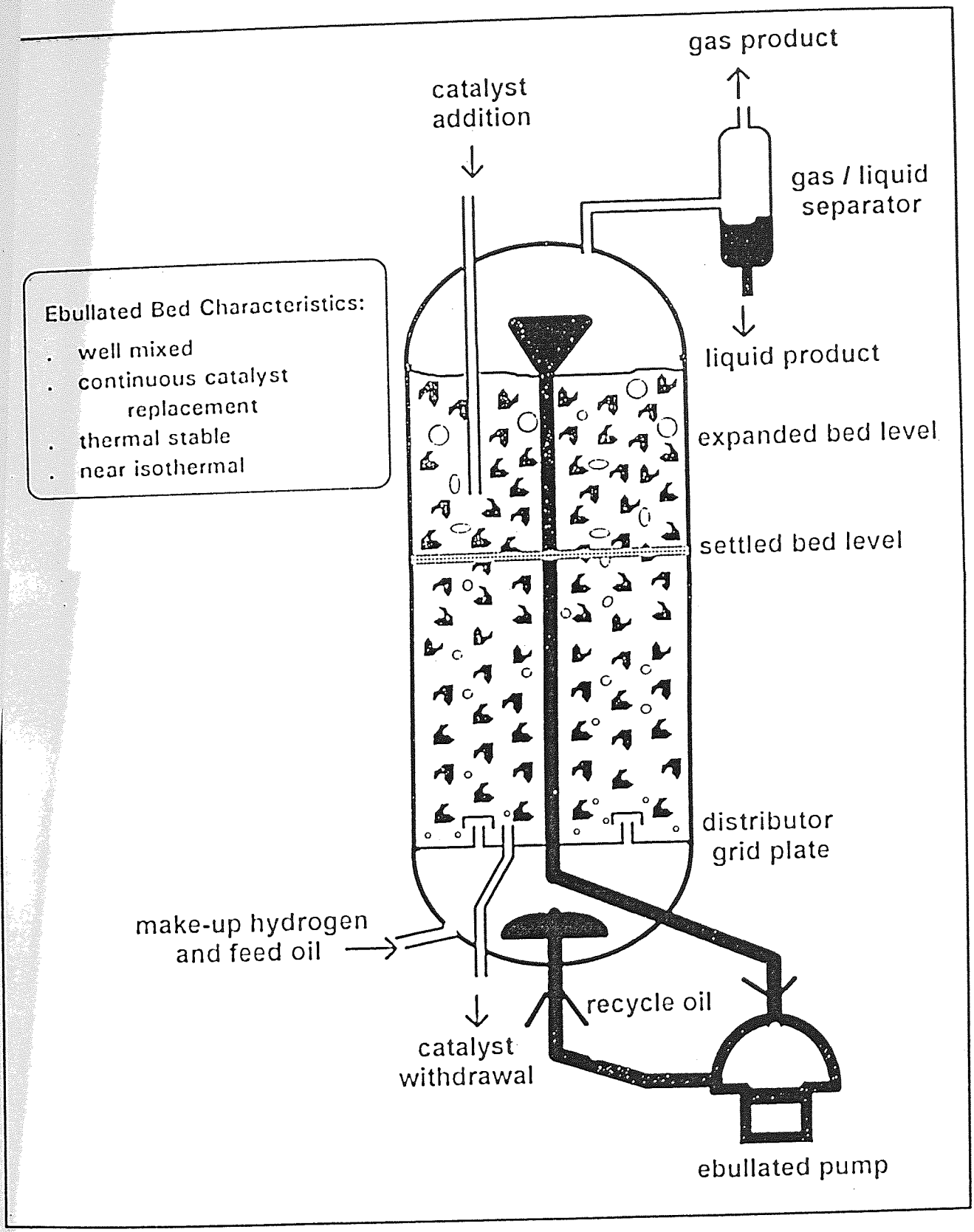

Figure 2.14. Ebullated Bed Reactor. Reactants Flow Diagram.

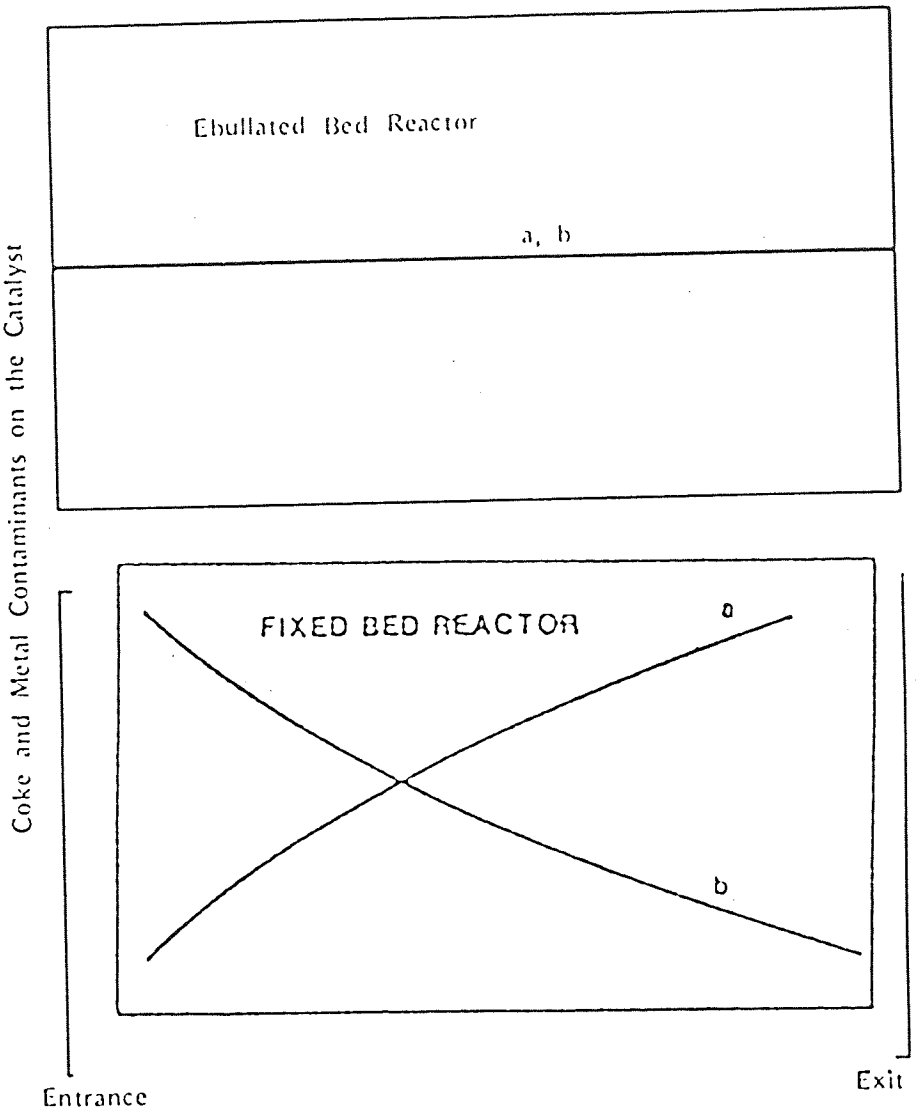

Figure 2.15. Coke and Metal Deposition Profiles on Catalysts Fixed Bed and Ebullated Bed Reactors (a: coke, b: metal)

Nalitham et al., (82) compared the performance of catalysts with unimodal and bimodal pore size distributions in a two stage coal liquefaction process. The required catalyst replacement rate for the bimodal catalyst was found to be only 1/4th the rate for the unimodal catalyst, thus indicating the potential advantage for the catalyst with a bimodal pore size distribution.

Similar improvements in performance with macroporous catalysts were also noticed by Rhee et al., (83). In that study the advantage of the macroporous catalysts was considered to derive primarily from the minimization of hindered diffusion effects. In a related study Wang and Guin., (84) investigated the effects of catalyst pore size distribution on deactivation rates under conditions of very rapid coke build-up using a model feed. The results of their studies revealed that macroporous catalysts accumulated higher coke loadings. However, in spite of their greater coke accumulations, the macroporous catalysts exhibited lower rates of activity decline and were able to retain their activity for a longer time period as compared to microporous catalysts.

Recently, Absi-Halabi and Stanislaus (85) examined the relationship between catalyst pore size and coke formation during the hydroprocessing of Kuwait vacuum residues and found that the amount of coke deposited on the catalyst increased as the percentage of pores larger than 250Å decreased. These data suggest that large molecules with a high coke-forming tendency, such as asphaltenes and polynuclear aromatics, spend more time within the narrow pores of the catalysts due to slow diffusion. This may lead to further reaction and condensation, polymerization and the formation of coke. Another interesting observation was the low coke formation for a unimodal pore catalyst having pore maximum in the 100-250Å diameter range. It is suggested that this range of pore size is large enough for the free diffusion of a large proportion of low molecular size asphaltenes and other heteroatom containing species. The surface area of such catalysts containing predominantly medium size mesopores are usually higher than the macropore catalysts and this in turn can be responsible for higher hydrogenation activity. The coke precursors such as olefins, carbonium ions, free radicals, and resin type polynuclear aromatics may be hydrogenated rapidly resulting in reduced coke formation.

Tamm et al. (7) have shown that concentrations of vanadium near the external surface are significantly higher for a small pore diameter catalyst (80 Å) than for a large pore catalyst, (1000 Å), indicating a poor metal distribution and increased diffusional limitations for the former (Figure 2.16). Improved metal distribution through the pellet

and longer catalyst life have been observed for large pore diameter catalysts by Jacobson et al. (60) and Plumail et al. (86a) and Stanislaus et al (86b). Bimodal catalysts were found to accommodate more metals than unimodal catalysts and for microporous catalysts (10-20 nm diameter range), vanadium was deposited only at the periphery of the particle. Its penetration into the particle did not exceed 10% of the particle diameter. In macroporous catalyst pellets of (100-1000 nm diameter range), vanadium was deposited homogeneously while in bimodal catalyst particles, vanadium deposition occured through the pellet, but mainly at periphery (Figure 2.17).

Particle Size. It is recognized that the effectiveness of a catalyst can be improved by decreasing the particle size and by maximizing the exposure of its surface. Literature data indicate the use of 0.8 to 1.6 mm diameter extrudates for long duration operation. Nielson et al. (87) have shown that, at lower pressure, the larger particle had a longer life than the smaller diameter catalyst, while at higher pressures, the latter had a longer life. However, the initial deactivation rate of the smaller catalyst was significantly higher than that of the large size catalyst at both pressures (Fig. 2.18). Similar results were also obtained by Tamm et al. (7) and Shah and Paraskos (88). Since a decrease in particle size maximizes the exposure of its surface, external cracking and metal removal reactions are enhanced leading to high concentrations of coke and metal deposits on the catalyst particles. Consequently the small size catalyst would lose its activity at a faster rate than the large size catalyst, as observed by several workers (7,60,88).

Effect of Catalyst Acidity

Coke deposition on alumina supported Ni-Mo or Co-Mo catalysts is strongly influenced by the acidity of the alumina support (89,90). High levels of organic nitrogen (from organic bases) found in coke have been attributed to the acidity effect (89,90). Recent studies have shown that a major part of the coke is accumulated on the alumina support and not on the Ni/Mo or Co/Mo crystallites (91, 44). It has been suggested that the activity loss caused by coke deposition is primarily due to the coke blocking the edges of the active MoS_2 crystallites (91). At high coke levels, pore blockage would also reduce catalytic activity. Increasing catalyst acidity by additives such as B, Si, F etc are known to enhance coke formation whereas PO_4 addition which neutralizes the strong acid sites leads to reduced coking.

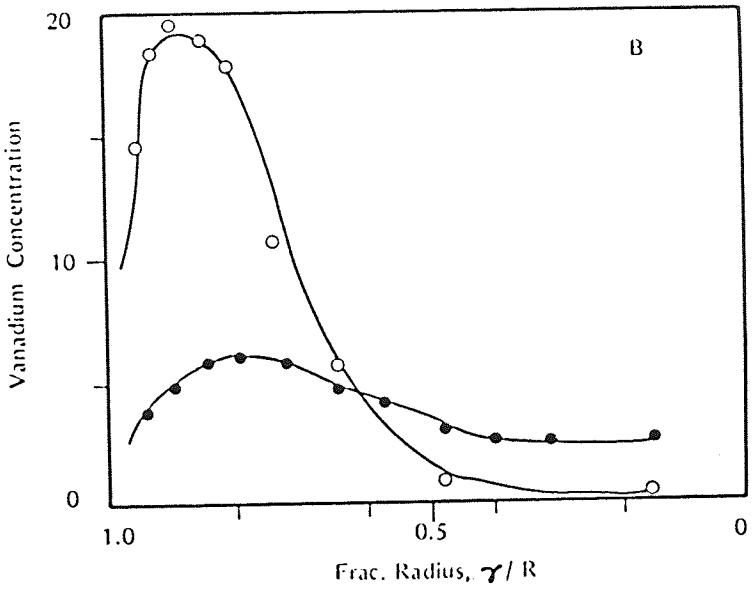

Figure 2.16. Effect of Pore Diameter on Vanadium Deposition

○ small pores, θv = 0.15

• large pores, θv = 0.20

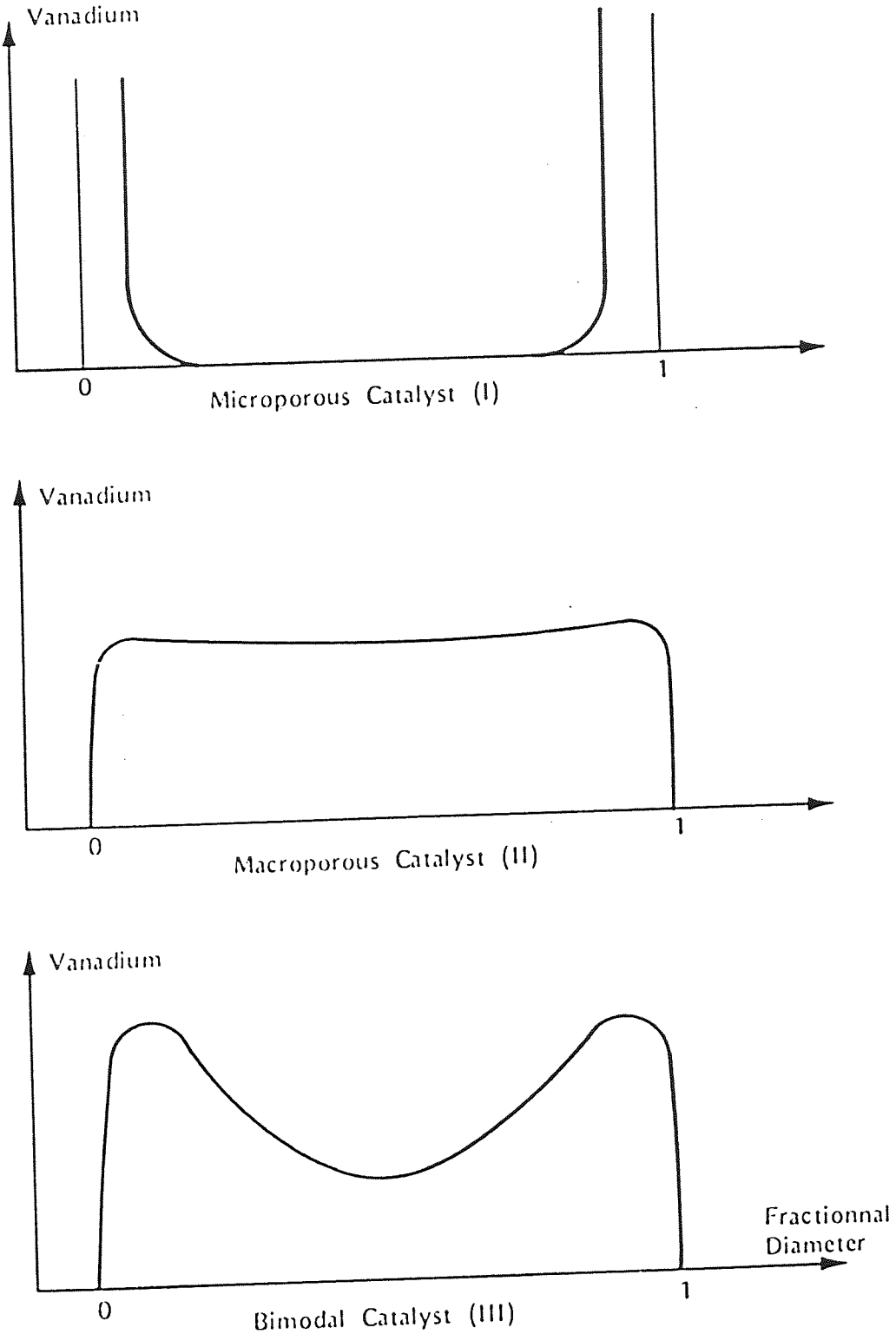

Figure 2.17. Effect of Pore Diameter on Vanadium Deposition.

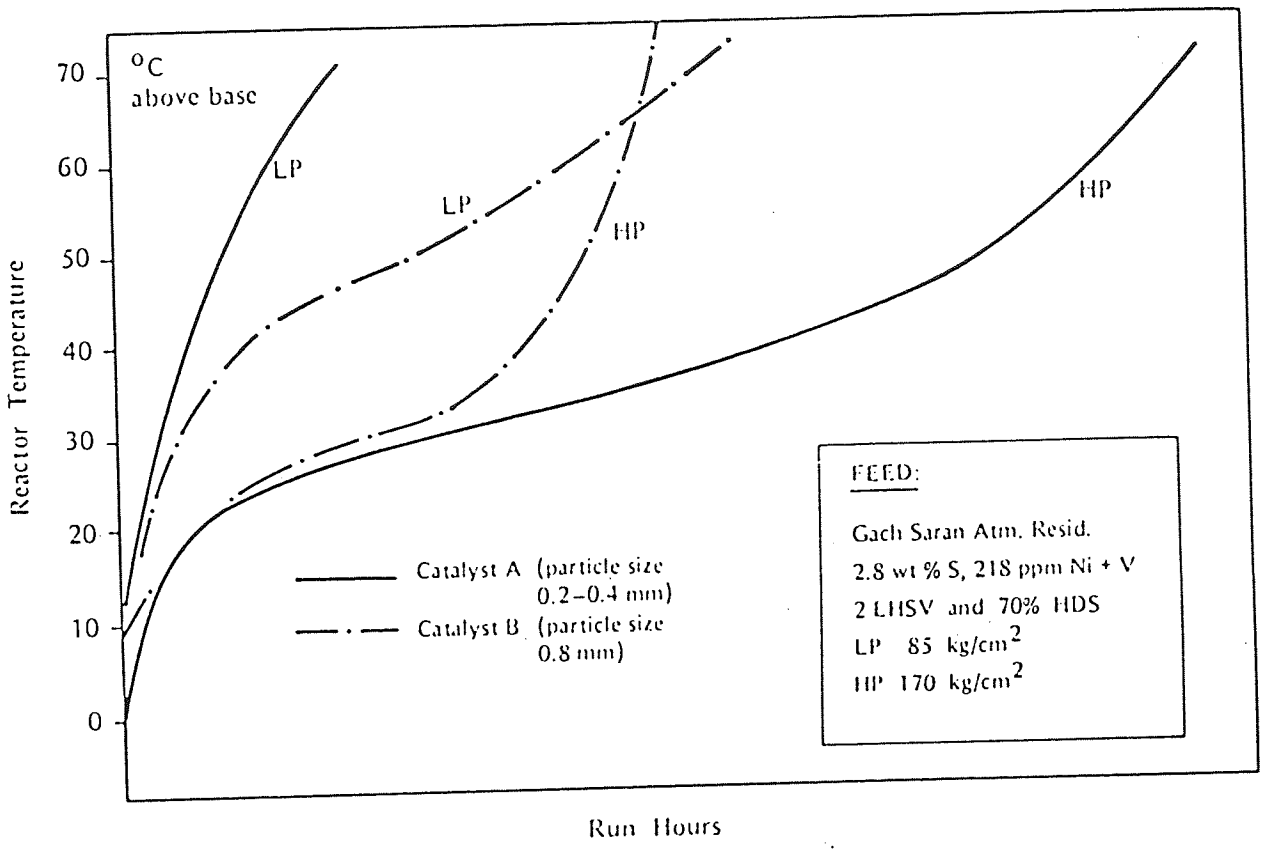

Figure 2.18. Influence of Pressure and Particle Size on Deactivation of Two Different Catalysts.

2.4. Reactivation of Residue Hydrotreating Catalysts

Since the catalysts used for hydrotreating of residual oil are found to deactivate as a result of the deposition of coke and metals, it is necessary to remove these contaminants from the catalyst in order to reactivate and reuse it. The primary objective of regeneration and/or rejuvenation is the recovery of the original activity of a deactivated catalyst.

The carbonaceous portion of the deposits is usually removed by combustion in an oxygen containing atmosphere. For the removal of the metal foulants deposited on the catalyst, chemical treatment is essential. Organic or inorganic acids can be used for the leaching of the deposited metals. The studies reported in the literature on the removal of coke and metals from deactivated hydrotreating catalysts in order to reactivate them are reviewed in the following sections.

2.4.1. Coke Removal (Regeneration)

Regeneration of hydrotreating catalysts by coke combustion and gasification has been studied extensively and the subject has been reviewed recently by Furimsky and Massoth (92). In addition to oxygen or air, gases such as CO_2, H_2, N_2O, O_3 and H_2O can be used for coke oxidation or gasification as indicated in the following reactions.

The main four modes of regeneration are:

$$C + O_2 \rightarrow CO_2 \quad (1)$$

$$C + H_2O \rightarrow CO + H_2 \quad (2)$$

$$C + 2H_2 \rightarrow CH_4 \quad (3)$$

$$C + CO_2 \rightarrow 2CO \quad (4)$$

Reactions (1) and (2) are generally fast while reactions (3) and (4) are too slow. Among these, attention has been focused mainly on oxidative regeneration.

In oxidative regeneration, the early stages of the reaction between the spent catalyst and oxygen are crucial. The coke oxidation comprises a number of exothermic reactions. Typical reactions include:

$$C + O_2 \rightarrow CO_2$$

$$2C + O_2 \rightarrow 2CO$$

$$4H_{org} + O_2 \rightarrow 2H_2O$$

$$S_{org} + O_2 \rightarrow SO_2$$

$$N_{org} + O_2 \rightarrow NO_2$$

$$MSx + yO_2 \rightarrow MOz + SO_2$$

$$MS_x + 2xO_2 \rightarrow M(SO_4)x$$

$$M(SO_4)x \rightarrow MO_z + xSO_2/SO_3$$

The carbon is oxidized, and the organic residue on the catalyst (H,S_{org}, N_{org}) and metals (Co, Mo, Ni, W, V, Fe and Al) are oxidized. As a result, any consideration of decoking must consider removal of carbon, possible removal of unwanted metals associated with carbon, oxidation of components of the catalyst with carbon, oxidation of components of the catalyst, and possible changes resulting from heat liberation during oxidation.

Temperature programmed oxidation studies have shown that the reactions of the organic and the inorganic portions of the spent catalyst with oxygen occur over wide temperature ranges (34,37,38,44) ie. 250°C to 500°C. The presence of coke with a wide range of reactivitiy has been reported by some workers (92,93). The combustion of the most reactive parts of the coke species in excessive amounts of oxygen may result in temperature runaways causing undesirable changes to the catalyst.

The rate of coke combustion generally depends on few main parameters, namely, start-up temperature, coke concentration oxygen content of the regeneration gas and the flow rate. Since the reactions which occur during coke combustion are highly exothermic, it must be carefully regulated to avoid the generation of excessive heat.

Most of the studies reported on the oxidative regeneration of coked hydrotreating catalysts are devoted primarily to elucidating carbon and sulfur removal mechanisms by temperature programmed oxidation techniques (37,38,93,94,95,96).

A few studies have been reported on the sintering of the active components of Co-Mo-Al_2O_3 catalysts during regeneration. Artega el al (97,98) observed that regeneration caused an increase of the surface exposure of both Mo and Co ions and produced a more active catalyst. They also noticed that the dispersion of Mo increase was also observed with increasing temperature (in the range 400 to 700°C), while that of cobalt decreased

apparently due to some of the cobalt entering the alumina lattice to form $CoAl_2O_4$ like species (98). In contrast, Dufresne et al (99) reported that sintering of the active molybdena phase can occur even at temperatures around 500°C. In a recent study by Furimsky (100), a significant loss in the surface area of the catalyst support was observed when the catalyst was regenerated in air containing 20% oxygen. Few studies have been reported on the structural changes occuring to the support and to the active catalyst components during oxidative regeneration of hydrotreating catalysts. Further work on the subject appears necessary with special attention to the early stages of regeneration.

2.4.2. Metal Removal (Rejuvenation)

In the case of coke and metal fouled spent residue hydroprocessing catalysts, regeneration by conventional procedures using nitrogen-air or steam-air under controlled conditions does not result in complete reactivation of the catalyst. While coke is removed completely, the metallic impurities remain on the catalyst and act as a diffusion barrier to the reactants. Therefore, to reactivate such metal-fouled spent catalysts it is necessary to remove the deposited metals by special treatments. The process of reactivation by the removal of deposited metals is referred to as rejuvenation. Selective removal of the contaminant metals without significantly damaging the physical and chemical characteristics of the original catalyst is an important requirement for efficient rejuvenation. A number of methods have been reported in the literature for leaching of metal foulants with chemical reagents from spent heavy oil hydrotreating catalysts (101,102,103,104,105). As the reagents effectiveness in selective removal of the deposited metals without significantly affecting the active metals, is an important factor in the rejuvenation process, it would be useful to discuss the principle and chemistry of selective leaching and separation of metals using chemical reagents.

Metals on spent hydrotreating catalysts are usually present as sulphides. It is, therefore, essential to find a chemical reagent that reacts with these sulphides. Also it should be possible to separate selectively the products of reaction. However, a selective leaching agent could act in two ways.

A chemical could be chosen that reacted with only one of the contaminants to produce a complex that dissolved in solution, or one could select a chemical that reacts with all

metals to produce complexes only one of which was soluble. In the first case, one would select complexing agents on the basis of their stability constants.

$$MS + H_2X = MX + H_2S$$

$$K = \frac{(MX)(H_2S)}{(MS)(H_2X)}$$

where K is high for a metal that should be removed and low for a metal that should not. In the second case, the complexing agent would be selected on the basis of solubility in a given solvent.

Beuther and Flinn (103) used organic reagents capable of forming water soluble metals complexes. The reagents screened for leaching included organic acids, such as oxalic, lactic, glycolic, phthalic and succinic acids, as well as acetylacetone, ethylenediamine, o-aminophenol and salicylaldehyde. No definite conclusions were established regarding the metal removal and catalytic activity improvement.

Mitchel et al. (104) used an aqueous solution of oxalic acid as reagent for removing vanadium sulphide from spent residue hydroprocessing catalyst prior to burning-off the coke. They claimed at least 30% removal of vanadium from the catalyst without affecting the active catalytic constituents. A process developed at IFP by Le Page et al. (106) involves treating the used catalyst with aqueous oxalic acid solution at 80°C after burning coke from the catalyst. Removal of at least 50% of the metallic impurities, (but less than 25% of catalytic constituents) with 80% recovery of initial activity has been reported in the process. Selectivity of the reagent for removing the major metal foulant was not reported by these workers.

Another process developed by Farrell et al. (107) involves treating the deactivated catalyst prior to coke burn-off with an aqueous solution containing a mixture of oxalic acid and aluminium nitrate or nitric acid. They achieved removal of at least 50% of the vanadium plus nickel contaminants and restoration of at least 70% of the original HDS activity. It is claimed that the deactivated catalyst should not be decoked prior to treatment with the regenerant solution, because the formation of SO_2 and/or SO_3 plus O_2 attacks most

hydrodesulphurization catalyst supports and also removes the active components of the catalyst. Beuther et al. (103) on the other hand stated that the chemical extraction of the metals from the coked catalyst would be quite difficult because the over-all metallo-organics are embedded in a coke matrix.

Recent studies by Hernandez (108) showed that oxalic and citric acid treatments of used catalyst after coke burning improved the equilibrium HDS activity of the catalyst (16.63%) compared with that of the fresh catalyst. However, in industrial catalysts, it is more important to maintain activity at a high level than to have a high initial activity accompanied by a steep decrease in activity. Another interesting observation reported by this author was that the hydrodemetallization HDM activity is enhanced by simple coke burning treatment.

Silbernagel et al. (109) have reported that contacting metal contaminated hydrodesulphurization catalyst with a heteropoly acid, such as molybdophosphoric acid to which dilute hydrogen peroxide is added, results in a significant enhancement in the rate and extent of carbon and metals removal. This is due to the fact that H_2O_2 helps maintain the heteropoly acid in the highest oxidation state which will effect the extraction of vanadium, and because H_2O_2 assists in oxidizing V^{4+} to V^{5+}, VO^{2+} to V_2O_5 and V_2S_2 to $VOSO_4$; in general, higher oxidation state species are more soluble. A somewhat similar process involving two steps has been reported by the same authors (105). The process involves first contacting the catalyst with a sulphiding reagent (H_2S/H_2) and then treating the sulphided spent catalyst with a heteropoly acid such as molybdophosphoric acid.

Anderson (110) discloses a method for removing vanadium by contacting a regenerated catalyst with a gas containing molecular oxygen at a temperature of 538°C, sulphiding at 400-870°C and washing with an aqueous mineral acid to remove the contaminated metal sulphide. An aqueous phase oxidation method for removing metal contaminants such as Ni, V, Fe, etc., from FCC has also been reported by Burke et al. (111). The process involves contacting the sulphided metals-contaminated catalyst with an aqueous solution containing soluble metal nitrate and nitrite ions. The oxidized catalyst is further treated with an aqueous oxidative wash in an aqueous peroxide solution and a reductive wash in an aqueous solution of SO_2.

Recently removal of 70-80% of the vanadium and 55-70% of the nickel without affecting the catalyst metals has been claimed by Hydrocarbon Research Inc. (112, 113). The process comprises:

One.removing process oil by solvent washing,

Two.treatment at 15-120°C with an aqueous solution of sulphuric acid and ammonium peroxydisulphate,

Three.washing-away the reagent, and

Four.burning the carbonaceous deposit at 430-480°C.

Deposited metals are removed, but the catalyst metals remain and initial activity is restored. The disadvantage of this process is the excessive amount of undesirable sulfate ions in the final catalyst.

In another patented process developed by Ioka et al. (114) the spent catalyst is treated with Cl_2 or NaClO in the presence of water at 50-100°C. Chlorinated V, Ni, and Co are leached while Mo is not leached-out during the chlorination process. It is reported that 83% V, 76% Ni and 81% Co and < 5% Mo are extracted in the process. The treated catalyst can be reused after calcination at 550°C for 2 hr. However, the relation between metals removal and catalyst activity improvement was not establsihed in this study. Poezd et al. (115) patented a simple method involving grinding of the spent catalyst into a powder, and adding ammonium molybdate solution to the mixture. The material is subsequently moulded into pellets, dried at 120-160°C and calcined at 500-550°C. This method should be described as re-impregnation rather than regeneration.

Marcantonio (116) introduced a process for recovery of metals (Ni, Co, Mo, V) from spent hydroprocessing catalysts by first roasting at 400-600°C and then contacting twice with aqueous solutions of ammonia and ammonium salts which improves the metal recoveries (especially for Cobalt) from ca 50% to ca 90%.

Recently, an excellent academic study of rejuvenation of deactivated hydrotreating catalyst has been carried out (102) followed by several recent publications in the area (119-124). Marafi et al. used oxalic acid to leach metals from a Co-Mo/Al_2O_3 catalyst used for hydroprocessing of an atmospheric residue to explore the mechanism and kinetics of leaching metal sulphides (119). For V removal, the best fit was obtained by a shrinking

core model, suggesting that mass transfer in the matrix of the coke deposited on the catalyst surface was rate controlling. It was suggested that leaching resulted from the formation of metal oxalates in the system.

$$MS_2 + 4H+ = M^{4+} + 2H_2S$$

$$M^{4+} + 2(C_2O_4)^{2-} = M(C_2O_4)_2$$

Based on the stability constants for complex formation with different metals, it was shown that V was most favourable, followed by that of Ni. Marafi et al. (123) extended their studies to include malonic and acetic acids and found the following order of efficiency for V removal: oxalic > malonic > acetic acid. The addition of aluminium nitrate improved the extraction efficiency, where as aluminium sulphate and ammonium nitrate did not. The effect of metals removal on surface area and HDS activity is shown in Table 2.7. This shows the improvement of activity in spite of the residual presence of the coke, confirming the contribution of metals to catalyst deactivation.

Table 2.6. Effect of Leaching on the Surface Area and Activity

Catalyst Type	Surface area (m^2g^{-1})	HDS (%)
Fresh	203	65
Spent	44	29
Leached with oxalic acid	100	36
Leached with oxalic acid + *Al(NO3)3*	125	46
Leached with malonic acid	105	42
Leached with malonic acid + *Al(NO3)3*	110	45

Controversial reports are found in the patents literature regarding the advantages and disadvantages of using spent catalyst in the sulfide (coked) and oxide form for metal leaching with acid reagents. Thus, for example, Silbernagel et al. (109) noticed that the leaching of sulfide forms of the spent catalyst with a heteropoly acid led to high removal of

vanadium. Similar observations were also made by Myerson and Ernst (124a) as well as by Babcock et al (124b) who reported that pretreatment of the spent catalyst with H_2S followed by extraction with acidic solution resulted in more selective removal of vanadium. On the other hand, a process involving calcination of the spent catalyst at 500°C in air, followed by acid leaching has been reported to be efficient for regeneration of petroleum hydrodemetallization - hydrodesulfurization catalysts (125,106,126).

Although extraction of metal deposits and substantial recovery of activity are reported in most of the patented processes discussed above, none of these processes has been commercialized due to such drawbacks as:

- Removal of catalytically active metals (Mo, Co or Ni) with the undesired V deposits.
- Dissolution of part of the alumina, resulting in changes in the structural integrity of the alumina support.
- Decrease in the mechanical strength of the catalyst.
- Process economically not feasible.

In addition, several important questions such as the mechanism of leaching, the preferred leaching route (e.g., sulfide or oxide form of the metals) for selective removal of foulant metals and for cost effectiveness, effect of leaching treatment on the distribution and dispersion of the catalytically active metals and the effect of leaching on the physical and mechanical properties, remain unresolved. There is interest in process development for spent catalyst rejuvenation, in view of the potential benefits of the rejuvenation process from environmental and economic aspects. Further research studies are hence justified to develop a cost effective route for the rejuvenation of spent residue hydroprocessing catalysts.

2.5. Utilization of Spent Residue Hydrotreating Catalyst

One possible approach is to use spent catalyst in catalyst preparation. This approach is fairly new and only very limited studies have been reported in the literature. Gardner et al. (127) investigated the possibility of preparation of an active hydrotreating catalyst composition from spent hydrotreating catalysts by mixing them with alumina-containing materials and shaping the mixture into compacted extrudates. The scope of this study was

very limited. Only one type of spent catalyst from a distillate hydrotreating unit was used in the catalyst preparation experiments. The spent catalyst used in this study contained no vanadium. Since spent catalysts from residue hydroprocessing units form a major portion of solid wastes in Kuwait refineries, utilization of such catalysts in the preparation of active hydrotreating catalysts would be highly desirable.

Spent residue hydroprocessing catalysts have a high potential for the preparation of active HDM catalysts with desirable properties. The scientific basis for this is explained below.

The effectiveness of a HDM catalyst depends primarily on two factors, namely, mass transfer and intrinsic catalyst activity. Heavy residues are a complex mixture of high molecular weight compounds, and contain a large percentage of heteroatoms. The removal of the heteroatoms from the molecules during catalytic hydrotreating occurs rapidly over the active surface of the catalyst. For the reactions to take place effectively the molecules must have access to the inner surfaces of the catalyst extrudates through appropriate channels and pores that allow large molecules (V and Ni) to diffuse easily from the outer surface of the extrudates to the inner pores and with time these metals will be deposited and block the pore mouth and cause the catalyst to deactivate (28). In order to slow the rate of deactivation and extend the catalyst life it is suggested that the amount of large pores should be increased.

The second factor that plays a significant role in the performance of a HDM catalyst is the nature and dispersion of the active sites. The active catalyst component used mainly is MoO_3 supported on alumina oxide (Al_20_3). The method of dispersion of the active components on the support surface by proper impregnation and activation procedure as well as the surface area of the alumina support, are of vital importance to obtain catalysts with high activity, selectivity and stability.

The catalysts should also have an adequate mechanical strength, normally expressed as the crushing strength of the catalyst extrudates and as the attrition rate. Therefore in any new development and manufacture of HDM Catalyst the above mentioned factors should be taken into consideration (33). Table 2.7 shows the characteristics of a typical HDM catalyst.

A wide pore catalyst will permit deep penetration of metals and accumulation of larger amounts of metal deposits within the pores. Furthermore, the residence time of

Table 2.7. Characteristic of a Typical HDM Catalyst

Catalyst Property	Specification
Chemical:	
MoO_3 (wt%)	3 - 8
Al_20_3 (wt%)	Balance
Physical:	
Surface area (m^2/gm)	100-200
Pore volume (ml/gm)	0.5 - 1.5
Mean pore diameter (A°)	200 - 300
Side crushing strength (lbs/mm)	2 - 4

A good HDM catalyst is thus characterized by:

- very high metal retention power (80-100%) of its own weight)
- very low coking tendency
- proper porosity and active area

asphaltenes and other coke precursors within the pores will be relatively low due to the more rapid diffusion through wide pores. Consequently the rate of coke formation will be reduced. Currently, the large pore HDM catalysts are manufactured from a fresh alumina base using conventional techniques for regulation of the pore size. The alternative way is to use highly-fouled spent residue hydroprocessing catalysts in HDM catalyst preparation. The reason behind this is that spent hydroprocessing catalysts contain larger amounts of metals such as vanadium and nickel (15 wt% and 5 wt% respectively) and above 4-6 wt % of active metal (Mo), which are known to be highly active for promoting HDM reactions (128). Furthermore, the carbonaceous material which is present in the spent catalyst (15 wt%) can create wide pores when used in HDM catalysts preparation (129). The development of such catalysts can have an advantage in reducing the serious environmental problems associated with spent catalyst disposal in Kuwait.

Despite these potential advantages, this area of research has not received much attention. There is a strong need for studies that can lead to the development of methods and technology for the utilization of spent hydroprocessing catalysts in the preparation of active HDM catalysts.

3.0. SCOPE OF RESEARCH

The use of catalysts in petroleum residue upgrading by hydroprocessing has shown a remarkable increase in recent years. Rapid deactivation of the catalysts together with the non-availability of effective methods for the regeneration has resulted in the generation of large quantities of spent catalysts as solid wastes in the refineries worldwide. Since these spent catalysts contain toxic materials, they are classified as hazardous wastes and their disposal in an environmentally safe way poses a major problem. Considerable interest exists in minimizing the spent catalyst problem. This can be done both by reducing the rate of catalyst deactivation and extending its life in the residue processing plant and by developing a cost-effective technology to reactivate the catalyst for re-use or by finding ways to use them in other applications.

A review of the literature on the subject (reported above) reveals the following.

1. Deactivation of residue hydroprocessing catalyst by coke and metals deposition involves complex processes that are influenced by several factors such as catalyst type, process conditions, feedstock properties, etc. Although coke is believed to be primarily responsible for the rapid deactivation of the catalyst during the early period of the process, the coking mechanism is not clearly understood. More specifically, studies on initial coking in catalytic hydroprocessing are relatively few and there is a need for further research in this area.
2. The technology of reactivation/rejuvenation of spent hydroprocessing catalysts is not yet well developed. Considerable commercial interest exists in the rejuvenation of these catalysts by selective removal of metal contaminants. This can reduce the environmental problems caused by waste catalysts in a profitable way.
3. Spent hydroprocessing catalysts containing coke and metal deposits have a high potential for use in the preparation of wide pore active hydrodemetalization catalyst by

mixing them with alumina. Only very limited studies have been reported in literature on this subject. There is a strong need for further research in this area.

Considering the above points, the scope for further work on hydroprocessing catalyst deactivation, reactivation and utilization appears to be enormous. In the present work attention will be focussed on the following studies with a view to answering some of the questions indicated above. However, studies related to the utilization of spent catalyst in preparing active HDM catalyst are not considered as part of the work repeated in this thesis.

1. Catalyst Deactivation

   Studies on the nature of initial coke formed during residual oil hydroprocessing and its effect on catalyst performance (i.e. influence of initial coke on different catalyst functions).

2. Catalyst reactivation studies by coke combustion.

   Since coke combustion is exothermic, the early stages of contact between the spent catalyst and oxygen in the decoking process are crucial. Special attention will be paid to the initial stages of coke combustion. The influence of initial regeneration conditions on the structural changes occuring to the support and to the active catalyst components will be investigated.

3. Spent Catalyst Rejuvenation by Leaching of Foulant Metals.

   From the literature review on this subject it is clear that several important questions such as the mechanism of leaching, the preferred leaching route (e.g. leaching prior to decoking or after decoking), the influence of additives on leaching efficiency, the effect of leaching treatment on the dispersion and distribution of the catalytically active metals, the effect of leaching on the physical and mechanical properties of the catalyst, etc. remain unresolved. As part of the present work systematic experiments will be conducted to study these aspects of leaching and develop an effective method for the rejuvenation of spent residue hydroprocessing catalysts.

4. Modelling of the Metal Leaching Process

Modelling of the metal leaching process from spent catalyst has received little or no attention in previous studies. As part of the present studies on spent catalyst rejuvenation by foulant metal leaching we have attempted to develop a model for the leaching process using different organic reagents.

All these studies will form the subject matter of the thesis which in addition to the three chapters (1. Introduction, 2. Literature Review and 3. Purpose and Scope of the thesis), will consist of 6 more chapters. Specific studies that will be covered in each chapter are summarized in the following Table.

SPECIFIC STUDIES COVERED IN EACH CHAPTER

1. Introduction .....
2. Literature Review .....
   - 2.1. Deactivation of Hydrotreating Catalyst .....
   - 2.2. Reactivation (Coke Removal and Metal Removal) .....
   - 2.3. Utilization of Spent Hydrotreating Catalyst .....
3. Scope of Research .....
4. Experimental Methods and Materials Investigation .....
5. Catalyst Deactivation Studies .....
   - 5.1. Deactivation of Industrial Fixed Bed and Ebullated Bed Residue Hydroprocessing Catalysts .....
   - 5.2. Investigation of Initial Coking and Its Role in Hydrotreating Catalyst Deactivation .....
     - a. Factors Influencing The Amount and Nature of Initial Coke .....
     - b. Effect of Initial Coke on Different Functions of The Catalyst .....
6. Spent Catalyst Reactivation by Coke Removal .....
   - 6.1. Investigation of Coke Removal Process .....
7. Spent Catalyst Rejuvenation by Leaching of Foulant Metals .....
   - 7.1. Comparative Study of The Effectiveness and Selectivity in The Removal of Foulant Metals From Spent Hydroprocessing Catalysts in Coked and Decoked Forms .....
   - 7.2. Role of Inorganic Salt Additives in Promoting Leaching Efficiency of Organic Acids .....
   - 7.3. Effect of Metal Leaching on Catalyst Characteristics and Performance ...
8. Modelling of the Metal Leaching Process .....
9. Summary, Conclusion and Recommendation .....
10. References .....

4.0. EXPERIMENTAL INVESTIGATION

The detailed experimental plan prepared for this investigation comprised the following tasks.

1. Catalyst deactivation problem analysis in industrial residue hydroprocessing operations by studying the physical, mechanical and chemical properties of fresh and spent catalyst samples from fixed bed ARDS and ebullated-bed units.
2. Studies on Catalyst Deactivation by coke deposition. Investigation of the influence of operating temperature and processing time, feed quality and catalyst acidity on the nature of the coke that deposits on the catalyst surface during the early period of the run and its role in catalyst deactivation.
3. Studies on Hydroprocessing Catalyst Regeneration. Investigation of coke removal (regeneration process) by studying the influence of the following parameters on regeneration.

    - Effect of oxygen concentration
    - Effect of flow rate
    - Effect of temperature

4. Rejuvenation of Spent Residue Hydroprocessing Catalyst. Investigation of metal leaching by organic complex-forming reagents with and without promoter, and a comparison between their selectivities for the removal of metal foulants (V and Ni).
5. Characterization and Performance evaluation of regenerated and rejuvenated hydrotreating catalyst and studies on the relationship between vanadium removal and catalyst surface area and HDS activity recovery.
6. Modelling of the Metal Leaching Process.

The materials, experimental unit, analytical and experimental procedures used in various studies are briefly described in the following section.

4.1. Materials, Sources and Procedures

4.1.1. Catalysts

Samples of spent residue hydrotreating catalysts were obtained from different levels of each of the four reactors of the atmospheric residue desulphurization (ARDS) units. Another batch of spent catalyst was received from the ebullated bed reactor of Kuwait National Petroleum Company. Samples of corresponding fresh catalysts for both units were also received, which contained NiO and MoO_3 supported on γ-alumina and were in the form of extrudates.

The spent catalyst contained residual oil, sulphur, carbon, vanadium and nickel deposits in addition to the catalyst metals (Ni and Mo) orginally present. Detailed information and characterization about the catalyst samples is described fully in Chapter 5.

4.1.2. Reagents and Chemical

Analytical reagent grade oxalic acid, hydrogen peroxide, aluminum nitrate and ferric nitrate used in the metal extraction experiments were obtained from Baker and BDH. The naphtha (boiling range 92 - 170°C) used in deoiling of the spent catalyst was obtained from KNPC refinery.

4.2. Equipment and Procedures

4.2.1. Micro-reactor Unit

A bench-scale fixed bed microreactor unit, designed and manufactured by Vinci Technologies was used for coking studies on hydrotreating catalyst. A schematic diagram of the reactor system is shown in Figure 4.1.

The CATATEST unit consisted of five parts:

- the liquid inlet
- the gas inlet
- the reactor
- the product outlet with the separator
- the preheating oven

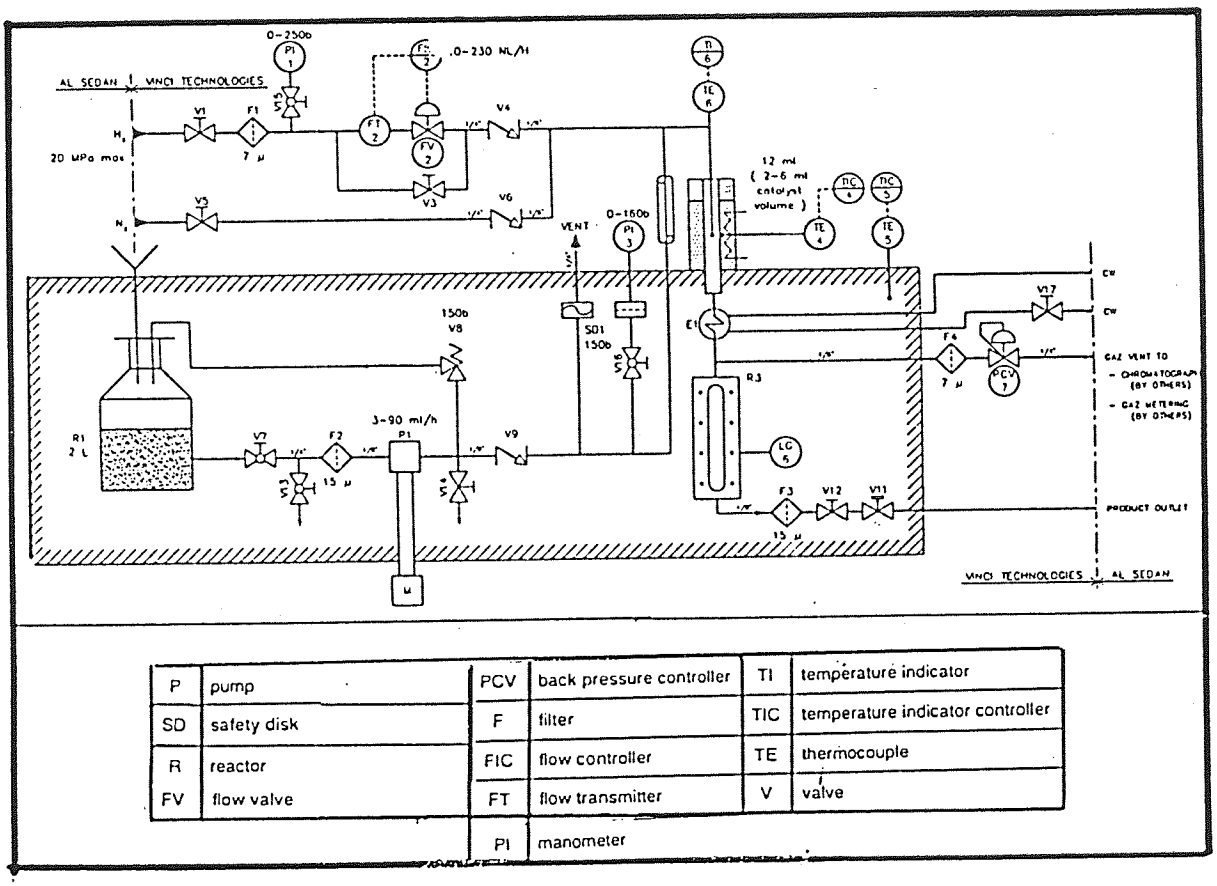

P	pump	PCV	back pressure controller	TI	temperature indicator
SD	safety disk	F	filter	TIC	temperature indicator controller
R	reactor	FIC	flow controller	TE	thermocouple
FV	flow valve	FT	flow transmitter	V	valve
		PI	manometer		

Figure 4.1. Bench-Scale Microreactor Unit for Heavy Feedstocks.

Liquid Inlet. This part of the unit includes a feed vessel (2*l*, atmospheric pressure) with an isolation valve (V7). Another valve (V13) is used to empty the feed vessel. The pump (P1) is protected with a filter (F2), and equipped with a priming valve (V14). This liquid feed line is protected with a check-valve (V9). This line also includes a nickel rupture disk (SD1) and a manometer (P13) equipped with a protection valve (V16).

Gas Inlet. This module consists of a hydrogen inlet stop valve (V1), a filter (F1) and a manometer (P11) with a protection valve (V15). The nitrogen inlet, consisting of a stop valve (V5), is T-branched after the check-valve (V4). For quick pressurization of the unit, the mass flow controllers can be by-passed with a manual valve (V3). This gas inlet module is protected by a check-valve (V4).

Two main operations can be performed with this module. The first one is nitrogen scavenging which is performed prior to conducting a new run with hydrogen. The second operation is the accurate control of the hydrogen flowrate, which can be adjusted instantaneously by tuning a new setpoint on the electronic rack.

Reactor. This sector of the bench-scale module unit begins at the gas-liquid mixing point after check valves V9 and V4. It is composed of the reactor itself (25 ml, 15 Mega Pascal, 550°C) and the cooler.

The heating zone of the reactor is equipped with its own high temperature safety device. There is an additional high temperature safety device for the fixed-bed. When the high temperature threshold is reached on the controller, the power supply to the furnace is shut down. At the high heat temperature threshold all power supplies (furnace and pump) are shutdown, but the instrumentation is kept in operation.

Product Outlet. This outlet consists of a high pressure gas-liquid separator-accumulator (LG6), a gas outlet filter (F4) located in front of a back pressure controller (PCV7) which assures a constant pressure in the unit by a continuous release of pressure, a product outlet filter (F3), a manual stop valve (V12) and a manual progressive valve (V11, microvalve) to create a pressure drop in order to ensure a smooth emptying of the high pressure accumulator-separator.

Preheating Oven. An oven is provided to ensure that feedstocks are preheated. The oven is temperature-controlled by means of an automatic device located on its front.

Control Rack. An electrical power rack pilots the unit.

The power supply for the unit is controlled by the main power switch. As the power is switched on, an indicator lamp lights up. Just below the main power switch, is the fuse instrumentation protection (5A).

Power buttons, with control lights are used to start, or shut-down the reactor furnace, the preheating oven and/or the pump. Each furnace zone has its own controller (ZONE 1). At the top of each controller is a security indicator that displays the heat temperature of the reactor, and two indicators that display the gas flow and potentiometer set point.

4.3. Procedures

4.3.1. Test Procedure for Deactivation Studies by Coke Deposition

The reactor was loaded with 14 ml of catalyst diluted with an equal volume of carborundum (Figure 4.2). The catalyst bed was placed in the reactor in such a way that it was in the mid-section of the reactor. Coarse carborundum was placed above and below the catalyst bed as shown in Figure 4.2. After the catalyst was loaded, the reactor was placed inside the furnace and tested for leaks with nitrogen under presurre (150 bar).

OPERATING PROCEDURE:

Calcination:

- Nitrogen was introduced at a flow rate of 10l/h under pressure (10 bar). The reactor was heated gradually to 450°C. These condtions were maintained for 2 h, following which, the reactor was cooled to 150°C.

Pre-sulphiding:

- Stop nitrogen flow
- Introduce 10% H_2S 90% H_2 gas stream (at 30 bar) into the reactor, flow rate; (10 *l*/h).
- Increase Temperature to 200°C.
- Maintain these conditions for 2 hours.
- Increase reactor temperature to 375°C while holding H_2S/H_2 gas flow rate (10l/h), and pressure 30 bar.
- Maintain the above conditions for 20 hours.

- Before injecting the feed bring the reactor temperature to the required level (as specified for particular run), and increase the oven temperature (50 - 130C).
- stop H_2S/H_2 gas flow and introduce Hydrogen, pressure (80 bar), flow rate (10l/hr).
- Prime and purge the system to assure the flow of the feed.
- Start the run by injecting the feed at a rate of 28 ml/h whilst maintaining reactor at specified operating conditions.
- Continue the run for the required time as specified in the experimental program.
- Collect product samples at specific time intervals.

Cleaning of the System.

- Close feed valve.
- Introduce naphtha in to the system after each run to clean the reactor (catalyst) and lines for 1 hour, flow rate 60 ml/min.
- Introduce nitrogen gas (10 bar) for drying for a period of 1 hour.
- Shut-down the unit.
- Unload the reactor, collect the catalyst sample and label it.
- The catalyst sample and product were then characterized as described in chapter 5, section 5.2..

Stripping Operating Procedure.

- Keep the product sample in a water bath at (50°C).
- Introduce nitrogen gas to strip H_2S gas from the product sample.

4.3.2. Deoiling

The spent catalyst was thoroughly washed with naphtha to remove the contaminated residual oil in a mechanical shaker. The clean catalysts was then dried in an oven at 120°C for 24 hours. The de-oiled spent catalyst and fresh catalyst were characterized as described in Chapter 5.

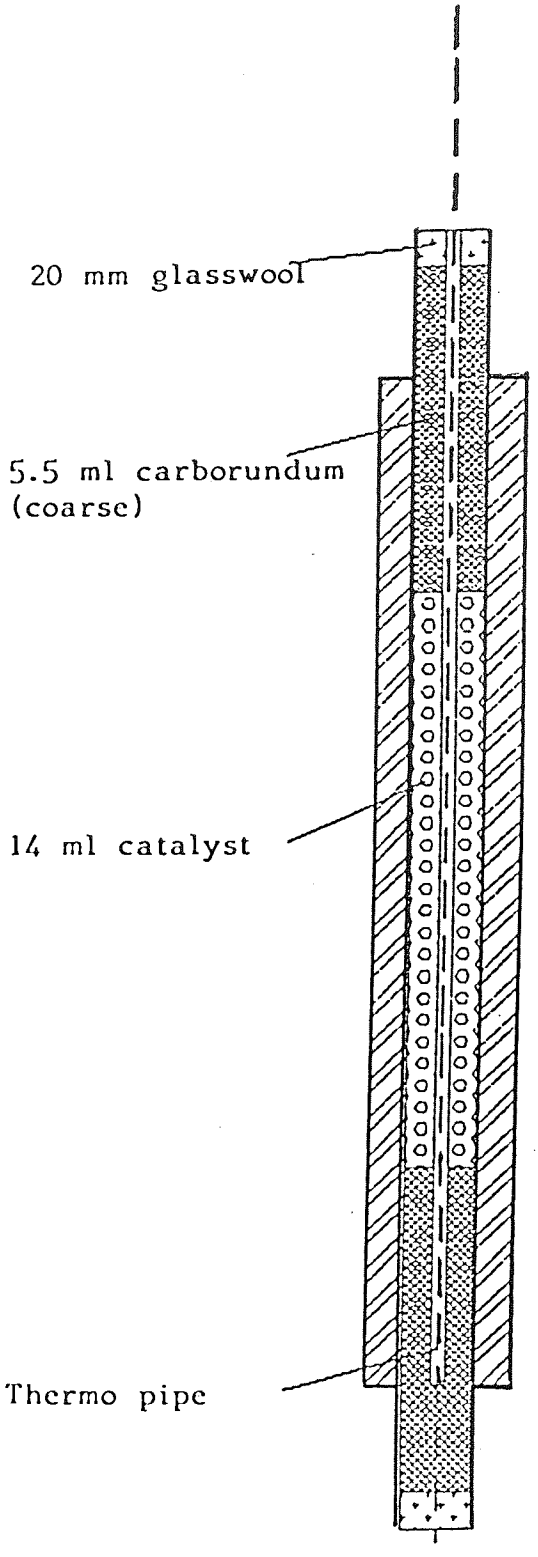

Figure 4.2. Schematic Diagram of the Loading of the Reactor.

Operating Parameters for Coking Studies:

Type of catalyst	:	$CoMo/Al_2O_3$
Hydrogen pressure	:	80 bar
Operating temperature	:	360, 380, 400, 420°C
Sulphiding	:	10% H_2S 90% H_2
Inlet Feed	:	Vacuum Gas Oil, or atmospheric residue
Liquid Hourly Space Velocity	:	$2h^{-1}$
H_2/Oil	:	360 ml/ml
Duration	:	1/2 h, 1 h, 3 h, 6 h, 24h.

4.3.3. Regeneration rig (Decoking)

A fixed bed reactor (volume 200 cc) length 70 cm and diameter 2 cm as shown in Figure 4.3. was used for decoking of the catalyst under controlled temperature conditions. 100g spent catalyst was charged to the reactor. The reactor was loaded with 50 ml of glass beads below and above the catalyst bed so that the catalyst remained at the center of the reactor. A thermocouple inserted into a thermowell at the center of the catalyst bed was used to monitor the reactor temperature during regeneration.

The following procedure was adopted. After loading the catalyst, nitrogen was passed at a rate of 100 l/h (27 cm^3/s) and the temperature was increased up to 370°C for 30 minutes, a mixture of 2% oxygen in nitrogen was passed for a period of 8 h at the same flow rate. The gas was then changed to 5% oxygen in nitrogen; the temperature was increased to 400°C and maintained for a period of 4h. The temperature was then increased up to 450°C; the regeneration gas was changed to air and flow maintained for a period of 2 h. Finally the reactor was cooled down to ambient temperature. The sample was collected and characterized as described in Chapter 6.

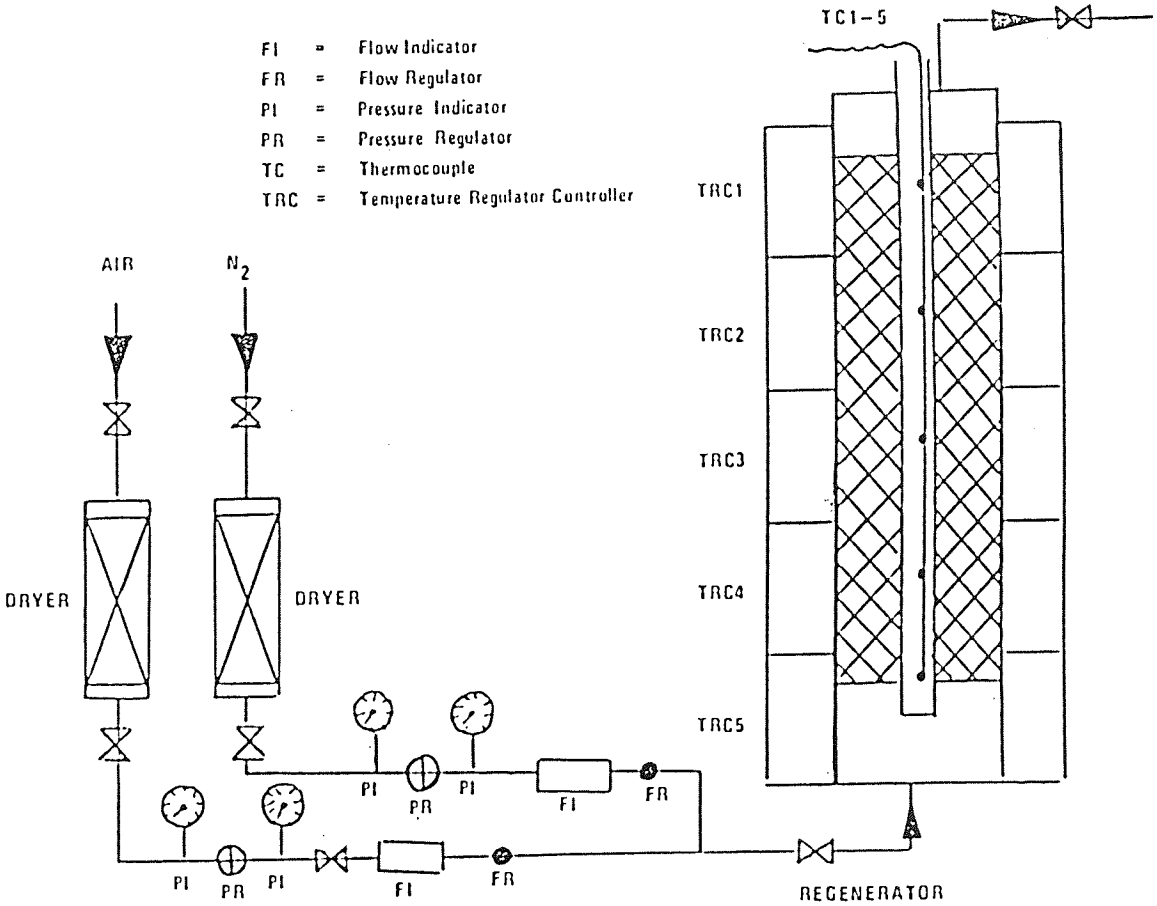

Figure 4.3. Regeneration Unit (Decoking).

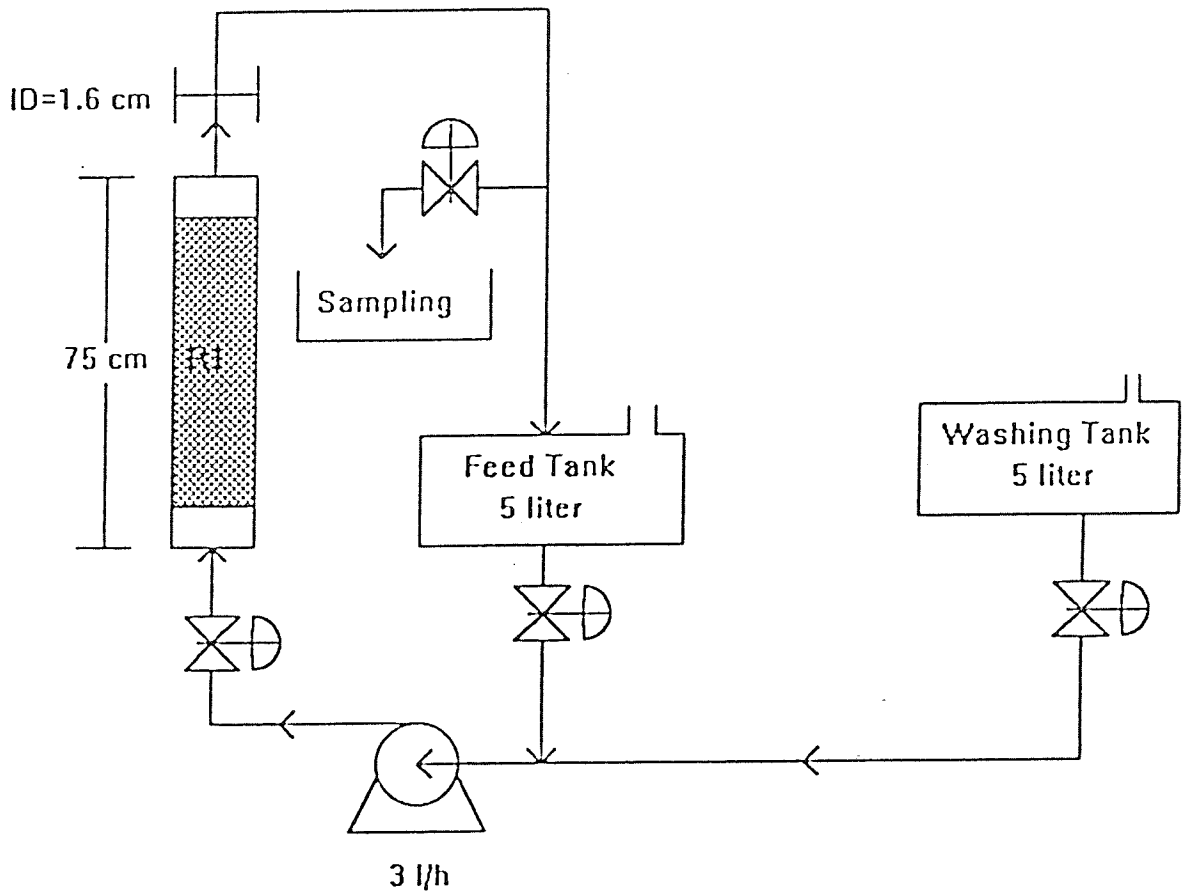

Figure 4.4. Bench-Scale Reactor for Metal Leaching.

4.3.4. Metal Leaching (Rejuvenation) Unit.

A special apparatus shown in Figure 4.4 was constructed for leaching of metals from the spent catalyst. It consisted of stainless steel fixed bed reactor ® of length 75 cm and diameter 1.6 cm, a dosing pump (P), and a glass reagent vessel. The reagent was pumped continuously through the catalyst bed from tbe bottom of the reactor (up-flow). The liquid product which was collected in the reagent vessel was recirculated continuously through the catalyst bed, at a rate of 3l/h, for the required period of time by the pump.

4.4. Characterization Techniques

The fresh and spent catalyst were characterized by measuring the physical, chemical and mechanical properties using standard procedures. Details of the procedure are described by M. Marafi (102). The equipment used for the various tests are listed in Table 4.1.

Surface Area. The surface areas of different catalyst samples were determined by the Brunauer-Emmet-Teller (BET) method. A Quantasorb adsorption unit (Quantachrome Corporation, U.S.A.) was used for BET adsorption isotherm determinations.

Pore Volume. The pore volume of catalyst samples was determined using water by the pore filling method.

Pore Size Distribution. Pore size distribution was measured with a Quantachrome Autoscan 60 mercury porosimeter. The method involves intrusion of mercury into the pores at different pressures (0 - 60000 psi).

Side Crushing Strength. A Quantachrome crushing strength analyzer was used to measure the side crushing strength of the catalyst pellets. The method determines particle crushing strength by measuring the force (in newtons, N) required to crush the particle.

Thirty pellets were tested from each catalyst sample and the average value was determined.

Average Length. The total length of 100 extrudates placed next to each other along their length was measured and the average length was calculated as the mean value.

Length Distribution. The catalyst particles in about 1g of the sample, obtained by riffling in a sample splitter, were classified by length with a digital vernier caliper into different groups, ranging from less than 0.5 mm to longer than 15 mm. The weights of the particles in the groups were determined and their percentages were obtained.

Bulk Density. The weight (g) of a known volume (100 ml) of the compacted catalysts was determined and the compacted bulk density was calculated as weight per unit volume (g/ml). A Quantachrome dual autotap apparatus was used for bulk density measurements.

Chemical Analysis. Inductively-coupled argon plasma (ICAP) spectroscopy (Jobin Yvon-model 24) was used to determine the concentration of different metals (V, Ni, Co, Mo, Fe) in the catalyst samples. The method involves atomizing the sample in a high temperature plasma and resolving the atomic spectra into atomic lines of each element by optical grating in an optical spectrometer.

Distribution Profiles of Contaminant Metals. A scanning electron x-ray microprobe analyzer (Jeol SXA-8600) was used for measuring the concentration profiles of contaminant metals across the catalyst pellet.

Thermogravimetric Analysis (TGA). A thermogravimetric analyzer (TGA model TGA-50, Shimadzu) was used to measure the weight changes in catalyst samples as a function of temperature. Section 5.1.3.3 gives detailed description of the procedure and principles of this technique.

Differential Thermal Analysis (DTA). A DTA-50, (Shimadzu) model differential thermal analyzer was used to measure thermal characteristics of a sample by measuring and recording both heating temperature and enthalpy. Section 5.1.3.4 describes procedure and principles of this technique.

Temperature Programmed Oxidation (TPO) Tests. Altimara (model AMI-1) TPO apparatus was used for characterizing coke deposits on spent catalysts. TPO profiles of gaseous products that evolved during temperature programmed oxidation of the catalyst sample were monitored using a GASLAB - 300 mass spectrometer and recorded as a function of temperature. Detailed procedure is described in section 5.1.3.2.

Nuclear Magnetic Resonance (NMR)

A solid state NMR, Buker-AMX-300 model was used to measure the aromaticity of coke deposits on treated catalyst. Detailed procedure and principles are described in section 5.2.6.2.

4.5. Catalyst Performance Evaluation Test Procedure for Leached Catalysts.

A fixed bed microreactor system was used for leached catalyst activity testing. Catalyst charges of 14 g were mixed with 5.5 g of carborundum and loaded in the reactor. Atmospheric gas oil containing 2% wt S was used as feed. The operating conditions were: Pressure: 40 bar, Temperature 350°C, H_2/oil/ratio: 400 ml/ml/h, LHSV: $6h^{-1}$. The catalyst was presulphided in the reactor. The presulphiding procedure involved passing 3 wt% CS_2 in atmospheric gas oil over the catalyst maintained at 300°C and 40 bars pressure. LHSV was adjusted to 6 h^{-1} and presulphiding was continued for three hours. The catalytic activity of catalyst samples by testing the hydrodesulphurisation of atmospheric gas oil (HDS) was established as described in Section 7.3.

Table 4.1. Techniques and Equipment Used for Full Characterization of Catalysts

	Catalyst Property	Technique Used	Equipment Available
1	Chemical Analysis		
		- XRF method	ARL-8410
		- ICAP spectroscopy	Jobin Yvon - 24
2	Elemental Analysis (C, H, N, S, O, etc.)	Elemental analyzer	1. ELCO, CHNS-932 2. SKALAR auto analyzer
3	Mechanical Properties		
a	Particle size (for materials <400μ)	X-ray scanning	Quantachrome Microscan 11
b	Bulk density	ASTM-D4164 procedure	Quantachrome dual autotap
c	Side crushing strength	Standard procedure (ASTM-D4179)	Quantachrome Crushing strength analyzer
d	Attrition and abrasion	ASTM-D4058-81	A cylindrical drum attrition
e	Bulk crushing strength	Shell method	Geomechanique bulk crushing strength machine
f	Pellet length and length distribution	Standard method	Digital vernier caliper (Mitutoya).
g	Real density and true volume	Standard method	Quantachrome Ultra pycnometer 1000.
4	Physical & Special Analysis		
a	Surface area	BET method	- Quantasorb adsorption unit. - Autosorb adsorption system
b	Pore volume and pore size distribution	Mercury intrusion technique	Quantachrome mercury porosimeter (Autoscan 60)
c	Specific surface area of metals	Chemisorption	Altamira AMI-1 adsorption system
d	Metal and carbon concentration profiles within the pellet	Electron microprobe analysis	Electron microprobe analyzer (Jeol) SXA-8600
e	Surface acidity and acid strength distribution	NH_3 chemisorption temperature programmed desorption	TPA/TPD apparatus (Altamira AMI-1)
f	Nature and proportion of different phases	XRD	XRD unit Philips (37-10)
g	Nature of coke in spent catalyst	Temperature programmed oxidation	TPO apparatus Altimira AMI-1
h	Aromiticity	NMR	Bruker-AMX-300

5.0. CATALYST DEACTIVATION STUDIES

5.1. Deactivation of Industrial Fixed Bed and Ebullated Bed Residue Hydroprocessing Catalysts.

5.1.1. Introduction

Petroleum residues upgrading through catalytic hydroprocessing is an important process in Kuwait refineries. Over 250000 barrels of atmospheric and vacuum residues are being processed daily in the three refineries of Kuwait National Petroleum Company (KNPC) bringing substantial economic returns to the country.

Two types of reactor technology are currently in use for residue hydroprocessing in Kuwait refineries. These include (1) fixed bed reactors and (2) ebullating bed reactors. The fixed bed reactor system is used for the hydrotreatment of atmospheric residue. A process flow diagram for the unit is shown in the previous chapter Figure 2.13.

The reactor section consists of four catalytic reactors operating in the trickle mode. Preheated feed and hydrogen enter the first reactor and the hydrotreated product leaves from the last reactor after passing through all four reactors in series. The first reactor is used as a guard bed to remove most of the metal impurities in the feedstock.

The remaining three reactors are used to remove sulphur and nitrogen and for partial conversion of residues to distillates by hydrocracking. Generally, in such fixed bed reactors, the catalyst is deactivated rapidly by metal deposition. The guard reactor is even plugged by metals and suspended solid deposits.

Problems linked to catalyst bed plugging by deposits do not usually occur in the ebullating bed reactor system. A schematic flow diagram of the ebullating bed reactor system is shown in Figure 2.14. The hydrogen-rich gas and the residual oil which has been preheated to the required temperatures and premixed in a specially designed mixer, are fed into the bottom of the reactor. The catalyst bed is maintained in an ebullated (expanded) state by an upward flow of the feed and the internal liquid recycle. Catalyst deactivation by coke and metals deposition can occur when various hydrotreating reactions (HDS, HDN, HDM, HYG & HC) are promoted by the catalyst. Therefore, in order to maintain a steady state activity, provision is made for periodic addition of fresh catalyst and withdrawal of the spent catalyst.

Although the catalyst deactivation in both types of reactor systems is generally believed to be caused by coke and metals deposits, specific information comparing the deactivation behaviour of catalysts in the multi-reactor, fixed bed atmospheric residue desulphurization (ARDS) process and the ebullated bed reactor is scarce in the open literature. In the present work a comparative study was made on the deactivation behaviour of industrial fixed bed and ebullated bed residue hydroprocessing catalysts.

5.1.2. Characterization of Fresh and Spent Residue Hydrotreating Catalysts.

Samples of fresh and spent catalysts used in different reactors of the atmospheric residue desulphurization unit of and in the ebullated bed reactor unit were acquired from Kuwait refineries and fully characterized. Table 5.1. presents the physical and mechanical properties of fresh and spent catalysts from various reactors of the ARDS unit. Table 5.2 presents the chemical properties of fresh and spent ARDS Catalysts. The catalyst characterization results for the ebullated bed reactor are presented in Tables 5.3 and 5.4.

The major objectives of this study were to:

(i) generate data on the characteristics of spent hydrotreating catalysts.

(ii) identify the extent and cause of deactivation of these catalysts, and to

(c) be able to compare the catalyst deactivation behaviour in fixed bed and ebullated bed reactors.

5.1.2.1 Chemical, Physical and Mechanical Properties of Fixed Bed ARDS Catalysts

The results presented in Table 5.2 show that in fixed bed residue hydroprocessing, catalyst samples discarded from different reactors (R1, R2, R3 and R4) connected in series contained substantially different concentrations of vanadium deposits. The vanadium concentration in the catalyst was highest (38 wt%) in the guard bed (R1) and lowest in the last reactor (R4) about 4.5 wt%. A similar trend is observed for nickel. The concentration of carbon deposits increased along the reactor series 1 to 4 in the order.

Guard Reactor 1< Reactor2 < Reactor 3 < Reactor 4. The amount of iron deposited on the catalysts was relatively small and decreased along the reactor series 1 to 4 with a maximum (0.19 wt%) in reactor 1 and a minimum in the last reactor. The sulphur contents of the spent catalysts from different reactors did not vary significantly. Since sulphur is

associated with both the metal and the coke deposits this trend is not unexpected. The spent catalyst also contained a certain amount of nitrogen; this. must have arisen from nitrogen compounds present in the feed. The nitrogen content of the spent catalyst increased with increasing coke content, indicating an association with the coke deposits. The quantities of other impurities, e.g. sodium and silicon, deposited on the catalyst during the hydrotreating process were relatively small and do not show significant variation between different reactors.

The physical properties of the catalyst samples from different reactors (Table 5.1) reveal the following. The catalyst in the last reactor had lost 70% of its original surface area whereas the losses in surface area for the 2nd and 3rd reactors in series were about 60%. In the guard bed reactor the loss was about 63%. The highest loss in surface area was suffered by the catalyst in the last reactor; this would be expected due the deposition of a large amount of coke (26.43 wt%). The side crushing strength of the spent catalyst in R1 was significantly increased whilst that in the others decreased relative to the fresh catalyst crushing strength. The largest loss in side crushing strength occured in catalyst from Reactor 4. In case of the guard bed reactor (R1) a large amount of vanadium was accumulated in the catalyst pores; this was probably responsible for the increased crushing strength. The bulk densities of the spent catalysts from all reactors were higher than that of the fresh catalyst. This correlated with the depostion of the highest amount of metal deposits in the guard bed (HDM Catalyst). Accumulation of metals simply fills the pores in the catalyst pellets and hence increases the bulk density. The largest increase of bulk density (100%) was found for the spent catalyst in the guard bed reactor (R1).

5.1.2.2. Chemical, Physical and Mechanical Properties of Ebullating Bed Catalyst

Unlike the fixed bed (ARDS) process, in the ebullating bed process the catalyst bed is maintained in an expanded state and, to maintain steady state activity, a portion of the spent catalyst is periodically withdrawn from the reactor and an equal amount of fresh catalyst added.

Table 5.1. Physical and Mechanical Properties of Fresh and Spent ARDS Catalyst in Fixed Bed Reactor

Catalyst Properties	Fresh Catalyst		Spent Catalyst			
	R1	R2, R3 & R4	R1	R2	R3	R4
Surface area (m^2/g)	199	257.2	55	77	101	104
Pore Volume (ml/g)	0.68	0.39	.05	.15	.19	.16
Bulk density (g/ml)	0.55	0.71	1.10	1.03	1.00	1.00
Side Crushing Strength (N/mm)	4.68	7.52	5.64	7.25	6.80	5.91

Table 5.2. Chemical Properties of Fresh and Spent ARDS Catalyst in Fixed Bed Reactor

Chemical Properties (wt %)	Fresh Catalyst		Spent Catalyst			
	R1	R2, R3 & R4	R1	R2	R3	R4
MoO_3	3.3	11.5	3.00	11.2	11.3	11.3
CoO	ND	3.65	ND	3.0	3.30	3.35
V_2O_5	ND	ND	38	34	9.7	4.50
NiO	1.1	<.02	6.90	5.8	2.90	2.10
Al_20_3	87.7	80.8	38	48	63	70.60
Fe_2O_3	0.06	0.1	0.19	0.1	0.11	0.10
SiO_2	0.57	0.5	0.41	0.42	0.43	0.43
C	-	-	13.50	17.8	23.4	26.43
H	-	-	1.70	2.25	1.50	1.9
N	-	-	0.17	0.25	0.30	0.28
S	-	-	4.6	6.25	5.90	5.30

Samples of fresh and spent Catalyst were characterized and the results are presented in Table 5.3 and 5.4. The spent catalyst contained large amounts of carbon (17.8 wt%), sulphur (13.13 wt%) and vanadium (18.4wt%). Its bulk density was considerably higher (120%) than that of the fresh catalyst. The surface area and crushing strength of the spent

catalyst were substantially lower than that of the fresh catalyst (79.66%, 20% respectively). The pore volume was remarkably low. Significant changes appeared in the length distribution of the catalyst particles; for example in the fresh catalyst a major percentage (74.75%) of the particles had lengths in the range 2.5 - 6.3 mm, whereas the spent catalyst contained only 29.9% of the particles in this range. The catalyst particles appear to break into smaller sizes during use in the ebullated bed process presumably because they are in continuous motion and subject to mechanical attrition. Obviously, such changes in the physical dimensions and bulk density of the catalyst affect the bed expansion behavior.

Table 5.3. Chemical Properties of Fresh and Spent Catalyst in Ebullating Bed Reactor

Chemical Properties (wt %)	Catalyst	
	Fresh	Spent
MoO_3	13	7.9
NiO	3.6	5.00
V_2O_5	-	18.4
Al_20_3	75.6	64.3
Fe_2O_3	< 0.05	0.14
Na_2O	< 0.03	2.40
SiO_2	< 0.05	< 0.1
C	-	17.8
H	-	1.3
N	-	0.19
S	-	13.13

5.1.3. Characterization of Spent Catalysts by Special Tests.

In addition to the physical, mechanical and chemical tests, some special tests were used to characterize the spent catalyst samples from fixed and ebullated bed reactors. These included electron microprobe analysis, temperature programmed oxidation (TPO), thermogravimetric analysis (TGA) and differential thermal analysis (TDA). These tests were primarily aimed at analysing the difference in the nature of coke and metal deposits on the catalyst in different reactors as an aid to understanding their role in catalyst deactivation.

Table 5.4. Physical and Mechanical Properties of Fresh and Spent Catalyst in Ebullating Bed Reactor

Catalyst Properties	Catalyst	
	Fresh	Spent
Surface Area (m^2/g)	331	67.3
Pore Volume (ml/g)	0.65	0.0958
Bulk density (g/ml)	0.564	1.24
Side crushing strength (N/mm)	1.94	1.554
Average length (mm)	3.72	3.18
Particle length distribution (wt %)		
< 0.5 mm	0	2.1
< 1.0 mm	0.3	5.7
< 1.6 mm	3.9	18.5
2.5 mm	17.8	19.5
2.5 - 6.3 mm	74.75	29.9
Pore size distribution (ml/g)		
> 250Å	0.23	0.0760
> 500Å	0.22	0.0750
1500 Å	0.19	0.0740
4000Å	0.15	0.0740

5.1.3.1. Distribution Profiles of Metals in Spent Catalysts from Fixed and Ebullated Bed Reactors.

Figure 5.1. shows the distribution profiles of vanadium within the spent catalyst pellets from various reactors in the fixed bed ARDS unit. Clearly that vanadium penetration into the catalyst pellet was deeper in Reactor 1 than in the other reactors. More vanadium accumulated near the outer surface than the interior of the catalyst pellet in all reactors; however, the vanadium distribution across the pellet cross section was higher and more uniform in Reactor 1 spent catalyst. The vanadium concentration inside the pellet decreased and that near the outer edge sharply increased in moving from the first to the last reactor.

The deeper penetration, and more even distribution, of vanadium in reactor 1 spent catalyst may be attributed to the larger pores in the catalyst loaded into this reactor. Since the residual oil feed containing the metals and other impurities first comes into contact with the catalyst in the guard bed reactor (R1), the metals tend to deposit first on the catalyst in this reactor as a result of the HDM reaction. The guard bed catalyst is designed to promote HDM reactions and contains macro-pores that allow easy diffusion of large metal-containing molecules into the active sites within the catalyst pores (33). This catalyst has a higher metal capacity than the others as demonstrated by the vanadium content of the spent catalysts (Table 5.2.).

In Figure 5.2, the distribution profiles of nickel in the spent catalyst from various reactors are shown. These demonstrate that nickel distribution within the pellet was more uniform than vanadium. This indicates that nickel-containing molecules in the residual oil diffuse more easily into the catalyst pores than the vanadium-containing species. This is in agreement with the results of Quan et al., (33) who reported that vanadium porphyrin is more reactive, and more controlled by diffusion, than the nickel porphyrins.

The distribution of the original catalyst materials (Mo and Co) show uniform profiles (Figures 5.3 and 5.4). This indicates that changes in the distribution of the catalytically active materials are insignificant during hydrotreating.

With regard to the ebullated bed reactor, vanadium was present in high concentrations near the external surface of the catalyst pellet and decreased to a minimum at the center (Figure 5.5). The other metals (Ni and Mo) were evenly distributed across the pellet.

5.1.3.2. Temperature Programmed Oxidation (TPO) Studies.

The spent catalyst samples collected from different reactors of fixed and ebullated process units were subjected to temperature-programmed oxidation with a gas mixture containing 5% O_2 in helium. This was performed in the temperature programmed oxidation unit (Al-Tamira, USA). A linear heating rate of 10°C/min. was used throughout, and the different gaseous products formed during coke oxidation were monitored as a function of temperature using a Gas Lab 300 mass spectrometer. The main purpose was to obtain information on the nature of the coke deposits on the catalysts in different reactors and their reactivities.

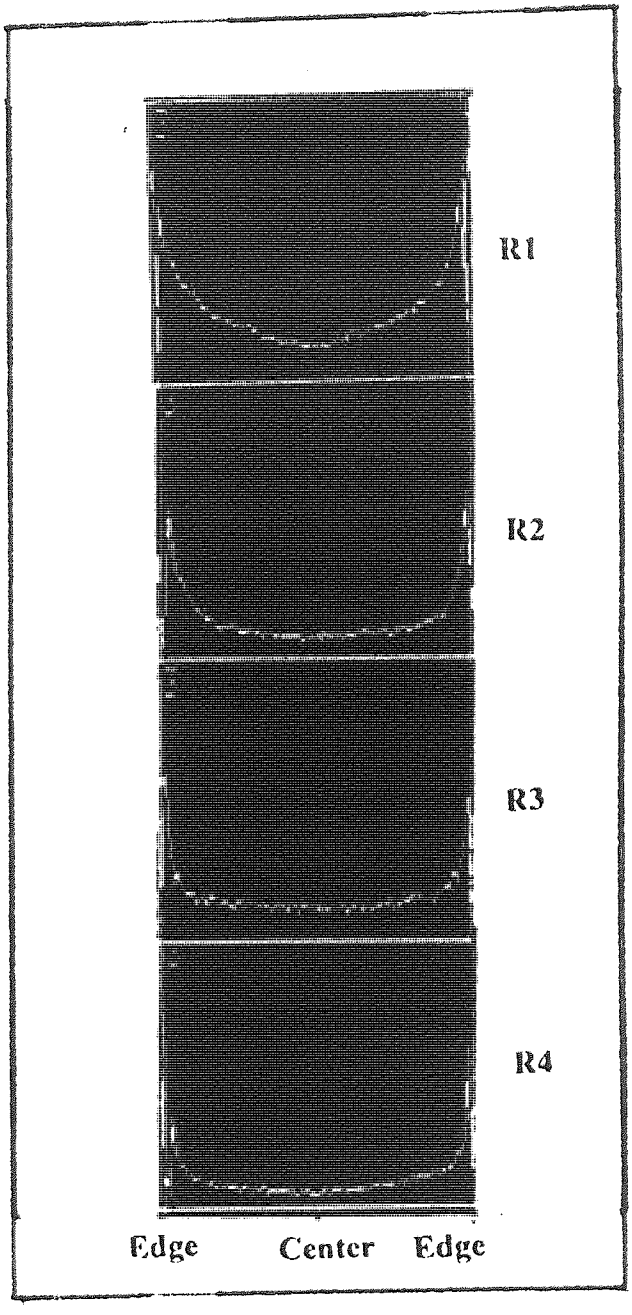

Figure 5.1. Vanadium Distribution Profiles Within Spent Catalyst Pellets from Various Reactors in ARDS Unit.

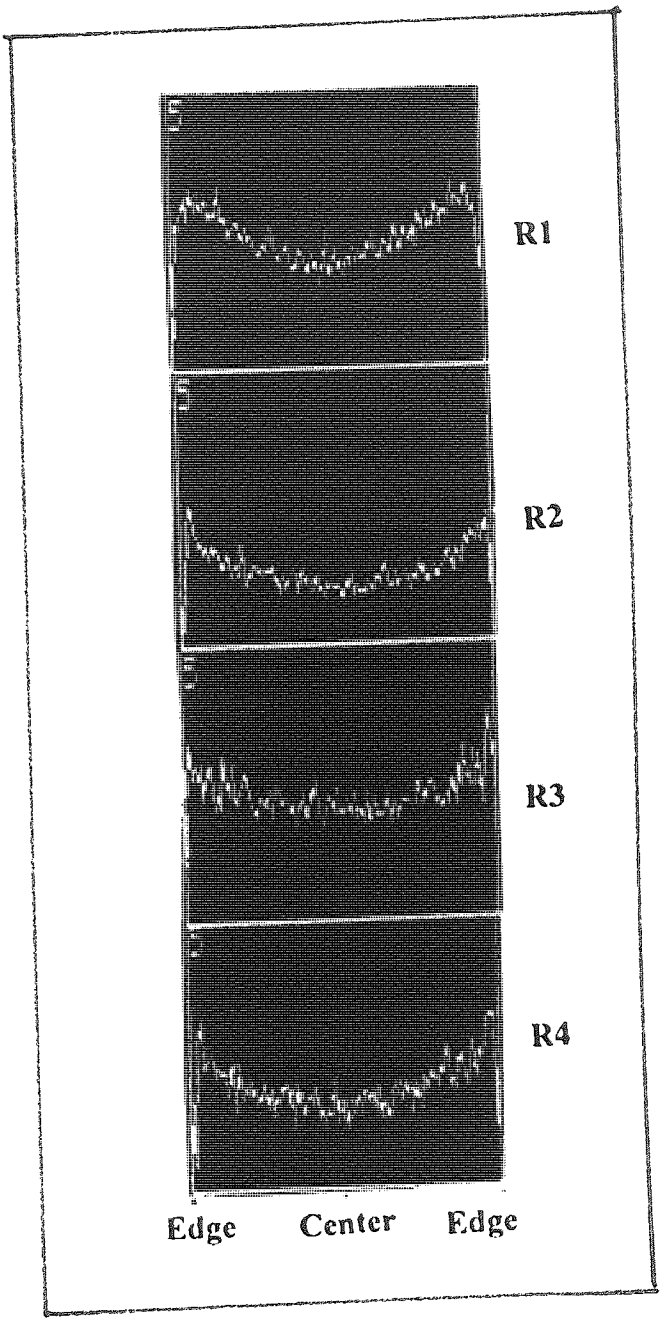

Figure 5.2. Nickel Distribution Profiles Within Spent Catalyst Pellets from Various Reactors in ARDS Unit

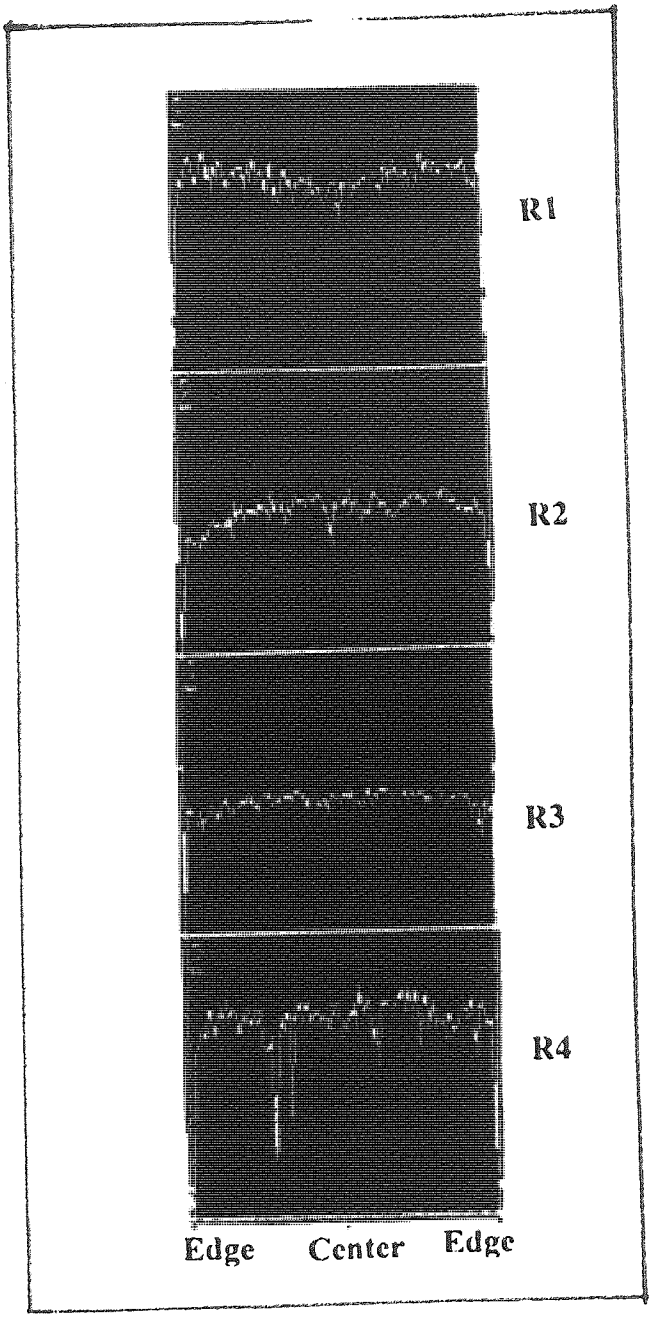

Figure 5.3. Molybdenum Distribution Profiles Within Spent Catalyst Pellets from Various Reactors in ARDS Unit

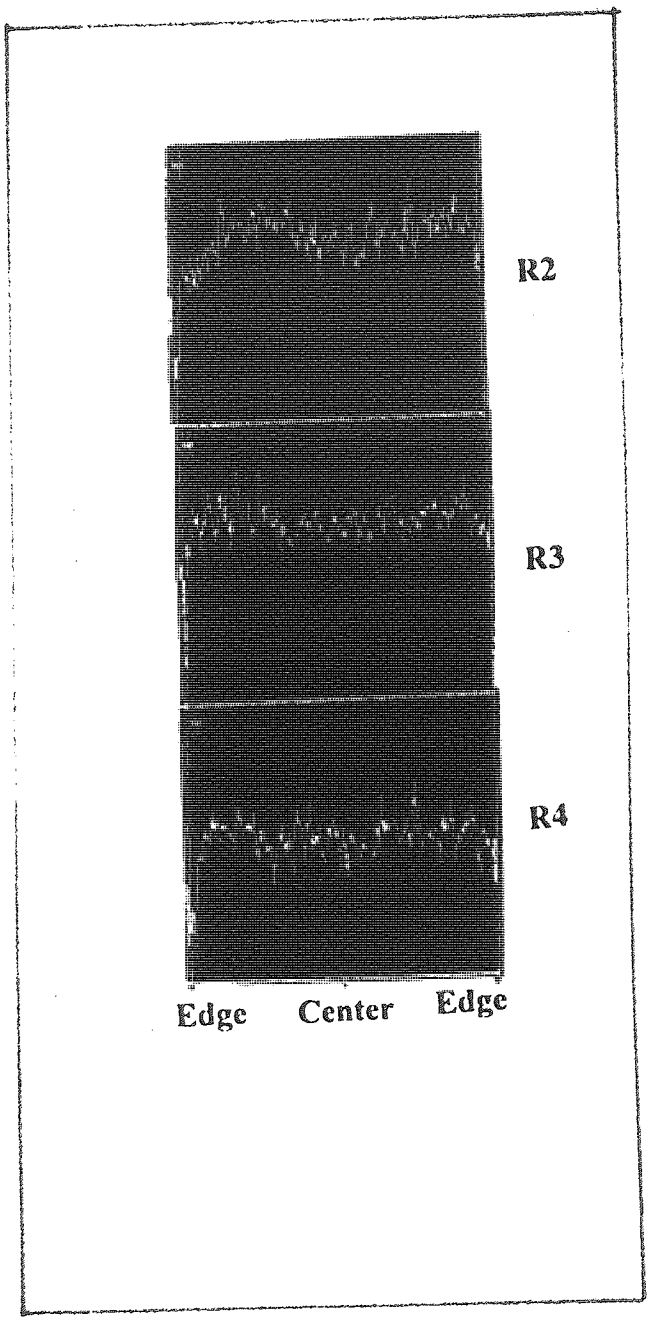

Figure 5.4. Cobalt Distribution Profiles Within Spent Catalyst Pellets from Various Reactors in ARDS Unit.

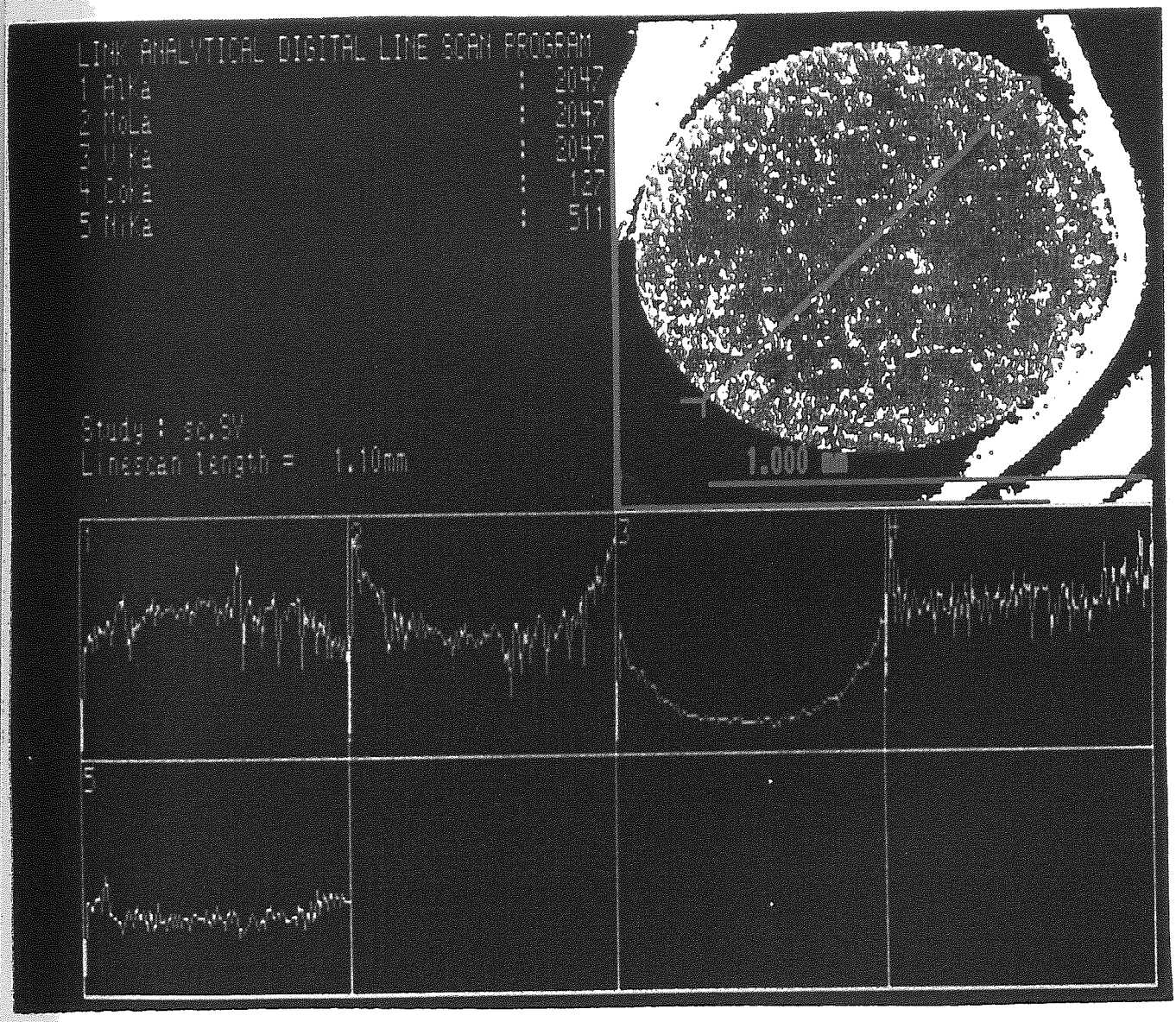

Figure 5.5 Distribution Profiles of Vanadium and Other Metals Within a Spent Catalyst Pellet in Ebullated Bed Reactor.

The TPO profiles of various gaseous products formed during the temperature programmed oxidation of a sample of the spent catalyst from the guard bed reactor (Reactor 1) are shown in Figure 5.6. Similar TPO profiles for the spent catalysts from the other three reactors in the ARDS unit and from the Ebullated Bed units are shown in Figures 5.7 - 5.10 . These demonstrate that various gases such as CO, CO_2, SO, SO_2, NO, NO_2 and H_2O are formed during a typical TPO run. This indicates the presence of C, H, S and N in the spent catalysts. The C, H, N and part of the sulphur are known to be associated with the coke deposits (30, 95). A major part of the sulphur in spent hydrotreating catalysts is usually associated with the metals, e.g., metal sulphides (128). Under the conditions used for TPO, the sulphur in the coke and metals is oxidized to both SO and SO_2, the nitrogen in the coke to NO and NO_2 and the carbon to CO and CO_2.

The peak shapes and peak temperatures of the various gases evolved during the TPO runs differ considerably for different catalysts. Thus, for example, in the case of the spent catalyst from the guard bed reactor, the TPO profiles of various gases demonstrate very broad peaks Figure 5.6. The SO and SO_2 profiles differ significantly from the others. Four distinct peaks at 180, 325, 415 and 600°C are observed for both SO and SO_2 formation, indicating that the combustion of the sulphur present in the spent catalyst occurs at these temperatures. The first SO and SO_2 peaks appear at a relatively lower temperature, namely 180°C. There is an absence of peaks for CO, CO_2, NO, and NO_2 coincident with the first SO_2 peak. This suggests that the form of which sulphur oxidizes at around 180°C is not associated with coke. As suggested by previous workers [Dufresne, (45); Yoshimura (38)], the first broad low temperature SO or SO_2 peak can be attributed to the oxidation of metal sulphides present in the catalyst. However, the spent catalyst used in the present work was from a residue hydrotreating unit and contained a substantial amount of vanadium sulphide in addition to Mo and Ni sulfides.

To check if the first SO_2 peak originated from the oxidation of all three types of metal sulphides, the TPO patterns of alumina-supported sulphides of Mo, Ni and V were studied individually. The results showed that both the vanadium and nickel sulphides oxidized with the formation of a major SO_2 peak around 180°C, whereas the MoS_2 oxidized over a wide temperature range (170 - 300°C) with two major broad peaks overlapping in the 250 - 300°C region and a shoulder peak at a relatively lower temperature (170°C).

A comparison of SO_2 profiles from these standard metal sulphides with that of the spent catalyst from Reactor 1 clearly indicated that the first (low temperature) SO_2 peak appearing around 180°C, and part of the second peak appearing around 300°C, result from

the oxidation of metal sulphides. For reactor 2 spent catalyst the sulphur oxides (SO and SO_2) exhibit the expected broad low temperature (180°C) peak resulting from the oxidation of metal sulphides. The second peak, and the associated broad shoulder of sulphur oxides, coincide exactly with the carbon oxide (CO and CO_2) formation profiles. The high temperature (600°C) SO and SO_2 peaks found in the case of the guard bed spent catalyst are also present for the second reactor spent catalyst but the corresponding CO_2 and NO_2 peaks are absent. The high temperature sulphur oxide peaks probably result from the oxidation of part of the vanadium sulphide. Spent catalysts from Reactors 1 and 2 contain substantially larger amounts of vanadium.

These data suggest that the combustion of coke deposits on the second reactor spent catalyst starts at about 200°C, reaches a maximum in the temperature range 300 - 325°C and is complete at about 470°C. The guard bed spent catalyst appears to contain some hard refractory type of coke which requires temperatures as high as 600°C for its oxidation. No such hard or refractory coke was present in this spent catalyst.

The TPO profiles of carbon and nitrogen oxides for the spent catalyst from reactor 3 are similar to those of Reactor 2 catalyst, except that the major peaks (Peak Nos. 2 and 3) are shifted to a high temperature range. For example, in the case of Reactor 2 spent catalyst, the major CO_2 (and NO_2) peak temperature was 325°C, whereas for Reactor 3 spent catalyst, this peak appears at 360°C. A similar shift is also observable in the next peak (Peak No. 3) which appears as an incompletely-resolved shoulder to Peak No. 2.

Interestingly, the three high temperature (>300°C) SO_2 peaks coincide exactly with the CO_2 and NO_2 peaks; this suggests that the sulphur oxidized at these temperatures is associated with the coke. The TPO data presented in Figure 5.6 indicate that coke oxidation occurs in three 3 distinct temperature regions, namely 320°C - 340°C, 400 - 420°C and 600°C, generating CO_2, SO_2 and NO_2.

It has been suggested that the nature of the coke (e.g., aromaticity, hardness, refraction) influences its reactivity as well as the maximum temperature required for removal by combustion (Furimsky and Massoth, (92). The results reported here indicate that a part of the coke present in the guard bed (Reactor 1) spent catalyst is very refractory and requires temperatures as high as 600°C for removal by oxidation.

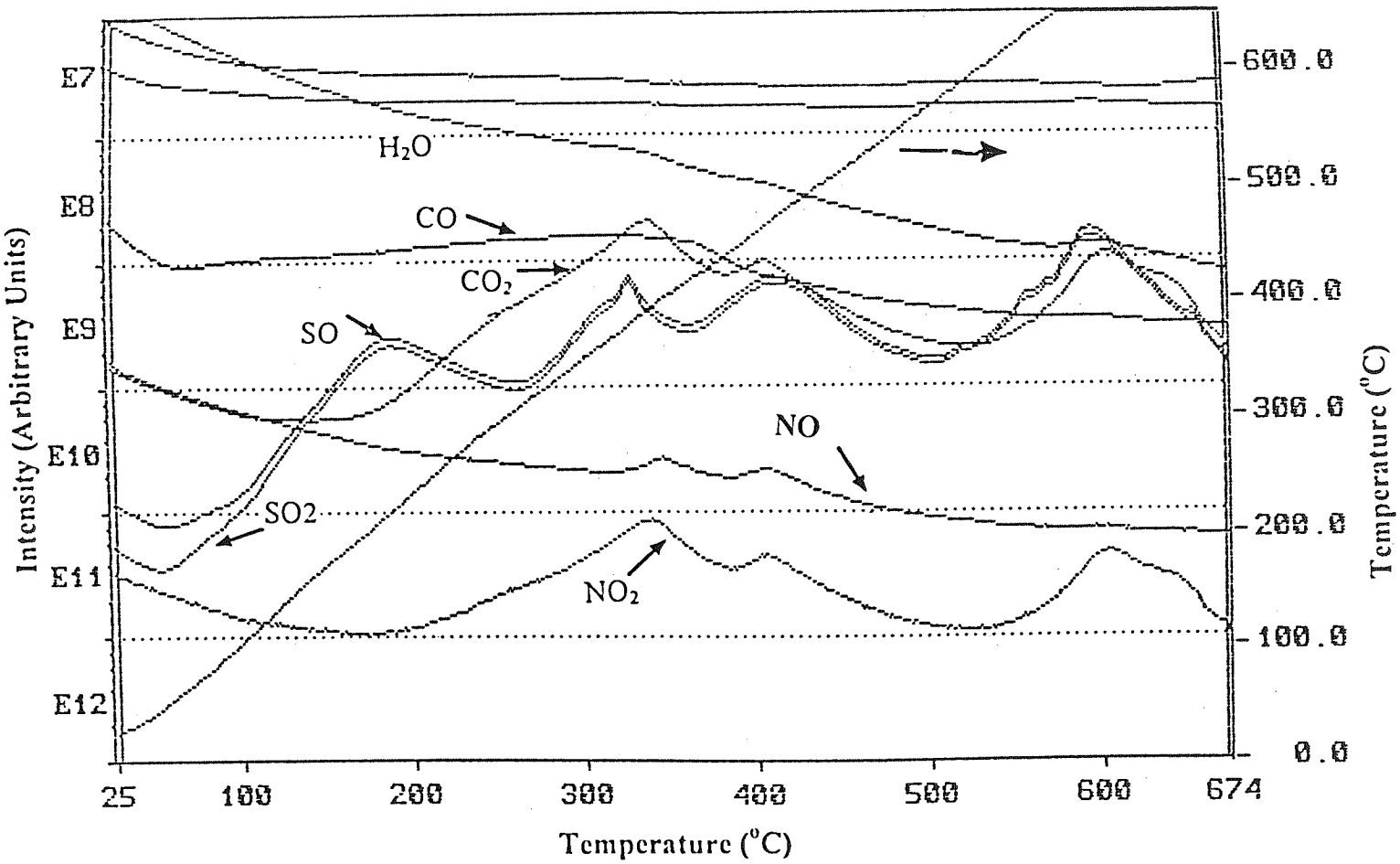

Figure 5.6 TPO profiles of Gaseous Products for Reactor-1 (Guard Bed) Spent Catalyst.

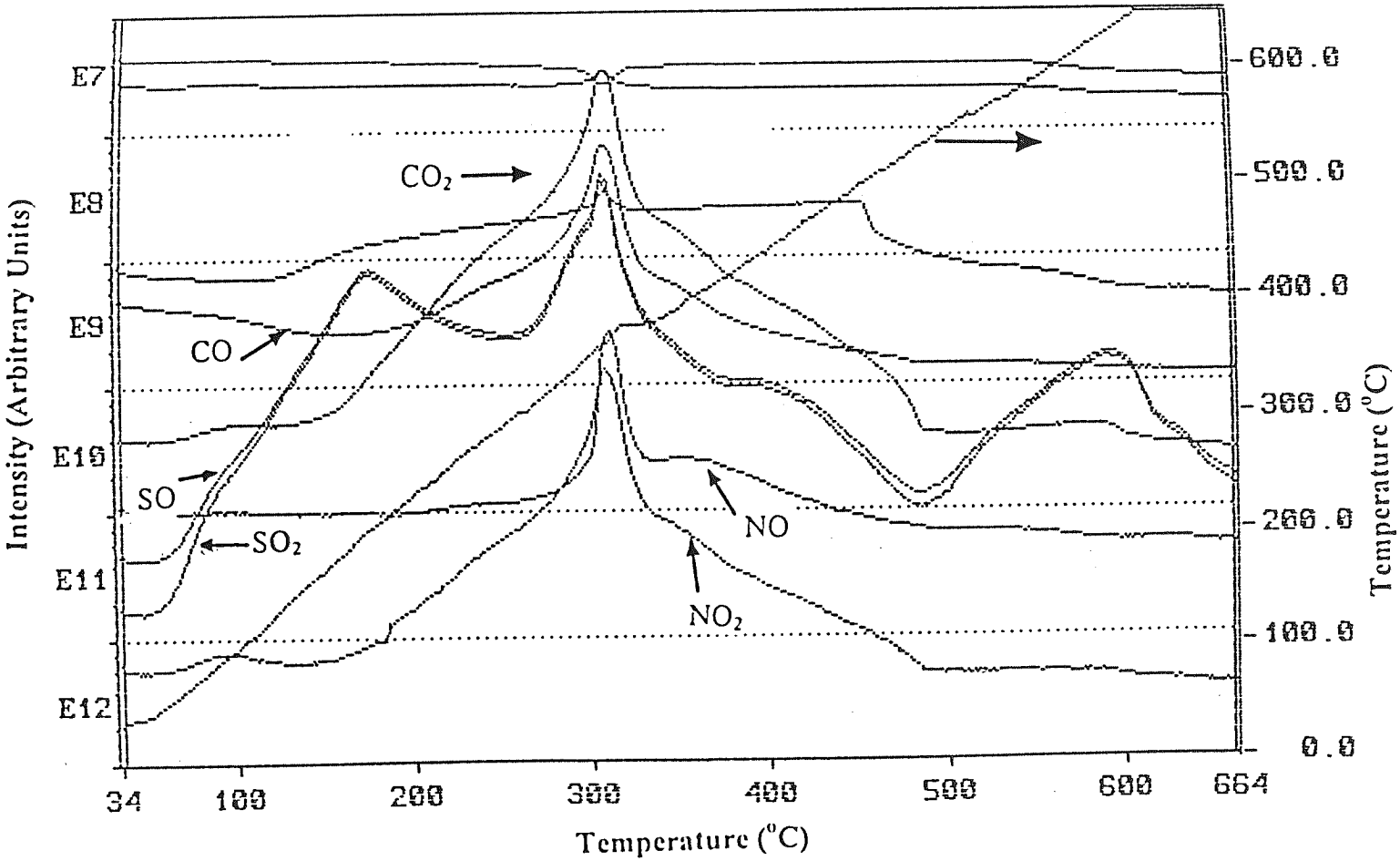

Figure 5.7. TPO Profiles of Various Gaseous Products for Reactor 2 Spent Catalyst.

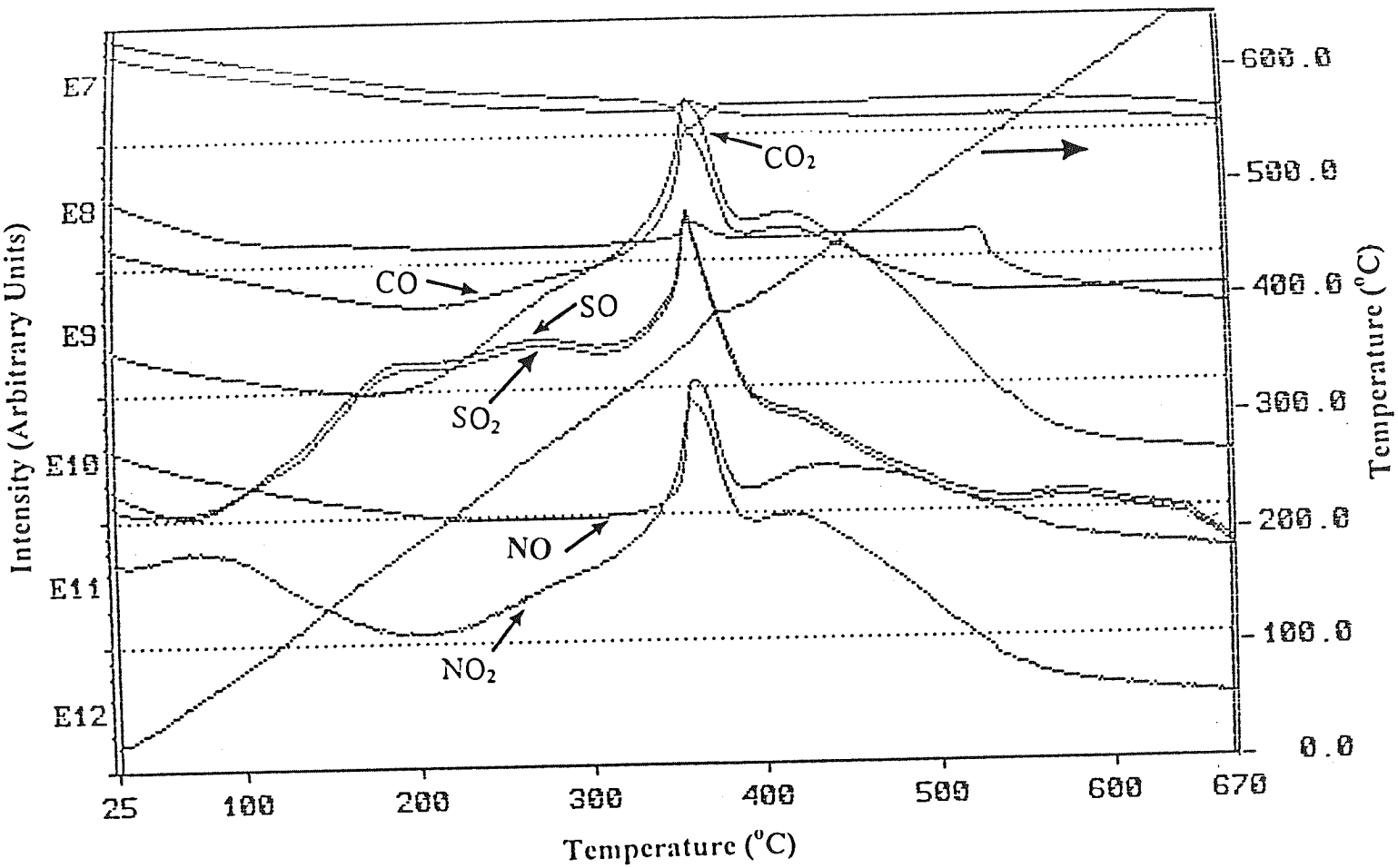

Figure 5.8. TPO Profiles of Various Gaseous Products for Reactor 3 Spent Catalyst.

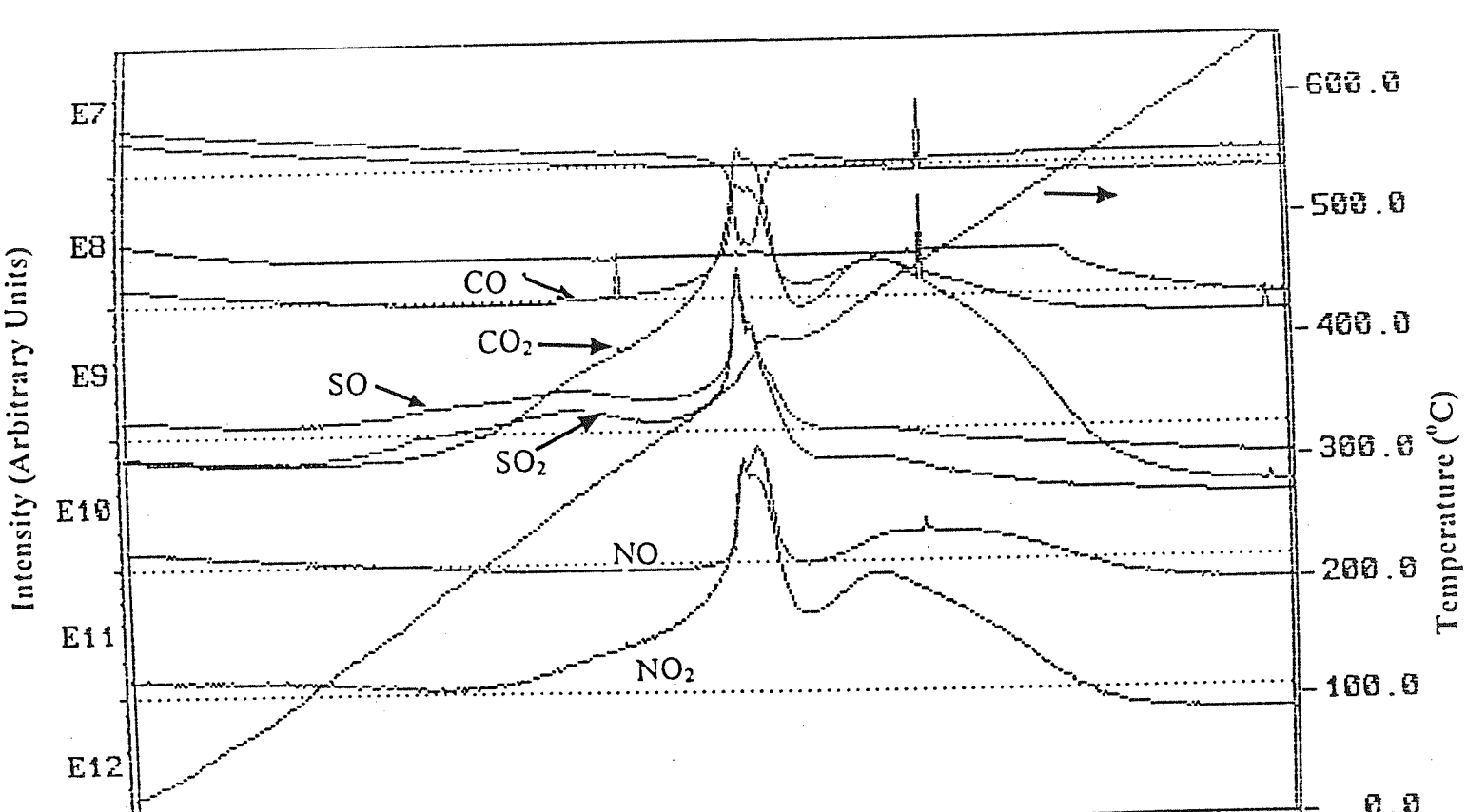

Figure 5.9. TPO Profiles of Various Gaseous Products for Reactor 4 Spent Catalyst.

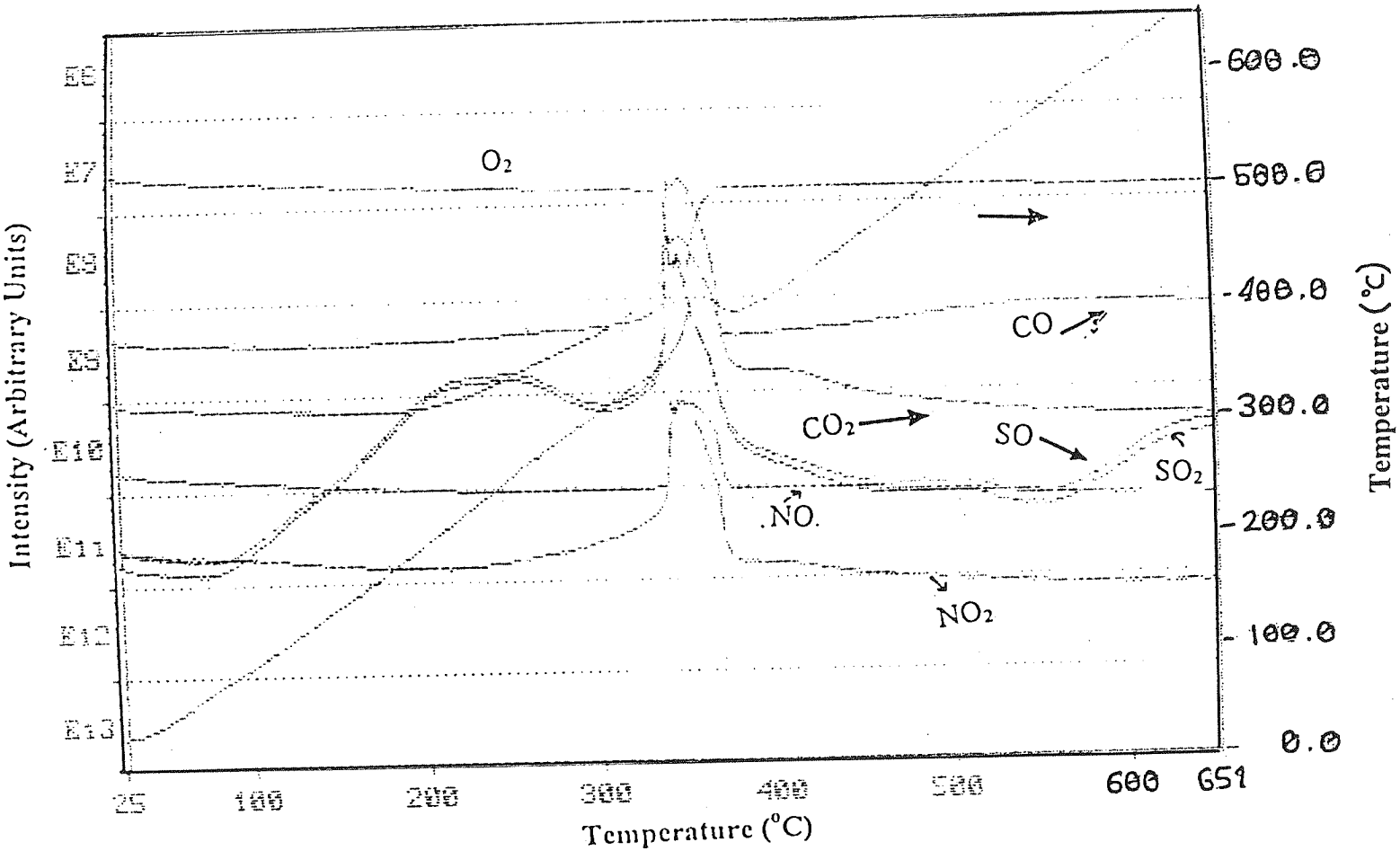

Figure 5.10. TPO Profiles of Various Gaseous Products for Ebullated-bed Spent Catalyst.

The trends in the formation of various gas products during the TPO of the spent catalyst from Reactor 2 show significant differences when compared with those of Reactor 1 spent catalyst. The peaks for various gases are sharper and well-defined. The formation of CO and CO_2 shows a prominent peak at 320°C, with shoulders above and below this temperature region. NO and NO_2 formation shows similar trends, with their peaks exactly coinciding with the CO_2 peaks. No high temperature CO_2 or NO_2 peaks are observed. The broad low temperature sulphur oxides (SO and SO_2) peaks are more resolved and appear as two peaks at 185°C and 250°C in the case of spent catalyst from reactor 3. One of the peaks coincides with the low temperature CO_2 and NO_2 peak at 250°C; this indicates that a part of the sulphur oxidizing at this temperature region is present in the coke.

The TPO profiles of various gaseous products for the ebullated bed spent catalyst are presented in Figure 5.10. The peaks for various gases are sharp and well-defined as in the case of ARDS reactor 4 spent catalyst.

Almost all gases (CO_2, CO, SO_2, NO_2 and NO) show a prominent peak around 350°C at which major coke oxidation occurs, indicating that the coke deposits on the ebullated bed catalyst contain C, S and N. Interestingly, for the ebullated-bed catalyst this major coke oxidant peak is at a temperature about 15°C lower compared with that of the ARDS spent catalyst from reactor 4. This can be attributed to the high V content of the H-Oil spent catalyst. For the sulphur oxides (SO and SO_2) the high temperature (>600°C) peak is formed in addition to the prominent sharp peak around 350°C as observed in the case of ARDS reactor 1 and reactor 2 spent catalysts. This confirms that the spent catalyst from the ebullated bed reactor contains high concentrations of vanadium sulphide which oxidizes at temperatures around 600°C.

It may be concluded that the coke present in the spent catalyst undergoes oxidation in three distinct temperature regions, producing oxides of carbon, sulphur and nitrogen. The coke oxidation was complete at temperatures around 500°C. The temperature at which coke combustion took place at a maximum rate, and the temperature needed for complete coke combustion, were about 35°C higher for the spent catalyst from Reactor 3 compared with that of Reactor 2. The exact reasons for this difference in coke combustion temperature are not clear. Analytical data indicated that the spent catalyst from Reactors 2 and 3 had similar coke contents, but differed in their vanadium contents. Reactor 2 spent catalyst had a much higher vanadium content than Reactor 3 spent catalyst. Vanadium is

known to enhance oxidation reactions, and it is commonly used as an oxidation catalyst. It is, therefore, possible to attribute the lower coke combustion temperature observed for Reactor 2 spent catalyst to its higher vanadium content. This is further confirmed by the fact that Reactor 3 and Reactor 4 spent catalysts, which had similar coke and vanadium contents, exhibited identical TPO patterns (Figures 5.8 - 5.9).

5.1.3.3. Thermogravimetric Analysis (TGA)

In thermogravimetric analysis, a small amount of the spent catalyst is heated in a current of air and the weight loss is recorded as a function of temperature. A linear heating rate (e.g., 10°C/min.) is normally used using a temperature programmed furnace. Inflections in the weight loss curve indicate phase changes due to oxidation or other thermal reactions. For example, the following chemical reactions can occur during coke combustion from a spent catalyst leading to phase changes and weight loss:

$C(s) + O_2(g) \rightarrow CO_2(g) + \Delta H$ cal/mole.

$S^{2-}(s) + O_2(g) \rightarrow SO_2(g) + \Delta H$ cal/mole.

The weight loss curves as a function of temperature can provide information about the reactivity of the materials and their thermal stability. The plateaus on the weight loss curve indicate stable phases over a temperature interval.

Figures 5.11 and 5.12 illustrate the weight loss curves as a function of temperature for the spent catalysts from two different reactors (R_2 & R_4). Three different temperature zones of weight loss are observable for spent catalysts. These three temperature zones can be classified as low (100 - 250°C), medium (300 - 450°C) and high (>600°C) zones. The largest weight loss occurs in the intermediate (300 - 450°C) range. The first inflection in the weight loss vs. temperature plot can be attributed to the loss of adsorbed moisture and light hydrocarbons and to the oxidation of metal sulphides. The large weight loss in the intermediate temperature region could be due to the oxidation of coke.

TPO results have shown that coke oxidation predominantly occurs between 300 and 450°C. The weight loss in the high temperature region is relatively small. In the case of the spent catalyst from the ebullated bed reactor (Fig. 5.13) the weight loss in the high temperature region (>600°C) was much higher than that with reactor 4 spent catalyst. This is to be expected, since the spent catalyst contained a substantial amount of vanadium

sulphide, and the weight loss in this region is caused by the removal of sulphur from vanadium sulphide by oxidation. Oxidation of a portion of the coke deposit that is more refractory may also partly contribute to the weight loss observed in the high temperature region. The TGA results are, in general consistent with the TPO data.

5.1.3.4. Differential Thermal Analysis (DTA)

In differential thermal analysis (DTA), changes in differential heat content of the sample are recorded as a function of the furnace temperature. The exothermal peaks indicate changes due to phase transitions, vaporizing, chemical changes, etc., and can be used to obtain information about the temperature at which chemical changes or phase transitions occur.

Figures 5.14, 5.15 and 5.16 show the DTA profiles for the three spent catalysts used in the present work. Three exotherms were apparent corresponding to the inflections in the TGA curves. Oxidative reactions of carbon, sulphur, nitrogen and hydrogen that occur during coke combustion are exothermic and yield a high heat of reaction. The first exothermal peak appears in the temperature region where the metal sulphide oxidation occurs. The second relatively large exothermal peak appears in the temperature region where major coke oxidation takes place. The third exotherm is relatively large for the spent catalyst from the ebullated reactor and corresponds with the third weight loss inflection temperature in the TGA curve.

In general, the DTA results support the conclusions reached in the TPO and TGA studies concerning the oxidation temperatures coke and metal sulfide.

5.1.3.5 Comparison between the Deactivation Pattern of Catalysts in Fixed Bed and Ebullating Bed Residue Hydroprocessing Units.

To obtain useful information on the deactivation pattern of the catalysts used in the fixed bed ARDS unit and the ebullating bed reactor, further consideration and comparisons between the physical, chemical and mechanical properties of both types of spent catalysts are presented below.

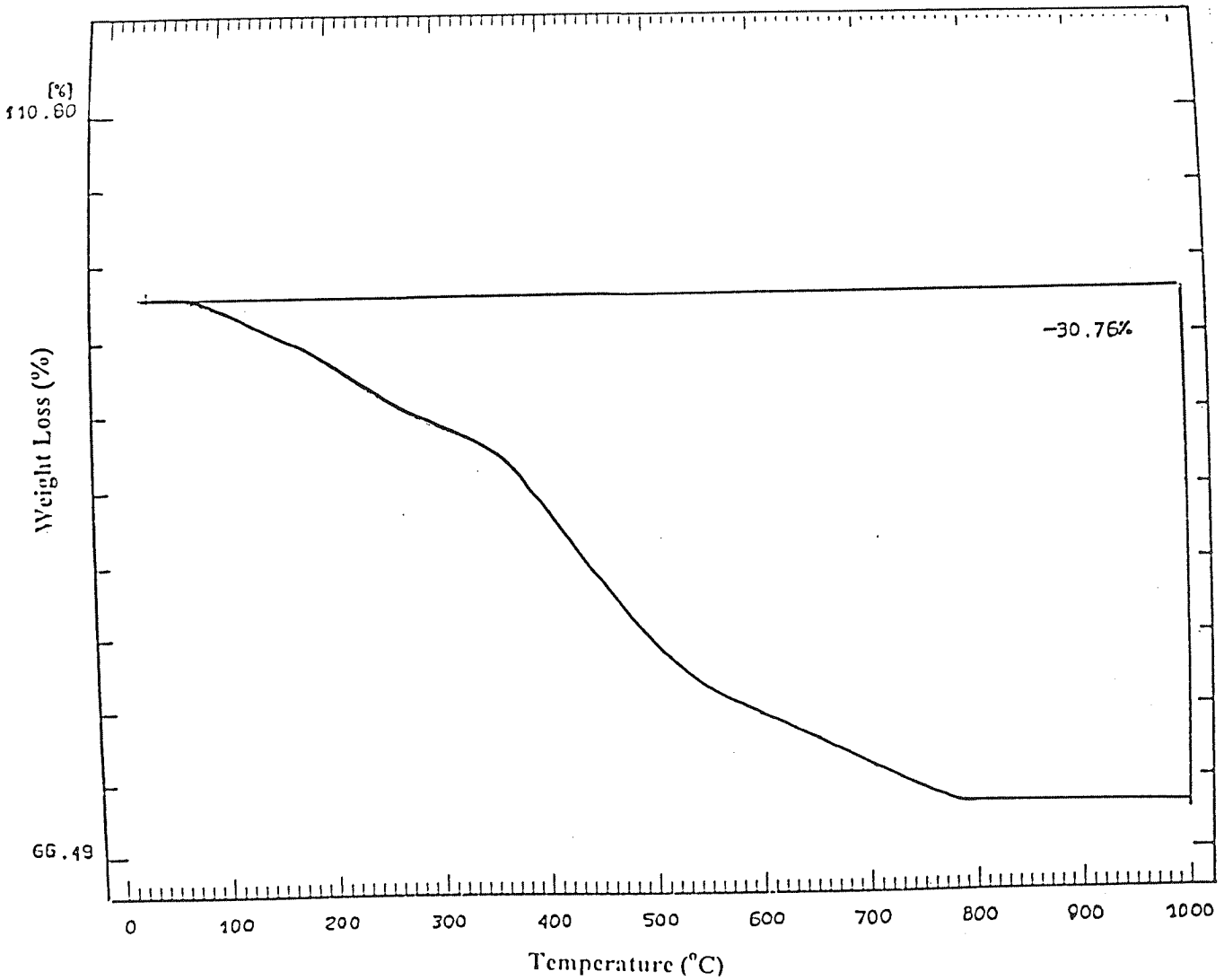

Figure 5.11. TGA Curve for Reactor 2 Spent Catalyst.

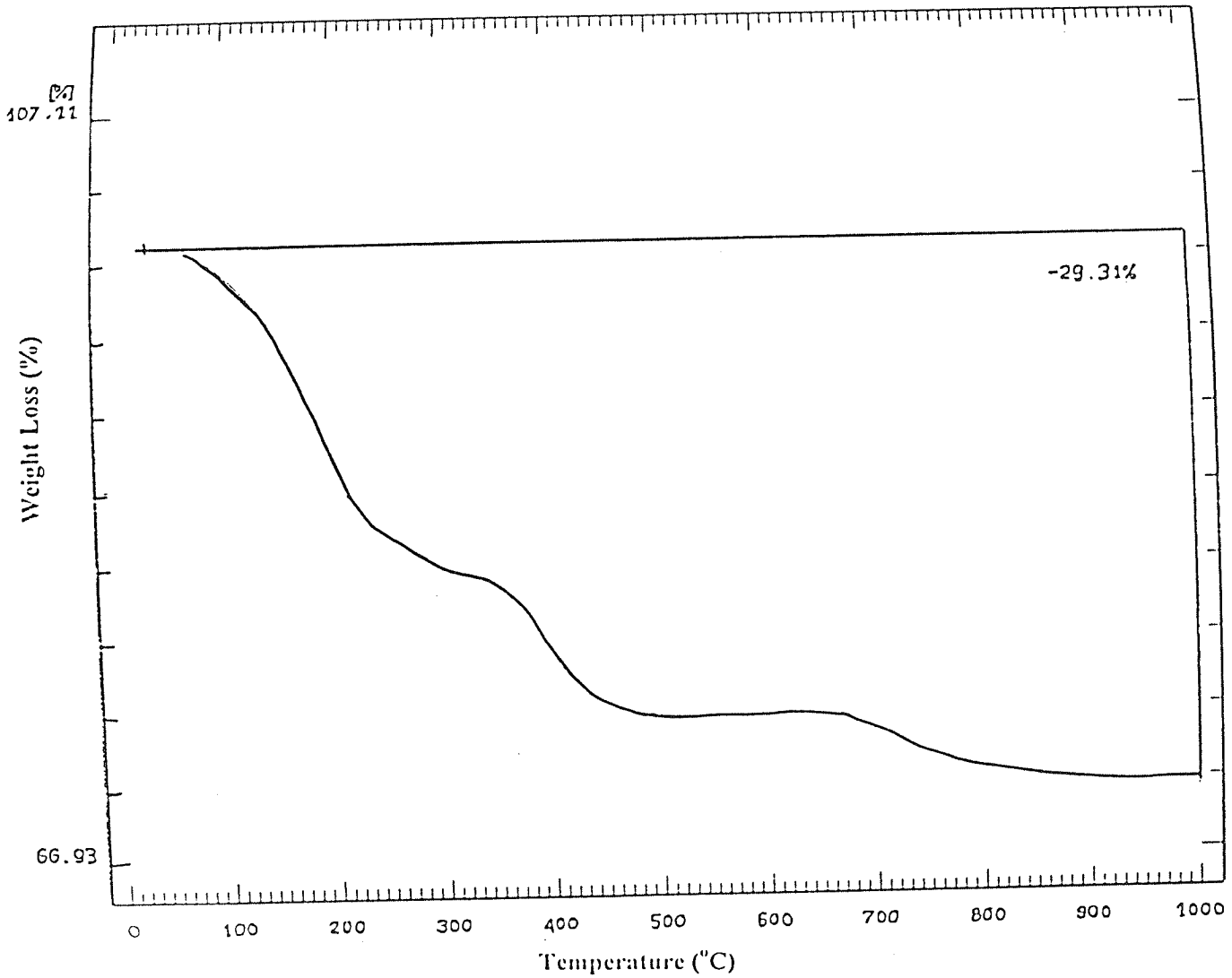

Figure 5.12. TGA Curve for Reactor 4 Spent Catalyst.

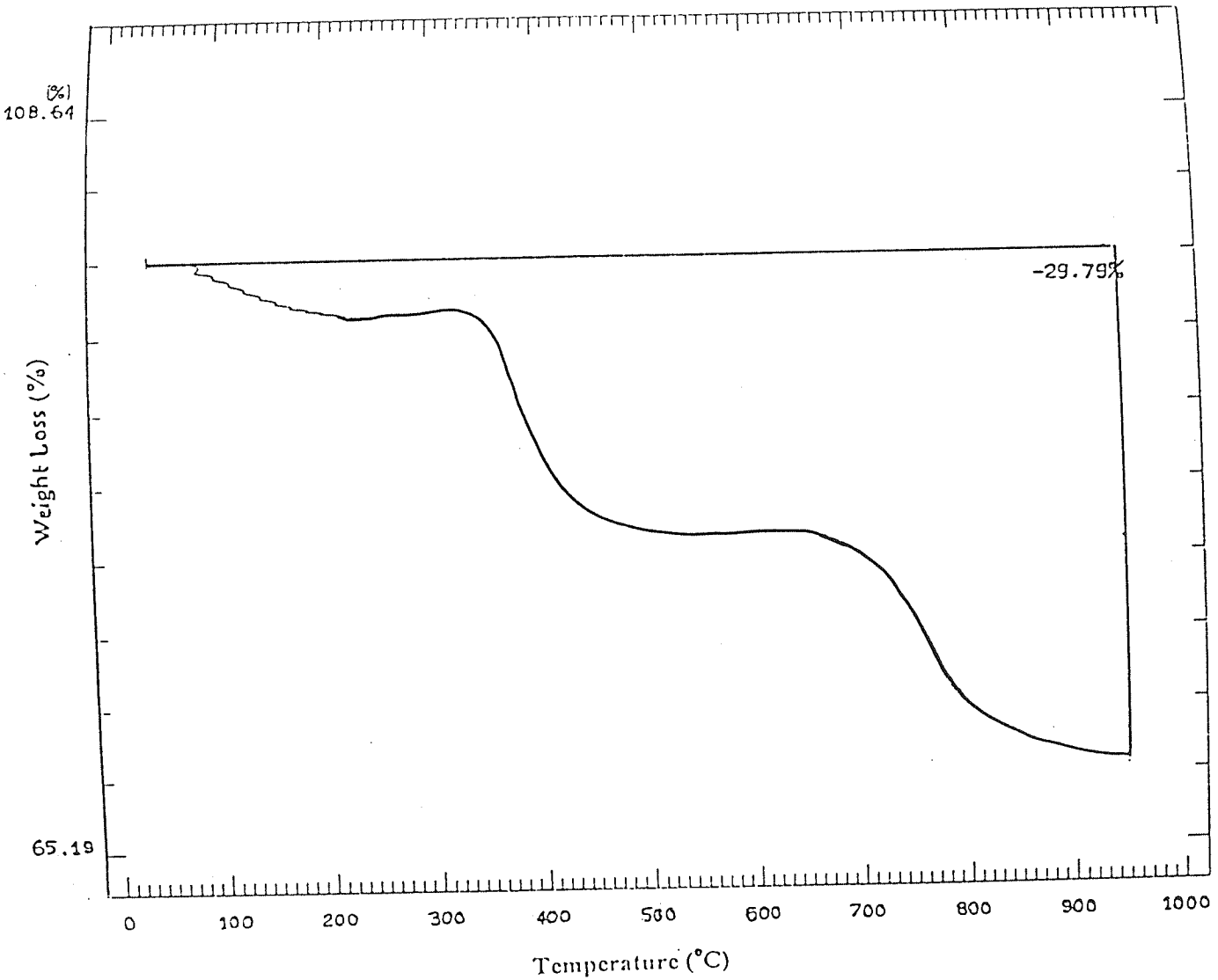

Figure 5.13. TGA Curve for Spent Catalyst from Ebullated-bed Reactor.

The carbon content of the catalyst in fixed bed reactors was found to increase from the entrance (Guard Reactor) to the exit (Last reactor). Thus in fixed bed units, the coke content of any catalyst pellet depends upon its location.

In an ebullating bed reactor, the catalyst particles are in continuous motion. Hence the coke content of a catalyst pellet does not depend upon its location. However, it would increase with increasing residence time in the reactor.

For both types of reactor, the major metal contaminants on the catalysts were vanadium and nickel. A small amount of iron was also deposited. In fixed bed reactors, contaminant metals deposition decreased from the entrance (Guard reactor) to the exit, whereas in the ebullating bed reactor, metals build-up depended primarily on the catalyst pellet residence time.

Since fresh catalyst is added and spent catalyst withdrawn periodically in ebullated bed reactors, and since the catalyst particles are in continuous motion, a portion of the catalyst which is not fully-deactivated by metal or coke deposition is also likely to be withdrawn. The spent catalyst from an ebullating bed reactor may, thus contain a mixture of highly contaminated or fouled, and partly fouled (low metal deposits), catalysts. This was confirmed by the observation that removal of carbon from the spent catalyst showed the presence of two types of particles, namely dark brown (highly fouled) and light brown or yellow (low metal contaminated) particles

Concentration profiles of vanadium across the catalyst pellet exhibited a maxima near the edge for samples from all reactors. The amount of vanadium penetrated and distributed within the pellet was however much larger for samples from the inlet reactor than for the outlet reactor. With catalyst from the ebullating bed reactor an edge concentration maxima for vanadium with a deeper penetration and distribution throughout the pellet was observed.

The surface area loss in catalyst samples from the fixed bed reactor system increased from the entrance to the exit. This observation is in line with the level of coke deposition which also increased from inlet to outlet.

In the case of the ebullating bed reactor the low metal-contaminated yellow particles had a higher surface area than the highly-fouled, dark brown catalyst particles.

Among other physical properties the average length and length distribution was significantly altered for catalyst pellets used in ebullating bed compared with those in the fixed bed. In the ebullated bed process the catalyst particles are in continuous motion;

hhence physical attrition of the particles to shorter lengths can occur more easily and result iin an increase in the percentage of smaller particles. The bulk density increase was similar ffor both ebullating bed and fixed bed catalysts and was caused primarily by the metal d deposits. The total pore volume was reduced by about 70-80%. The loss in the volume of p pores of less than 250 ¦ diameter was more pronounced.

In the ebullating bed hydrotreating process where the catalyst is in contact with the h heavy oil and hydrogen under dynamic conditions at high temperature and pressure, (decline in catalyst activity is caused not only by deposition of metals and coke, but also by (changes in the physical and mechanical properties of the catalyst.

Considerable changes in the physical dimensions (length and diameter) of the catalysts (occur by pellet breaking and attrition under the dynamic conditions of the process. As a result, the bed uniformity will be affected. If the particle dimensions are small (i.e. if the distribution is more towards fine particles) a large proportion of the catalyst will tend to float over the top of the bed hence affecting the mixing pattern. In addition, carry-over of catalyst fines will also take place to downstream vessels.

...Increase in the bulk density of the catalyst, which results from metals deposition will affect the bed expansion behaviour. Catalyst particles with a higher density will tend to sink to the bottom. A higher bulk density will, thus, require more ebullating fluid flow to achieve the required bed expansion in order to maintain the requisite catalyst contact with the oil and hydrogen.

5.2. INVESTIGATION OF INITIAL COKING AND ITS ROLE IN HYDROTREATING CATALYST DEACTIVATION

The spent catalyst analysis and characterization data presented in the previous section clearly indicate that coke deposition on the catalyst is a major cause of catalyst deactivation in the hydrotreating of petroleum oils. Despite intensive efforts by catalyst scientists to study catalyst deactivation by coke deposition, understanding of the nature of coke and its effect on different functions of the catalyst remains incomplete. In particular, the factors which influence the initial coking, and its role in catalyst deactivation, appear to have received little attention.

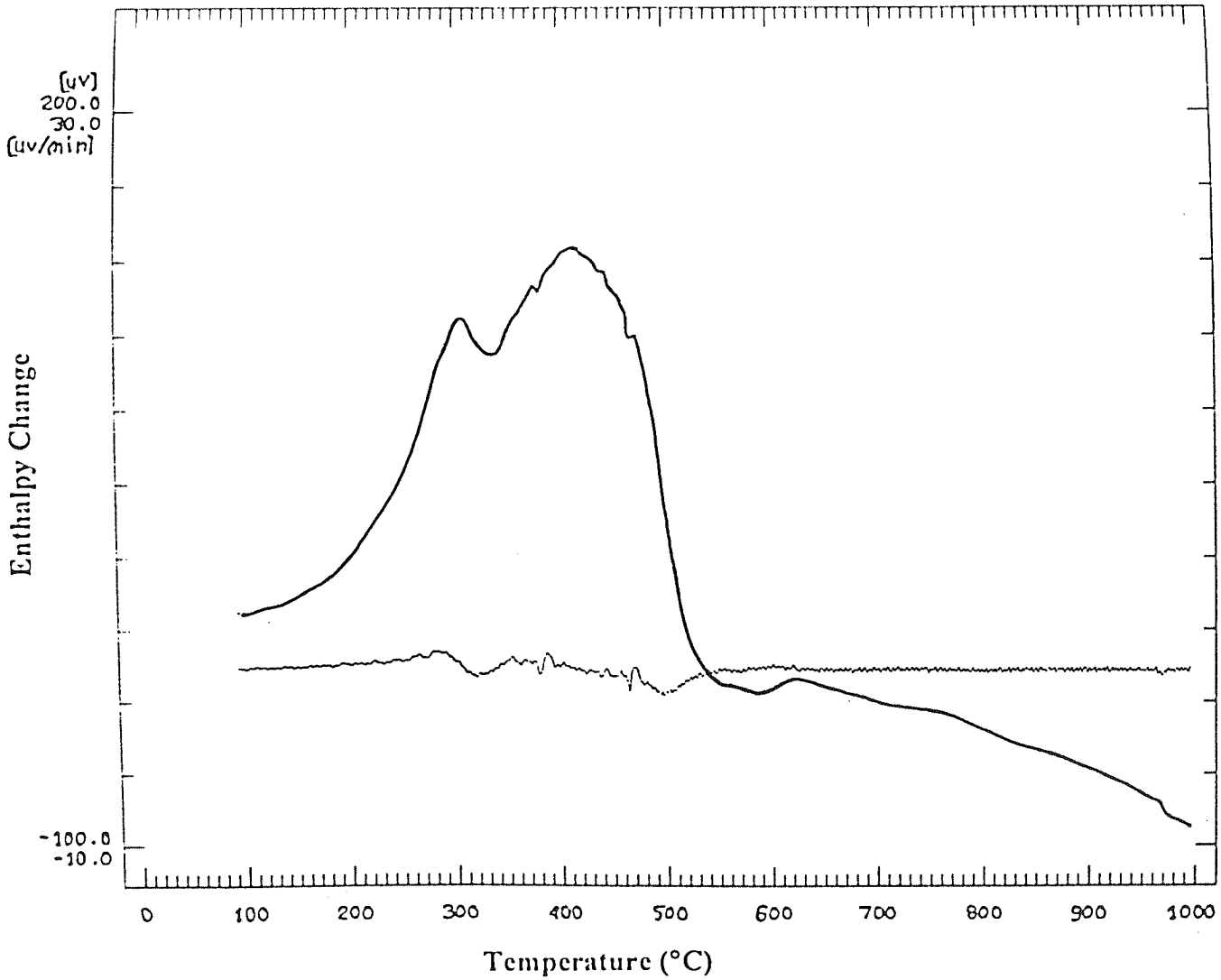

Figure 5.14. DTA Curve for Reactor 2 Spent Catalyst.

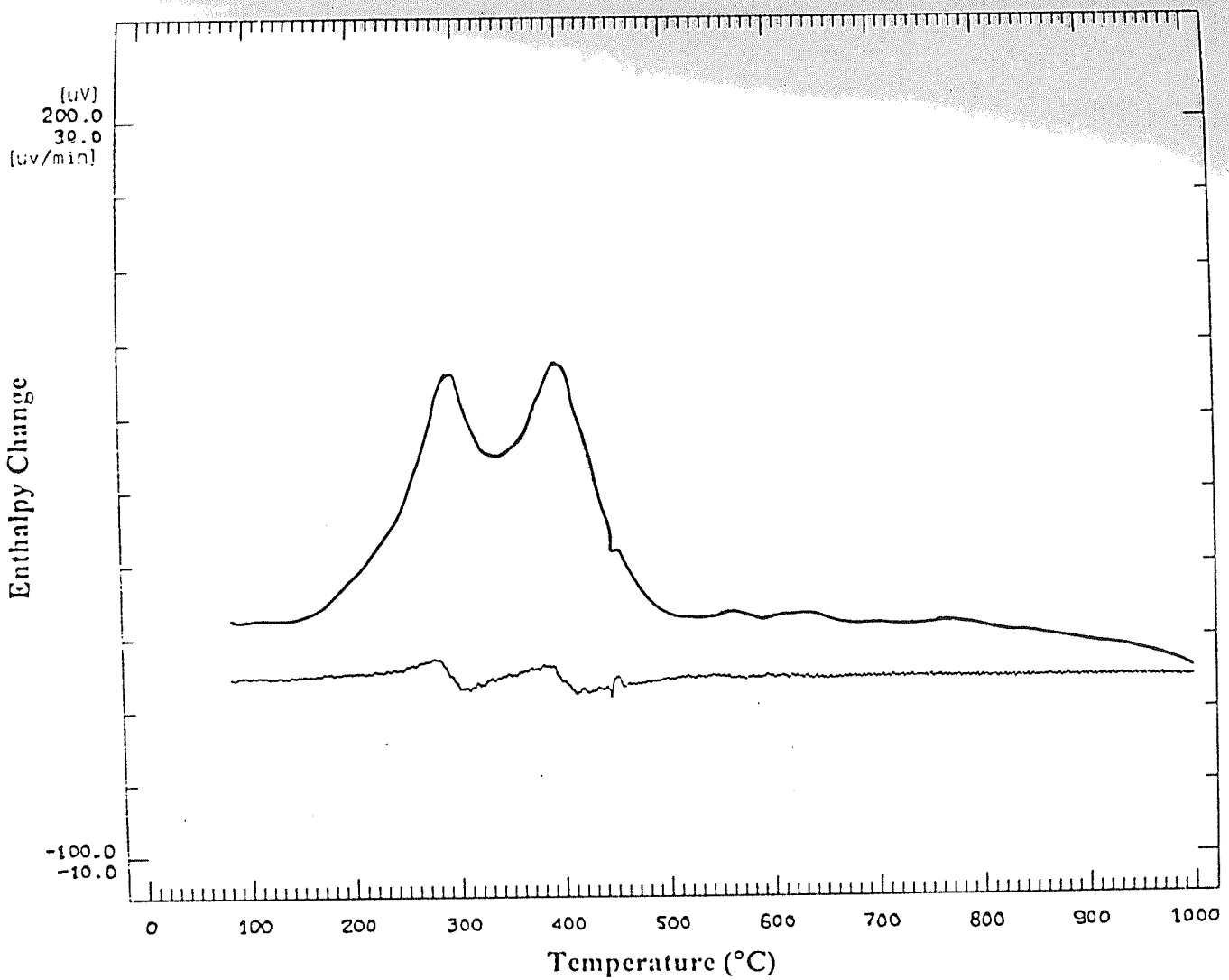

Figure 5.15. DTA Curve for Reactor 4 Spent Catalyst.

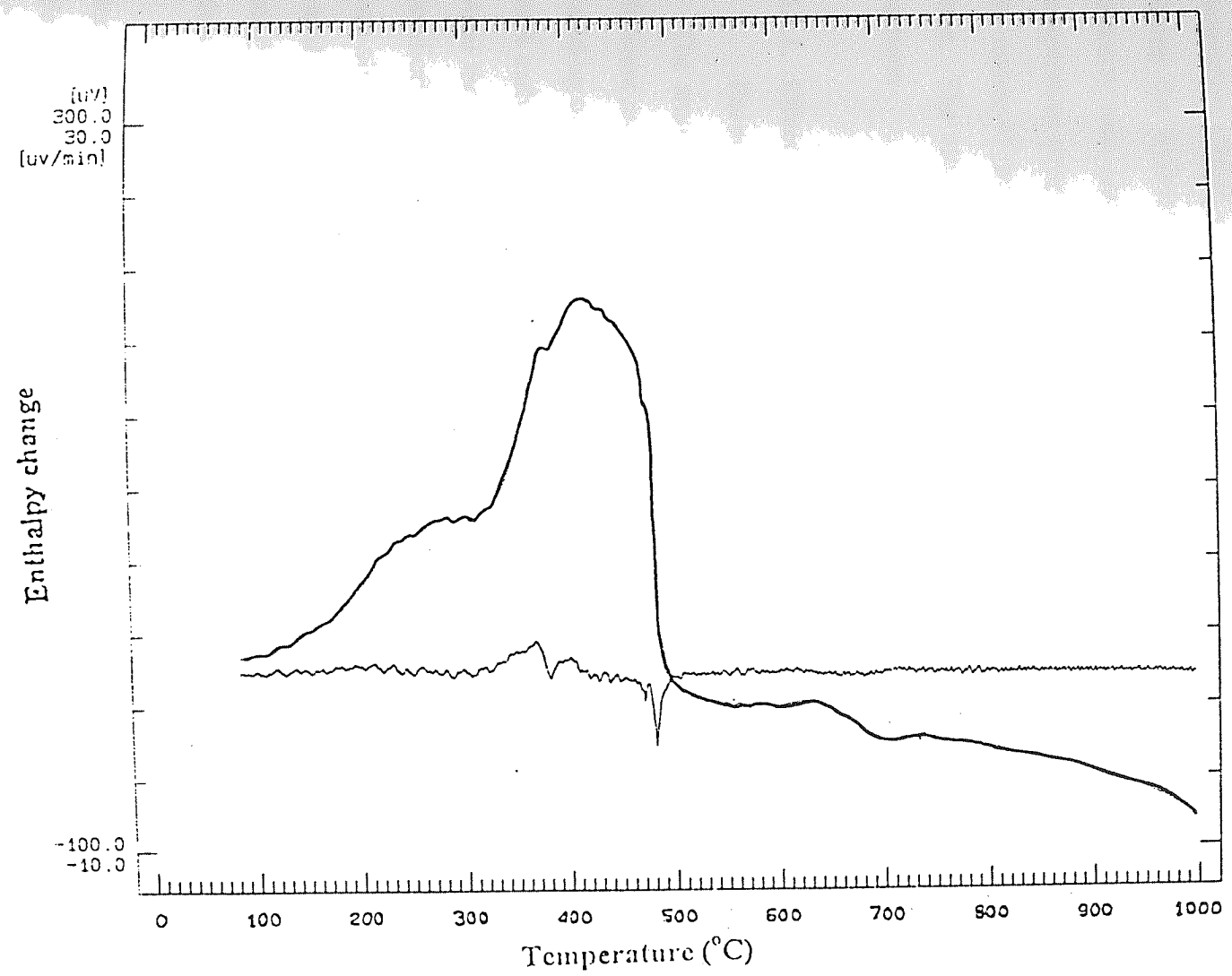

Figure 5.16. DTA Curve for Ebullated-bed Spent Catalyst.

In the present study a series of gas-oil hydrotreating runs of different duration ranging, om 30 minutes to 24 hours, were conducted. The objective was to gain a clear nderstanding of the nature of coke deposited on the catalyst during the early period of the peration and its role in catalyst deactivation. The influences of other important arameters related to the process, catalyst and feedstock variation on the formation of coke uring the hydrotreating process were studied. Detailed characterization of the coke eposits was carried out using various techniques, e.g. solid state ^{13}C NMR and mperature programmed oxidation (TPO) techniques, to gain a deeper understanding of ie nature of the initial coke and to examine how its properties change with processing me. The results of the various studies are presented and discussed in the following ections.

.2.1. Effect of Processing Time and Operating Temperature on Coke Formation

The amount of coke deposited on the catalyst during VGO hydroprocessing at two ifferent reactor temperatures is plotted as a function of run time in Figure 5.17. The coke uild-up on the catalyst surface was rapid during the early hours of the run. More than 10 vt% carbon was deposited on the catalyst within the first 3 hours of operation at 400°C. After the rapid coke build-up during the initial period coking slowed down and tended to evel-off or reach an equilibrium value within 24 h. Similar high initial coke deposition vas also observed at a lower operating temperature of 380°C. The results suggest that a apid coke buildup on the catalyst starts as soon as the feed is introduced and reaches a naximum of 17% wt within 24 h. This initial coke is likely to be responsible for the rapid leactivation of the catalyst during the early period of the hydrotreating process.

The data presented in Figure 5.17 also shows that an increase in temperature results in ncreased coke deposition on the catalyst. High temperatures usually enhance lehydrogenation, cracking and aromatization reactions at elevated temperatures. Condensation and polymerization of the olefinic and aromatic coke precursors may occur it elevated temperatures leading to an increase in coke deposition.

5.2.2. Effect of Feedstock Type on Coke Formation on Hydrotreating Catalyst.

Two different feeds, namely vacuum gas oil and atmospheric residue were used to evaluate the influence of feedstock type (or quality) on the extent of coke deposition on catalyst surface during hydrotreating. The characteristics of the two feeds are presented in Table 5.5. The hydrotreating experiments were conducted under identical conditions for both feeds.

The amount of coke deposited on the catalyst after different times during VGO and atmospheric residue hydrotreating are compared in Figure 5.18. Clearly a larger amount of carbon was deposited on the catalyst from atmospheric residue than from VGO. Interestingly, for the residual oil feed, the coke deposition on the catalyst was more rapid during the early hours of the run. Thus, for example, about 12 wt% carbon was deposited on the catalyst during the first 60 min. of operation with atmospheric residue feed, compared with only 3.4wt% carbon with VGO feed over the same period. After the rapid coke build-up during the initial period, coking slowed down and tended to level off within 24 h as observed by others (9,30, 130).

The difference in coke formation rates with the two feeds may be attributed to the variation in their composition. The atmospheric residue contains asphaltenes, which are totally absent in the vacuum gas oil. In addition, the residue contains a significantly higher amount of Conradson carbon residue (CCR). Aromatic and nitrogen compounds are also present in larger concentrations in the atmospheric residue than in the VGO.

Polynuclear aromatics, asphaltenes and Conradson Carbon Residue materials are known to have high coking tendencies. Wivel et al. (29) studied coke formation on hydrotreating catalysts using various feeds and found that the amount of coke formed on the catalyst increased with an increase in the amount of polynuclear aromatics in the feed. Absi-Halabi et al. (30) have suggested that a major source of coke is asphaltenes precipitated from solution at reaction temperature. This is supported by the results of Beuther et al (48) who identified coke with an asphaltene-like character in their aged catalyst. Higher concentrations of nitrogen in the feed also can lead to rapid coke build-up on the catalyst surface, since the nitrogen-containing compounds are strongly adsorbed on the surface and contribute to coke formation.

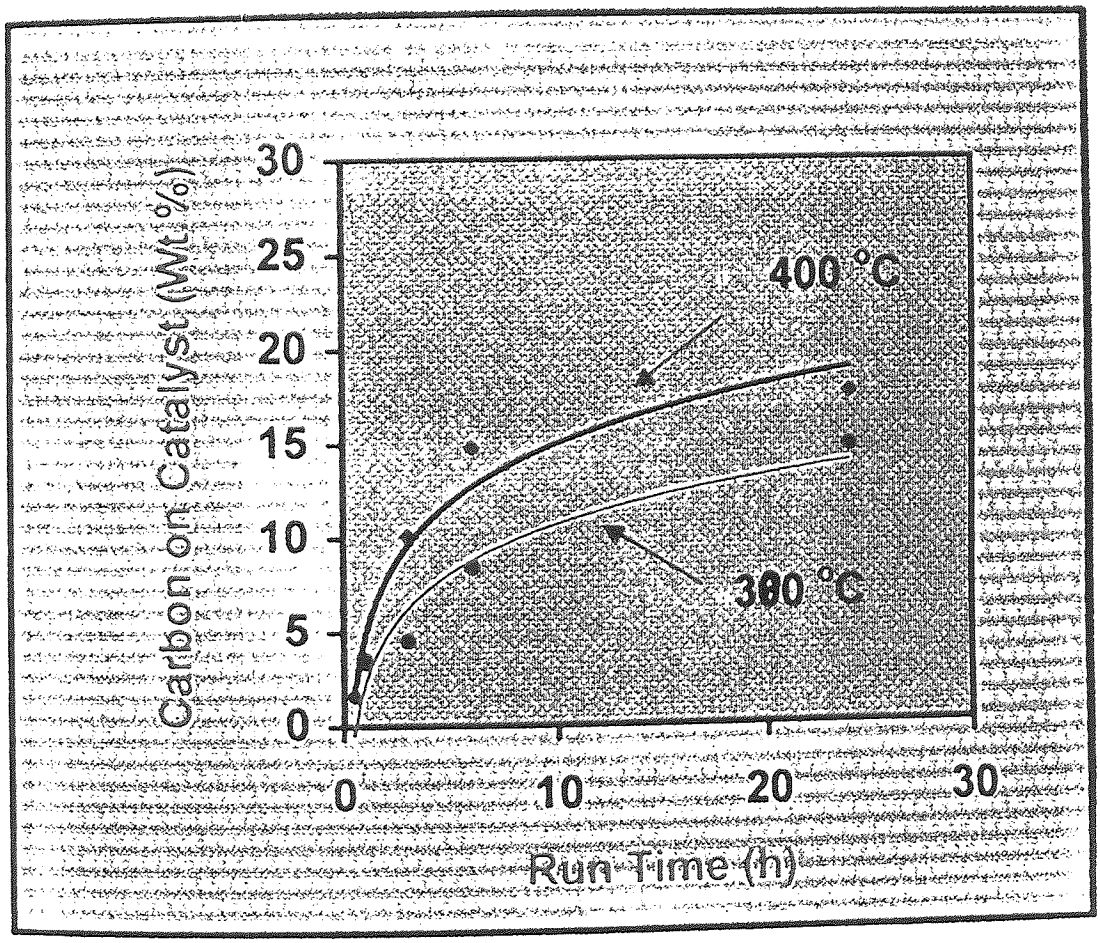

Figure 5.17. Carbon Deposition on Catalyst Vs. Run Time for VGO Feed.

Table 5.5. Feed Characteristics.

Test	Ref. No.	Unit	Sample Name	
			VGO	ATMR Treated
Desity 15°C	IP 190	g/ml	0.9040	0.9304
Gravity	IP 200	API	24.94	20.49
Total Sulfur	Coloumax	% wt	0.3902	0.534
CCR	IP 13	% wt	0.017	5.2
Asphaltene	IP 143	% wt	NIL	1.3
Ash Content	IP 4	% wt	0.0002	0.05
Metals	ICAP	µg/g	ND	6
Ni				
V	ICAP	µg/g	ND	10
Elemental Analysis				
C	-	% wt	86.4	85.9
H	-	% wt	12.97	13.2
Total (N_2)	Kjeldahl	% wt	0.11	0.21
Distillation	D1160	°C		
	IBP		184	354
	50%		467	546
	FBP		545	592

VGO = Vacuum Gas Oil

ATMR = Atmospheric Residue

CCR = Conradson Carbon Residue

API = American Petroleum Institute

ND = Not detected

- = Not available

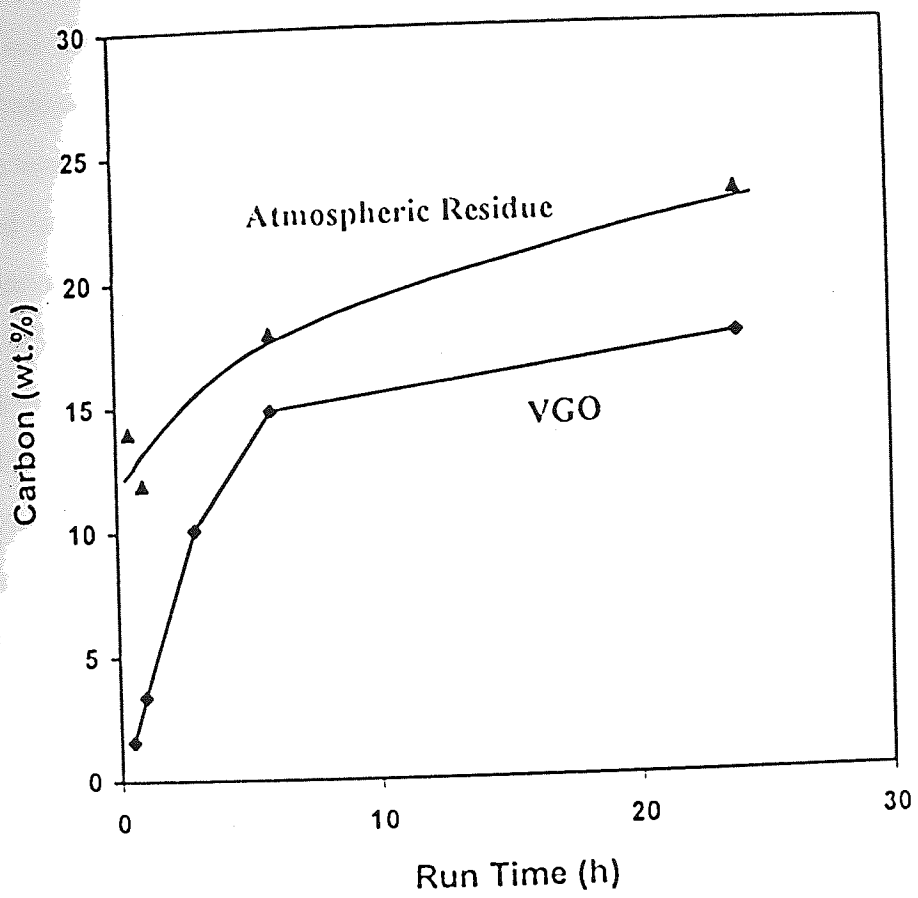

Figure 5.18. Amount of Coke Deposited at Different Times During VGO and Atmospheric Residue Hydrotreating.

.2.3. Influence of Initial Coking on Catalyst Surface Area and Porosity

The surface area and pore volume of the used catalyst samples from the different runs of arying durations were measured to gain additional information on the influence of initial oke on catalyst deactivation by loss of surface area and porosity. Catalyst surface area loss vith different feeds (VGO and atmospheric residue) are compared in Figure 5.19 (a). The urface area decline is plotted as a function of processing time for both feeds. The drop in urface area was particularly large for the catalyst used in the atmospheric residue ydroprocessing compared that used in VGO hydroprocessing. The decrease of surface rea was particularly high during the initial period (first 1-3 h) for both feeds. A similar rend is observable in the pore volume loss Figure 5.19(b). The loss of pore volume was emarkably high during the early hours of the run for the residual oil feed compared with he VGO feed. These losses in surface area and pore volume could be attributed to the oke deposition, since both parameters decrease in parallel with increasing amount of coke n the catalyst.

The micropores present in the fresh catalyst contribute significantly to its total surface area. Blockage of these micropores by coke deposition can be expected to lead to both loss of ore volume and surface area. A large loss in surface area of the catalyst occured within he first 3 h of the process with the residual oil feed. The coke deposition in the catalyst during this period was also very high (Figure 5.17). It is likely that much of the coke formed during the early hours of the run are deposited in the micropores of the catalyst leading to a substantial loss in the surface area and pore volume.

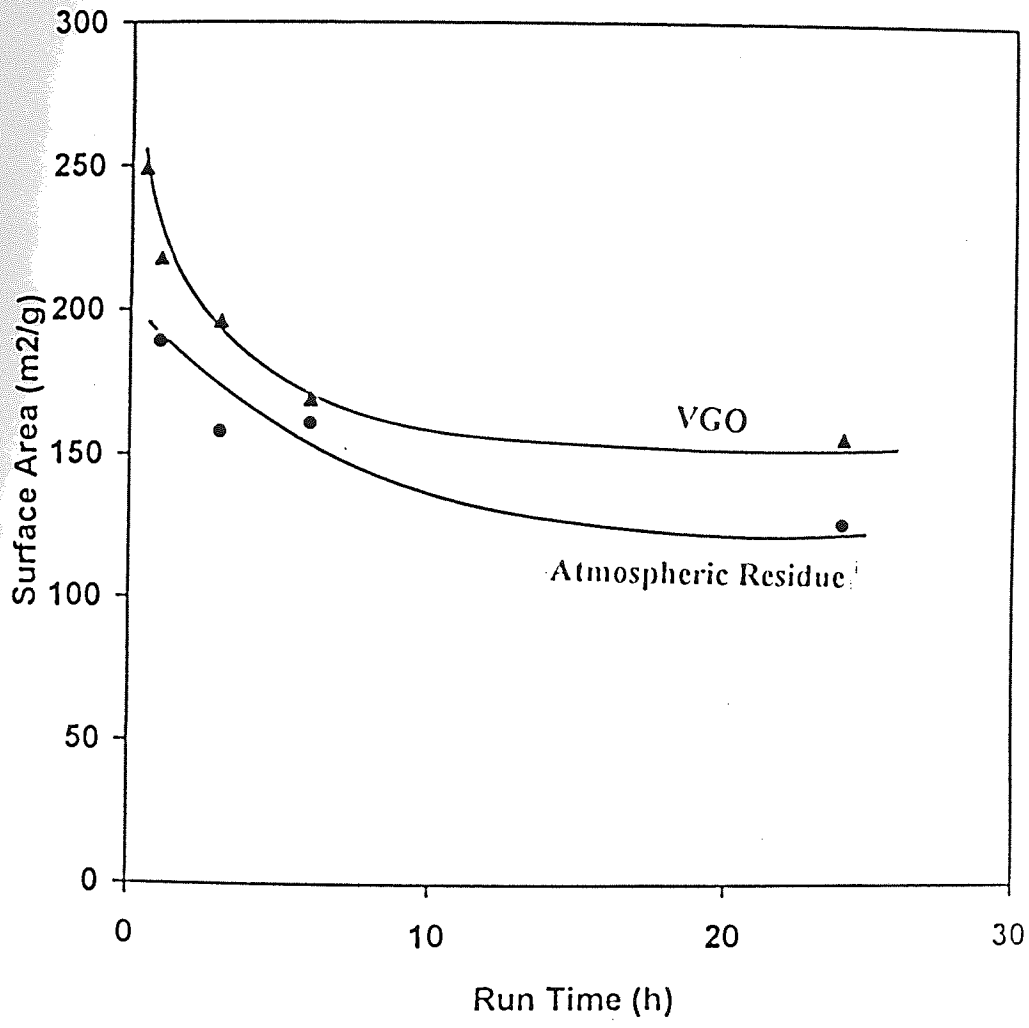

Figure 5.19a. Effect of Initial Coke on Catalyst Surface Area.

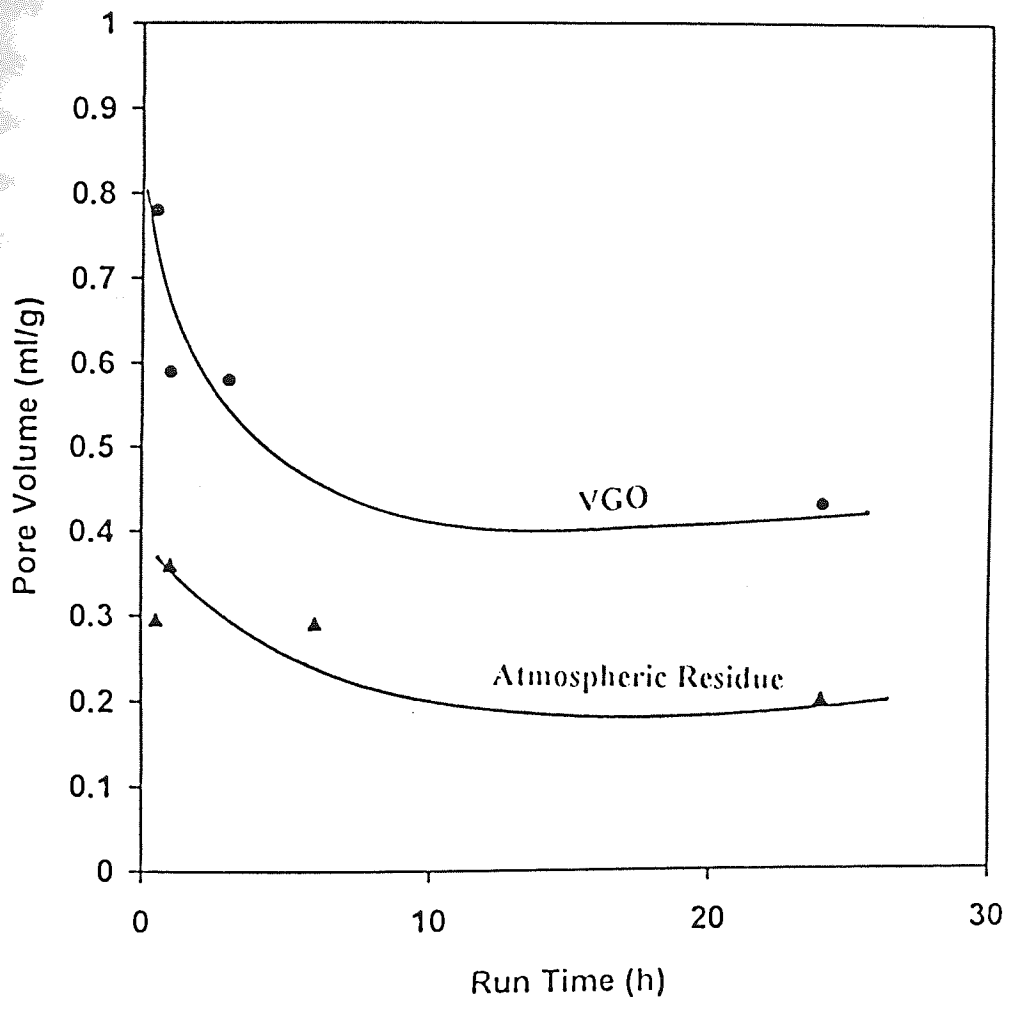

Figure 5.19b. Effect of Initial Coke on Catalyst Pore Volume.

These conclusions are confirmed by the pore size distribution data. Changes in the pore ze distribution of coked catalysts containing varying amounts of coke were examined. A ercury porosimeter (Quantachrome model Autoscan-60) was used to measure pore size istribution. The results are presented in Tables 5.6 and 5.7. The initial coke deposited uring the early hours of the run had a significant effect on the pore size distribution of the atalyst. Pores smaller than 50 and 100Å diameter appear to be affected more than the thers by the initial coke deposits. Thus, during the first one hour of operation at 380°C Table 5.6), the total volume of micropores of diameter <50Å are reduced by 67% (from .1156 ml/g to 0.0378 ml/g). The narrow mesopores (50-100Å diameter) were not ppreciably affected during the first 1 h, but they became progressively blocked by coke ith increasing time on stream. Thus, within 6 h of operation, 71% of the pore volume ontributed by the very narrow (50 - 100Å dia) meso pores were lost. Large mesopores nd macropores were not affected to any significant level by the initial coke deposits. hus, for example, even with the deposition of a large amount of coke (17 wt%) during the irst 24 h operation, the drop in the volume of macropores was only about 28%. onversely, the micropore and the small mesopore volumes were reduced, by 97% and 0% respectively, during the same period.

Catalyst pore size distribution, therefore plays an important role in catalyst deactivation y coke deposition, particularly during the early stages of the run.

Table 5.6. Pore Size Distribution of Catalysts Coked for Different Durations

Run Time	Pore Volume Distribution (ml/g)						Total Pore
(h)	<50 Å	50-100 Å	100-250 Å	250-400 Å	400-4000 Å	>4000 Å	Volume (ml/g)
resh	0.1156	0.2774	0.055	0.024	0.21	0.0241	0.7061
	0.0378	0.2338	0.0706	0.0142	0.153	0.0196	0.529
	0.0377	0.1774	0.05	0.0156	0.1696	0.0369	0.4872
	0.0264	0.08	0.0316	0.015	0.1504	0.0224	0.3258
4	0.0029	0.0266	0.0368	0.011	0.1478	0.0493	0.2744

2.4. Effect of Initial Coke on Catalyst Functions.

The influence of initial coking on HDS and HDN reactions was investigated by analysis the hydrotreated products for sulphur and nitrogen contents. The HDS and HDN rcentages were then plotted as a functions of coke on the catalyst for both VGO and mospheric residue feeds. The results presented in Figure 5.20 for the VGO feed clearly monstrate that the HDN function of the catalyst was deactivated more rapidly by the itial coke than the HDS function. Similar trends are also observable for the atmospheric sidue feed (Figure. 5.21).

A considerable difference is observable between the VGO coked and atmospheric sidue coked catalysts in their activity for promoting HDS reaction. With the VGO feed, e catalyst activity decline for promoting HDS was very slow, i.e. the drop in HDS tivity in 24 h was < 6%. Conversely, the catalyst used for atmospheric residue sulphurization shows a rapid deactivation. This has been due to the larger amount of oke deposited on the catalyst with the residual oil feed compared with VGO feed. It is so likely that the initial coke from the residual oil feed which contains metals and a igher concentration of nitrogen, had a more severe deactivating effect on the HDS nction of the catalyst.

A comparison of the HDS and HDN activity data presented in Figure 5.20 and 5.21 dicates for both types of feeds different degrees of deactivation of HDS and HDN nctions of the catalyst with similar coke levels. Hence the deposited coke affected the DS and HDN functions of the catalysts differently. A possible explanation for this bservation may be offered in terms of the mechanism of HDS and HDN reactions and the ctive catalytic sites involved in promoting these reactions.

he catalytic active sites in sulphided Co-Mo/Al_20_3 and Ni-Mo/Al_20_3 catalysts that are esponsible for promoting various hydrotreating reactions such as HDS, HDN and ydrogenation (HG) are known to be sulphur vacancies in MoS_2 crystallites and in the ixed sulphide phase (Co-Mo-S or Ni-Mo-S). The MoS_2 crystallites remain dispersed on he alumina surface as hexagonal slabs , and the promoter atoms (Co or Ni) are located at he active edges of the MoS_2 slab forming a highly active phase known as Co-Mo-S or Ni-Mo-S phase (131). Coke deposition may cover these active edges leading to decrease in heir activity for promoting various reactions.

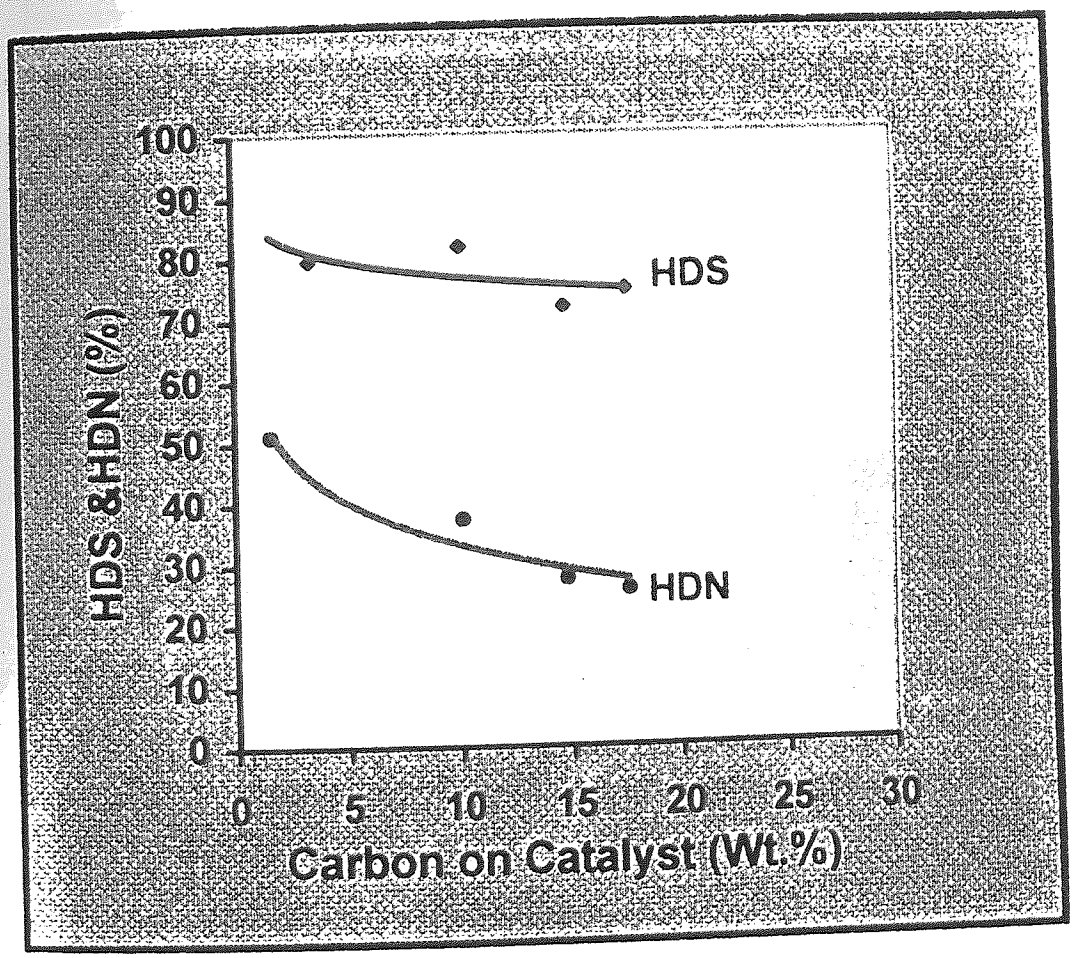

Figure 5.20. Effect of Coke Deposition on HDS and HDN Reactions for VGO Feed.

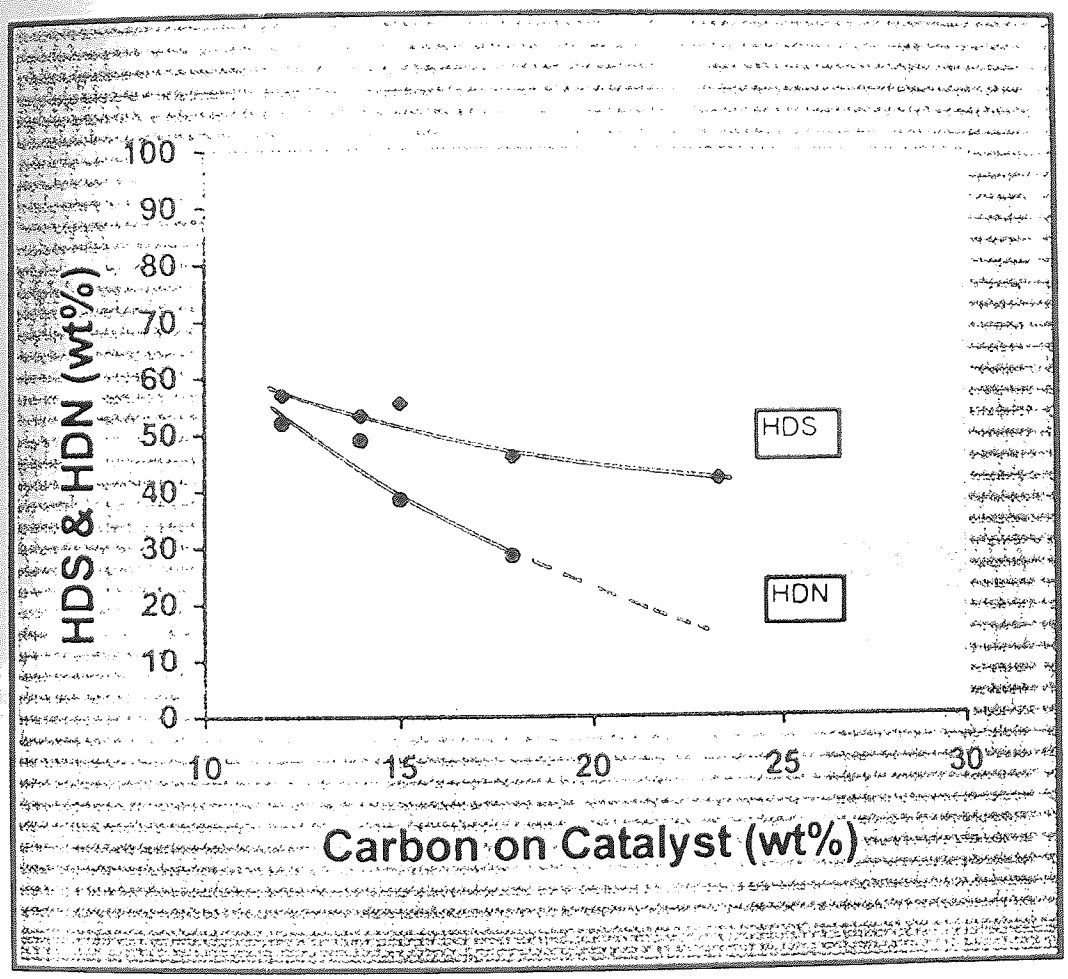

Figure. 5.21. Effect of Coke Deposition on HDS and HDN Reactions for Atmospheric Residue Feed.

Various kinetic studies with model compounds have indicated the presence of two istinct types of catalytic sites (i.e., sulphur vacancies): one is responsible for ıydrogenolysis of the heteroatom, and the other is responsible for hydrogenation (132). Specific geometric arrangements of sulphur vacancies with various degrees of uncoordination appear to be required for hydrogenation and hydrogenolysis. Corner sites and edge sites can display different degrees of sulphur vacancies and promotes different reactions (132,133). Corner sites with 2 or 3 sulphur vacancies (i.e. a higher Mo oxidation state) are primarily responsible for the hydrogenation reaction(HG). Hydrogenolysis sites could be on edges at a lower oxidation state or a combination of a sulphur vacancy and a SH group.

The difference in the deactivation rates observed in the HDS and HDN reactions with coke deposition during the initial stages of the run was probably due to the difference in their reaction mechanisms. The mechanism of HDS and HDN reaction of heterocyclic sulphur and nitrogen compounds is such that thiophenic sulphur compounds can undergo direct hydrogenolysis of the carbon - sulphur bond on the hydrogenolysis sites in the catalysts prior to HG of the heterocyclic ring. On the other hand, in the case of nitrogen containing heterocyclic rings, HG of the aromatic heterocyclic ring is essential before hydrogenolysis of the carbon-nitrogen bond can take place. It is likely that the initial coke was preferentially deposited on the higher oxidation state HG sites leading, in turn, to their deactivation. HDN activity of the catalysts will consequently show a large decrease with coke deposition. Recent studies by Diaz et al., (134) have continued the loss in activity caused by coke blocking the edges and corners of the active MoS_2 crystallites. The present results clearly demonstrate that the hydrogenation function of the catalyst that involves the corner sites (with 2 or 3 sulphur vacancies or a higher Mo oxidation state) is affected more than the hydrogenolysis function by the initial coke deposits.

5.2.5. Relation Between Catalyst Acidity and Its Coke Forming Tendency.

γ-Alumina is commonly used as a support material in conventional hydrotreating catalysts that contain sulphides of Mo and Co or Mo and Ni active catalyst components.

The alumina support not only provides the required porosity and surface area for the dispersion of the active catalyst components, but also contains acidic and basic sites that take part in some of the reactions occurring in the hydrotreating process. Both Bronsted

id Lewis-type acid sites have been shown to be present on the surface of activated umina (135). Coke deposition on alumina supported Ni-Mo or Co-Mo catalysts can be trongly influenced by the acidity of the alumina support. Recent studies have shown that major part of the coke accumulated on hyrotreating catalyst is present on the alumina support and not on the NiMo or CoMo crystallites. Although coke deposition on the catalyst, which is a major cause of catalyst deactivation, cannot be completely eliminated, it can be minimized by proper design of the catalyst's acidic and hydrogenation functions.

To be able to prepare a new generation of hydrotreating catalysts for reduced coking, it is necessary to gain a detailed knowledge of the relationship between the catalyst's acid function and its coke-forming tendency. The acidity of the alumina support by certain additives was therefore modified. A series of such catalysts with varying acidities were used to investigate the catalyst's acidity effect on hydrotreating catalyst deactivation by coke formation using VGO as feed.

Sodium and fluoride ions were used to modify catalyst acidity. Two different concentration levels of each of these additives were used to modify the acidity to different levels. The acid strength distribution of the conventional and modified catalysts were examined by temperature programmed desorption of ammonia.

Ammonia TPD patterns of the conventional CoMo catalyst and three other catalysts containing Na and F ions are illustrated in Figure 5.22. Two major peaks with maxima around 100 and 200°C are demonstrated in the TPD spectrum of the conventional Co-Mo/γ-Al_2O_3 catalyst. The low temperature (100°) and high temperature (200°C) peaks can be attributed to the desorption of ammonia from weak and strong acid sites, respectively.

With the addition of sodium (5 wt%), the high temperature peak is decreased considerably indicating that the strong acid sites on the catalyst are neutralized by the sodium ions. Conversely, with a 2 wt% fluorine addition, the high temperature peak increased whilst the low temperature peak decreased slightly. Further increase of fluorine level to 5% in the catalyst resulted in a large increase in the high temperature peak with a significant reduction in the low temperature peak. These results indicate that the addition of fluoride ions increases the number of strong acid sites in a conventional Co-Mo/γ-Al_2O_3 catalysts system whereas sodium ions neutralize the strong acid sites. Catalyst acidity decreases in the following sequence:

Co-Mo-F (5%) > Co-Mo-F (2%) > CoMo > CoMo-Na (5%)

A comparison of the amount of coke deposited on the various catalysts in one hour of VGO hydrotreating at 400°C is shown in Figure 5.23. Similar data for the run conducted at 380°C are presented in Figure 5.24. The lowest amount of carbon deposition occured on the conventional Co-Mo catalyst. Increasing the number of strong acid sites in the catalyst by fluoride addition lead to a substantial increase in coke deposition. Coke formation is believed to proceed through the polymerization and condensation of olefinic and aromatic materials. Since strong acid sites enhance the cracking, condensation and polymerization reactions, the observed increase in the coke deposition with the fluoride addition to the catalyst is not unexpected. The data presented in Figure 5.24 also show increased coke formation with sodium addition to the catalyst. This is surprising since the addition of sodium is known to neutralize the strong acid sites of alumina. This is confirmed by the ammonia TPD results presented in Figure 5.22. Weakly acidic catalysts are generally believed to reduce coke formation. The increase in the amount of coke deposition on hydrotreating catalysts with sodium addition therefore remains to be explained.

It is likely that sodium addition to alumina-supported Co-Mo catalyst plays a role in modifying the hydrogenation function of the catalyst in addition to neutralizing the strong acidity. Sodium can interact with the Mo forming a stable sodium molybdate; such stable molybdates have been observed in the case of addition of Ca and Mg to $CoMo/Al_2O_3$ catalysts. The interaction of the added sodium with Mo can suppress the hydrogenation and hydrogenolysis functions of the catalyst. Thus, with sodium-containing catalysts, hydrogenation of coke precursors, will occur at a lower rate, and as a result, the coke deposition will increase.

5.2.6. Nature of the Initial Coke

To gain a deeper understanding of the nature of the initial coke and to examine how its characteristics change with processing time the coke deposition on the catalysts from different runs were characterized using techniques such as temperature programmed oxidation (TPO) and solid state carbon-13 cross-polarization magic angle spinning nuclear magnetic resonance (CP/MAS ^{13}C NMR) spectroscopy.

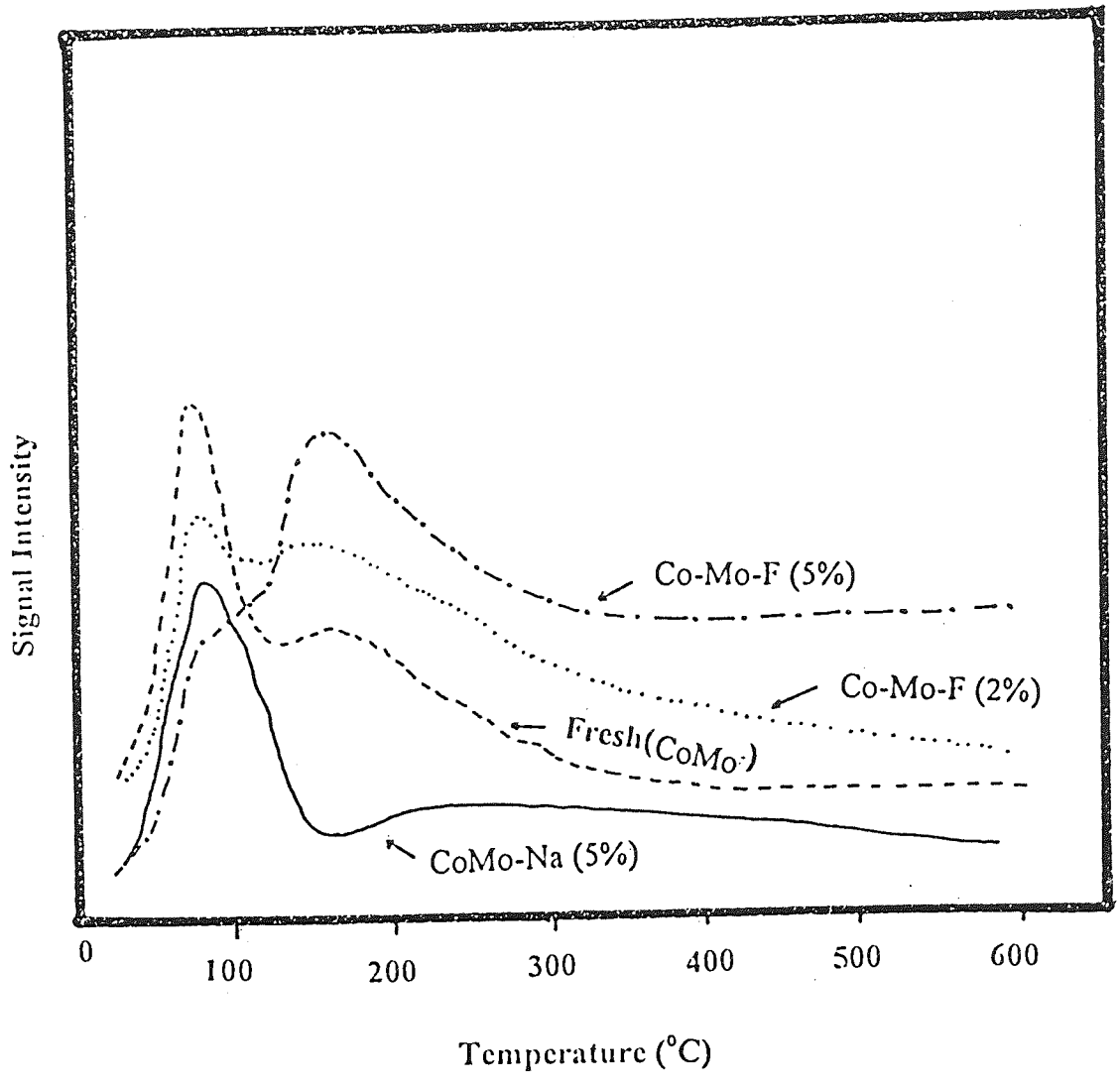

Figure 5.22. Ammonia TPD Patterns for A Conventional Co-Mo/Al_2O_3 Catalyst Before and After Adding Sodium or Fluorine.

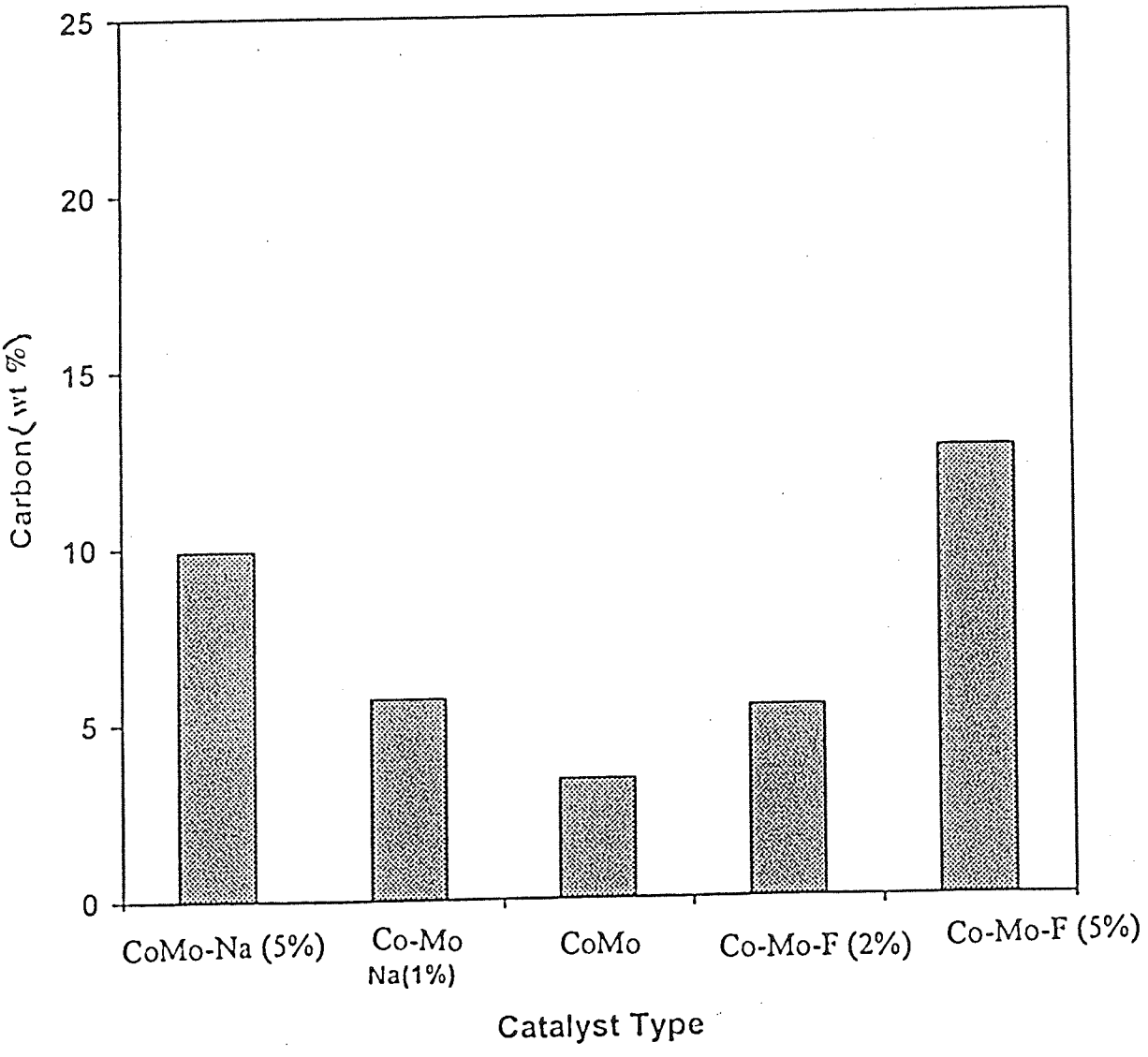

Figure 5.23. Effect of Catalyst Acidity on Coke Deposition During VGO Hydrotreating (T-400°C).

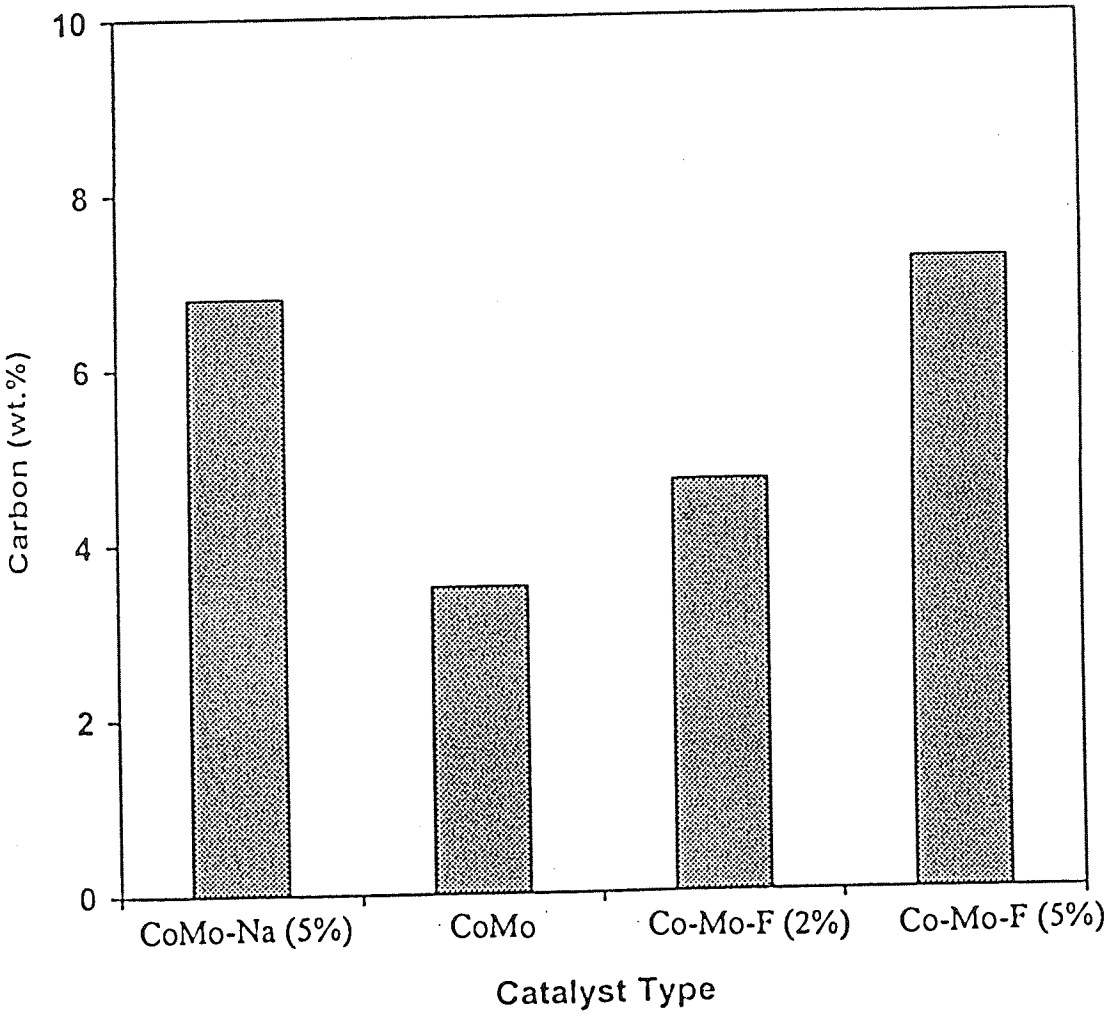

Figure 5.24. Effect of Catalyst Acidity on Coke Deposition During VGO Hydrotreating at 380°C

5.2.6.1. Coke Characterization by TPO.

Using the TPO technique, the different gaseous products formed during coke oxidation and the temperature profiles can provide valuable information about coke composition and its reactivity. Used catalyst samples from the runs conducted at 380°C for different duration (1 and 24 h) were subjected to TPO with a gas mixture containing 5% O_2 in helium. The different gaseous products formed during the coke oxidation were monitored as a function of temperature using a Gas Lab 300 mass spectrometer. A linear heating rate of 10°C/min was used throughout. The purpose was to obtain information on the reactivity of initial coke deposits as well as on the changes that occur in the nature of the coke deposits with increasing reaction time.

Figures 5.25a and 5.25b show the trends in the formation of various gaseous products during the TPO of catalysts coke for different durations at 380°C. Combustion products from a typical TPO run show the presence of CO, CO_2, SO, SO_2, NO, NO_2 and H_2O which indicates that the coke deposit is composed mainly of C, H, S and N. Under the conditions used for TPO the sulfur in the coke was oxidized into both SO and SO_2, the nitrogen into NO and NO_2, and the carbon into CO and CO_2.

The profiles of formation of SO and SO_2, and of CO and CO_2, show similar trends. However the formation of NO and NO_2 exhibit a different TPO profiles, particularly, at high temperatures. The profiles for the catalyst coked for a very short duration (1 hour) shows very broad peaks (Figure 5.25a) while the catalyst from the long duration run shows sharp peaks (Figure 5.25b) for all gases. Thus, for example, the CO and CO_2 formation profiles for the 1-h run catalyst exhibit very broad peaks covering the temperature region of 250 to 550°C. Conversely, the long-duration run catalyst shows two distinct maxima around 280°C and 440°C for both CO and CO_2 formation. This indicates that the coke combustion occurred predominantly in these two temperature regions.

The results of this study indicate that part of the coke deposited on the catalyst during the first 24 h of operation is more reactive and burns off easily at a relatively low temperature (i.e., 280°C). The other part of the coke is probably more refractory and requires a higher temperature (i.e., 440°C) for oxidation. In the case of very short duration runs (e.g., 1 h) the CO_2 formation tends to extend over a wide temperature range 250 to

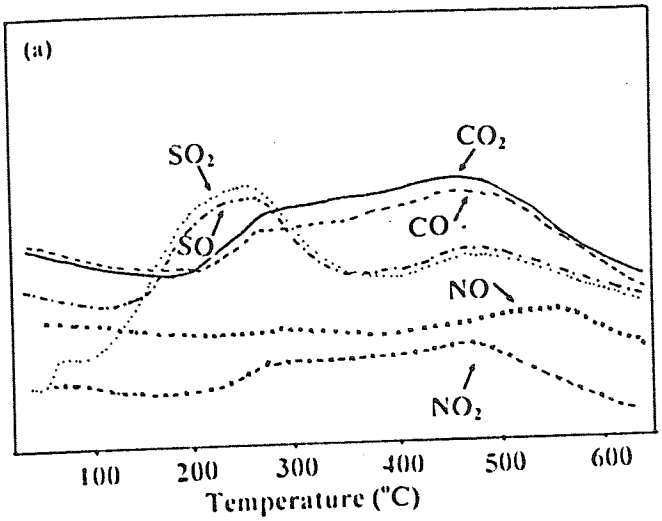

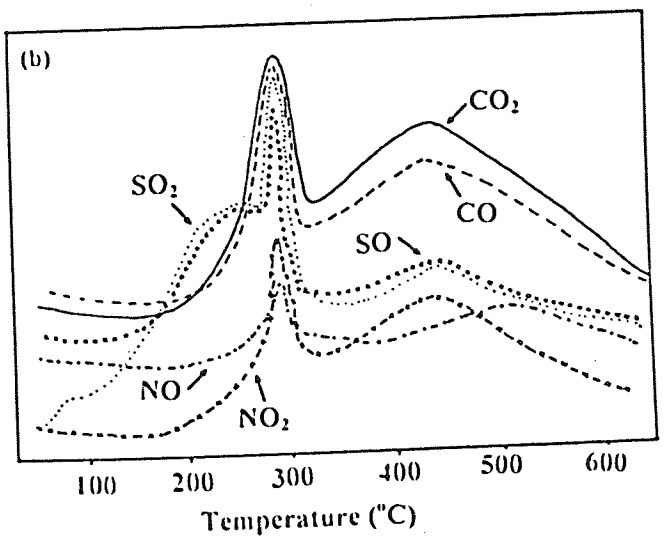

Figure 5.25 (a and b). Profiles of Various Gaseous Products Formed during the TPO of Coked Catalysts. (a) Run time = 1 hour; (b) Run time = 24 hours.

550°C) with two broad, less resolved peaks around 270 and 470°C. A variety of coke species with a wide range of reactivities are likely to be present in the initial coke deposited within the first hour of operation. Part of this initial coke is probably strongly adsorbed or bound to the support require and therefore a higher temperature for removal by oxidation.

The more reactive, easily combustible coke appears to contain little or no sulphur, but an appreciable amount of nitrogen. A part of the nitrogen present in the catalyst is oxidized with the coke producing NO and NO_2 peaks coinciding exactly with those for CO and CO_2 peaks. Another part of the nitrogen in the coke is oxidized only into NO at a temperature higher than that for carbon combustion, indicating that it is probably buried deeply below the coke layer and strongly bound to the catalyst's surface. Its oxidation occurs only after the coke layer is removed by combustion.

5.2.6.2. Coke Characterization by ^{13}C NMR Spectroscopy. Recently ^{13}C NMR has become a powerful tool for structural characterization of coke deposits. In the solid state, different types of carbon atoms can be resolved and it is possible to calculate the aromaticity of the deposited coke. In the present work, ^{13}C NMR spectra of the catalyst samples coked with different feedstocks at different operating temperatures were measured using a cross-polarized magic angle spinning (CP/MAS) technique to obtain information on the influence of feedstock quality and operating temperatures on coke aromaticity. Particular attention was paid to information on the nature of the initial coke deposited on the catalyst during the first 24 h period.

Figure. 5.26 compares the solid state ^{13}C NMR spectra of spent catalyst used in the hydrotreating of two different feeds, namely, vacuum gas oil and atmospheric residue, for a duration of 1 h. A similar comparison of the ^{13}C NMR spectra of spent catalysts from a longer duration (24 h) run for both feeds is shown in Figure 5.27. Peaks of aromatic carbon and aliphatic carbon are indicated in these spectra. All the spectra contain both aliphatic and aromatic carbons; however, the peak areas due to both types of carbon vary significantly with the feedstock and processing time.

The concentration of aromatic carbon in the coke was calculated as follows and the results are presented in Table 5.7 together with the total carbon (wt%).

$$\text{Aromatic carbon (\%)} = \frac{Area\ under\ aromatic\ carbon}{Total\ (aromatic\ +\ aliphatic\ carbon)\ peak\ area} X\,100$$

Table 5.7 shows that the coke deposited on the catalyst from the residual oil feed was significantly more aromatic in character than that from the VGO feed. This can be attributed to the presence of high concentrations of Conradson Carbon Residue (CCR) and asphaltenic materials in the residual oil feed. Studies have shown that initial coke formed in the catalyst consists of adsorbed asphaltenes (30). It is believed that the basic nitrogen atoms present in the asphaltene molecules lead to preferential adsorption of the asphaltenes on the catalyst surface during the early stages of hydroprocessing. The asphaltenes consist of condensed aromatic sheets. It is likely that the highly aromatic asphaltenic and high molecular weight CCR materials in the residual oil contribute to the formation of highly aromatic coke on the catalyst during the initial period.

The results presented in Figure 5.26 and Table 5.7 indicate that the coke formed on the catalyst during the first 1 h operation of 380°C was more aromatic in character than that in the 400°C run. However, at higher run lengths (e.g., 24 h), an opposite trend appeared i.e., the coke on the catalyst at 400°C was slightly more aromatic than that formed at 380°C.

This is not unexpected since high temperatures promote condensation of polynuclear aromatics to more aromatic coke with increasing processing times. This trend of increased coke aromaticity with temperature is in agreement with the results of some similar earlier studies (41, 136).

Figure 5.28 illustrates the ^{13}C NMR spectra of spent catalyst samples used for hydroprocessing VGO over different run lengths. Similar results for the atmospheric residue feed are presented in Figure 5.29. The coke deposited on the catalyst within the first one hour of the operation was considerably more aromatic in nature, and the aromaticity decreased on increasing the processing time from 1 h to 24 h. It is likely that the initial coke containing highly aromatic materials adsorbed on the catalyst were subsequently hydrogenated on the catalyst surface forming less aromatic materials. The initial coke thus changed its aromatic character significantly within 24 h of operation; However, with further increase of time on-stream, the deposits can undergo cracking and condensation reactions resulting in an increase in their aromaticity (95) in long duration

Table 5.7. Effect of Feedstock Quality on Coke Aromaticity.

Reaction Temperature (°C)	Run Duration (h)	VGO		Atmospheric Residue	
		Carbon (wt%)	Coke Aromaticity (%)	Carbon (wt%)	Coke Aromaticity (%)
400	1	3.4	40	11.9	75
	6	14.8	-	17.9	-
	24	17.6	19	23.3	49
380	1	3.5	71	-	-
	6	8.4	25	-	-
	24	17.0	16	-	-

runs. The results of the present short duration runs clearly demonstrate that the initial coke deposits were highly aromatic and changed to a less aromatic coke within 24 h. This is consistent with the mechanism proposed by Beuther et al., (48) for coke deposition on sulphide catalysts during hydrodesulfurization of petroleum residues.

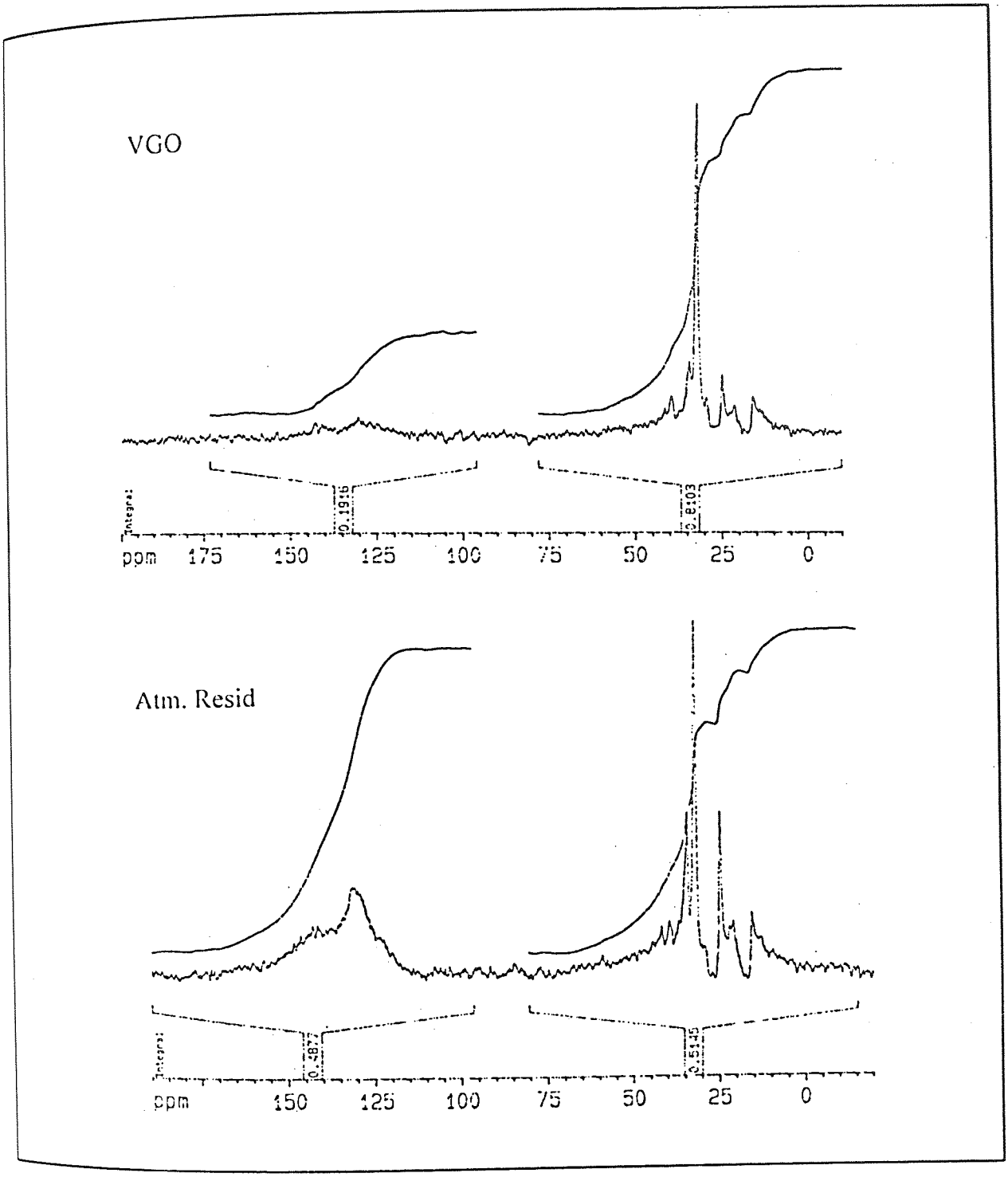

Figure. 5.26. Comparison of the Solid State ^{13}C-NMR Spectra of Coked Catalyst used in Hydrotreating VGO and Atmospheric Residue Feeds for 1 h.

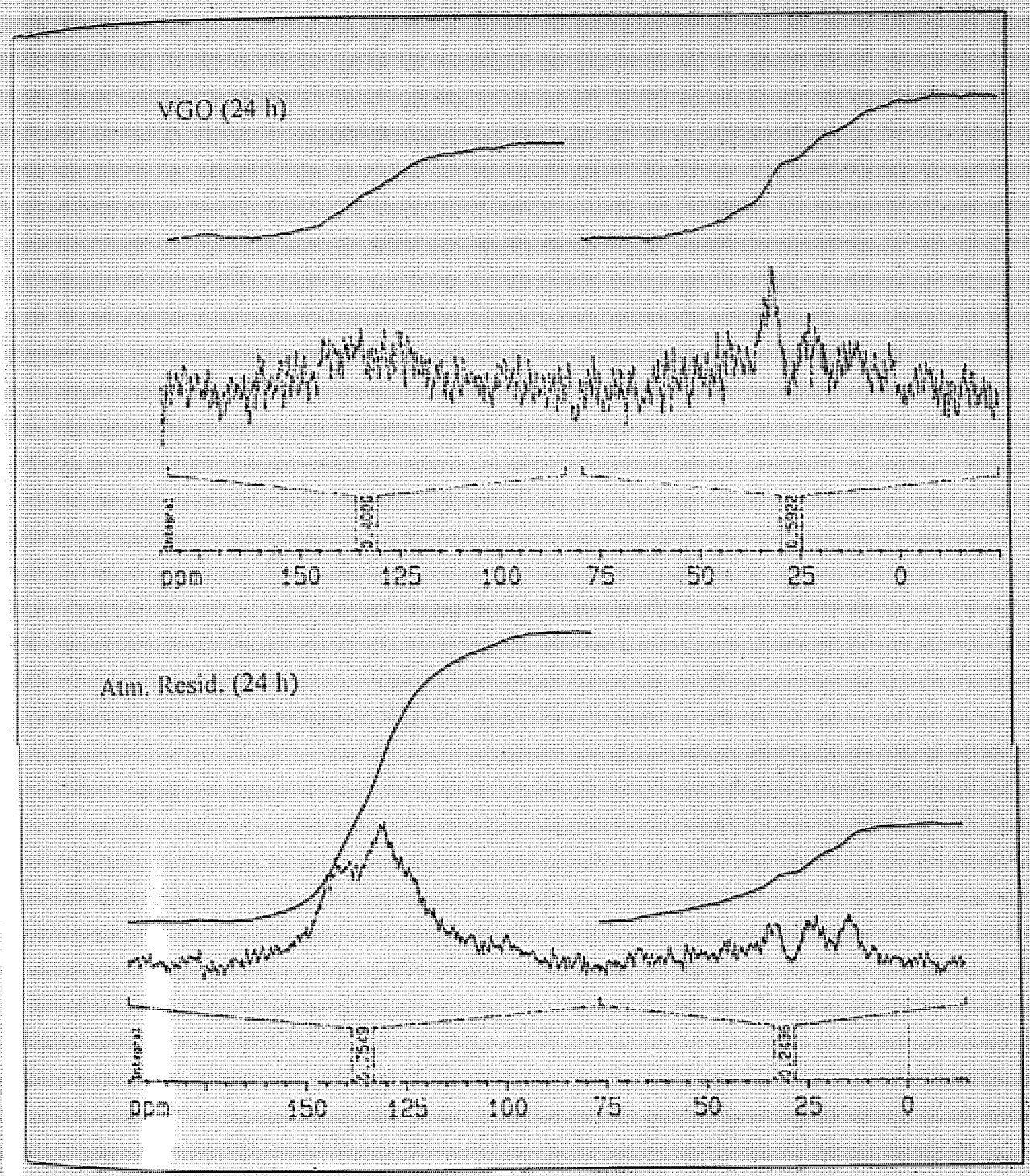

Figure. 5.27. Comparison of the Solid State ^{13}C-NMR Spectra of Coked Catalyst Used in Hydrotreating VGO and Atmospheric Residue Feeds for 24 h.

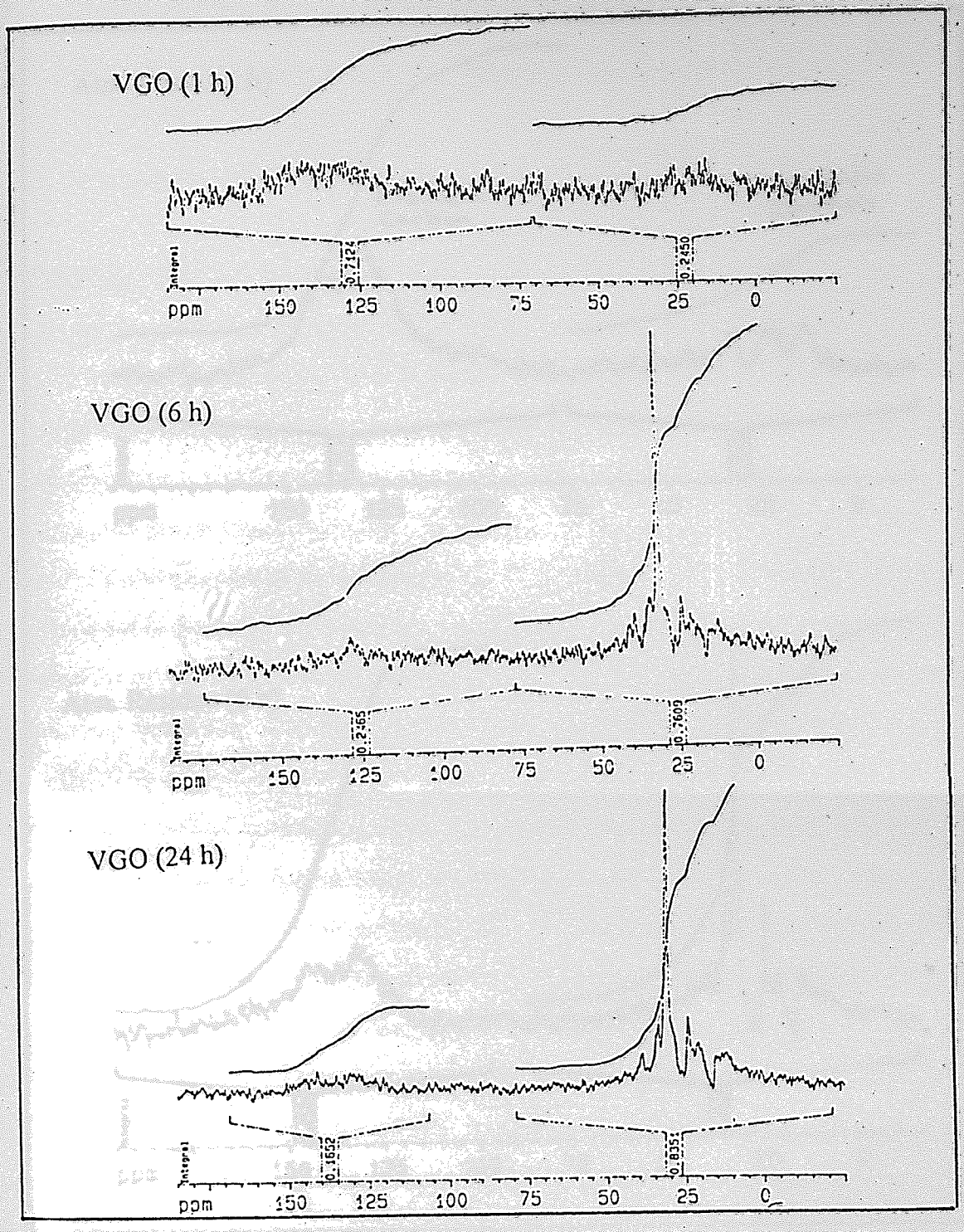

Figure. 5.28. Solid State ^{13}C-NMR Spectra of Coked Catalyst Used in VGO Hydroprocessing for Different Durations (T=380°C).

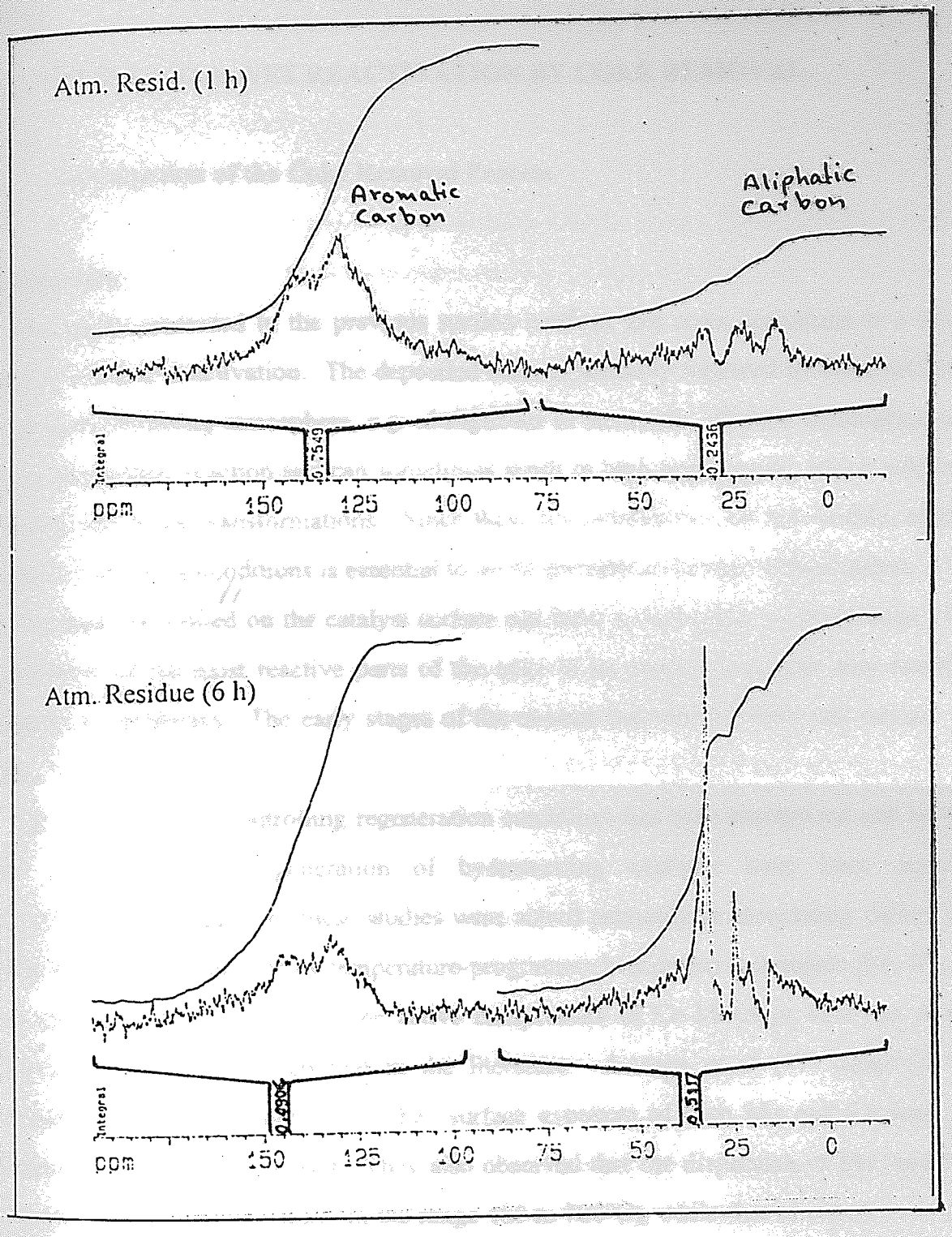

Figure. 5.29. Solid State ^{13}C-NMR Spectra of Coked Catalyst After Hydroprocessing of Atmospheric Residue for Different Durations.

6.0. SPENT CATALYST REACTIVATION BY COKE REMOVAL

6.1.. Investigation of the Coke Removal Process.

Introduction

The results presented in the previous section confirm that coke deposition is a major cause of catalyst deactivation. The deposited coke is normally removed by combustion in an oxygen-containing atmosphere, e.g. nitrogen-air or steam-air. Carbon combustion is a highly exothermic reaction and can sometimes result in high temperature, which enhances sintering and phase transformations. Since these transformations are irreversible, careful control of decoking conditions is essential to avoid permanent damage to the catalyst.

The deposits formed on the catalyst surface can have a wide range of reactivities. The combustion of the most reactive parts of the coke in an excess of oxygen may result in temperature runaways. The early stages of the contact between the coke and oxygen are crucial.

The importance of controlling regeneration conditions has been recognized and several studies on oxidative regeneration of hydrotreating catalysts have been reported (92,93,94,99,101). Most of these studies were aimed primarily at elucidating carbon and sulfur removal mechanisms by temperature-programmed oxidation techniques (94, 99). A few studies on the sintering of the active components of Co-Mo-Al_20_3 catalysts during regeneration have been reported in the literature. Arteaga et al (97) observed that regeneration caused an increase of the surface exposure of both Mo and Co ions and produced a more active catalyst. They also observed that the dispersion of Mo increased with an increase in temperature (in the range 400 to 700°C), while that of cobalt decreased apparently due to some of the cobalt entering the alumina lattice to form $CoAl_2O_4$ like species (98). In contrast, Dufresne et al (94a) reported that sintering of the active molybdena phase can occur even at temperatures around 500°C. Few studies have been reported on structural changes occurring to the support and to the active catalyst components during oxidative regeneration of hydrotreating catalysts. More specifically, the influence of start-up regeneration conditions on catalyst structural properties has received little attention.

The key to the control of undesirable changes, such as sintering and phase transformation, occurring in hydrotreating catalysts during oxidative regeneration is to understand the factors which enhance them. A systematic study was therefore conducted on the effect of parameters such as temperature, gas flow rate and oxygen concentration on the sintering of an industrial gas-oil hydrotreating catalyst during regeneration . Chemical changes and phase transformations occurring in the catalyst during regeneration were also examined.

The results revealed that during the decoking process extensive surface area loss occurred due to sintering at high (>5%) oxygen concentrations and high flow rates of the regeneration gas. Increasing the initial combustion temperature above 440°C led to considerable sintering of the catalyst. Pore size distribution data of the catalysts decoked at different temperatures showed a progressive pore enlargement with increasing temperature. At temperatures above 700°C a substantial loss of molybdenum from the catalyst together with phase transformations in the alumina support occurred. Details of the study together with discussion of the results are presented below.

A deactivated hydrotreating catalyst from a commercial gas-oil desulphurization plant was used for the decoking experiments.

Table 6.1. Catalyst Characteristics

Catalyst Properties	Fresh	Used
MoO_3 (wt. %)	15.7	15.1[a]
CoO (wt.%)	4.1	4.0[a]
Carbon (wt.%)	-	10.5
Sulphur (wt %)	-	6.5
Surface area (m^2/g)	240	108
Pore volume (ml/g)	0.54	0.22

[a]Coke free basis

The characteristics of the catalyst together with that of the fresh catalyst are summarized in Table 6.1. The catalyst was thoroughly extracted with toluene to remove the residual gas oil, and then dried at 110°C. The regeneration experiments were carried out in a fixed bed

tubular reactor system which is described in detail in Chapter 4. In a typical experiment 100 g spent catalyst was charged to the reactor. Coarse carborundum was placed below and above the catalyst bed so that the catalyst remained at the center of the reactor. Thermocouples inserted into a thermowell at the center of the catalyst bed were used to monitor the reactor temperature at various points.

After loading the catalyst, dry nitrogen was passed at a rate of 1.5 L/h/gm cat., and the temperature was increased to 150°C at a rate of 100 °C/h. After maintaining the temperature at 150°C for 1 h, the regeneration gas containing the desired oxygen content was passed. The conditions were then adjusted to the desired regeneration temperature and gas flow rate. The regeneration was then continued for 8 h under these conditions. The reaction time was fixed at 8 hours for all the studies. This was based on preliminary experiments which indicated that most of the coke was removed within this period at the base conditions selected for study (i.e. temperature 400°C, gas flow rates 1.5 L/h/gm cat., and oxygen concentration 5 vol%). Finally, the remaining coke on the regenerated catalyst was completely burned by introducing air. The reactor was then cooled down to room temperature in a stream of nitrogen, and the catalyst was unloaded and characterized. Table 6.2 summarizes the regeneration conditions used in the investigation.

Table 6.2. Regeneration Conditions

Regeneration Parameter	Oxygen content effect	Flow Rate effect	Temperature effect
Temperature (°C)	400	400	300-800
Oxygen Content (5 vol.%)	1.5 - 20	5.0	5.0
Flow rate per gram catalyst (l/h)	1.5	0.5 - 4.0	1.5

Samples of the regenerated catalysts were characterized and changes in surface area, pore volume and pore size distribution were monitored. Chemical changes and phase transformation in the catalyst were also examined. The surface areas of the catalysts were determined by nitrogen adsorption (BET method) using a Quantasorb adsorption unit manufactured by Quantachrome Corporation, USA. Pore volume and pore size distribution

were determined by mercury porosimetry. X-ray diffraction patterns of the catalysts were obtained using a Phillips PW-1410 x-ray spectrometer.

The rate of carbon combustion generally depends upon three main parameters, namely, start-up temperature, oxygen content of regeneration gas and the flow rate. Initial studies were focused on the influence of these parameters on catalyst characteristics. The aim was to obtain a better understanding of the changes brought about to the physico-chemical characteristics of the catalyst by changes in the regeneration parameters, and hence to establish optimum conditions to minimize catalyst deactivation by sintering and phase transformations during regeneration.

During the decoking process extensive loss of surface area and activity occurred at high (>5%) oxygen concentrations (Figure 6.1) and high flow rates (>3 l/h/g.cat) of the regeneration gas (Figure 6.2). This is explainable in terms of the formation of hot spots in the catalyst bed. At higher oxygen concentration or flow rates, coke burning rates are high and an excessive amount of heat will be generated on the catalyst surface leading to sintering of the catalyst. The optimum gas flow rate (around 2 lit/h/gm of catalyst) observed under the condition of this study (Figure 6.2), appears to be adequate for controlled burning of most of the coke without formation of hot spots which could damage the catalyst.

At very low gas flow rates, a relatively large percentage of carbon remained unburned. This was verified from the carbon analysis of the catalysts of some runs which were terminated before air was introduced. When air was introduced at the end of the run, it is likely that excessive heat was generated due to the rapid burning of the remaining coke causing some sintering of the catalyst and loss of surface area. This probably explains the low surface area observed for the catalyst regenerated at very low gas flow rates (Figure 6.2).

A significant loss in surface area due to sintering of the catalyst support was observed recently by Furimsky when the catalyst was regenerated in air containing 20% oxygen (100). Under the conditions of the present study, start-up oxygen concentrations above 5% in the regeneration gas were found to result in catalyst sintering. This reflects the importance of controlling excessive oxygen availability to prevent hot spots in the regeneration bed. However, higher oxygen concentrations could be used if localized

temperatures are better controlled and hot spots are avoided, as in the design of some commercial regeneration units (94b).

The regeneration temperature was varied between 300 and 800°C and its effect on important physical and chemical properties was examined. The data presented in Figure 6.3 shows that the temperature of decoking had a very significant effect on the catalyst surface area and pore volume. A catalyst regenerated at 300°C had a substantially lower surface area than those regenerated with temperatures in the range 370 - 440°C, presumably due to incomplete coke combustion. Studies using temperature-programmed oxidation of coke in spent hydrotreating catalysts (34,95,96,) have shown a sharp increase in CO_2 formation with a maximum at temperatures around 400°C. This indicates that most of the coke on the catalysts can be removed by combustion at around this temperature region.

An increase of initial regeneration temperature above 440°C resulted in extensive sintering as indicated by pore enlargement and a drastic drop in surface area. This was presumably due to a very high combustion rate and excessive heat generation. Pore size distribution data of the catalysts decoked at different temperatures demonstrate a progressive increase in the amount of large pores (Figure 6.4). Thus, for example the catalyst regenerated at 400°C had a maximum pore volume around 0.006-0.008 micron pore diameter. On increasing the regeneration temperature to 600°C and 700°C, the pore maxima shifted to about 0.025 micron, and 0.040 micron diameter, respectively. Further increase of temperature to 800°C, resulted in a large increase of the pore diameter with a maximum around 2 micron. The large loss in surface area at temperatures above 600°C is probably due to the influence of Mo in enhancing alumina sintering and phase transformation (137).

X-ray diffraction (XRD) patterns of the catalysts regenerated at different temperatures showed no significant changes on increasing the temperatures up to 500°C. Above this temperature new peaks were observed corresponding to molybdenum trioxide ($2\theta = 25.5°$ and 27.50°) and aluminium molybdate ($2\theta = 23.5°$). The peaks corresponding to γ-alumina became sharp and narrow with progressive increase of temperature indicating enhanced crystallinity and sintering. The XRD-pattern of the sample regenerated at 800°C showed the presence of α-alumina, indicating that phase transformation of γ-alumina has occurred.

Chemical analysis of the regenerated catalysts indicated that temperatures up to 600°C had no significant effect upon the composition of the catalyst (Figure 6.5). At 700°C and above, a substantial decrease in the amount of molybdenum was observed, whereas, the cobalt content was not significantly affected. These results are in agreement with the earlier finding that calcination temperatures above 700°C lead to volatilization of molybdenum from the catalyst (23). The results show clearly demonstrate care must be exercised to control the temperature around 400°C during the early period of decoking, since high temperatures cause sintering, phase transformation and substantial loss of molybdenum and lead to irreversible deactivation of the catalyst.

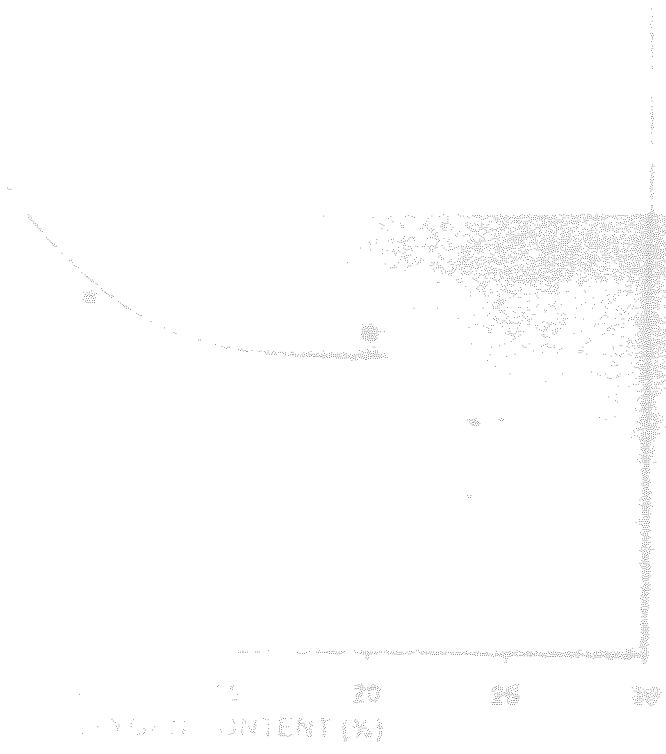

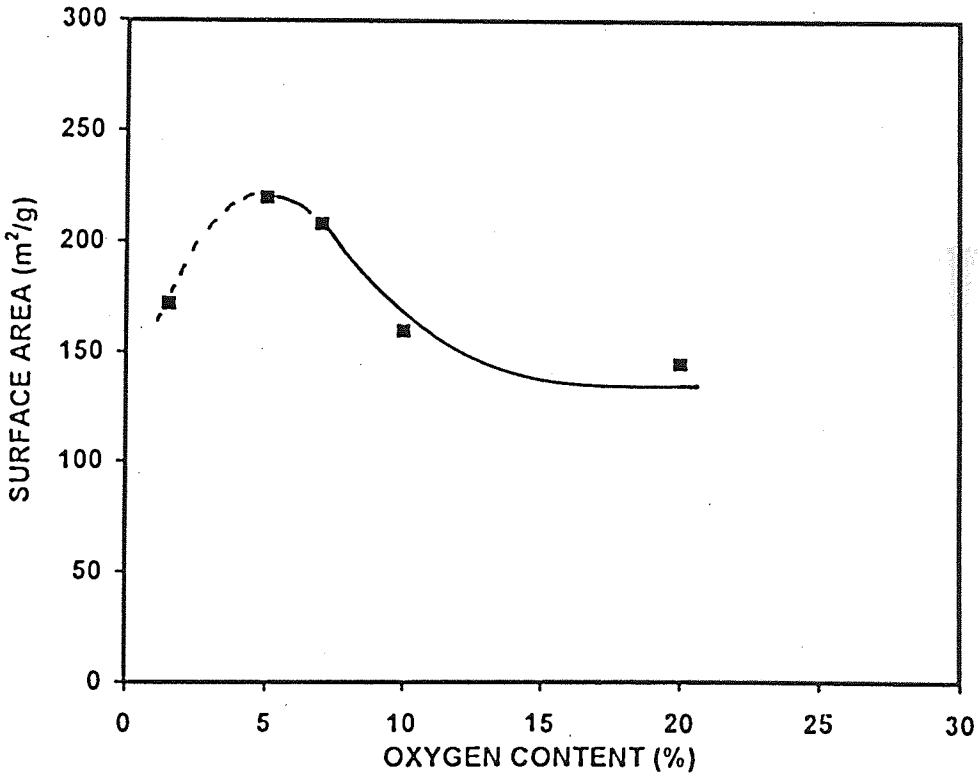

Figure 6.1. Effect of Oxygen Content of the Regeneration Gas on Catalyst Surface Area.

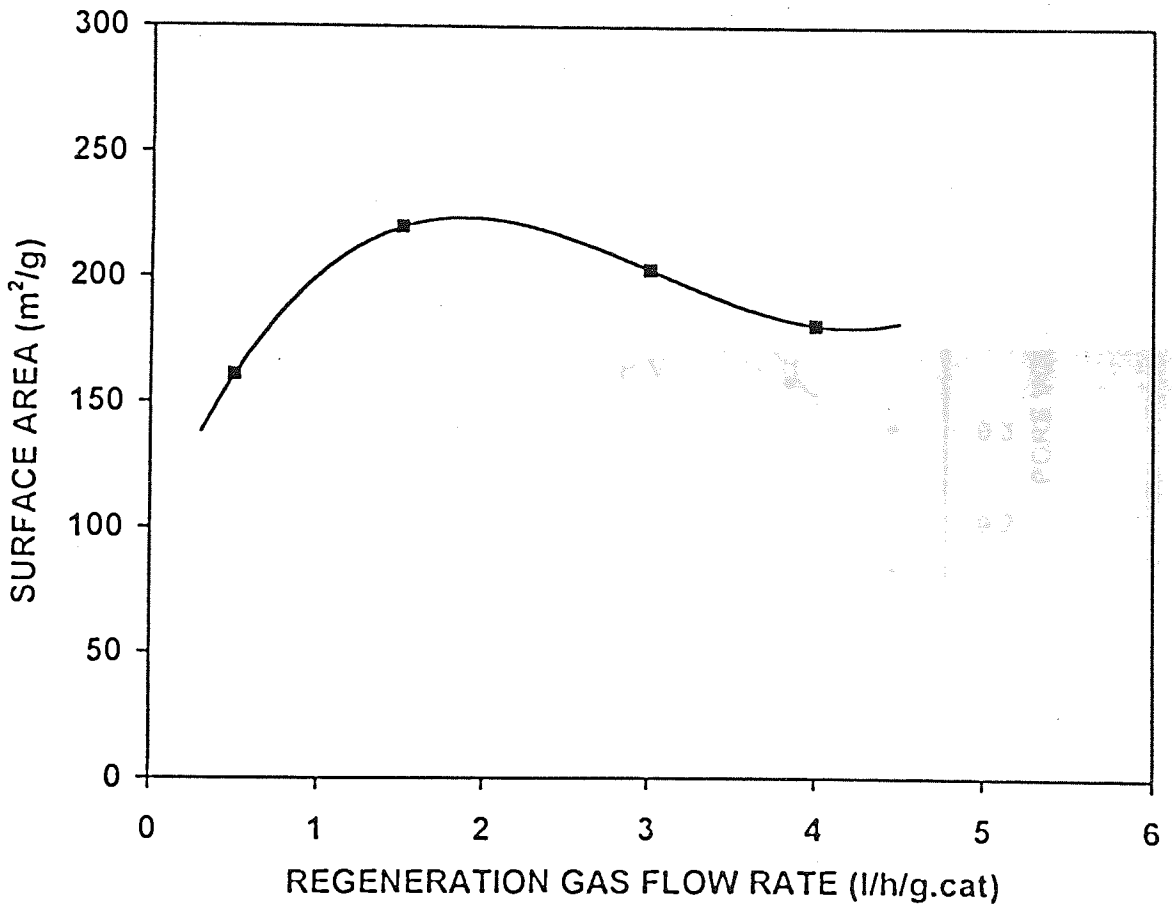

Figure 6.2. Effect of Regeneration Gas Flow Rate on Catalyst Surface Area.

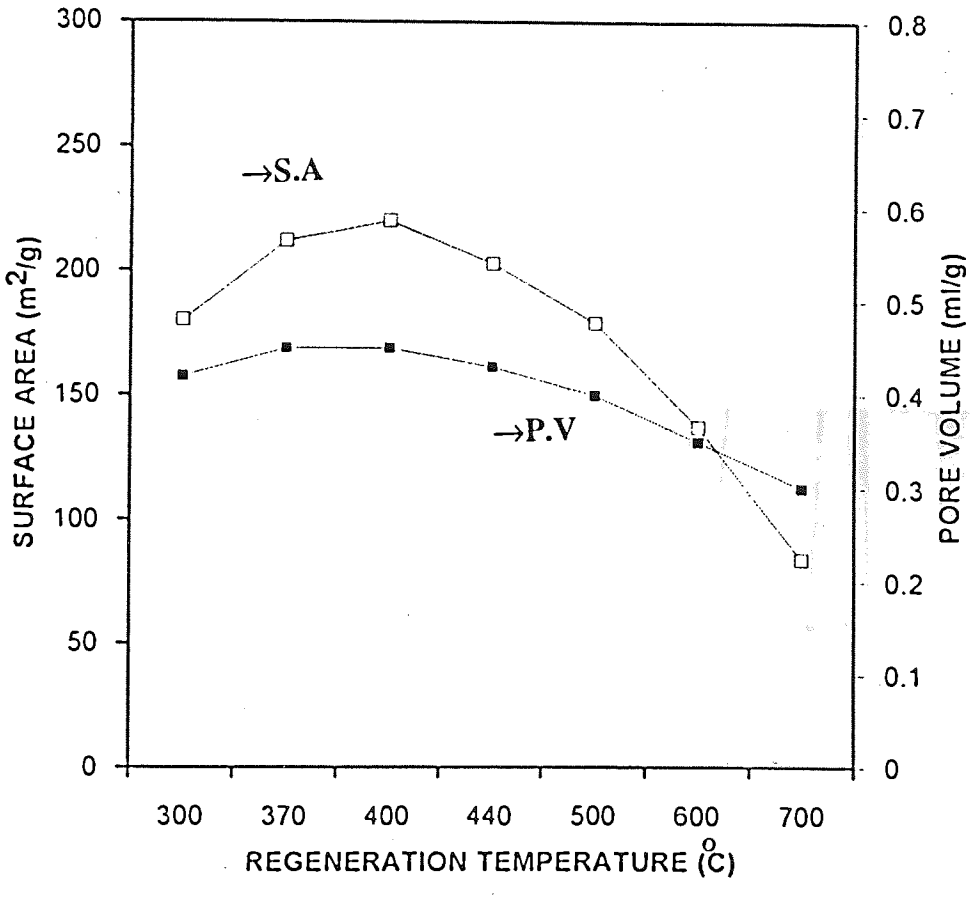

Figure 6.3. Effect of Regeneration Temperature on Catalyst Surface Area and Pore Volume.

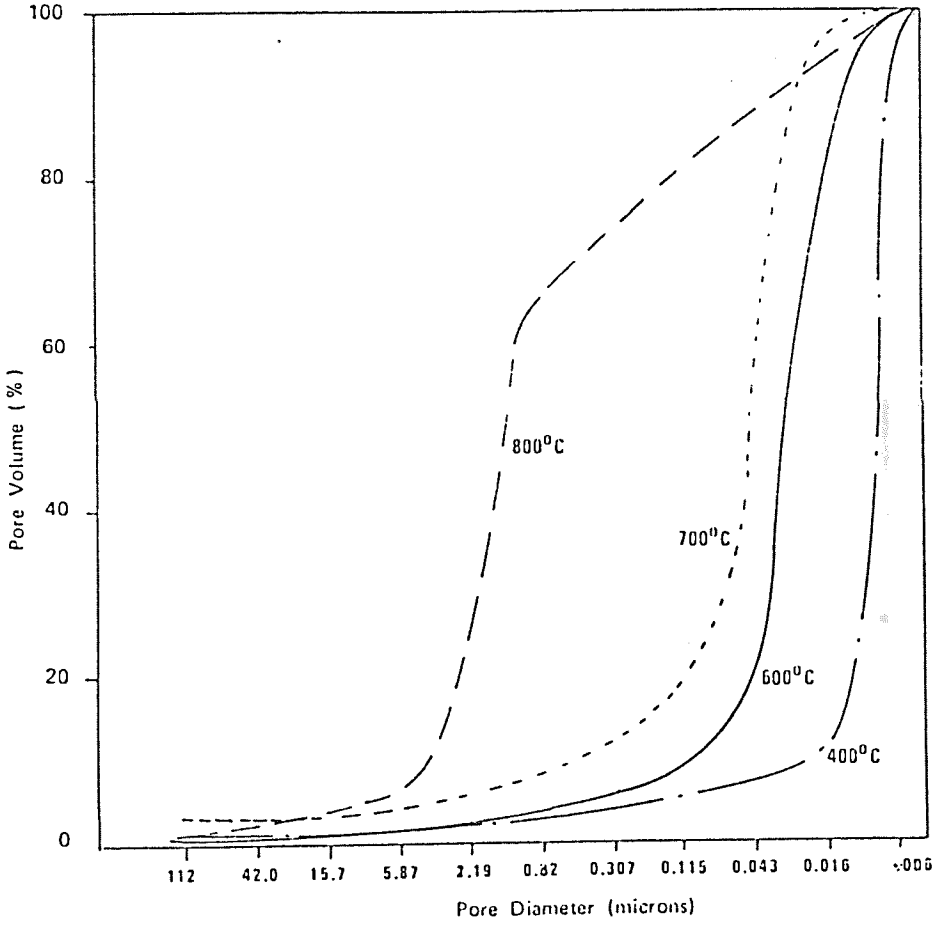

Figure 6.4. Effect of Regeneration Temperature on Catalyst Pore Size Distribution.

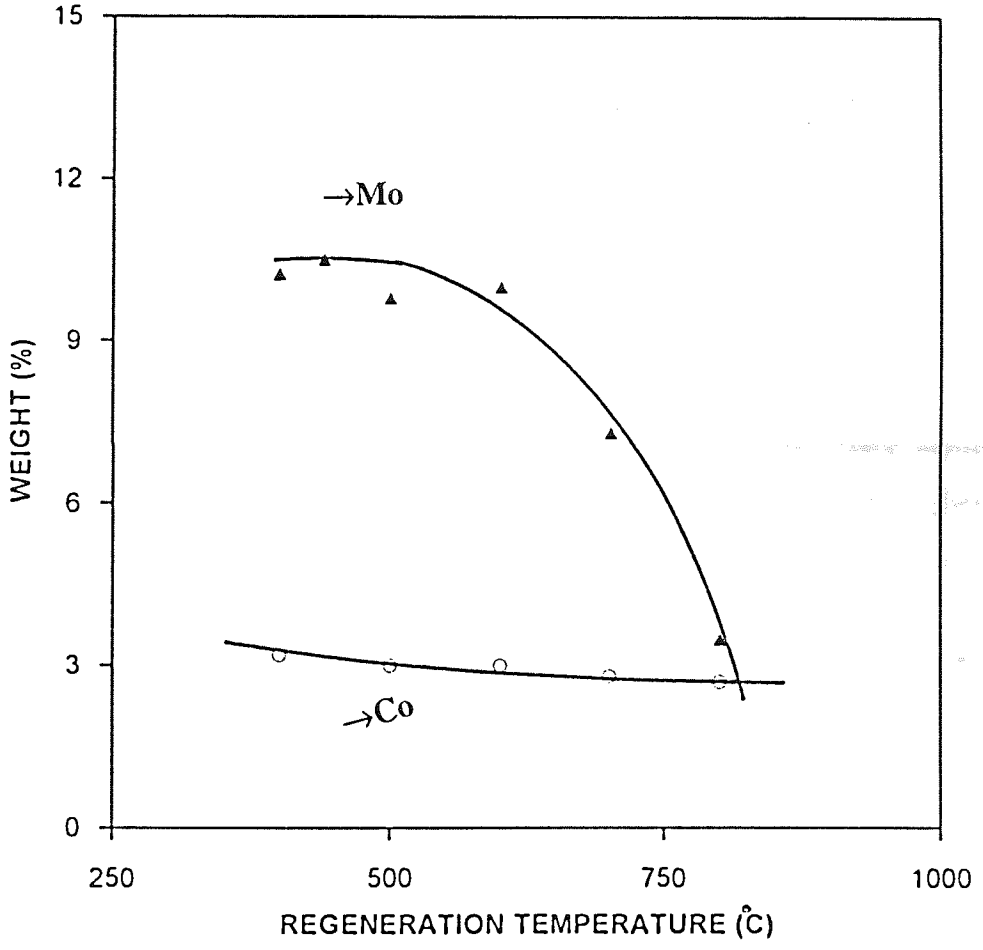

Figure 6.5. Effect of Regeneration Temperature on Active Metals Content of the Catalyst.

7.0. SPENT CATALYST REJUVENATION BY LEACHING OF FOULANT METALS

Catalysts used in the upgrading of petroleum residues are deactivated by coke and metal (V and Ni) deposits originating from the heavy feedstock (7,130,139). The foulant metals are usually concentrated near the outer surface of the pellet; they tend to plug the pore mouths and markedly reduce the active surface area available within the inner pores of the catalyst (9,33). To reactivate the catalyst both the coke and metal deposits have to be removed from the catalyst surface. Regeneration by conventional procedures using nitrogen-air or steam-air removes only the coke deposits (93,101). The metallic impurities remain on the catalyst and act as a diffusion barrier for the reactants. If the contaminant metals can be removed selectively by chemical treatment without significantly affecting the useful physical and chemical properties of the catalyst, then the catalyst can be rejuvenated and reactivated (101,102).

Several workers have attempted to rejuvenate metal-fouled spent residue hydrotreating catalysts by selective removal of the deposited metals by chemical treatment (101,102,138,103,106,126,108,120). The reagents used to remove the metals include organic and inorganic acids, alcohols, ketones, dioxane, peroxy compounds and chlorine based chemicals. In most of these studies the vanadium extraction was not selective. Excessive removal of the catalytically-active metals (Mo and Co) occured together with the undesired foulant metal (vanadium).

Furthermore, several important questions such as the mechanism of leaching, the preferred leaching route (coked or decoked form of the spent catalyst) for better selectivity in removing vanadium deposits, and the effect of metal leaching treatment on the physical and mechanical properties of the catalyst as well as upon the distribution of catalytically active metals were not addressed.

In the present work, a major emphasis was placed on the factors influencing the selectivity of vanadium leaching and on the mechanism of the leaching process. The effectiveness of leaching vanadium from coked (sulphide) and decoked (oxide) forms of spent residue hydrotreating catalyst using oxalic acid was investigated. The influence of oxidizing agents such as H_20_2 and ferrite nitrate on the leaching efficiency of organic acids was also studied. Samples of the spent and leached catalysts were characterized for surface

area, porosity, chemical composition and metal distribution profile within the catalyst pellet. The samples were also tested for HDS activity recovery and the relationship between the amount of vanadium removed and the recovery of surface area, pore volume and HDS activity was examined. The results of all these studies are presented and discussed in the following three sections (7.1., 7.2 & 7.3).

7.1. Comparative study of the effectiveness and selectivity in the removal of foulant metals from spent hydroprocessing catalysts in coked and decoked forms.

Two routes were used to leach the foulant metals from the spent residue hydroprocessing catalysts. In the first, de-oiled spent catalyst containing coke and deposited metals in sulphide form was chemically treated to leach the metal foulants. In the second, de-oiled spent catalyst was decoked by controlled combustion of coke and the resultant coke-free catalyst containing metals in oxide forms was subjected to leaching. Oxalic acid, a chelating agent that can form soluble metal complexes, was used for metal leaching via both routes. The spent and treated catalysts were characterized and the improvements in surface area, pore volume and hydrode-sulphurization (HDS) activity of the catalysts were compared. The primary aims of the study were to compare the effectiveness of the two routes for selectively leaching the deposited vanadium from coked and decoked forms of spent catalyst and to recommend the preferred leaching route for better activity recovery.

7.1.1. Comparison of foulant metals leaching from coked and decoked catalysts by oxalic acid and oxalic acid + H_20_2 reagents

A series of leaching experiments were conducted on coked and decoked spent catalysts using oxalic acid and oxalic acid mixed with an oxidizing agent such as hydrogen peroxide. The experimental procedure used for leaching is described in detail in Chapter 4. The amount of vanadium removed from the two types of spent catalysts by oxalic acid alone are compared in Fig. 7.1. This shows that the extent of vanadium leaching from the decoked spent catalyst was considerably higher than that from the coked catalyst. Thus for example, about 55% wt. of vanadium was removed from the decoked catalyst in 8 h, whereas less than 4% is leached from the coked catalyst under the same conditions.

The addition of hydrogen peroxide to oxalic acid resulted in to a large increase in the extraction of vanadium from the coked catalyst (Fig. 7.2), but did not significantly affect removal from the decoked catalyst (Fig. 7.3). Similar results were observed for nickel extraction from both types of catalysts by oxalic acid and oxalic acid + H_2O_2 reagents (Table 7.1).

A possible explanation for the observed differences in the leaching behavior of decoked and coked catalyst related the oxidation state of the metals present. In the coked spent hydrotreating catalyst, the metals are present primarily as sulphides in lower oxidation states (140,128). During decoking carbon is burnt in an oxygen-containing atmosphere. As a result, it is possible that low-valence metal sulphides are oxidized to high-valence metal oxides and sulphates. Salts or complexes of metals in a higher oxidating state are known to be more soluble than the corresponding lower-oxidation state species. The observed difference in the leaching behavior of coked and decoked catalysts in oxalic acid could thus be attributed to the different oxidation states of the metal species present, which in turn influences their degree of reactivity and the nature and solubility of the complex formation. In decoked catalysts, the higher oxidation state favors the formation of soluble oxalate complexes, and thus higher leaching rate may be expected.

The enhanced leaching observed in the presence of H_2O_2 is in line with the above mechanism. H_2O_2 is an oxidizing agent, and, under acidic conditions, can oxidize the low-valence metal sulphides to high-valence metal ions that can readily form soluble complexes with oxalate ions in the leaching solutions. Thus, a synergistic effect between H_2O_2 and oxalic acid appears to be responsible for the improved leaching activity. Clearly, the presence of an oxidizing agent is helpful in leaching foulant metals by such complexing agents as oxalic acid because, in the oxidized state, vanadium and other metal ions are complexed more easily by oxalate ions kept in solution.

Further evidence for this theory is provided by the leaching experiments on decoked catalysts with oxalic acid in the presence and absence of H_2O_2. Figure. 7.3 shows that oxalic acid alone was very effective in leaching vanadium and the addition of H_2O_2 did not significantly improve leaching performance. Since the metals in the decoked catalyst are already present in a higher valency state, they are more easily attacked by oxalic acid to form soluble oxalate complexes, and leaching is therefore very effective.

Table 7.1. Influence of H_2O_2 on Nickel Extraction.

	Amount of nickel leached (wt %)[a]	
	Coked catalyst	**Decoked catalyst**
Oxalic acid	3.6	60.3
Oxalic acid + H_2O_2	47.0	76.5

[a]Amount of nickel leached after 8 h of treatment.

7.1.2. Selectivity for vanadium removal

Selective removal of the main foulant metal (i.e. vanadium) from the catalyst pores without significantly affecting the catalytically-active metals (e.g. molybdenum) is an important requirement for efficient rejuvenation and reactivation of the metal-fouled spent hydroprocessing catalyst. In Figure. 7.4 the amount of molybdenum leached is plotted against the amount of vanadium removed for coked and decoked catalysts with an oxalic acid + H_2O_2 reagent system. The amount of molybdenum removed along with vanadium was substantially higher for the decoked than for the coked catalyst. Since molybdenum is an active HDS catalyst component, its removal in substantial quantities may be expected to reduce the catalyst activity. The above results clearly indicate that in practice it would be more effective to conduct the leaching before, rather than after, decoking (Route 1).

7.1.3. Effect of metal leaching by different routes on the catalyst surface area, pore volume and HDS activity.

The surface area, pore volume and HDS activity of spent catalysts rejuvenated by leaching by different routes were determined. The results are compared with those of untreated spent catalyst and the corresponding fresh catalyst in Table 7.2. The surface area and pore volume of the spent catalyst (fouled by coke and metal deposits) were, respectively, about 22 and 25% of the fresh catalyst.

The removal of the foulant metals from the spent catalyst by leaching results in an improvement in surface area and pore volume, the degree of improvement being different for different leaching reagents and routes. Leaching of the coked catalyst with oxalic acid alone did not result in any significant improvement in surface area and pore volume whereas with the oxalic acid + H_2O_2 reagent, the surface area was increased remarkably (from 52 to 141 m^2/g). In the case of decoked catalyst the improvement in surface area and pore volume are substantially higher even for the sample treated only with oxalic acid. In general, the surface area recovery appears to be a function of vanadium removal.

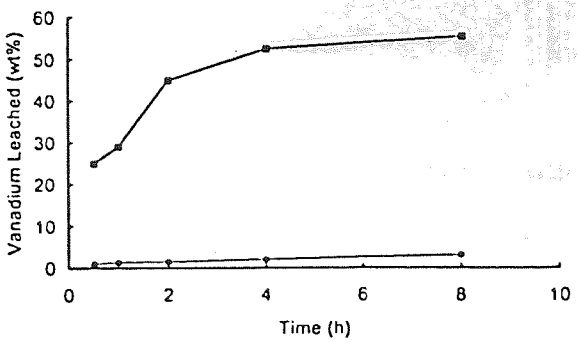

Figure. 7.1. Comparison of vanadium leaching from coked and decoked spent catalysts by oxalic acid. (●) Coked; (■) decoked.

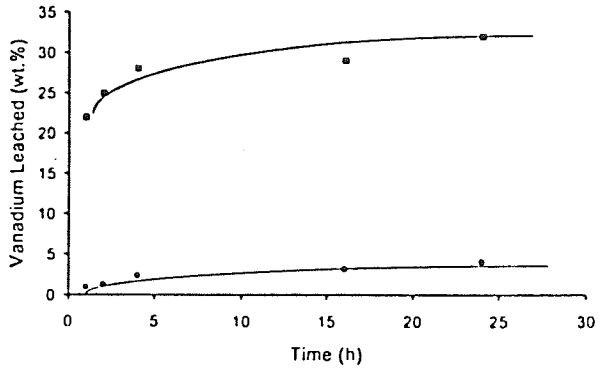

Figure. 7.2. Effect of hydrogen peroxide addition on the efficiency of oxalic acid for vanadium removal from coked spent catalyst (●) Oxalic acid; (■) oxalic acid (0.66M) + H_2O_2 (0.66 M).

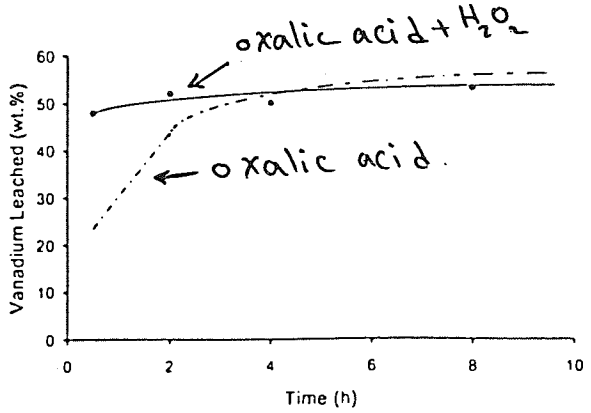

Figure. 7.3. Effect of hydrogen peroxide on the efficiency of oxalic acid for vanadium leaching from decoked spent catalyst. (○) Oxalic acid (0.66M); (●) oxalic acid (0.66M) + H_2O_2 (0.66M).

The HDS activity of the spent catalyst was very low, which is not surprising in view of its low surface area and pore volume caused by fouling by coke and metal deposits. Leaching of deposited vanadium prior to decoking with oxalic acid + H_2O_2 reagent mixture resulted in a substantial recovery of HDS activity although all the carbon deposits remained on the catalyst. The results indicate that coke deposition has less effect on deactivation than do the metal deposits.

Decoking of the leached catalyst leads to a further increase in HDS activity. For the catalyst leached after decoking, there was only partial recovery in catalyst activity even though the increase in surface area and pore volume resulting from metals leaching was high. This may be attributed to the leaching of a large quantity of molybdenum with the vanadium. Figure. 7.4. shows that the amount of molybdenum removed with vanadium was substantially higher for the decoked than for the coked catalyst. Thus, in the decoked catalyst, the advantage of surface-area gain resulting from vanadium removal appears to be offset by excessive molybdenum leaching.

Table 7.2. Surface area, pore volume and HDS activity of fresh, spent and treated catalysts

No.	Catalyst type	Leaching agent	Surface area (m^2/g)	Pore volume (ml/g)	HDS activity (%)	Relative HDS activity[a]
1	Fresh	-	240	0.48	61	100
2	Spent	-	52	0.12	17	28
3	Leached but not decoked	Oxalic acid alone	65	0.15	21	34
4	Leached but not decoked	Oxalic acid + H_2O_2	141	0.27	52	85
5	Leached and decoked (Route 1)	Oxalic acid + H_2O_2	181	0.43	59	97
6	Decoked and leached (Route 2)	Oxalic acid + H_2O_2	197	0.46	36	59
7	Decoked and leached	Oxalic acid alone	180	0.42	37	61

aThe relative HDS activity is based on the activity of fresh catalysts taken as 100.

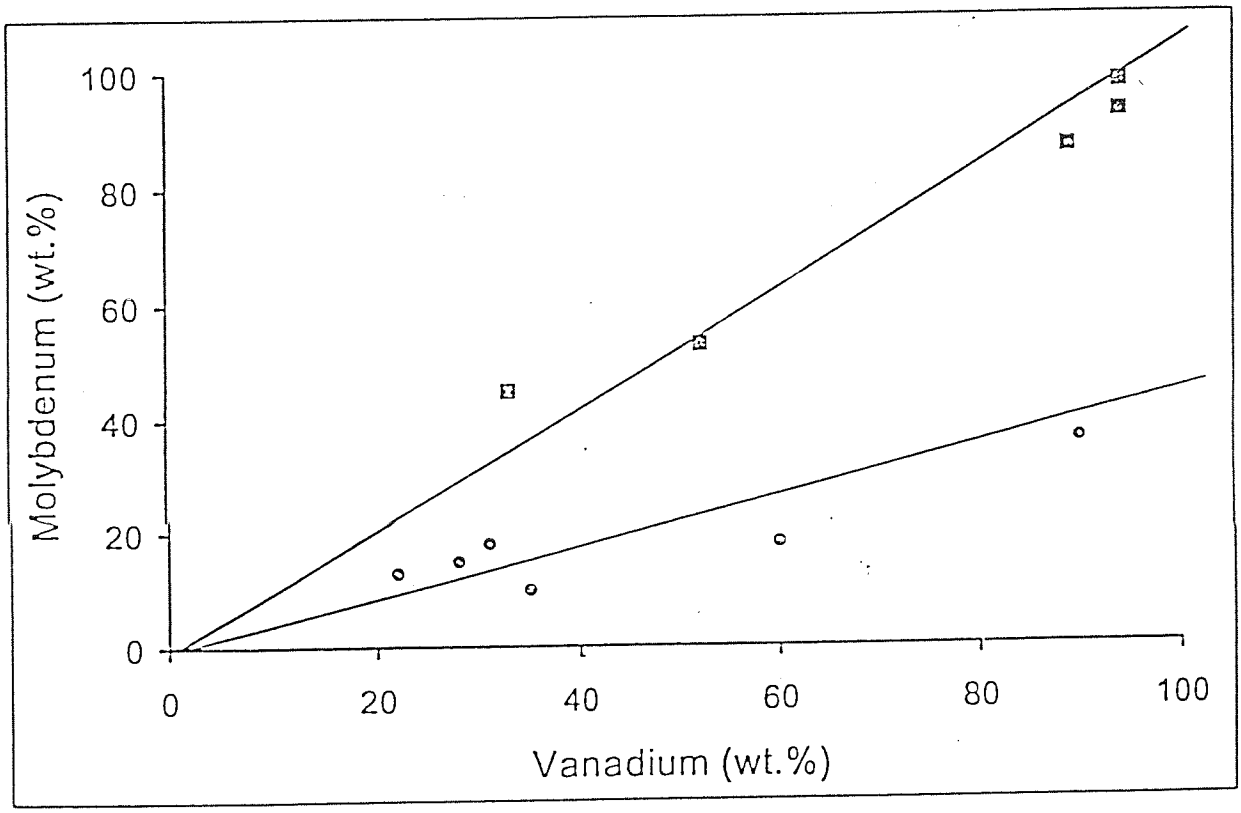

Fig. 7.4. Vanadium leached vs. molybdenum leached for coked and decoked catalysts with oxalic acid + H_2O_2 reagent (■) Decoked; (●) coked.

7.1.4. Conclusions

A comparative study was made on the leaching of metal foulants from spent hydroprocessing catalyst in coked and decoked forms using oxalic acid and oxalic acid mixed with an oxidizing agent such as H_2O_2. Oxalic acid alone showed very poor activity for leaching foulant metals from coked spent catalyst, but was very effective on decoked spent catalyst. The addition of hydrogen peroxide to oxalic acid enhanced the efficiency of leaching from coked spent catalyst, but not from decoked spent catalyst. The selectivity for removal of the major metal foulant (vanadium) was better and activity recovery was higher for the catalyst rejuvenated by metal leaching prior to decoking.

7.2. Studies on the Leaching of Foulant Metals with Ferric Nitrate-Organic Acid Mixed Reagents.

In the previous study (reported in Section 7.1. a comparison was drawn between the efficiency of oxalic acid for selective leaching of metal foulants from coked and decoked forms of spent residue hydroprocessing catalyst. The influence of adding an oxidizing agent such as H_2O_2 to oxalic acid, on the leaching efficiency was also examined. Oxalic acid alone showed very poor activity for leaching foulant metals from coked spent catalyst, but was very effective on decoked spent catalyst. Addition of hydrogen peroxide to oxalic acid enhanced the efficiency of leaching from coked spent catalyst, but not from decoked spent catalyst. The selectivity for removal of the major metal foulant (vanadium) was better and activity recovery was higher for the catalyst rejuvenated by metal leaching prior to decoking.

These results suggest that a mixture of an oxidizing agent and an organic complexing agent would be more effective and selective for vanadium leaching from coked spent catalyst. Therefore, other selected oxidizing agents were tested for their efficiency in selectively promoting the leaching of foulant metals (141,142). The influence of mixing ferric salts (e.g. ferric nitrate and ferric sulphate) to some organic acids, namely, oxalic, and tartaric acid in selective extraction of foulant metals from coked spent catalyst is reported in this section.

7.2.1. Influence of ferric nitrate on the leaching efficiency of different acids.

Leaching experiments were carried out using two different organic acids, namely, oxalic and tartaric acids, with or without ferric nitrate addition. De-oiled, but not decoked, spent catalyst from the atmospheric residue hydrodesulphurization unit of Kuwait National Petroleum Company (KNPC) was used in the experiments.

Figure. 7.5 shows the influence of ferric salts on the efficiency of oxalic acid for vanadium extraction from the spent catalyst. Clearly oxalic acid alone had a very poor activity for leaching vanadium from the spent catalyst, the adding of ferric nitrate to oxalic acid substantially enhances its efficiency for vanadium extraction. Ferric nitrate was more effective than ferric sulphate in enhancing the leaching efficiency of oxalic acid. Figure. 7.6. shows a similar effect from ferric nitrate on nickel extraction by oxalic acid. An increase in the concentration of oxalic acid from 0.33 to 0.66M substantially enhanced both vanadium and nickel leaching (Figures. 7.5 and 7.6). A similar accelerative influence of ferric nitrate for vanadium and nickel leaching was observed with tartaric acid (Figure. 7.7).

Consideration of the various steps involved in the leaching process may assist understanding of the role of ferric nitrate in promoting the leaching efficiency of organic acids. The process of leaching normally involves the following individual steps: (a) diffusion of leaching reagent to the solid liquid interface, (b) reaction between the solid and the reagent to form a product, (c) dissolution of the product, and (d) diffusion of the dissolved product away from the interface. Any combination of the above steps may control the rate of leaching away from the interface and the amount of material leached. In spent hydrotreating catalysts, the metals are present as sulphides (106). In such systems, the leaching reactions can be expected to be of the overall form:

$$MS_x + 2xRCOOH \longrightarrow M(RCOO)_{2x} + x\,H_2S$$

In aqueous systems, such reactions can be expected to proceed in three stages, e.g. for oxalic acid.

$$H_2C_2O_4 \rightleftharpoons 2H^+ + C_2O_4^=$$

$$MS_x + 2xH+ \rightleftharpoons M^{2x+} + xH_2S$$

$$M^{2x+} + xC_2O_4= \rightleftharpoons M(C_2O_4)x$$

which will be controlled by the ionization constants of the acids, and the equilibrium constants of the metal sulphides and the metal/organic acid complexes. The ease of formation of the metal ion, its reaction with the complexing agent, and dissolution of product depend to a large extent on the oxidation state of the metal in the metal compound.

In the present study ferric nitrate had an accelerating influence on the dissolution of metals such as vanadium and nickel in oxalic acid when the metals were present as sulphides in coked catalyst. The role of ferric nitrate in promoting the leaching efficiency of oxalic acid and other acids is not clear. In mineral processing, ferric salts are extensively used to enhance the acid leaching of certain metals, e.g., Zn, Cu and Ni, from their sulphide ores (141,142). A galvanic mechanism has been proposed by some workers to explain the catalytic effect of ferric ions. Galvanic interactions can cause an enhanced dissolution of one or more of the electrochemically coupled minerals, and cathodic protection (no dissolution) of other minerals. The minerals (or metal salt) with the lower rest potential will react anodically and dissolve rapidly, whereas cathodic behavior (no dissolution) may be imposed on the mineral possessing the higher rest potential. Mechanism based on the redox potential of the Fe^{3+}/Fe^{2+} couple have been proposed to explain the catalytic role of Fe^{3+} ions in leaching metals from sulphide ores (143). This implies that in systems involving oxidative leaching, the rate and selectivity of leaching different metals can be controlled by varying the redox potential of a given electrolyte or by using appropriate redox couples.

Ferric nitrate is a good oxidizing agent. Its role in enhancing the leaching of metals by acid reagents is therefore to oxidize the low valent metal sulphides to higher oxidation states which may be more easily attacked by the acid reagent or complexing agent. In the oxidized state vanadium would be complexed more easily by oxalate ions and kept in solution. These results lend additional support to the earlier suggestion that a synergistic mechanism involving oxidizing and complexing reactions is responsible for the enhanced leaching of metals from coked spent hydrotreating catalysts.

7.3. Effect of Metal Leaching on Catalyst Characteristics and Performance.

In the metal-leaching process, the catalyst is treated with chemical reagents to remove the contaminant metals from the catalyst surface, the major objective being to rejuvenate the catalyst. It is important that no major damage occurs to the useful properties of the catalyst. Information on the physical, chemical and mechanical properties of the treated-

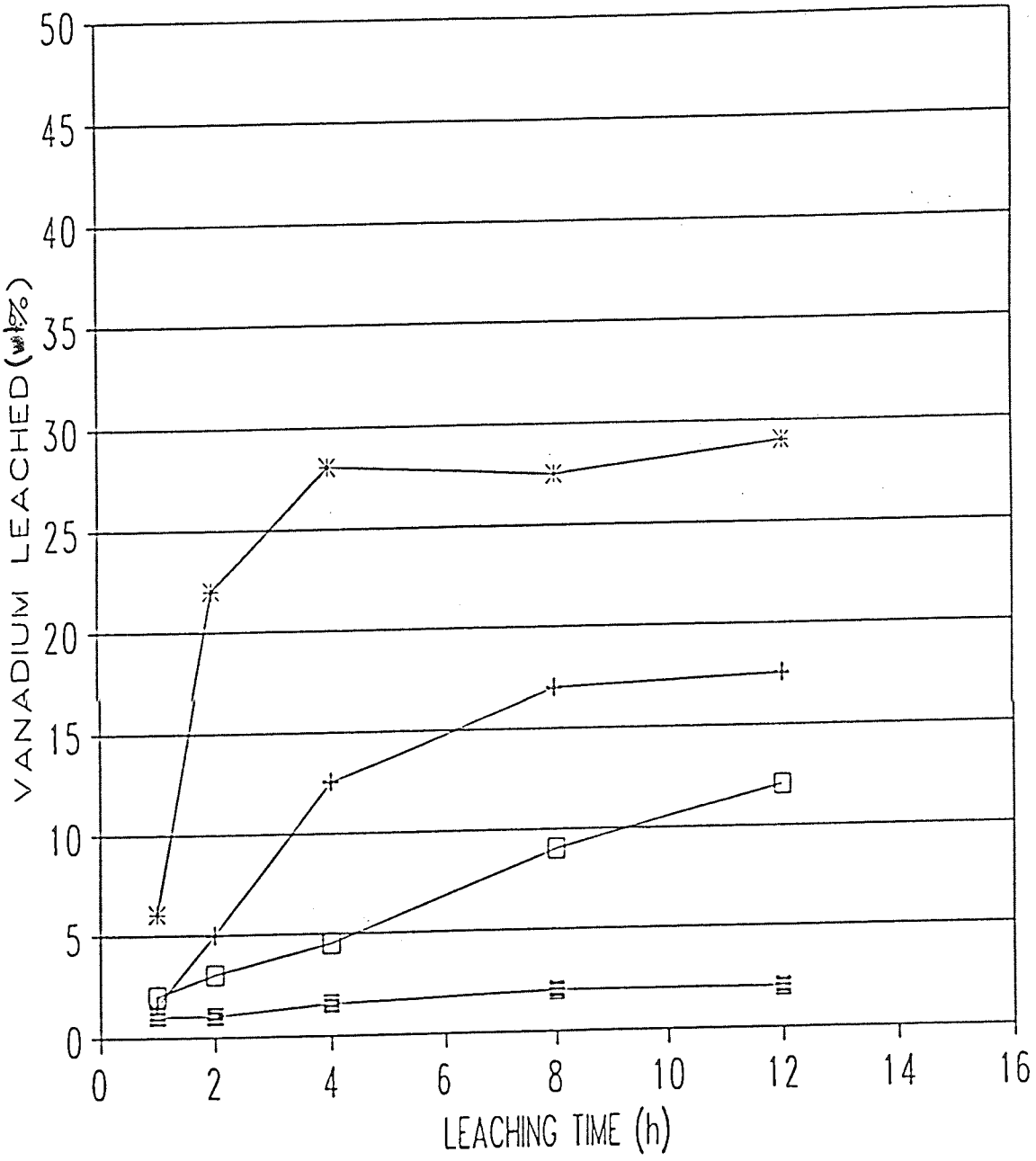

Figure. 7.5. Effect of ferric salts on the efficiency of oxalic acid for vanadium removal. (■) Oxalic acid (0.66 M), (*) oxalic acid (0.66 M) + ferric nitrate (0.66 M), (+) oxalic acid (0.33 M) + ferric nitrate (0.66 M), (□) oxalic acid (0.66 M) + ferric sulphate (0.66 M).

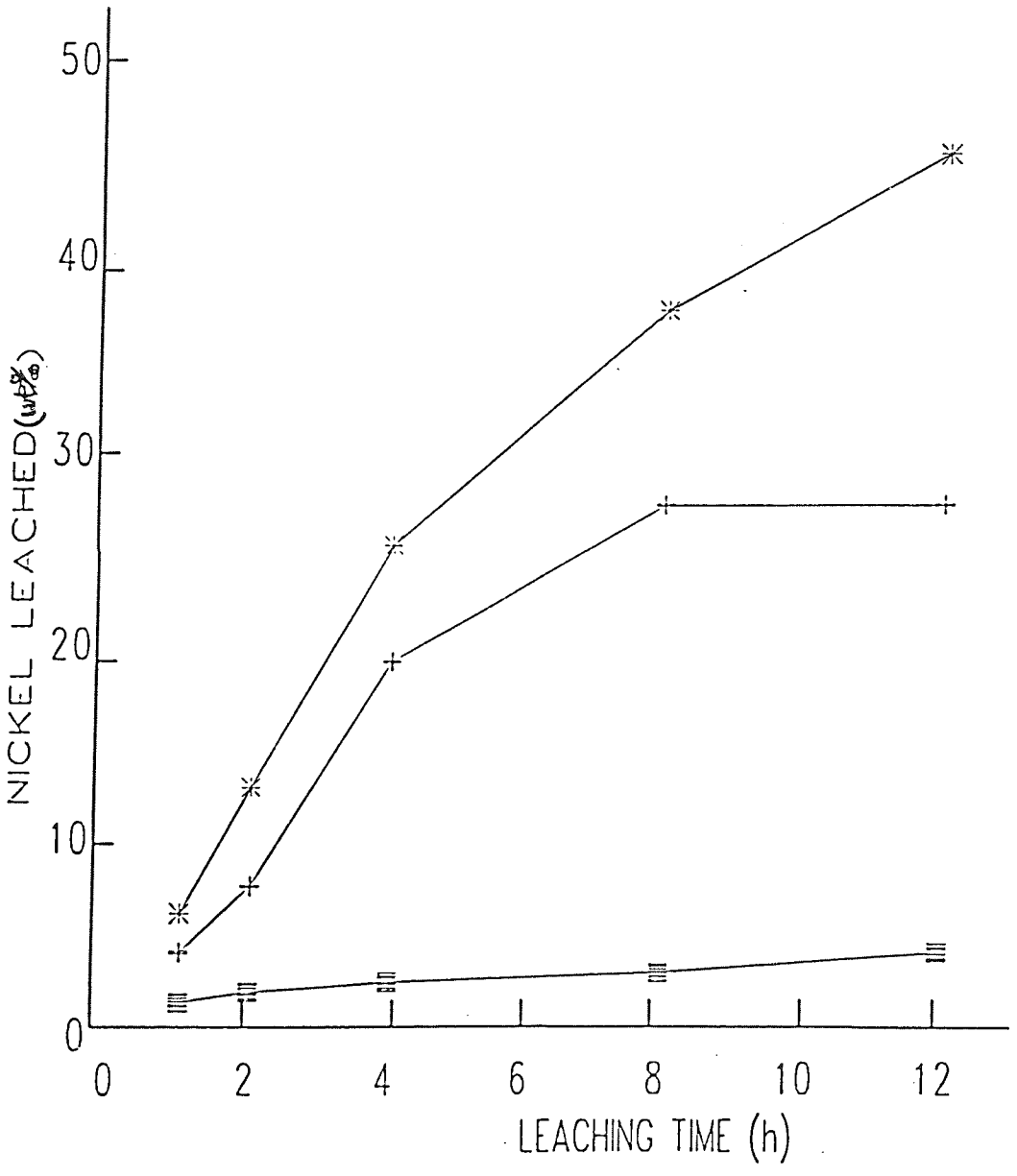

Figure. 7.6. Effect of ferric nitrate on the efficiency of oxalic acid for nickel extraction. (▣) Oxalic acid (0.66 M), (+) oxalic acid (0.33 M) + ferric nitrate (0.66 M), (*) oxalic acid (0.66 M) + ferric nitrate (0.66 M)..

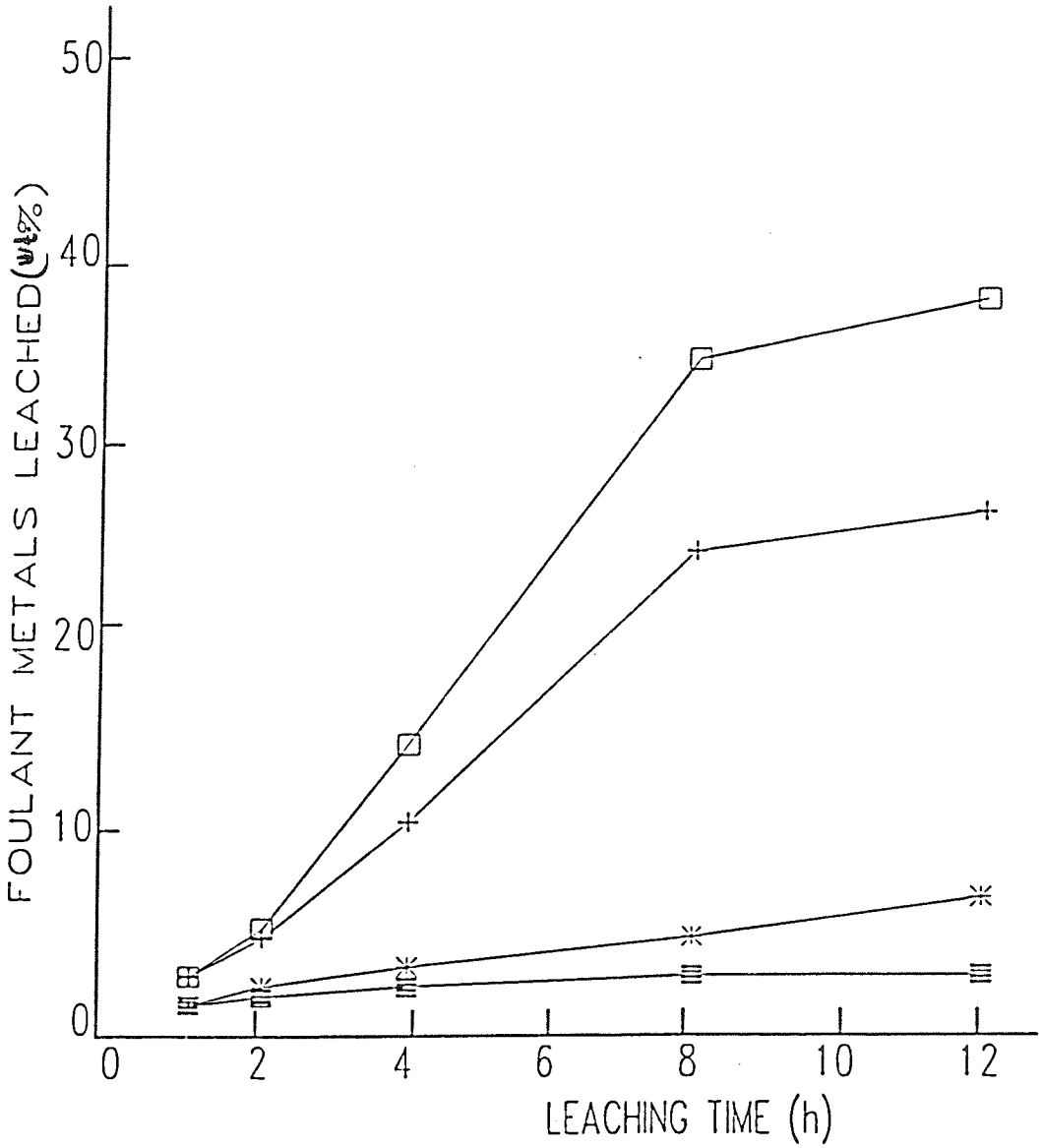

Fig. 7.7. Effect of ferric nitrate on the efficiency of tartaric acid for vanadium and nickel removal. (■) Vanadium leached by tartaric acid (0.66 M), (+) vanadium leached by tartaric acid (0.66M) + ferric nitrate (0.66 M), (*) nickel leached by tartaric acid (0.66 M), (□) nickel leached by tartaric acid (0.66 M) + ferric nitrate (0.66 M).

samples of spent catalyst and treated catalyst were, therefore, characterized for their surface area and porosity. The influence of chemical treatment on the distribution of the foulant metals (V and Ni) and the active catalyst metals (Co and Mo) within the catalyst pellet were determined by electron microprobe analysis. X-ray diffraction patterns of fresh, spent and treated catalysts were examined to determine whether any phase changes had occurred in the catalyst as a result of the leaching treatment. The samples were also subjected to an activity test for hydrodesulphurization, and activity recovery as a result of the rejuvenation process was evaluated. The relationships between the amount of vanadium removed and the recovery of surface area, pore volume and HDS activity were carefully examined.

7.3.1. Relation between the extent of vanadium removal from the spent catalyst and surface area and pore volume improvement.

The surface area and pore volume of treated spent catalysts are plotted as a function of (%) vanadium extracted in Figure 7.8. Clearly both the surface area and pore volume increased substantially with increasing vanadium extraction.

An interesting point to note in Figure 7.8.demonstrates that even an initial extraction of 5-10% V from the spent catalyst leads to a significant increase in surface area. This was particularly high up about 30% vanadium removal. Extraction of more vanadium above this level (up to 90%) did not result in an appreciable increase in surface area.

7.3.2. Effect of vanadium leaching from the spent catalyst on its HDS activity.

The HDS activities of the leached spent catalysts were determined in a fixed bed microreactor using atmospheric gas oil containing 2 wt% sulphur as feed. Activity data presented in Figure 7.9. shows that about 85% of the catalyst's initial HDS activity was regained upon removal of about 30% vanadium from the spent catalyst, although all carbon deposits remained on the catalyst. No appreciable increase in HDS activity occured with further extraction of vanadium from the spent catalyst (Figure. 7.9). This trend is similar to that observed for the surface area improvement with vanadium removal (Figure. 7.8).

Some explanation of these observations can be advanced in terms of the location of the vanadium in the spent catalyst. Electron microprobe analysis of the spent catalyst showed that high concentrations of vanadium were present near the edge of the catalyst pellet (Figure. 7.10). Such large accumulations may block the pore mouths and make the surface within the pores inaccessible to the reactants. Hence, the catalyst is deactivated by pore mouth plugging (33,9).

A simple model representing pore plugging by foulant metal deposition is shown in Figure 7.11. It is possible that during the catalyst life on-stream, the narrow pores (C) rapidly become plugged simply because of the small pore mouth diameter. As the catalyst use continues progressively larger pores become plugged until the catalyst performance reaches the lowest permissible limit. Obviously at this stage some large pores (as represented by A) that lead to the pellet's interior are still accessible to the feed. This is evidenced by the 52 m^2/g surface area of the spent catalyst. If the catalyst pellet had been totally plugged the surface area would have been less than 1 m^2/g.

Leaching the foulant metal deposits from the pore mouths should open the pores and consequently increase the surface area of the catalyst. A real gain in surface area and activity will be achieved only when the amount of vanadium removed is sufficient to open the small and medium sized pores providing access to the active sites within the internal pores. It appears that less than 30% of the total vanadium deposited on the catalyst was responsible for pore mouth plugging and the obstruction of much of the catalyst surface area within the pores. The improvement in surface area and HDS activity of the catalyst were very high up to about 30% vanadium removal from the spent catalyst.

Figure 7.10. shows the effect of leaching on the distribution profiles of vanadium and other metals within a pellet of coked spent catalyst: the untreated spent catalyst contains large concentrations of vanadium near the edge, whereas the treated catalyst, contains a considerably decreased amount of vanadium near the edge. The results indicate that during the chemical treatment, the vanadium accumulated near the outer edge at the pore mouths was leached out gradually, thus opening up the pores. In agreement with this, the pore volume and catalyst surface area were found to increase with increasing vanadium removal. The unleached vanadium remaining in the treated catalyst was not concentrated at the pore mouths, but distributed uniformly within the pellet.

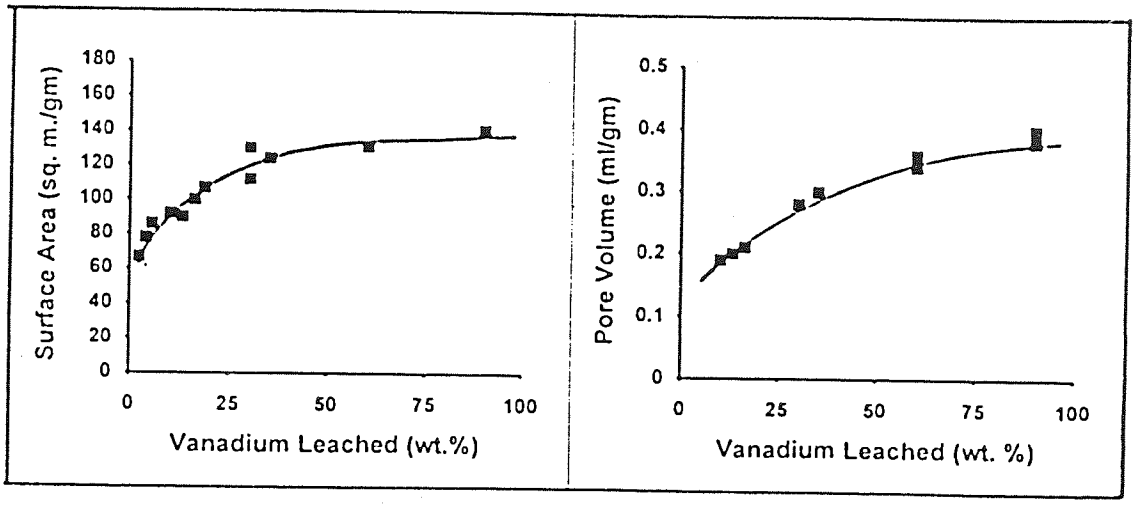

Figure. 7.8. Relation between vanadium removal and surface area and pore volume.

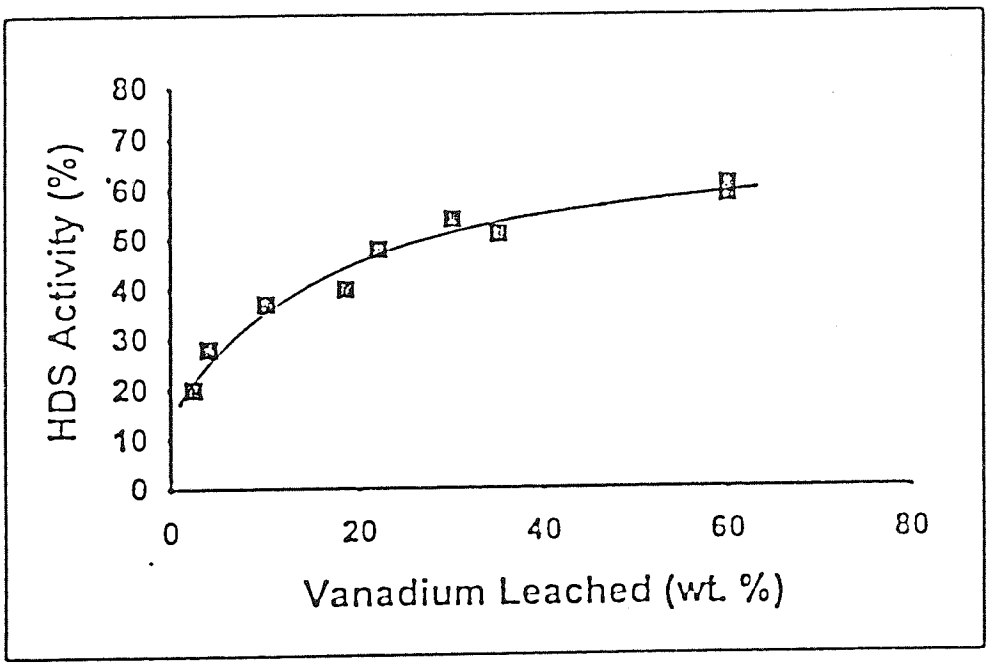

Figure. 7.9. Effect of vanadium leaching on desulphurization activity.

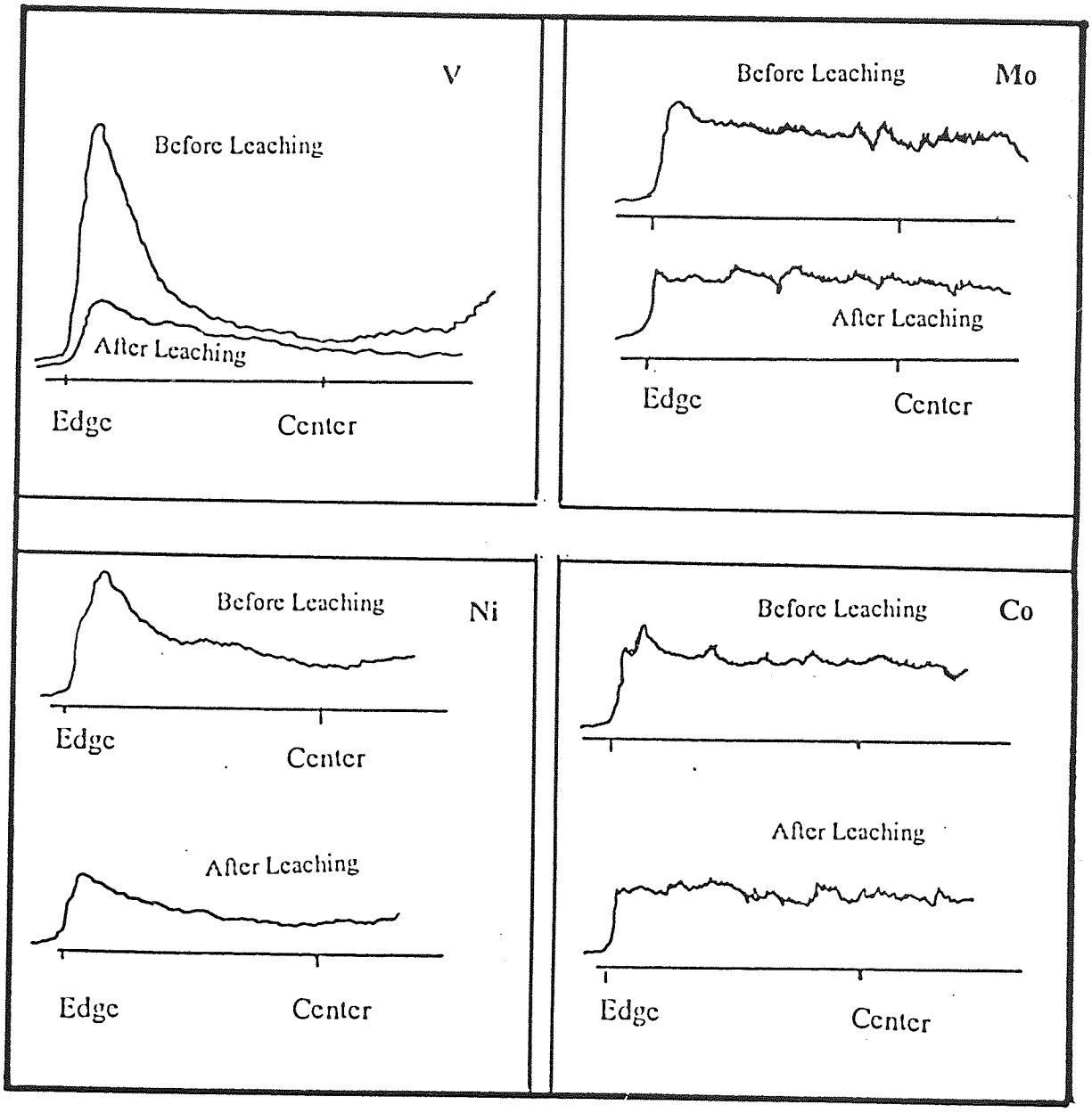

Figure. 7.10. Distribution Profiles of V, Ni, Mo, and Co in Spent Catalyst before and after Leaching.

Nickel penetrated further than the vanadium into the interior of the pellet. Nickel extraction by chemical reagents changed the distribution pattern; the concentrations of nickel at the edge and on the interior surfaces were decreased by leaching. The unleached nickel appears to be well distributed within the catalyst pellet. The distribution profiles of catalyst metals (Co-Mo) in coked spent catalyst pellets before and after leaching are also included in Figure 7.10. In the coked samples, both cobalt and molybdenum concentrations were slightly higher near the edge than at the center, whereas after leaching, the metals appeared to be redistributed.

XRD patterns of fresh, spent and treated catalysts were measured to determine whether any structural or phase changes had occurred in the catalyst and in the γ-alumina support as a result of the leaching and decoking (rejuvenation) treatments. The results presented in Fig. 7.12. show identical XRD patterns for the fresh and rejuvenated catalysts. The γ-alumina phase structure of the support is retained in the spent and leached catalysts. In the unleached spent catalyst, a diffuse peak (d value = 2.59) showed that vanadium was present as V_2S_3 either as small crystallites or amorphous material. No peaks corresponding to nickel, molybdenum or cobalt sulphides or other phases were detected. It is likely that these metals remain well dispersed in the form of small crystallites. The XRD results clearly indicate the absence of phase changes in the γ-alumina support as a result of the leaching treatment.

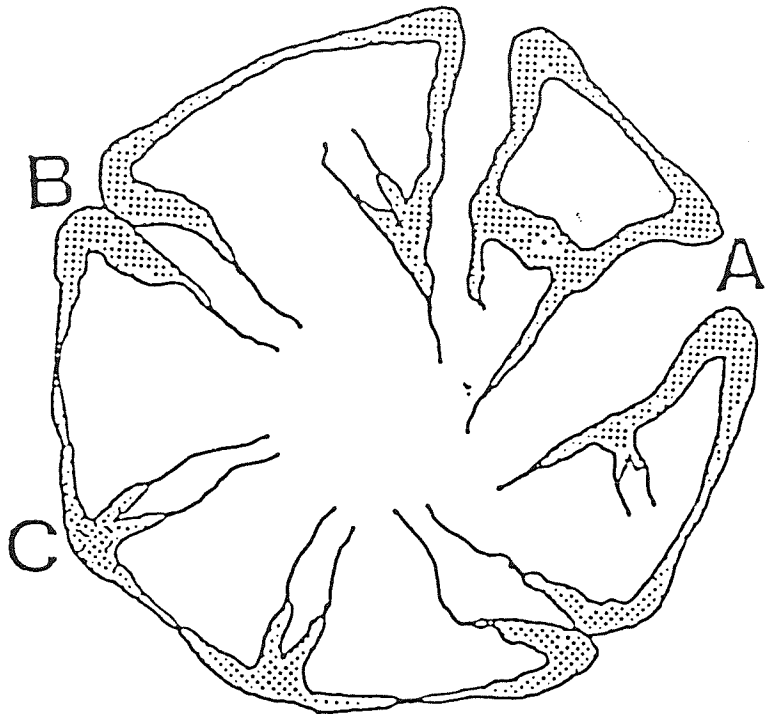

Figure 7.11. Representation of Pore Plugging by Foulant Metal Deposits. (A: large pores; B: medium-sized pores; C: micropores).

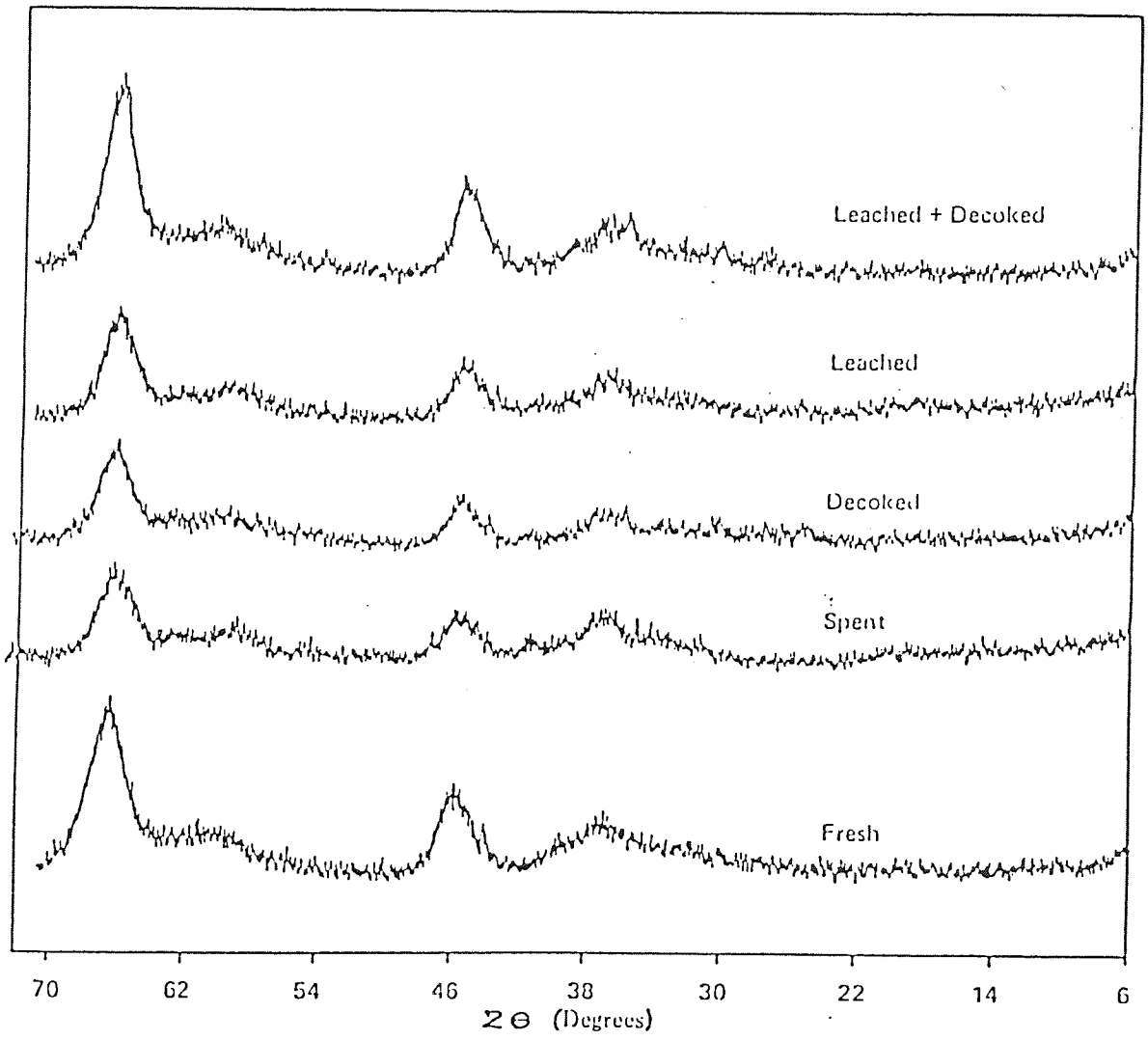

Figure. 7.12. X-ray diffraction patterns of fresh, spent, leached and rejuvenated catalysts.

7.3.3. Summary and Conclusions

Samples of spent and chemically-treated catalysts were characterized for surface area, porosity and chemical composition. The samples were also tested for HDS activity recovery as a result of the rejuvenation process, and the relationship between the amount of vanadium removed and the recovery of surface area, pore volume and HDS activity was examined. The results of the studies revealed that the surface area and pore volume increased substantially with increasing vanadium extraction from the spent catalyst and the HDS activity showed a parallel increase. Improvements in surface area and the HDS activity were substantial up to 30% vanadium removal but did not significantly improve for vanadium extraction above this level. More than 85% of the catalysts initial HDS activity was recovered by removal of about 35% vanadium from the catalyst, although all carbon deposits remained on the catalyst.

These results have been explained in terms of the location of vanadium in the spent and treated catalysts and its role in catalyst deactivation. Electron microprobe analysis was used to determine the distribution profiles of vanadium and other metals (Mo, Co and Ni) within pellets of treated and untreated spent catalysts. The untreated spent catalyst contained large concentrations of vanadium near the outer edge, whereas the treated catalyst pellets contained substantially decreased amount of vanadium near the edge. Redistribution of V, Co, Mo and Ni within the pellet as a result of leaching was observed. X-ray diffraction pattern of the rejuvenated catalyst was identical to that of fresh catalyst. No peaks corresponding to alumina phases other than γ-alumina were observed indicating the absence of phase changes in the γ-alumina support as a result of the leaching treatment.

8.0. MODELLING OF THE METAL LEACHING PROCESS

In the research program on the rejuvenation of spent residual oil hydrotreating catalysts (102), a comparison was made between the efficiencies of different organic acids for selective leaching of metal foulants from coked and decoked forms of spent catalyst (106,123). The influence of adding an oxidizing agent such as hydrogen peroxide or ferric nitrate to organic acids (e.g. oxalic acid) on the leaching efficiency, and the metal leaching kinetics and mechanism were also examined (121,122). The spent and leached catalysts were characterized by standard procedures. Table 8.1. shows some of the catalyst characterization properties at various stages of deactivation and leaching. The results of these studies were discussed in previous sections.

This section describes the development of a model for foulant metals leaching from the spent catalyst. Since the process initially involves extraction of the deposited metals from the pore mouths until the pore structure is exposed followed by the removal of the metals from the pore structure, both kinetic and mass transfer aspects were considered in the model.

8.1. MODEL DEVELOPMENT

Two important observations were made during the experimental investigation. Firstly, the metal deposition, especially of vanadium, is located mainly in the region close to the catalyst extrudate outer boundaries. Secondly, the leaching of spent catalysts cannot be described satisfactorily by either a kinetic control or diffusionai control mechanism (119). Metal deposits removal by leaching appears to be take place in two stages as shown in Figure 8.1. The change-over from the first to the second stage appears to occur after a particular process time, t_θ of 3 to 5 hours depending on the leaching agent, which has considerable influence on both the reaction kinetics and mass transfer coefficients. Hence, it is necessary to examine the physical phenomena involved in the removal of metal foulants by leaching in spent catalysts more carefully, before a reliable model can be developed.

The effective diffusivities of the leaching agent, De, were determined using the following approximation (144).

$$De = \varepsilon^2 D$$

where D is the diffusion coefficient [145, 146] and ε is the catalyst porosity listed in Table 8.1. The data in Table 8.2, shows that the effective diffusivity with the three leaching agents changes with the catalyst porosity according to the progress of the catalyst

rejuvenation. The effective diffusion rates with different leaching agents are higher in the second stage than in the first stage. Moreover, the overall leaching rates of the three acids (Table 8.2) were in the order:

oxalic acid > malonic acid > acetic acid.

Table 8.1. Catalyst Properties

Catalyst Property	
Metal Contents in Spent Catalyst (wt%)	
Vanadium	14.9
Nickel	3.1
Molybdenum	1.07
Cobalt	3.99
Average Pore diameters, R (Å)	80
Pellet Radius, R_c (cm)	0.06
Porosity, ε variation due to catalyst status	
Spent Catalyst before leaching	0.12
Spent Catalyst after 1st stage leaching	0.35
Spent Catalyst after 2nd stage leaching	0.42
Fresh Catalyst	0.48
Density, ρ_b variation due to catalyst status (g/cm^3)	
Spent Catalyst before leaching	1.21
Spent Catalyst after 1st stage leaching	1.09
Spent Catalyst after 2nd stage leaching	0.97
Fresh Catalyst	0.73

Table 8.2. Mass Transfer and Kinetic Data for Vanadium Leaching @ 0.66M and 50°C

Parameter	acetic acid	malonic acid	oxalic acid
Diffusion coefficient, D (cm^2/s) $x10^5$	1.908	1.881	2.088
Effective Diffusivity, De (cm^2/s) $x10^7$			
Spent Catalyst before leaching	2.75	2.70	3.01
Spent Catalyst after 1st stage leaching	23.4	23.0	25.6
Spent Catalyst after 2nd stage leaching	33.6	33.2	36.8
Fresh Catalyst	43.9	43.3	48.1
Overall Leaching Rate* (wt%/s) $x10^5$	18.06	31.25	41.48
Thiele Modulus			
1st stage leaching	2.36	4.17	4.96
2nd stage leaching	0.28	0.49	0.58

* Average rate from a complete test.

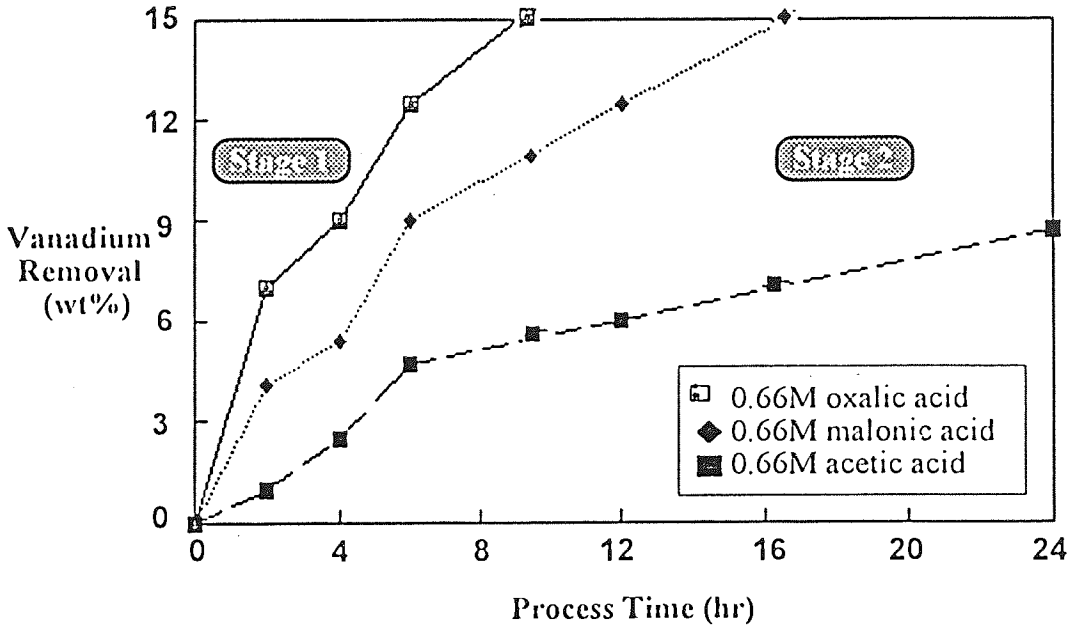

Figure 8.1. Effect of leaching agent on vanadium removal @ 323K.

From the experimental data, the leaching reaction is relatively slow and hence a pseudo steady-state can be assumed. Thus, the combined effect of the diffusion and reaction rates on metal leaching can be conveniently examined by the Thiele Modulus analysis which provides a measure of the controlling regime. It is defined as the ratio between the reaction rate to the diffusional rate, i.e.

$$\Phi^2 = \frac{\mathcal{R}_p^2 \, k}{De} = \frac{\mathcal{R}_p^2}{De} \frac{\text{Reaction Rate}}{(C_{A_s})^n}$$

where $\mathcal{R}_p$ is the catalyst pellet radius, k is the pseudo first order rate constant, and D_e, the effective diffusion coefficient of the leaching agent. The improvement in the intraparticle mass transfer due to foulants removal however, modifies the Thiele Modulus as shown in Table 8.2. For the 1st stage of vanadium leaching, Φ^2 is well above 2.0 indicating that the reaction is controlled by internal mass transfer. In contrast for the 2nd stage leaching Φ^2 is <1 which suggests that the process is under kinetic control.

At the optimal space velocity used (36.3h^{-1}), the external mass transfer resistance to the leaching agent is assumed to be minimal and hence, the overall rate depends mainly on the internal mass transfer and reaction kinetics. The metal foulants are believed to plug the catalyst pores and be partially deposited along the main channels. This restricts passage of the leaching agents to reach the fouled pores. Hence, intraparticle mass transfer can be assumed initially to be rate limiting. However, as leaching progresses, the intraparticle transfer is gradually improved inside the catalyst substrate pore network and chemical reaction becomes rate limiting. Values of the effective diffusivity are given in Table 8.2. The De after the first stage of leaching is 8.5 times greater than that before leaching starts. A schematic representation of the proposed reaction scheme is shown in Figure 8.2. The leaching process is considered to involve two operations:

1. removal of metal foulants along the main mass transfer channels (macropores) connected to the micropores until the pore structure begins to resume that of the fresh catalyst, and
2. removal of metal foulants from the pore structure.

In the first stage, metal deposits restrict the transfer of the leaching agents and effluents within the pore network, and therefore intraparticle mass transfer is the rate limiting step. The situation can be represented by 'A' progressing to 'B' as illustrated in Figure 8.2. The mass balance can be expressed as,

$$\frac{t}{\tau_D} = -2 \frac{r^2}{R^2} [\ln(R) - \ln(r)] + [1 - \frac{r^2}{R^2}] \qquad (1)$$

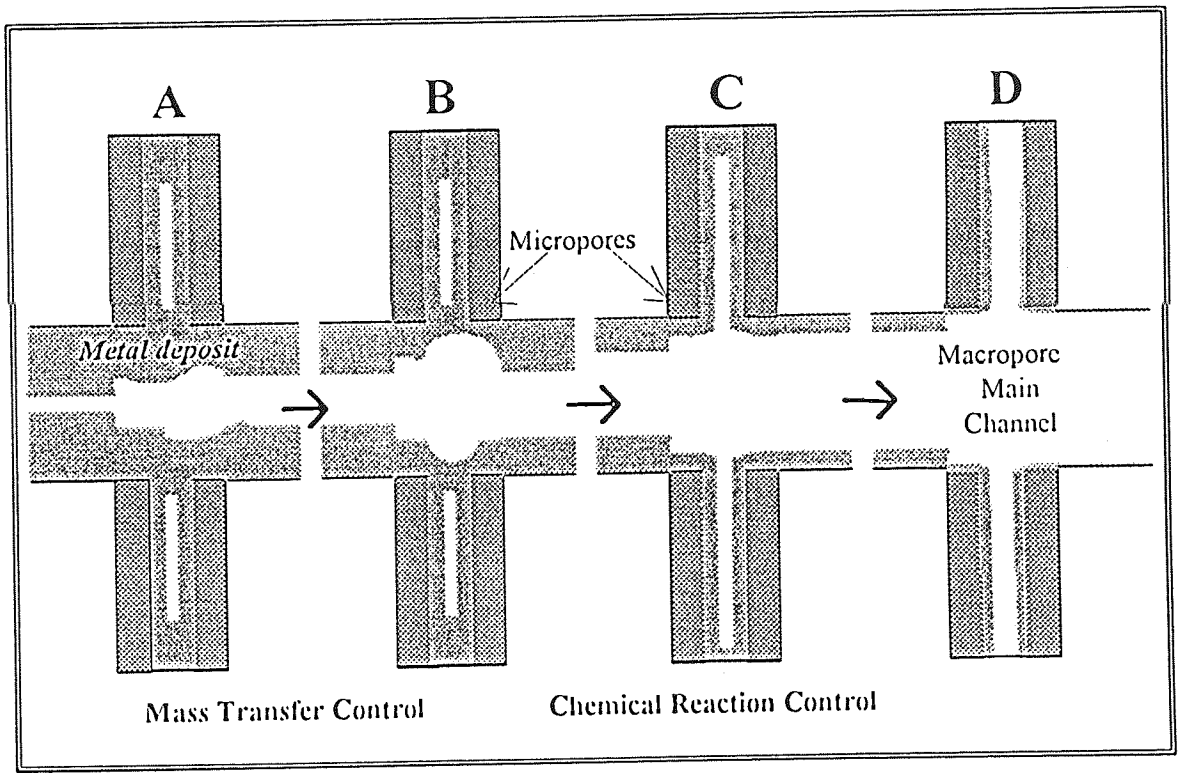

Figure 8.2. A Schematic Representation of the Two Metal Leaching Stages in a Catalyst Network.

and

$$\tau_D = \frac{R^2 \rho_B}{4 C_A De} \quad (2)$$

In terms of the fraction conversion, Equation (1) can be expressed as:

$$\frac{t}{\tau_D} = 2 (1 - \chi) \ln(\sqrt{1-\chi}) + \chi \quad (3)$$

where χ is the fractional conversion and is defined as:

$$\chi = \frac{\text{amount leached}}{\text{total foulants}} = 1 - \frac{r^2}{R^2} \quad (4)$$

Assuming a first order reaction the chemical kinetics of the leaching process can be represented schematically in the situation progressing from 'B' to 'C' and then to 'D' as shown in Figure 8.2. According to Levenspiel (147), the chemical kinetics of the leaching process on a cylindrical pore can be represented by:

$$\frac{t}{\tau_K} = 1 - \frac{r}{R} \quad (5)$$

where

$$\tau_K = \frac{R \rho_B}{k C_A} \quad (6)$$

In terms of fractional conversion, Equation (5) becomes:

$$\frac{t}{\tau_K} = 1 - \sqrt{(1 - \chi)} \quad (7)$$

Equations (3) and (7) form the basis of the proposed model. The fractional conversion from both equations is expressed in terms of a normalized process time which is different with respect to the controlling step. When the reaction rate is much faster than that of mass transfer, i.e.,

$$k >> De \qquad (8)$$

the rate is under diffusional control. Detailed model development is given in Appendix A.

8.2. APPLICATION

A typical plot of the simulated fractional conversion for kinetic control (Curve A) and mass transfer control (Curves B1 and B10) against the normalized process time is given in Figure 8.3. The difference between Curves B1 and B10 is that the mass transfer rate in B1 is assumed ten times faster than in B10 whilst the reaction rates are the same in both cases. When $\tau_K = \tau_D$, represented by Curves A and B1, the rate controlling mechanism can switch from kinetics to mass transfer or vice versa, at $t/\tau = 0.715$ and $\chi = 92\%$ where the two curves intersect. When $\tau_K = 10\tau_D$, the process is definitely under diffusional control. As illustrated, Curves A and B10 intersect at $t/\tau = 0.05$ and $\chi = 8\%$, at which the rate controlling mechanism gradually switches to the reaction rate. However, all these lines show a monotonic increase in conversion with process time and do not exhibit the two-stage characteristics obtained experimentally as given in Figure 8.1. This can be overcome by using the two model equations together with τ_K and τ_D as a function of the switch in mechanism. The precise time for the switch and the conversion with process time curves can be generated in the following procedure.

Initially, the values of τ_D and τ_K are calculated from Equations (2) and (6) respectively, and their ratio, Ψ becomes,

$$\Psi = \frac{\tau_D}{\tau_K} = \frac{R\,k}{4\,De} \qquad (9)$$

Assuming that the rate limiting mechanism switches when the fractional conversion and the normalized process time determined from Equations (3) and (7) are equal, then Ψ can be expressed as:

$$\Psi = \frac{1 - (\sqrt{1 - \chi})}{2\,(1 - \chi)\,\ln(\sqrt{1 - \chi}) + \chi} \qquad (10)$$

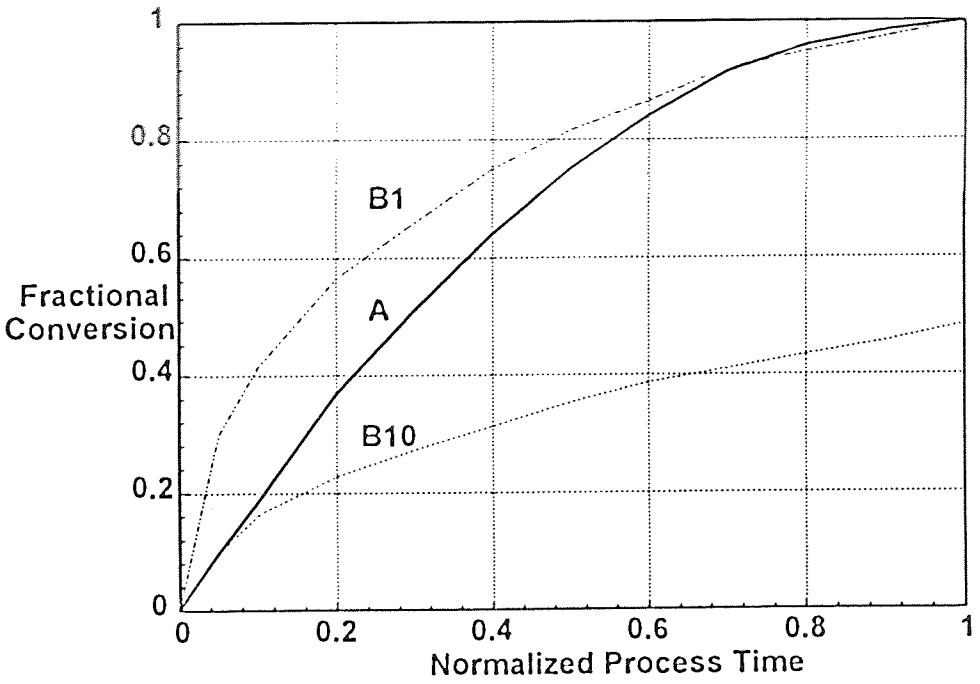

Figure 8.3. Preliminary simulated results.

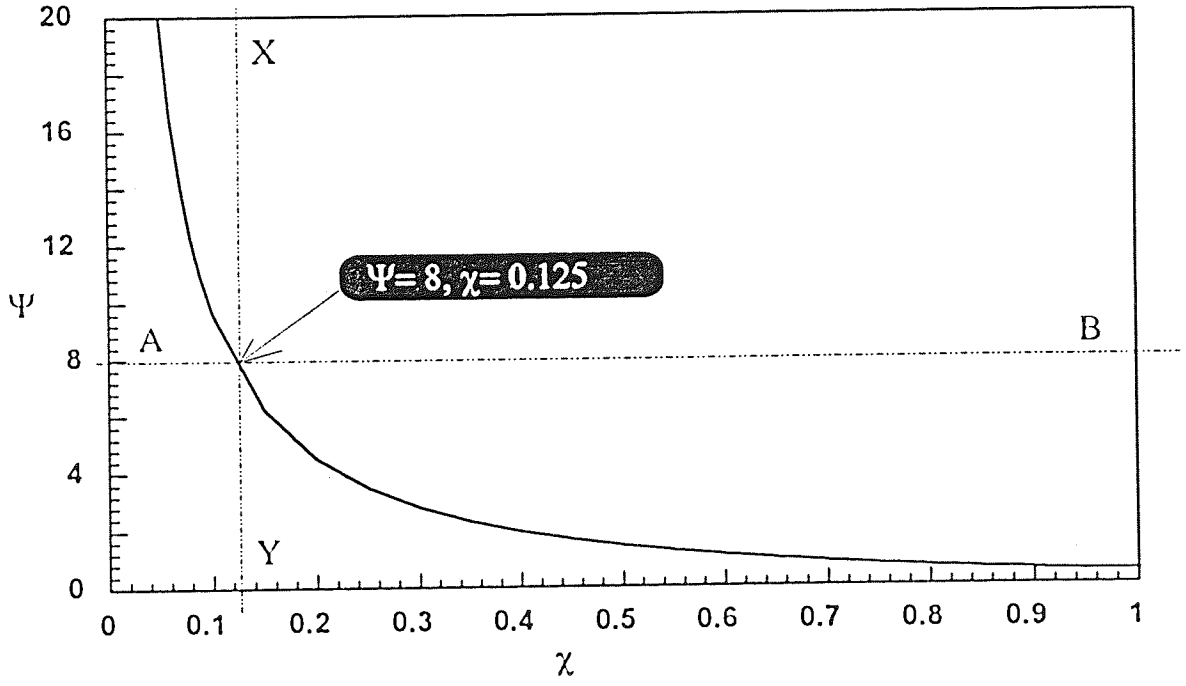

Figure 8.4. The characteristic curve of Ψ with χ.

For any value of Ψ determined from Equation 9, the conversion χ_θ at t_θ, the time when the mechanism switches, χ_θ can be evaluated from Equation (10) using a predictor-corrector procedure. Alternatively, χ_θ can be read directly from Figure 8.4, which shows a plot of χ versus Ψ. For example, for $\Psi = 8$, the value of χ_θ is 0.125. When Ψ is close to 1, χ_θ equals to unity a single diffusional or kinetic control model, depending on circumstance, will be satisfactory.

Taking the maximun value of the total process time, τ_{max}, as

$$\tau_{max} = \tau_D \text{ (1st Stage)} + \tau_K \text{ (2nd Stage)} \qquad (11)$$

Equations (3) and (7) can then be rearranged with the corresponding boundary conditions to yield,

- At $0 \leq t \leq t_\theta$, the leaching time under diffusion control is:

$$t_D = \tau_{max} [2 (1 - \chi) \{\ln(\sqrt{1 - \chi})\} + \chi] \qquad (12)$$

and

- At $t_\theta \leq t \leq \tau$, the leaching time under kinetic control is:

$$t_K = \tau_{max} (\sqrt{1 - \chi_\theta} - \sqrt{1 - \chi}) \qquad (13)$$

Finally, the total process times for leaching using different agents can be calculated from the expression:

$$\tau = t_D \text{ (1st Stage)} + t_K \text{ (2nd Stage)} \qquad (14)$$

To demonstrate application of the model, the experimental data for vanadium removal using 0.66M oxalic, malonic and acetic acids at 323K as reported in Figure 8.1, are used. The required parameters and values are given in Table 8.3. After normalizing the conversions, a comparison between the simulated results and experimental data at Ψ = 2.51, 1.93 and 1.16 for oxalic, malonic and acetic acid respectively, is shown in Figure 8.5. The simulated values are represented by lines and the experimental data by different symbols. The characteristic of the two reaction stages are well illustrated in the first two cases but it does not for the acetic acid leaching. The model prediction fits the

experimental data very well with both oxalic and malonic acids leaching, at the moderate reaction but lower diffusion rates. The simulated results for acetic acid, which has lower reaction and diffusion rates, follow similar trends to the experiment data but with minor differences in magnitude. This may be due to the Ψ value for acetic acid leaching being near unity, at which the switch mechanism fails. The values of the total process time for each leaching agent are given in Table 8.3 and they are less than the maximum process time but close to the experimental values. An improvement of the model to include the stochiometric ratio can be found in Appendix B (Smith, 1997).

Table 8.3. Required Parameters used in the Developed Model.

Parameter	Acetic Acid	Malonic Acid	Oxalic Acid
1st Stage τ_D (hr)	27.78	16.33	12.44
2nd Stage τ_K (hr)	23.99	8.47	4.96
Ψ	1.16	1.93	2.51
χ_θ	0.862	0.4928	0.3824
τ_{max} (hr) from Eqn. (11)	51.77	24.80	17.40
τ (hr) from Eqn. (14)	49.49	18.86	13.40

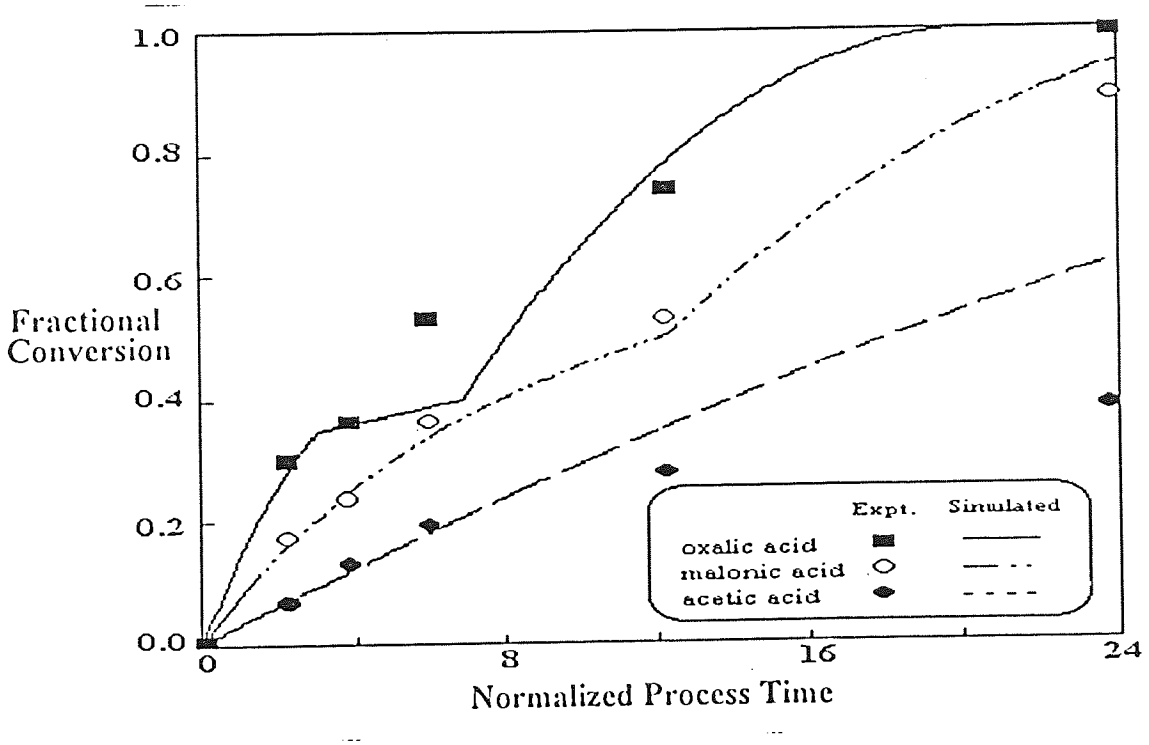

Figure 8.5. Comparison of experimental data with simulated results.

8.3. CONCLUSIONS

A simple model was developed for foulant metals leaching from the spent catalyst. The leaching process is considered to involve two consecutive steps: (i) removal of metal foulants along the main mass transfer channels connected to the narrow pores until the pore structure begins to develop; and (ii) removal of metal foulants from the pore structure. Both kinetic and mass transfer aspects were considered in the model development, and good agreement was observed between experimental and simulated results.

9.0. CONCLUSIONS AND RECOMMENDATIONS

The steadily increasing market demand for transportation fuels together with the new environmental regulations adopted to reduce harmful emissions from the use of petroleum products have led refiners to invest heavily in residue upgrading technologies by the catalytic hydrogen addition route. The catalysts used in the residue hydrotreating processes deactivate rapidly by fouling of the active surface by coke and metal deposits. Effective methods for the reactivation of the coke and metal-fouled spent catalysts from residue hydroprocessing units are not currently available. This has led to the generation of large quantities of spent catalysts as solid wastes in the refineries. The spent catalysts are classified as hazardous wastes and their disposal in an environmentally-acceptable way is not an easy task. Considerable interest exists in minimizing the extent of spent catalyst disposal. This could have been achieved by extension of the catalyst life, by slowing down catalyst deactivation rate, together with effective reactivation of the deactivated catalyst for reuse.

In the present work attention was focused on hydroprocessing catalyst deactivation and its reactivation. As a first step, the information available in the literature on the subject, namely, hydroprocessing catalyst deactivation and its reactivation by the removal of coke and metal foulants was reviewed. The areas for further research work on the subject were then identified and a detailed experimental plan was prepared. This comprised;

1. Catalyst deactivation problem analysis in industrial residue hydroprocessing operations by studying the physical, mechanical and chemical properties of fresh and spent catalyst samples from fixed bed ARDS and ebullated-bed units.
2. Studies on Catalyst Deactivation by coke deposition. Investigation of the influence of operating temperature and processing time, feed quality and catalyst acidity on the nature of the coke deposited on the catalysts surface during the early period of a run and its role in catalyst deactivation.
3. Studies on Hydroprocessing Catalyst Regeneration. Investigation of the coke removal (regeneration) process by studying the influence of the following parameters on regeneration.
   - Effect of oxygen concentration
   - Effect of flow rate
   - Effect of temperature

4. Rejuvenation of Spent Residue Hydroprocessing Catalyst. Investigation of metal leaching by organic complex forming reagents with and without promoter, and a comparison between their selectivities for the removal of metal foulants (V and Ni).
5. Characterization and performance evaluation of regenerated and rejuvenated hydrotreating catalyst, and studies on the relationship between vanadium removal and catalyst surface area and HDS activity recovery.
6. Modelling of the Metal Leaching Process.

The results are briefly summarized below together with the conclusions drawn from them.

1. Catalyst Deactivation Problem Analysis in Industrial Residue Hydroprocessing Operations.

A comparison between the characteristics of spent catalysts from two different types of reactor units, namely fixed bed and ebullating bed hydroprocessing units was made and the deactivation pattern of the catalysts in both types of reactor systems was examined. Catalysts from both types of reactor were deactivated primarily by deposition of carbon and metals, particularly vanadium and nickel.

In the fixed bed unit, which consisted of a series of reactors, the first two reactors were deactivated predominantly by foulant metal (vanadium) deposits, whereas the last two reactors were deactivated primarily by coke deposition.

The rate of coke deposition on the catalyst increased from the entrance to the exit whereas the rate of metals deposition decreased.

In the ebullating bed reactor, since the catalyst particles are in continuous motion, the coke or metal contents of the catalyst would not be expected to depend on the location of the catalyst in the reactor. However, considerable changes in the physical dimensions (pellet length distribution) were noticed for the spent catalysts from this reactor unit. Vanadium concentration within a catalyst pellet was a maximum near the outer edge and decreased to a minimum at the centers. This indicates that pore mouth plugging by vanadium deposits was the main cause of deactivation in residue hydroprocessing units.

2. Studies on Hydrotreating Catalyst Deactivation by Coke Deposition.

In these studies, particular attention was paid to the nature of initial coke deposited on the catalyst surface and its role in catalyst deactivation. The results of the studies revealed that coke deposition was very rapid during the early hours of the run reaching as high as 14% within 3 hours. This initial coke was responsible for the rapid catalyst deactivation. An increase in temperature (360 → 380 → 400°C) increased carbon deposition on the catalyst due to enhancement of dehydrogenation, cracking and aromatization reactions. The influence of initial coke on catalyst surface area and porosity was significant. A large loss (36%) in the surface area and pore volume of the catalyst occurred within the first 6 h of the process. Pore size distribution analysis indicated that coke formed during the early period of the run was predominantly deposited in the micropores of the catalyst.

Catalyst acidity and feedstock quality were found to have a remarkable influence on the amount and the nature of initial coke deposited on the catalyst surface. The TPO profiles for the gases formed (SO, SO_2, CO, CO_2, NO, NO_2 and H_2O) from coke at different processing times were significantly different, indicating differences in the nature of the coke. The HDN and HDS were affected differently by the initial coke deposits.

3. Studies on Hydroprocessing Catalyst Regeneration by Coke Removal.

A systematic study was conducted on the effect of parameters such as temperature, regeneration gas flow rate and oxygen content of regeneration gas on coke removal by combustion from a spent Co-Mo/Al_2 O_3 hydrotreating catalyst. The primary objective of the study was to understand the influence of these key parameters on the sintering and phase transformation of hydrotreating catalysts during the decoking step. Since the early stages of contact between the spent catalyst and oxygen in the decoking process are crucial, special attention was paid to the initial stages of coke combustion. The influence of start-up regeneration conditions on the structural changes occurring to the support and to the active catalyst components was investigated. The results revealed that during the decoking process extensive surface area loss occurred due to sintering at high (>5%) oxygen concentrations and high flow rates of the regeneration gas. Increasing the initial combustion temperature above 440°C led to considerable sintering of the catalyst. Pore size distribution data of catalysts decoked at different temperatures showed a progressive pore enlargement with increasing temperature. At temperature above 700°C a substantial

loss of molybdenum from the catalyst occurred, together with phase transformations in the alumina support.

4. Spent Catalyst Rejuvenation by Leaching of Foulant Metals.

The major area of study was into factors influencing the selectivity of vanadium leaching and the mechanism of the leaching process. Two routes were used to rejuvenate spent residue hydroprocessing catalysts by leaching foulant metals. In the first, deoiled spent catalyst containing coke and deposited metals in sulfide form was chemically treated to remove the metal foulants. In the second, deoiled spent catalyst was decoked by controlled combustion of coke and the resultant coke-free catalyst, containing metals in oxide form, was subjected to leaching. Oxalic acid, a chelating agent which is able to form soluble metal complexes, was used for metal leaching in both routes. The influence of adding an oxidizing agent such as H_2O_2 to oxalic acid, in particular its effect on the leaching efficiency, was examined in both routes. The spent and treated catalysts were characterized and the improvements in surface area, pore volume and hydrodesulphurization-activity of the catalysts were compared.

The selectivity for leaching of the major metal foulant (vanadium) was better, and activity recovery was higher, for the catalyst rejuvenated by metal leaching prior to decoking. The addition of oxidizing agent to the acid reagent was found to enhance the efficiency of leaching from coked spent catalyst, but not from decoked spent catalyst. The efficiency of two different organic acids (e.g. oxalic acid and tartaric acid) and two different oxidizing agents (H_2O_2 and Ferric nitrate) in selectively leaching the metal foulants were compared. The study showed that oxalic acid-ferric nitrate reagent was superior to other reagent systems in terms of selectivity of vanadium leaching as well as for surface area, pore volume and activity recovery. The role of oxidizing agents (e.g. ferric nitrate) in enhancing the leaching of foulant metals from coked spent catalyst was attributed to a synergistic effect involving oxidation of low valent metal sulfides to higher oxidation states which may be easily attacked by the complexing acid reagent.

Since it is important that no major damage is done to the useful properties of the catalyst in the metal leaching process, the treated catalysts were fully characterized by different techniques. Electron microprobe analysis was used to determine the distribution profiles of vanadium and other metals (Mo, Co, and Ni) within pellets of treated and

untreated spent catalysts. The untreated spent catalyst contained large concentrations of vanadium near the outer edge, whereas the treated catalyst pellets contained much lower amounts. Redistribution of V, Co, Mo and Ni within the pellet was observed as a result of leaching. The x-ray diffraction pattern of the rejuvenated catalyst was identical to that of fresh catalyst. No peaks corresponding to alumina phases other than γ-alumina were observed, indicating the absence of phase changes in the γ-alumina support as a result of leaching. The surface area and pore volume increased substantially with increasing vanadium extraction from the spent catalyst; the HDS activity showed a parallel increase. Improvements in surface area and the HDS activity were substantial upto 30% vanadium removal but vanadium extraction did not significantly improve above this level. More than 85% of the catalyst initial HDS activity was recovered by removal of about 35% vanadium from the catalyst, although all carbon deposits remained on it.

5. Modelling of the Metal Leaching Process.

A model was developed for foulant metals leaching from the spent catalyst. Since the leaching process initially involves extraction of the deposited metals from the pore mouths until pore structure develops followed by the removal of the metals from the pore structure, both kinetic and mass transfer aspects were considered in the model development. Good agreement was obtained between the experimental leaching results and simulated values based on the model showed.

RECOMMENDATIONS

The environmental problems posed by the disposal of spent catalysts as solid wastes are well recognized and there is considerable interest in finding methods for their safe disposal or utilization. In the present research, attention was focussed upon the deactivation and reactivation of spent hydroprocessing catalysts. Particular emphasis was given to the factors influencing the removal of coke and metal foulants from the spent catalyst in order to rejuvenate it. The study resulted in a deeper understanding of the deactivation mechanisms and led to the optimization of process parameters for decoking and selective leaching of the deposited foulant metals.

In spent catalyst rejuvenation by metal leaching, metals-containing leach liquid is generated as a waste product. The leach liquids contain various metals such as V, Ni &

Mo. Recovering the useful metals from the solution by ion-exchange method and recycling of the leaching reagent would improve the process economics. The potential environmental problem posed by the leach liquid would also be solved. Alternatively, the metals-containing solution can be used in catalyst preparation. Since the liquid is acidic and contains active catalyst materials (Co, Ni & Mo), it can be used as a peptizing agent and for incorporating the catalytically-active metals into the alumina support during the kneading step.

However rejuvenation and reuse of the spent catalyst does not completely solve the spent catalyst environmental problem. After two cycles of reactivation and reuse, further rejuvenation may not be possible and the catalyst has to be eventually disposed of as solid waste. Therefore, alternative disposal options for the waste spent catalysts should be explored. One possibility is the utilization of the coke and metals-containing spent catalyst in the preparation of wide pore active hydrodemetalization (HDM) catalysts by mixing them in certain proportions with boehmite in the form of fine powder followed by kneading and extrusion. The coke present in the spent catalyst would help to enlarge the pores and the metals can promote hydrotreating reactions.

Considering the above, the following recommendations are made for further research,

1. To investigate various options for the utilization of the metals-containing leach liquid, including the possibility of utilizing them in catalyst preparation.
2. To develop methods for the utilization of coke and metals fouled spent hydroprocessing catalysts in preparing active HDM catalyst.
3. To explore alternative options for utilization and safe disposal of spent catalysts including metals recovery and recycling.

NOMENCLATURE

Symbols

C_A	leaching agent concentration, mol/cm^3
D	diffusion coefficient, cm^2/s
De	effective diffusivity, cm^2/s
k	reaction rate constant, g/s
l	pore length, Å
n	order of reaction
r	radial coordinate of pores
r_θ	radial coordinate of pores
R	pore radius, Å
R_c	catalyst radius, cm
t	process time, h

Greek Symbols

χ, χ_θ	fractional conversion at any radial coordinate and at r_θ respectively
ε	porosity
Φ^2	Thiele Modulus
ψ	ratio between total process time due to kinetic control and diffusional control
τ	dimension at total process time, h
π	pi, a constant
ρ	molar density, g/cm^3

Subscripts

A	leaching agent
B	metal foulant
D	diffusional control
i	initial
K	kinetic control
o	initial conditions
s	surface conditions
θ	radial position where controlling regime to be switched

References

1. J.G. Speight. The Chemistry and Technology of Petrolem. Marcel Dekker Inc.: 1980, New York.
2. J.F. Le Page. Resid and Heavy Oil Processing, Technip. 1992, Paris.
3. W.I. Beaton and R.J. Bertolacini. Resid Hydroprocessing at Amaco. Catal. Revs., Sci. Eng.33, 281-317, 1991.
4. G. Heinrich, M. Valais, M. Passot, and B. Chapotel. Mutations of World Refining: Challenges and Answers. Thirteenth World Petroleum Congress, Paper No. 18 (1), 1991.
5. I. E. Maxwell; J. E. Naber; and K. P. de Jong., The Pivotal Role of Catalysis in Energy Related Environmental Technology. Appl. Catal. A: General, 113, (2): 153-174, 1994.
6. B. Delmon. New Technical Challenges and Recent Advances in Hydrotreatment Catalysis. Catalysis Letter, 22:1-32, 1993.
7. P.W Tamm,. H.F. Harnsberger, and A.G. Bridge. Catalyst Ageing in Hydroprocessing. Industrial and Engineering Chemistry Process Design and Development, 20:263-270, 1981.
8. C.H. Bartholomew. Catalyst Deactivation, Chemical Engineering, 12:96-112, 1984.
9. S.T. Sie. Catalyst Deactivation by Poisoning and Pore Plugging to Petroleum Processing in "Catalyst Deactivation" (B. Delmon and G.F. Froment, Eds.), Elsevier, p.545, 1980, Amsterdam.
10. L. Reyes, C. Zerpa and J.H. Krasuk. Catalyst Deactivation in HDM of Heavy Deasphalted Oils. In "Catalyst Deactivation" (B. Delmon and G.F. Froment, Eds.), Elsevier, 88:85-95, 1994, Amsterdam.
11. L.L. Hegedus, and R.W. McCabe. Catalyst Poisoning in "Catalyst Deactivation" (Eds. B. Delmon and G.F. Froment), Elsevier, p. 471, 1980, Amsterdam.
12. H. Wise. Mechanism of Catalyst Poisoning by Sulfur Species. In "Catalyst Deactivation" (Eds. C.H. Bartholomew and John B. Butt), Elsevier, 68:497-504, 1991, Amsterdam.

13a. C.H. Bartholomew, P.K. Agrawal and J.R. Katzer. Sulphur Poisoning of Metals in "Advances in Catalysis, 31:135-242, 1982.

13b. J. Barbier et al. Adv. Catal. 37, 279 (1990).

14. G.F. Huttig. Disc. Farad. Soc. 8, p. 215 (1950).

15. A.E.B. Presland, G.L. Price and D.L. Trimm, Progress in Surface Science, 3,63, 1972,

16. M. Moayeri, and D.L. Trimm. Reorganization of Nickel Under Steam Reforming Conditions. Farad. Soc. Trans. 73, p. 1245, 1977.

17. E. Ruckestein. New Mechanism of Sintering and Redispersion Induced by Spreading and Wetting (Eds. C. H. Bartholomew and J. B. Butt), "Catalyst Deactivation", 68:585-596, 1991.

18. W.M. Gitzen, Alumina as a Ceramic Material. Amer. Cer. Soc., 1970. Columbia.

19. J.E. Wanke, Models for Sintering of Supported Metal Catalysts in Progress in Catalyst Deactivation (J.L. Figuerido, Ed.), p. 315, 1982.

20. E. Ruckenstein, Sintering and Catalytic Implications. A Surface Thermodynamic Approach (Eds. B. Delmon and G.F. Froment), In "Catalyst Deactivation" 993:33-52, 1994.

21. B. Delmon, and P. Grange. The Role of Chemical Transformation of Solids in Aging and Deactivation of Catalysts, in "Progress in Catalyst Deactivation) J.L. Figueiredo, Ed.), p. 231, 1982.

22. J.R. Rostrup-Nielsen. Catalytic Steam Reforming, in Catalysis Science and Technology, 5:245, 1983.

23. A. Stanislaus and K. Al-Dolama. Effect of Thermal Treatment on the Concentration and Distribution Profiles of Molybdenum, Cobalt and Nickel in Co-Mo/Al_20_3 and Ni-Mo/Al_20_3 Catalysts. J. Cataly. 101:536, 1986.

24. A.G. Bridge Catalytic Hydrometallation of Heavy Oils, Studies in Surface Science and Catalysis 53: 363-383, 1990.

25. P. N. Hannerup and A. C. Jacobsen. A Model for the Deactivation of Residue HDS Catalyst. ACS Div. Petrol. Chem. 28. p.576, 1983.

26. H. Beuther and B. K. Schmid, Reaction Mechanism and Rates in Residue HDS, Proceeding. 6th World Petrol. Congr. Section III, p. 297, 1963.

27. D. S. Thakur and M. G. Thomas., Catalyst Deactivation in Heavy Petroleum and Synthetic Crude Processing. Ind. Eng. Chem. Process Des. Dev. 23, 349, 1984.

28. F.M. Dautzenberg; J. Van Klinken: K.M.A. Pronk; S.T. Sie and J.B. Wiffels, Catalyst Deactivation Through Pore Mouth plugging during residue desulphurization. ACS Symposium Series 65, 254-265, 1978.

29. P. Wivel, P. Zeuthen and A.C. Jacobson. Initial coking and deactivation of hydrotreating catalysts by real feeds. In Catalysis Deactivation. Elsevier pp. 257-265, 1991.

30. M. A. Halabi, A. Stanislaus and D.L.Trimm. Coke formation on catalysts during hydroprocessing of heavy oils. Applied Catalysis. 72:193-215, 1991.

31. J. Bartholdy, and B.H.Cooper. Metal and coke deactivation of resid hydroprocessing catalysts. American Chemical Society of Petroleum Chemistry. Preprints 38: 386-390, 1993.

32. C. J. Pereira and J. W. Beekman. Modelling of hydrodemetallation catalysts. Ind. Eng. Chem. Res. 28, 222 (1989).

33. R.J. Quan; R.A. Ware, C.W. Hung and J.Wei. Catalytic hydrometallation of Petroleum. Advances in Chemical Engineering 14:95-257, 1988.

34. P. Zeuthen, P.Blom and F.E.Massoth. Characterization of nitrogen on aged hydroprocessing catalyst by temperatures programmed oxidation. Applied Catalysis 78:265-276, 1991.

35. F. Melo, Fans, P.Grange and B.Delmon. Interactions of asphaltene with sulfided cobalt-molybdenum on alumina catalysts. Applied Catalysis, II: 281-290, 1984.

36. E. Furimsky. Deactivation of molybdate catalysts by nitrogen bases. Erdol and Kohle 35:455-464, 1982.

37. P. Zeuthen, P. Bolm, B. Muegge and F. E. Massoth. Temperature programmed sulfidation and oxidation of Ni-Mo/alumina catalysts and reaction with ammonia. Applied Catalysis, 68:117-126, 1991.

38. Y. Yoshimura et al. Oxidative regeneration of spent molybdate and tungstate hydrotreating catalysts. Energy and Fuels 8: 435-445 (1994).

39. M. Ternan, E. Furimsky and B.I. Parsons. Nature of coke in residue hydroprocessing catalysts. Fuel processing technology, 2:45-54, 1979.

40. A. Nishijima, H. Shimada, Y. Yoshimura, R.Sato and N. Matsubayashi. Deactivation of molybdenum catalysts by metal and carbonaceous deposits during the hydrotreating of coal liquids and heavy petroleums. Studies in Surface Science and Catalysis 34:39-58, 1987.

41. D.J. Sajkowski, M.A. Pacheco, T.H.Plasch, T.H. Fleisch and B.L. Meyers. Deactivation of Coal Liquefaction Catalysts Proceedings of the 9th International Congress on Catalysis, Chemical Institute of Canada, 1988, Ottawa.

42. J.G. Speight, Initial reactions in the coking of residue. American Chemical Society, Petroleum Chemistry Division's preprints 32:413-418, 1987.

43. K.P. de Jong, D. Reinalda and C.A.Emeis. Coke depostion in trickle bed reactors during heavy oil processing. Studies in Surface Science and Catalysis 88:155-66, 1994.

44. J. Van Doorn and J. A. Moulijn. Carbon deposition on Catalyst. Catalysis Today, 7:257-266, 1990.

45. P. Dufresne, F. Valeri and S. Abotteen. Continuous Developments of Catalyst Off-Site Regeneration and Presulfiding, Studies in Surface Science and Catalysis 100: 253 - 262, 1996.

46. J.V. Sanders, J.A. Spink and S.S. Pollack. The Structure of Carbon Deposits on HDS Catalysts. Applied Catalysis 5:65-76, 1983.

47. R. Bacaud, M.Besson, M. Oberson P.Bussiere, H.Charcosset, G.Djega-Maria Dassou and B. Nickel. Coking of iron sulfide catalysts during hydroliquefaction of Coal. Studies in Surface Science and Catalysis 34: 289-301, 1987.

48. H. Beuther, O.A. Larson and A.J. Perrotta. The mechanism of coke formation on catalysts. Studies in surface science and catalysis 6:271-282, 1980.

49. C.H. Bartholomew. Catalyst deactivation in hydrotreating of residue. Presented at the American Institute of Chemical Engineers Spring Meeting, March 28-April 1, 1993, Houston.

50. E. E. Wolf and E. Alfani. Catalyst deactivation by coking. Catalysis review science and engineering. 23:329-371, 1982.

51. E.A. Cotte and J.L. Calderon. Studies on asphaltenes pyrolysis. American Chemical Society. Division Petroleum Chemistry Division Preprints, 26:538-545, 1981.

52. E. Fitzer, K. Muller and W. Schaffer. Chemistry and Physics of Carbon. Marcel Dekker, Vol. 7, 237-248, 1971, New York.

53. M. A. Halabi, A. Stanislaus, F. Owaysi, Z. H. Khan and S. Diab. Hydroprocessing of heavy residues: Relation between operating temperature, asphaltene conversion and coke. Studies in Surface Science and Catalysis. 53:201-212, 1990.

54. S. Eser and R.G. Jenkins. Carbonization of Petroleum feedstocks I: Relationships between chemical constitution of the feedstocks and mesophase development. Carbon 27:877-887, 1989.

55. M.F. Oxenreiter, C.G.Frye, G.B.Hoekstra and J.M. Srokae. Paper presented at the Japanese Pet. Inst. Nov. 30, 1972.

56. W.F. Arey, N.E. Blackwell and A.D. Reichie. Advances in Desulfurization of Residual Reactions and Asphalts. 7th World Petroleum Congress, p. 167, 1967, Mexico.

57. F.A. Audibert and P. Duhaut. Residual Reduction by Hydrotreatment. Paper presented at the 35th Midyear Meeting of the American Petroleum Institute Division of Refining, p. 992, May 13-15, 1970, Houston.

58. N.Takayama, S. Kurita, M. Sato, and T. Kwan. Distribution of Vanadium and Nickel Deposits Inside Desulfurization Catalysts. Nippon Kagaku Zasshi, 92, p. 834-8, 1971.

59. N. Todo et al. Kogyo Kagaku Zasshi, 74, p.563, 1971.

60. A.C. Jacobson, In "Surface Properties and Catalysis by Non-Metals (J.P. Bonnelle, Ed), Reidel Publishing Company, p. 305, 1983.

61. R. Galiasso et al. Deactivation of Hydrodemetallization Catalyst by Pore Plugging. Fuel, 62, p. 817, 1983.

62. J.M. Bogdanor and H.F.Rase. Characterisitics of a Commercially Aged Ni-Mo/Al_20_3 Hydrotreating Catalyst: Component Distribution, Coke Characteristics, and Effects of Regeneration. Ind. Eng. Chem., Prod. Ref. Dev. 25, p. 220, 1986.

63. H. Lovink. Petroleum Upgrading Technology Course; Supplementary Material, Vol. 1, D4-1, 1994, KISR.

64. A.M. Henke. Oil and Gas Journal 68, 97, 1970.

65. T. Oktsuka. Hydrodesulfurization of Petroleum Resids. Catal. Rev. Sci. Eng. 16, 291, 1977.

66. J.G. Speight. The desulphurization of heavy oils and residues. Marcel Dekker Inc. 1981.

67. B. G. Silbernagel and K. L. Riley. Heavy feed hydroprocessing deactivation. The chemistry and impact of vanadium deposits. Studies in Surf. Sci. Catal. 6, 313-321, 1980.

68. B. Meugge and F.E. Massoth. Comparison of Hydrotreating Catalyst Deactivation, by coking with vacuum Gas oil vs. Anthracene. Catalyst Deactivation, Eds. C. H. Bartholomew and J. B. Butt., 68; 297-304, 1991.

69. F.E. Massoth and G. Muralidhar. Proc. 4th Int. Conf. on the Chemistry and traces of Molybdenum Climax Molybdenum Co., p. 343, 1982.

70. S. H. Yang and C. M. Satterfield, J. Catal. 81, p. 168, 1983.

71. E. Furimsky and Y. Yoshimura. In Handbook of Heat and Mass Transfer. Vol 3, Kinetics, Catalysis and Reactor Engineering (N. Cheremissinaff, Editor), Gulf Publishing Co., 1988.

72. J.M. Pazoz, J.C. Conzalez and A.J. Salazar. Effect of Catalyst Properties and Operating Conditions on Hydroprocessing High Metal Feeds. Ind. Eng. Chem. Proc. Des. 22, p.653, 1983.

73. J.R. Kriz. Can. J. Chem. Eng., 72, p. 85, 1994.

74. A. Stanislaus, M.A. Halabi, F. Owaysi and Z. Hameed. Effect of temperature and pressure on hydroprocessing of Kuwait Vacuum Residues. KISR Publication No. 2756, 1988.

75a. S.S. Shih, P.N. Angevine, R.H. Heck and S. Sawruk. Catalyst Assessment for Upgrading Short Contact Time SRC to low sulfur boiler fuels. ACS, Div. Fuel Chem., 25, p. 152, and ACS Symp. Ser. 156, p. 175, 1981.

75b. M. Absi-Halabi & A. Stanislaus. Effect of process conditions and catalyst properties on catalyst deactivation in residue hydroprocessing. Presented at ACS Symposium on "Deactivation and Testing of Hydrocarbon Conversion Catalysts", Chicago, USA, August 20-24, 1995.

76. F.M. Dautzenberg and J.C. Deken. Reactor Developments in hydrotreating and conversion of residues. Catal. Rev. Sci. Eng. 26, p. 421, 1984.

77. C.A. McKnight and V. Nowlonv. Metals Accumulation and Practicle Mixing in a Commercial Residue Hydroprocessing with continuous Catalyst Addition. ACS 205th National Meeting, March 28-April 2, 1993, Denver.

78. A. Stanislaus, M.A. Halabi and K. Al-Dolama. Comparative study of deactivation of residue hydroprocessing catalysts from fixed bed and Ebullating bed reactors. KISR No. 2752.

79. J. Wei and R. G. Wei. Metal Deposition profiles in Hydrodemetallation. Chem. Eng. Comm, 13, p. 251, 1982.

80. R. Agarawal and J. Wei. Hydrodemetallation of Nickel and Vanadium porophyrins Intra particle Diffusion. Ind. Eng. Chem. Proc. Des. Dev. 23, p. 515, 1984.

81. B.G. Johnson, F.E. Massoth and Bartholdy . Diffusion and Catalytic Activity Studies on Fresh and Resid Deactivated HDS Catalytsts. AICHE J. 32, 12, p. 1980-87, 1986.

82. R.V. Nalitham, J.M. Lee and C. W. Lamb. Two Stage Coal Liquefaction Process Performance with Close Coupled Reactors. Fuel Processing Tech. 17, p. 13, 1987.

83. Y.W. Rhee, J.A. Guin and C.W. Curtis. Energy and Fuels, 3, p. 391, 1989.

84. W.P. Wang and J.A. Guin. A Comparison of unimodal and bimodal catalyst deactivation behavior in a model compound system with rapid coke deposition. Fuel Processing Tech. 28, p. 149, 1991.

85. M.A. Halabi and A. Stanislaus. Studies on Hydroprocessing of Vacuum Residue: Relationship between Catalyst Activity, Deactivation and pore size Distribution. OAPEC/IFP workshop on catalysts in the downstream operations, 1994, Paris.

86a. J.C. Plumail, Y. Jacquin, G. Martino and H. Toulhoat. Effect of the pore size distribution on the Activities of Alumina supported Co-Mo Catalysts in the Hydrotreatment of Boscan Crude. Preprints, ACS Div. Petrol. Chem., 28, p. 562, 1983.

86b. A. Stanislaus, M. Absi-Halabi, F. Owaysi, Z. Hameed and K. Al-Dolama. H-Oil Catalyst specifications assessment: Effect of Catalyst Pore Size Distribution. KISR Publication No. 4013 (1992).

87. A. Nielsen, B. H. Cooper and A.C. Jacobson. Composite Catalyst Beds for Hydroprocessing of Heavy Residue. Preprints, ACS, Div. Petrol. Chem. 26, p. 440, 1981, Denmark.

88. Y.T. Shah and J.A. Paraskos. Ind. Eng. Chem. Proc. Des. Div, 20, pp. 470, 1981.

89. E. Furimsky. The Catalytic Removal of Sulfur, Nitrogen and Oxygen from Heavy Gas Oil. AICHE. J. 25, 2, p. 306-11, 1979.

90. J.H.K. Choi and M.R. Gray. Structural Analysis of Extracts from Spent Hydroprocessing Catalysts. Ind. Eng. Chem. Res., 27, 9, p. 1587-95, 1988.

91. F. Diaz, B.C. Gates, J.T. Miller, D.J. Sajkosvski and S.G. Kukes. Hydrotreating Catalyst Deactivation by Coking. Ind. Eng. Chem. Res. 29, p. 12, 1990.

92. E. Furimsky and F. E. Massoth. Regeneration of Hydroprocessing Catalysts. Catalysis Today 17, 537-660 (1993).

93. Y. Yoshimura and E. Furimsky. Oxidative Regeneration of Hydotreating Catalysts. Appl. Catal., 23, p. 157. 1986.

94a. Y. Yoshimura, T. Sato, H. Shimada, N. Matsubayashi, M. Imanura, A. Nishima and S. Yoshitomi. Oxidative Regeneration of Molybdate and Tungstate Hydrotreating Catalysts. ACS Div. Petrol. Chem. Preprints, p. 32, 1993.

94b. P. Dufresne, N. Brahma, F. Valeri and S. Abotteen. Off-Site Catalyst Regeneration and Presulfiding of Hydroprocessing Catalysts. Arabian Journal for Science and Engineering. V. 21, No. 2, 255-261, 1996.

95. P. Zeuthen, B.H.Cooper, F.T. Clark and D. Arters. Characterization and Deactivation Studies of Spent Resid Catalyst from Ebullating Bed Service. Ind. Eng. Chem. Res., 34, pp. 755-762, 1995.

96. J. Van Doorn, J.T. Bosch, R.J. Bakkum and J.A. Moulijn. Temperature Programmed Oxidation Analysis of Hydrotreating Catalyst. Stud. Surf., Sci. Catal., 34 p. 391, 1987.

97. A. Artega, A. Fierro, J.L.G. Delannay and E. Delmon. Simulated deactivation and regeneration of an industrial Co-Mo/ Al_2O_3 Catalyst. Influence of the regeneration temperature. Applied Catal. 26, 227, 1986.

98. A. Artega, A. Fierroj. L.G., P. Grange and B. Delmon. Simulated Regeneration of an Industrial Co-Mo/γ-Al_2O_3 Catalyst. Influence of the Regeneration Temperature. Applied Catal. 34, 89, 1987.

99. P. Dufresene. Hydrotreating Catalyst Regeneration. ACS Div. Petrol. Chem. Preprints p. 54, 1993, Denver.

100. E. Furimsky. Effect of coke and catalyst structure on oxidative regeneration of hydroprocessing catalysts. Fuel Processing Technology, 27, pp. 131-147, 1991.

101. D.L. Trimm. Deactivation, Regeneration and Disposal of Hydroprocessing Catalysts. Catalysts in Petroleum Refining. D.L. Trimm et al., (editors), Elsevier Science Publishers. 58: 41-60, 1990.

102. M. Marafi, The Regeneration of Deactivated Hydrotreating Catalyst, M.Phil. Thesis. The University of Aston, Birmingham, 1988.

103. H. Beuther and R. Flinn. Technique for Removing Metal Contaminants from Catalyst, Ind. Eng. Chem., Vol. 2, No. 1, p. 53, 1963.

104. D.S. Mitchel, Rafael, A.G. Bridge and J. Jaffe. Catalyst Rejuvenation with Oxalic Acid. U.S. Patent, 2, 791, 989, 1974.

105. R.R. Mohan, B.G. Silbernagel and G.H. Singhal. Regeneration of Spent Hydrodesulphurization Catalysts with Heteropoly Acids and Hydrogen Peroxide. U.S. Patent 4, 268, 415, 1981.

106. J. F. P. Le Page, P. Baumgartner and P. Duhant. Process for Regeneration Catalysts Used for Hydrotreating Hydrocarbons. British Patent 1, 245,358, 1971.

107. D.R. Farrell and J.W. Ward. Method for Rejuvenating Hydroprocessing Catalysts. U.S. Patent 4, 089, 806, 400, 1978.

108. J.O. Hernandez. On the use of spent Hydrodesulfurization Catalyst. Presented before the American Chemical Society, Meeting, 12 - 17 September 1982, Kansas City.

109. B.G. Silbernagel, R.R. Mohan, G.H. Singhal. Regeneration of Spent Hydrodesulfurization Catalysts Employing Presulphiding Treatment and Heteropoly Acids. U.S. Patent 4, 272, 400, 1981.

110. A. Anderson. Removing Contaminants from Silica-Based Cracking Catalysts. U.S. Patent 3, 173, 882, 1977.

111. E.H. Burke, J.S. Yoo, J.A. Karch and J. Yuan Sun. Catalyst Demetallization with a Reductive SO_2 Wash. U.S. Patent 4, 243, 550, 1981.

112. P. Ganguli. Regeneration of Spent Catalysts from Coal Liquefaction and Petroleum Residual Processing Operations. 17th IECEC Proceedings, pp. 825 - 830, 1982.

113. J.H. Everston. Hydrocarbon Research Inc. Regeneration of Metals Contaminated Hydrocarbon Process Catalyst. U.S. Patent 3, 240 - 208, 1983.

114. IOKA, Masatada, Shimizu, Toshiharu. Regeneration of Metals Contaminated Hydrocarbon Process Catalyst. U.S. Patent 3, 240, 208, 1983.

115. O.F. Poezd, Lipknol, B.A., Sutyrin, A.M. Maslova. Regeneration of a Spent Catalyst for Hydrofining of Petroleum Raw Material , U.S.S.R. 825, 136, 1981.

116. P.J. Marcantonio. Leaching Metals from Spent Hydroprocessing Catalysts with Ammonium Sulfate. U.S. Patent 4, 554, 138, 1985.

117. S. Takase and A. Inone. Regeneration of Spent Hydrotreating Catalysts by Burning Coke - In Molecular Oxygen and Extracting Vanadium and/or Nickel Residues in Alcohol. Europ. Pat. Appl. E. P. 156, 226, 1985.

118. R. Z. Pyreh and R. S. Rickard. Vanadium Recovery from Carbonaceous Ore or Scrap - by Two/Stage Oxidising Roast Followed by Weak Acid Leach. U.S. Patent. 4, 115, 110, 1978.

119. M. Marafi, A. Stanislaus. Regeneration of Spent Hydroprocessing Catalysts: Metals Removal. Applied Catalysis, 47, 85 - 96, 1989.

120. M. Marafi, A. Stanislaus, C.J. Mumford and M. Fahim. Rejuvenation of Spent Residue Hydroprocessing Catalyst by Leaching of Foulant Metals. Studies in Surface Science and Catalysis, 53, 213, 1990.

121. A. Stanislaus, M. Marafi and M. Halabi. Studies on the Rejuvanation of Spent Catalysts: Effectiveness and Selectivity in the Removal of Foulant Metals from Spent Hydroprocessing Catalysts in Coked and Decoked Forms. Applied Catalysis A: General, 105, 195-203, 1993.

122. M. Marafi, A. Stanislaus, M. Absi-Halabi. Heavy Oil Hydrotreating Catalyst Rejuvenation by Leaching of Foulant Metals with Ferric Nitrate - Organic Acid Mixed Reagents. Applied Catalysis B: Environmental 4, 19 - 27, 1994.

123. M. Marafi, A. Stanislaus and C. J. Mumford. Studies on Rejuvenation of Spent Residue Hydroprocessing Catalyst by Leaching: Influence of Inorganic Salt Additives on the Leaching Efficiency of Organic Acid. Catalysis Letter 18, 141-151, 1993.

124a. A. Myerson and W. R. Ernst. Regeneration of HDS Catalysts. U.S. Patent 4, 698, 321, 1987.

124b. K. W. Babcock, L. H. Hiltzik, W. R. Ernst and J. D. Carruthers. Appl. Catal., 51: 295, 1985.

125. T. D. Chan and G. Martino. Method for regeneration of catalyst deactivated by metal deposition. French Patent 2, 589, 368 (1987).

126. M. R. Reda. Regeneration of spent hydroprocessing catalyst. 1. Effect of the iron (II)/iron (III) redox couple on the selectivity of the removal of metals. Ind. Eng. Chem. Res. 30, 2148 (1991).

127. Gardner, L. E., and D. R. Kidd. Preparation of Hydrotreating Catalyst from Spent Catalysts. U.S. Patent No. 4, 888, 316, 1989.

128. H. Thoulhoat, R. Szymanski and J.C. Plumail. Interrelation betwen initial pore structure, morphology and distribution of accumulated deposits and life times of hydrodemetallization catalysts. Catalysis Today 7: 531-568, 1990.

129. Walendziewski. Preparation of Large Pore Alumina Support for hydrodesulphurization catalysts. Applied Catalysis A: general, 96, pp. 163-174, 1993.

130. G. Gualda. Coke versus metal deactivation of residue hydrodemetallization catalysts. Studies in surface science and catalysis, Vol. 88: 145 - 154, 1994.

131. H. Topsoe, Clausen, B.S. Topsoe, N. Y., and Zeuthen, P. Progress in the design of hydrotreating catalysts based on fundamental molecular insight. Studies in Surface Science and Catalysis, 53: 77 - 120, 1990.

132. C. Moreau and P, Geneste. Factors affecting reactivity of organic model compounds in hydrotreating reactions. In theoretical aspects of Heterogeneous Catalysis, Edited by J. B. Moffat, Van Reinhold, 256 - 289, 1990.

133. M. Daage and R. R. Chianelli. Structure function relations in molybdenum sulfide catalysts: The rim-edge model. Journal of Catalysis 149: 4124 - 427, 1994.

134. F. Diaz, B. C. Gates, J. T. Miller and S. G. Kukes, Hydrotreating Catalyst deactivation by coking. Ind. Eng. Chem. Res. 29, 1999, 1990.

135. J. B. Peri. Infrared spectroscopy in Catalytic research. Catalysis Science and Technology p. 171 - 220, 1984.

136. N. O. Egiebor and M. R. Gray. 13C-NMR characterization of Organic Residue on Spent Hydroprocessing, Hydrocracking and Demetallization Catalysts. Applied Catalysis, 55:81-91, 1989.

137. A. Stanislaus, M. Absi-Halabi and K. Al-Dalama. Studies on deactivation of Hydrotreating Catalysts: Role of Molybdena and Additives on Sintering and phase

transformations of MoO_3/α-Al_2O_3 systems. Studies in Surface Science and catalysis, 53; 22P, 1990.

138. I.S.J. Hildebrandt, R.O. Koseoglu, J.E. Duddy and D.E. Sherwood. Rejuvenation and reuse of High Activity Catalysts for Hydroprocessing High Metal Residue. ACS preprints, Vol. 38, No. 1, 40, 1993.
139. D. S. Thakur and M. G. Thomas. Catalyst Deactivation in Heavy Petroleum and Synthetic Crude Processing. Appl. Catal. 15, 197, 1985.
140. T. H. Fleisch, B. L. Meyers, J. B. Hall and G. L. OH. Multitechnique Analysis of Used Hydrotreating Catalyst. J. Catalyst. 86, 147, 1984.
141. J. H. Canterford, P. T. Davey and G. T. S. Samabourakis. The Influence of Ferric Ion on the Dissolution of Copper from Lump Oxide Ore: Implications in Solution Mining. Hydrometallurgy, 15, 93, 1985.
142. G. Demopoulos and P. A. Distin, Ferric Chloride Leaching of Sulfidized Chaleopyrite. Hydrometallurgy. 10, 111, 1983.
143. F. K. Grunwell, Kinetics and Mechanism of the Oxidative Dissolution of a Zinc Sulfide Concentrate in Ferric Sulfate Solutions. Hydrometallurgy, 19, 227, 1987.
144. R. C. Reid, J. M. Prausnitz and B. E. Poling. The Properties of Gases and Liquids McGraw-Hill, 4th Edition, 1987, New York.
145. "International Critical Tables", Vol. 5, McGraw-Hill, 1929, New York.
146. API, Technical Data Book - Petroleum Refining, Refining Department, American Petroleum Institute, Washington DC, 5th Edition, Chapters 4 and 13, 1992.
147. O. Levenspiel Chemical Reaction Engineering. John Wiley & Sons, 2nd Edition, 1972, New York.
148. E.L. Smith, Head of Chemical Engineering and Applied Science. Aston University, Birmingham, England. 1997 (Private Communication).

APPENDIX A

The foulant metal leaching operation for spent catalyst involves:

1. Removal of metals until pore structure develops.
2. Removal metals from pore structure.

According to Levenspiel (1972), the chemical kinetics of the process, assuming first order reaction on a cylinder, can be written as:

$$\frac{-dM}{dt} = k \text{ x } Conc.\ leachant \text{ x } S.a$$

$$= \quad k\ C_A \text{ x } 2\ \pi r\ l$$

$$-dM = -\rho\ dV$$

$$= -\rho d[\pi r^2 l]$$

$$= -\pi\rho l\ d[r^2] = -2\pi\rho l r dr$$

$$= k\ C\ 2\ \pi r\ l\ dt$$

$$\therefore \quad -\int_R^{rc} dr = \frac{Kc}{\rho} \int_o^t dt$$

$$t = \frac{\rho}{k c_A} \left[R - r_e\right]$$

$$\tau = -\frac{\rho}{k c_A} R$$

$$\therefore \frac{t}{\tau} = 1 - \frac{re}{R}$$

$$\text{If } 1-X_B = \frac{\text{Vol. unreacted core}}{\text{total vol.}} = \frac{\pi r^2 l}{\pi R_c^2 l} = \left[\frac{r}{R_c}\right]^2$$

$$\therefore \frac{t}{\tau} = 1 - \left[1 - X_B\right]^{1/2}$$

or,

$$\frac{\text{amount originally present} - \text{amount leached}}{\text{amount originally present}} = \left[\frac{r}{R_c}\right]^2$$

$$\frac{t}{\tau} = 1 - \frac{\text{amount original} - \text{amount leached}}{\text{amount original}}$$

If leaching is mass transfer controlled, we may write:

$$Q_A = D\frac{dc}{dr} \qquad \text{Diffusion equation}$$

$$\frac{-dN_A}{dt} = 2\pi r l . Q_A$$

$$= 2\pi r l . Q_A \text{ at surface}$$

$$\frac{-dN_A}{dt} = 2\pi r l . D_e \frac{dc}{dr}$$

$$\frac{-dN_A}{dt} \int_R^r \frac{dr}{r} = 2\pi D_e l \int_{C_{AS}}^{C_{AO}} dc$$

$$\frac{-dN_A}{dt} \ln \frac{r}{R_c} = -2\pi D l C_{AS}$$

Now $N_A = \rho V$

$= \rho \pi r^2 l$

$dN_A = \rho \pi l d[r^2]$

$= 2\rho \pi l r \cdot dr$

$$2\pi \rho l \int r \left(\ln \frac{r}{R_c} \right) dr = 2\pi D_e l C_{AS} \int dt$$

$$\int r \ln \left(\frac{r}{R_c} \right) dr = \frac{D_e}{\rho l} C_{AS} \int dt$$

$$= -\int \left[r \ln(r) - r \ln(R_c) \right] dr = \frac{D_e}{\rho} C_{AS} t$$

$$= \left(\frac{r^2}{2} \ln r - \frac{r^2}{4} - \frac{r^2}{2} \ln R_c \right)_R^r = \frac{D_e}{e} C_{AS} t$$

$$\frac{R_c^2}{4} + \frac{r^2}{2} \ln r - \frac{r^2}{4} - \frac{r^2}{2} \ln R_c = \frac{D_e}{\rho} C_{AS} t$$

$$\frac{-r^2}{2} (\ln R_c - \ln r) + 1/4 \left[R_c^2 - r^2 \right] = \frac{D_e}{\rho} C_{AS} t$$

At r=0, t=τ

$$\frac{R_c^2}{4} = \frac{D_e}{\rho} C_{AS} t \; . \; \tau$$

$$\frac{t}{\tau} = -2 \frac{r^2}{R_c^2} \left(\ln R_c - \ln r \right) + 1 - \frac{r^2}{R_c^2}$$

Now $$\frac{\text{amount leached}}{\text{total}} = \frac{\pi R_c^2 \, l - \pi r^2 l}{\pi R_c^2 \, l} = 1 - \frac{r^2}{R_c^2} = X$$

$$\frac{t}{\tau} = 2 (1-x) \left[- \ln R + \ln \left[R_c \sqrt{(1-x)} \right] \right] + X$$

$$\frac{t}{\tau} = 2 (1-x) \ln \left(\sqrt{1-x} \right) + X$$

In essence, the model consists of the following rate equations. For chemical reaction control:

$$\frac{t}{\tau} = 1 - (1-x)^{1/2} \qquad \text{(A1)}$$

For diffusion control:

$$\frac{t}{\tau} = 2 - (1-x) \ln \left(\sqrt{1-x} \right) + x \qquad \text{(A1)}$$

APPENDIX B

The model can be improved by including the stoichiometric ratio of the leaching reaction, as well as the estimation of diffusion rate during the leaching process. The mathematical development is as follows:

The leaching process:

$$aA + mM \longrightarrow \text{products}$$

(Acid) (Metal)

For "Diffusion Control", assume diffusion of A through carbon (coke) deposited in pore to the shrinking core boundary in a "steady-state" process.

Then for $r_c > r > R_o$.

$$\text{Diffusion Rate} = -2\pi r . D_e . \frac{dC_A}{dr} = K$$

Separating variables and integrating to get

$$-\int_{C_{A_O}}^{0} dC_A = \frac{K}{2\pi D_e} \int_{R_O}^{r_c} \frac{dr}{r}$$

$$\text{Hence, } C_{A_O} = \frac{K}{2\pi . D_e} (\ln r_c - \ln R_o)$$

$$\text{or } K = \frac{2\pi D_e . C_{A_O}}{\ln(r_c / R_o)} \qquad \text{(B1)}$$

where,

r_c = shrinking core radius

R = particle radius

R_o = initial radius of unblocked pore

Equation B1 gives the Diffusion Rate, K, for any value of r_c.

Metal Distribution Rates

$$= 2\pi r_c \cdot \frac{dr_c}{dt} \cdot \sigma_M \cdot \left(\frac{a}{m}\right) \qquad \text{(B2)}$$

where σ_M is the no. of moles of metal (M) in unit volume of fouled pore (before leaching). Note the need to include the stoichiometric ratio a/m.

Equations (B1) and (B2) separating variables and integrating:

$$\frac{D_e \cdot C_{A_O}}{\sigma_M \left(\frac{a}{m}\right)} \int_o^t dt = R_o^2 \int_1^{(r_c/R_o)} \left(\frac{r_c}{R_o}\right) \cdot \ln\left(\frac{r_c}{R_o}\right) \cdot d\left(\frac{r_c}{R_o}\right)$$

This leads to

$$\frac{D_{e.C_{A_O}}}{\sigma_M (a/m)} \cdot \frac{t}{R_o^2} = \frac{1}{2} \ln\left(\frac{r_c}{R_o}\right) \cdot \left(\frac{r_c}{R_o}\right)^2 \cdot - \left(\frac{r_c}{R_o}\right) \cdot \frac{1}{4} + \frac{1}{4}$$

This process is complete when $r_c = R$ and $t = \tau$.

$$\frac{D_e . C_{A_O}}{\sigma_M (a/m)} \cdot \frac{\tau}{R_o^2} = \frac{1}{2} \ln\left(\frac{R}{R_o}\right) \cdot \left(\frac{R}{R_o}\right)^2 - \left(\frac{R}{R_o}\right)^2 \cdot \frac{1}{4} + \frac{1}{4}$$

or

$$\frac{D_e . C_{A_O}}{\sigma_M (a/m)} \cdot \frac{4}{R_o^2} . \tau = \ln\left(\frac{R}{R_o}\right)^2 - 1 + \left(\frac{R_o}{R}\right)^2 \qquad \text{(B3)}$$

To solve Equation B3, a value for $\frac{R_o}{R}$ must be either known or estimated. For example, if we let $\frac{R}{R_o} = 3$, then the RHS of (B3) equals 1.3; for $\frac{R}{R_o} = 10$, RHS of (B3) equals 3.6.

Nomenclature

M	Metal foulant
V	Volume of the pore, 10^{-28} meter.
X_B	Fractional conversion
Q_A	Molar flux, mole/cm^2/s
N_A	No. of mole, mole
C_{A_S}	Surface concentration of leaching agents, mole/cm^3
r_c	Shrinking core radius, cm
R_o	Initial radius of unblocked pore, $\mathring{A}$
σ_m	No. of moles of metal
C_{A_O}	Bulk concentration of leaching agent, mole/cm^3

APPENDIX C

List of Publications and Technical Reports:

Refereed Journals/Books

1. Studies on Hydrotreating Catalyst Deactivation by Coke Deposition: Influence of feedstock quality on initial coking. A paper will be presented on Catalyst in Fuel Processing and Environmental Protection, ACS, Division of Petroleum Chemistry, Las Vegas, USA, Sept. 7-11, 1997. A paper will be published in Catalysis Today. In press.
2. Rejuvenation of Residual Oil Hydrotreating Catalysts by Leaching of Foulant Metals Modelling of the Metal Leaching. M. Marafi, A. Stanislaus, E.K.T. Kam and M. Absi-Halabi. Applied Catalysis A: General Vol. 147, No. 1, 1996, p. 35-46.
3. Factors Controlling Sintering of Co-Mo/Al_2O_3 Hydrotreating Catalyst During Oxidative Regeneration. A Stanislaus, M. Marafi and M. Absi-Halabi. The Arabian Journal for Science and Engineering (AJSE). Catalysis in Petroleum Refining, Volume 21, No. 2, 1996. p. 273-281.
4. Residual oil hydrotreating catalyst rejuvenation by leaching of foulant metals: effect of metal leaching on catalyst characteristics and performance. A. Stanislaus, M. Marafi and Absi-Halabi. Hydrotreating Technology for Pollution Control, Edited by M. Occelli and R.R. Chianelli, Marcel Dekker, New York, 1996. p. 327-336.
5. Heavy oil hydrotreating catalyst rejuvenation by leaching of foulant metals with ferric nitrate-organic acid mixed reagents. Marafi, A. Stanislaus and M. Halabi. Applied Catalysis B: Environmental. Vol. 4, 1994. p. 19-27.
6. Studies on the Rejuvenation of Spent Catalysts: Effectiveness and Selectivity of Foulant Metals Removal from Spent Hydroprocessing Catalysts in the Coked and Decoked Forms. Stanislaus, M. Marafi and M. Halabi. Applied Catalysis A: General, Vol. 105, 1993. p. 195-203.
7. Studies on Rejuvenation of Spent Residue Hydroprocessing Catalysts by Leaching of Foulant Metals: Influence of Inorganic Salt Additives on the Leaching Efficiency of Organic Acids. Marafi, A. Stanislaus and C.J. Mumford. Catalysis Letters Journal, Vol. 18, 1993, p. 141-151.
8. Rejuvenation of Spent Residue Hydroprocessing Catalyst by Leaching of Foulant Metals. Marafi, A. Stanislaus, C.J. Mumford and M. Fahim. Published in Studies in Surface Science and Catalysis. Vol. 53, 1990. p. 213-223.
9. Regeneration of spent hydroprocessing catalysts: metals removal. Marafi, S. Stanislaus, C.J. Mumford and M. Fahim. Applied Catalysis Journal, Vol. 47, 1989, p. 85-96.
10. The Regeneration of Deactivated Hydrotreating Catalysts. M. Marafi. M. Phil. Thesis. 1988.

Conference Proceedings

11. Development of a process to rejuvenate the spent hydroprocessing catalysts from Kuwait refineries. M. Marafi. Paper to be presented in 15th World Petroleum Congress, Forum 20, Beijing, China. October 1997.

12. Studies on Hydrotreating Catalyst Deactivation by Coke Deposition: Influence of feedstock quality on initial coking. A paper will be presented on Catalyst in Fuel Processing and Environmental Protection, ACS, Division of Petroleum Chemistry, Las Vegas, USA, Sept. 7-11, 1997.

13. Spent Catalyst Rejuvenation: A Route for Minimizing Catalyst Composition. M. Marafi, M. Halabi and A. Stanislaus. A paper presented in OAPEC-IFP joint Workshop on "Improving the Efficiency in refining operations and its economical yield", France, June24-27, 1997.

14. Rejuvenation of Spent Heavy Residue Hydroprocessing Catalyst from Kuwait Refineries. M. Marafi. A paper presented in OAPEC Symposia on "Refining Industry in the Arab Countries and the Challenges for the 21st Century", Cairo, 1996.

15. Effect of Initial Coking on Hydrotreating Catalyst Functionalities and Properties. M. Marafi and A. Stanislaus. Prepr. Am. Chem. Soc. Pet. Chem. Volume 41, No. 3, 1996, p. 604-608.

16. Rejuvenation of Spent Residue Hydrotreating Catalysts: A Comparative Assessment of the Efficiency of Different Acid Reagent on Selective Leaching of Foulant Metals from Coked Spent Catalyst. M. Marafi, A. Stanislaus and M. Absi-Halabi. Presented at Europ-CAT-II, September 3-8, 1995. MECC, Maastricht, The Netherlands.

17. Residual Oil Hydrotreating Catalyst Rejuvenation by Leaching of Foulant Metals: Effect of Metal Leaching on Catalyst Characteristics and Performance. A. Stanislaus, M. Marafi and M. Absi-Halabi. Prepr. Am. Chem. Soc. Pet. Chem. 39, 4, 1994, p. 627-631.

18. Comparative evaluation of rejuvenation of spent residue hydroprocessing catalysts in the decoked (oxidic) and coked (sulfided) form. Stanislaus, M. Marafi and M. Absi-Halabi. Presented at ACS conference, March 28-April 2 on Regeneration, Reactivation and Reworking of Spent Catalysts. ACS Division petroleum Chemistry pre-prints Vol. 38(1), 1995, p. 62-66.

19. Rejuvenation of hydrotreating catalysts: comparative evaluation of coked and decoked catalyst. M. Marafi, A. Stanislaus and M. Halabi. Kuwait-Japanese Symposium, 3-7 Nov. 1993. KISR, Kuwait, p. 99-107.

20. Recycling of Deactivated Hydrotreating Catalysts. A Viable Approach in Solving Refineries Solid Wastes Problem. M. Marafi, A. Stanislaus and C.J. Mumford. Published in Chemistry in Industry, Proceedings Part I. 1992. p. 153-164.

21. A comparative study of the efficiency of three different organic acids for selective leaching of metal foulants from spent residue hydroprocessing catalysts. M. Marafi, A. Stanislaus, and C.J. Mumford. Presented at 1st Tokyo Conference on Advanced

Catalytic Science and Technology, Tokyo, 1990. Published in Catalytic Science and Technology, (Kodakausha publishing Co., Tokyo), Vol. 1, 1991, p. 389-391.

22. Studies on the Rejuvenation of Spent Catalysts: a Comparative Study of the Efficiency of Three Different Organic Acids for Selective Leaching of Metal Foulants from Spent Residue Hydroprocessing Catalysts. M. Marafi, A. Stanislaus and C.J. Mumford. Proceedings, Catalytic Science and Technology, Vol. 1, 1990. p. 389-392.

Technical Reports

23. Optimization of a Continuous Process for the Rejuvenation of Spent Hydroprocessing Catalysts. M. Marafi, M. Absi-Halabi, A. Stanislaus, E.K.T. Kam, F. Jassem and F. Abu-Seedo. Final Report (PT001C). June 1997.

24. Preliminary Economic Assessment of Novel Catalyst Rejuvenation Process. M. Marafi, E.K.T. Kam, A. Stanislaus and M. Absi-Halabi. Technical Report No. 5, KISR 4987 (1997).

25. Rejuvenation of Spent Hydroprocessing Catalysts: Studies on the Separation and the Utilization of the Spent Catalyst. M. Marafi, M. Absi-Halabi, A. Stanislaus. F/ Jassem, F. Al-Kharsan and J. Al-Fadhli. Technical Report No. 4, KISR 4986 (1997).

26. Rejuvenation of Spent Hydroprocessing Catalysts: Studies on the Removal of Coke and Metal Deposits from the Spent Catalyst. M. Marafi, A. Stanislaus, F. Jassem, and F. Abu-Seedo. Technical Report No. 3, KISR (1996).

27. Studies on the Nature and Effect of Coke Deposition on Hydrotreating Catalysts. M. Marafi, A. Stanislaus, M. Al-Samhan, J. Al-Fadhli. Final Report, KISR No. 4745, (1996).

28. Studies on characterisation, deactivation and rejuvenation of spent residue hydroprocessing catalysts. M. Marafi, A. Stanislaus, F. Jasem. Technical Report, KISR No. 4618, (1995).

29. Studies on Deactivation by Coke Deposition in Hydrotreating Catalysts: Effect of Temperature and Time on the Nature of Coke Deposits. M. Marafi, A. Stanislaus, S. Al-Jadi, Y. Mirza. Technical Report KISR No. 4591. (1995).

30. Detailed Equipment Designs for a Continuous Mode Process for Spent Catalyst Rejuvenation. M. Marafi, M. Absi-Halabi, E. Kam, and A. Stanislaus. Technical Report KISR 4513, (1994).

31. Studies on Development of a Process to Rejuvenate Spent Residue Hydroprocessing Catalyst. A. Stanislaus, M. Halabi, F. Owaysi, M. Marafi, H. Al-Zaid and K. Al-Dolama, KISR 3394, (1990).

32. Studies on Leaching of Metal Foulants from Spent Residue Hydrodesulphurization Catalysts. A. Stanislaus, M. Halabi, M. Marafi, F. Owaysi and H. Al-Zaid, KISR 3110, (1989).

33. M. Marafi. Enhanced Oil Recovery. KISR, 1726 (1985).

34. Marafi and M.M. Ismail. Reclamation of Used Motor Oil. Final Report 1316 (June 1984).

35. Kuwait Heavy Crude Oil Handbook. Z. Hameed and M. Marafi. KISR 1124, (1983) (Confidential).

36. Crude Oil Assay. K. Marron and M. Marafi. 1981. (Confidential).